NUREG/CP-0091
Vol. 6

Han

Proceedings of the U.S. Nuclear Regulatory Commission

Fifteenth Water Reactor Safety Information Meeting

Volume 6
- Decontamination and Decommissioning
- Accident Management
- TMI-2

Held at
National Bureau of Standards
Gaithersburg, Maryland
October 26-29, 1987

U.S. Nuclear Regulatory Commission

Office of Nuclear Regulatory Research

Proceedings prepared by
Brookhaven National Laboratory

Available from

Superintendent of Documents
U.S. Government Printing Office
P.O. Box 37082
Washington D.C. 20013-7082

and

National Technical Information Service
Springfield , VA 22161

NUREG/CP-0091
Vol. 6
R2, R3, R4

Proceedings of the U.S. Nuclear Regulatory Commission

Fifteenth Water Reactor Safety Information Meeting

Volume 6
- Decontamination and Decommissioning
- Accident Management
- TMI-2

Held at
National Bureau of Standards
Gaithersburg, Maryland
October 26-29, 1987

Date Published: February 1988

Compiled by: Allen J. Weiss

Office of Nuclear Regulatory Research
U.S. Nuclear Regulatory Commission
Washington, DC 20555

Proceedings prepared by
Brookhaven National Laboratory

ABSTRACT

This six-volume report contains 140 papers out of the 164 that were presented at the Fifteenth Water Reactor Safety Information Meeting held at the National Bureau of Standards, Gaithersburg, Maryland, during the week of October 26-29, 1987. The papers are printed in the order of their presentation in each session and describe progress and results of programs in nuclear safety research conducted in this country and abroad. Foreign participation in the meeting included twenty-two different papers presented by researchers from Belgium, Czechoslovakia, Germany, Italy, Japan, Russia, Spain, Sweden, The Netherlands and the United Kingdom. The titles of the papers and the names of the authors have been updated and may differ from those that appeared in the final program of the meeting.

PROCEEDINGS OF THE
15th WATER REACTOR SAFETY INFORMATION MEETING

October 26-29, 1987

Published in Six Volumes

GENERAL INDEX

D ACKER
CEA FRENCH ATOMIC ENERGY COMMISSION
DEMT/SMTS/RDMS
GIF S/YVETTE 91191
FRANCE

H. ADACHI
JAPAN ATOMIC ENERGY RES. INSTITUTE
TOKAI-MURA
IBARAKI 319-11
JAPAN

L. J. AGEE
ELECTRIC POWER RESEARCH INSTITUTE
3412 HILLVIEW AVENUE
PALO ALTO CA 94303
USA

H. AKIMOTO
JAPAN ATOMIC ENERGY RES. INSTITUTE
TOKAI-MURA
IBARAKI 319-11
JAPAN

P. ALBRECHT
UNIVERSITY OF MARYLAND
DEPT. OF CIVIL ENGINEERING
COLLEGE PARK MD 20742
USA

D. J. ALEXANDER
OAK RIDGE NATIONAL LAB
P.O. BOX X, BLDG 4500-S
OAK RIDGE TN 37831
USA

R. P. ALLEN
BATTELLE PACIFIC NORTHWEST LAB.
P.O. BOX 999
RICHLAND WA 99352
USA

K. K. ALMENAS
UNIVERSITY OF MARYLAND
COLLEGE PARK MD 20742
USA

A. ALONSO
MADRID POLYTECHNICAL UNIVERSITY
JOSE GUTIERREZ ABASCAL, 2
MADRID 28006
SPAIN

M. AMIN
SARGENT & LUNDY
55 E. MONROE
CHICAGO IL 60603
USA

P. S. ANDERSEN
DYNATREK, INC.
2115 E. JEFFERSON STREET
ROCKVILLE MD 20852
USA

J. M. ANDERSON
BECHTEL
15740 SHADY GROVE RD.
GAITHERSBURG MD 20850
USA

F. ARAYA
JAPAN ATOMIC ENERGY RES. INSTITUTE
3000 TRINITY DR.
LOS ALAMOS NM 87544
USA

W. C. ARCIERI
ENSA, INCORPORATED
15825 SHADY GROVE ROAD
ROCKVILLE MD 20850
USA

K. H. ARDRON
CENTRAL ELECTRICITY GENERATING BOARD
BOCD
GLOUCESTER
UK

J. G. ARENDTS
EG&G IDAHO, INC.
P.O. BOX 1625
IDAHO FALLS ID 83415
USA

D. A. ARMSTRONG
WASHINGTON PUBLIC POWER SUPPLY SYS.
3000 G. WASH. WAY-P.O. BOX 968
RICHLAND WA 99352
USA

A. ARNAUD
CEA FRENCH ATOMIC ENERGY COMMISSION
CEN CADARACHE
ST. PAUL LEZ DURANCE 13115
FRANCE

W. W. ASCROFT-HUTTON
HM NUCLEAR INSTALLATIONS INSPECTORATE
BAYNARDS HOUSE CHEPSTOW PLACE
LONDON W24TF
UK

V. G. ASMOLOV
I. V. KURCHATOV INST. OF ATOMIC ENERGY
KURCHATOV SQUARE
MOSCOW 123182
USSR

D. AXFORD
ATOMIC ENERGY OF CANADA, LTD
15 ISABEL STREET
PETAWAWA ONTARIO K8H1Z1
CANADA

W. J. BABYAK
WESTINGHOUSE BETTIS ATOMIC PWR LAB
P.O. BOX 79
WEST MIFFLIN PA 15122
USA

A. J. BAKER
HM NUCLEAR ISTALLATIONS INSPECTORATE
ST. PETERS HOUSE, BALLIOL ROAD
BOOTLE MERSEYSIDE L203LZ
UK

J. L. BALLIF
SCIENTECH
P.O. BOX 1406
IDAHO FALLS ID 83403-1406
USA

W. H. BAMFORD
WESTINGHOUSE
P. O. BOX 2728
PITTSBURGH PA 15230
USA

M. C. BAMPTON
BATTELLE PACIFIC NORTHWEST LAB
P.O. BOX 999
RICHMOND WA 99352
USA

K. K. BANDYOPADHYAY
BROOKHAVEN NATIONAL LAB
BLDG. 129
UPTON NY 11973
USA

R. A. BARI
BROOKHAVEN NATIONAL LAB
BLDG 130
UPTON NY 11973
USA

B. R. BASS
OAK RIDGE NATIONAL LAB.
P.O. BOX Y
OAK RIDGE TN 37831
USA

J. A. BAST
GENERAL ELECTRIC COMPANY
P.O. BOX 1072
SCHENECTADY NY 12301
USA

R C BAUER
WESTINGHOUSE BETTIS ATOMIC PWR LAB
P.O. BOX 79
WEST MIFFLIN PA 15122
USA

K .R. BAUMGARTEL
GESELLSCHAFT FUR REAKTORSICHERHEIT
SCHWERTNERGASSE 1
KOELN 8046
FRG

S. L. BAXTER
UNIVERSITY OF MARYLAND
4100 CONNECTICUT AVENUE
BALTIMORE MD 21045
USA

P. D. BAYLESS
EG&G IDAHO, INC.
P.O. BOX 1625
IDAHO FALLS ID 83415
USA

A. BECERRA
INSURGENTES SUR 1776
MEXICO CITY
MEXICO 01030
MEXICO

R. J. BEELMAN
EG&G IDAHO, INC.
P.O. BOX 1625
IDAHO FALLS ID 83415
USA

J. G. BENNETT
LOS ALAMOS NATIONAL LAB.
P.O. BOX 1663, MS J570
LOS ALAMOS NM 87544
USA

E. D. BERGERON
SANDIA NATIONAL LABORATORIES
P.O. BOX 5800, DIV 6413
ALBUQUERQUE NM 87185
USA

K. D. BERGERON
SANDIA NATIONAL LABORATORIES
P.O. BOX 5800
ALBUQUERQUE NM 87185
USA

E. BESWICK
CENTRAL ELECTRICITY GENERATING BOARD
BOOTHS HALL, CHELFORD ROAD
KNUTSFORD CHESHIRE WA168QG
UK

P. BEZLER
BROOKHAVEN NATIONAL LABORATORY
BLDG. 129
UPTON NY 11973
USA

M. J. BIRD
UKAEA/AEE WINFRITH
DORCHESRER
DORSET DT28DH
UK

D. P. BIRMINGHAM
BABCOCK & WILCOX
1562 BEESON STREET
ALLIANCE OH 44601
USA

M. M. BLEAKLEY
UKAEA/SRD
WIGSHAW LANE, CULCHETH
WARRINGTON WA34NE
UK

J. L. BOCCIO
BROOKHAVEN NATIONAL LABORATORY
BUILDING 130
UPTON NY 11973
USA

B. R. BOHER
FRAMATOME
254 RAINPRINT SQUARE
MURRYSVILLE PA 15668
USA

J. M. BOONE
DUKE POWER
422 SOUTH CHURCH ST.
CHARLOTTE NC 28242
USA

R. B. BORSUM
BABCOCK & WILCOX CO
7910 WOODMONT AVE., SUITE 220
BETHESDA MD 20814
USA

W. M. BOWEN
BATTELLE PACIFIC NORTHWEST LAB
P.O. BOX 999
RICHLAND WA 99352
USA

D. R. BRADLEY
SANDIA NATIONAL LABORATORIES
P.O. BOX 5800
ALBUQUERQUE NM 87185
USA

M. BRANDANI
ANSALDO
VIA D'ANNUNZIO 113
GENOVA 16129
ITALY

R. J. BREEDING
SANDIA NATIONAL LABORATORIES
P.O. BOX 5800, DIV 6413
ALBUQUERQUE NM 87185
USA

D. BREWER
DUKE POWER
422 SOUTH CHURCH ST.
CHARLOTTE NC 28242
USA

I. BRITTAIN
UKAEA/AEE WINFRITH
DORCHESRER
DORSET DT28DH
UK

J. M. BROUGHTON
EG&G IDAHO, INC.
P.O. BOX 1625
IDAHO FALLS ID 83415
USA

B. J. BUESCHER
EG&G IDAHO, INC.
P.O. BOX 1625
IDAHO FALLS ID 83415
USA

N. E. BUTTERY
CENTRAL ELECTRICITY GENERATING BOARD
BERKELEY NUCLEAR LABORATORIES
BERKELEY GLOUCESTERSHIRE GL139PB
UK

A. L. CAMP
SANDIA NATIONAL LABORATORIES
P.O. BOX 5800, DIV 6412
ALBUQUERQUE NM 87185
USA

N. G. CATHEY
EG&G IDAHO, INC.
P.O. BOX 1625
IDAHO FALLS ID 83415
USA

S. CHAKRABORTY
EIR-EIDG. INST. FUR REAKTORFORSCHUNG
WURENLINGEN CH5303
SWITZERLAND

Y. CHEN
INSTITUTE OF NUCLEAR ENERGY RESEARCH
P.O. BOX 3-3
LUNG-TAN TAIWAN 32500
ROC

J. C. CHEN
LEHIGH UNIVERSITY
WHITAKER LAB #5
BETHLEHEM PA
USA

T. CHEN
ADVANCED NUCLEAR FUELS CORP.
2101 HORN RAPIDS RD., P.O. BOX 130
RICHLAND WA 99352
USA

H. S. CHENG
BROOKHAVEN NATIONAL LAB
BLDG 475B
UPTON NY 11973
USA

J. CHENG
UNIVERSITY OF MARYLAND
DEPT. OF CIVIL ENGINEERING
COLLEGE PARK MD 20742
USA

A. CHEUNG
WESTINGHOUSE
P.O. BOX 355
PITTSBURGH PA 15230
USA

O. K. CHOPRA
ARGONNE NATIONAL LAB
9700 S. CASS AVE-BLDG 208
ARGONNE IL 60439
USA

J. CHRISTENSEN
BATTELLE PACIFIC NORTHWEST LAB
P.O. BOX 999
RICHLAND WA 99352
USA

R. CLASPER
UKAEA/SRD
WIGSHAW LANE, CULCHETH
WARRINGTON WA34NE
UK

J. W. CLEVELAND
SEA CONSULTANTS, INC.
2001 GATEWAY PLACE, SUITE 610-W.
SAN JOSE CA 95110
USA

M. COLAGROSSI
ENEA/DISP
VIA VITALIANO BRANGATI 48
ROME 00144
ITALY

R. K. COLE
SANDIA NATIONAL LABORATORY
P.O. BOX 5800, DIVISION 6418
ALBUQUERQUE NM 87185
USA

M. W. CONEY
CENTRAL ELECTRICITY GENERATING BOARD
CERL-KELVIN AVE
LEATHERHEAD KT227SE
UK

I. COOK
UKAEA
CULHAM LABORATORY
ABINGTON OXFORDSHIRE OX1438D
UK

K. V. COOK
OAK RIDGE NATIONAL LAB
P.O. BOX X, 4500S
OAK RIDGE TN 37831
USA

B. A. COOK
EG&G IDAHO, INC.
P.O. BOX 1625
IDAHO FALLS ID 83415
USA

W. R. CORWIN
OAK RIDGE NATIONAL LAB
P.O. BOX Y, BLDG. 9204-1
OAK RIDGE TN 37831
USA

R. COWARD
MPR ASSOCIATES, INC.
1050 CONNECTICUT AVE N.W.
WASHINGTON DC 20036
USA

S. R. COWNE
BALTIMORE GAS & ELECTRIC
CALVERT CLIFFS - P.O. BOX 1535
LUSBY MD 20657
USA

W R CRAMOND
SANDIA NATIONAL LABORATORY
P.O. BOX 5800
ALBUQUERQUE NM 87185
USA

M. W. CRUMP
COMBUSTION ENGINEERING
1000 PROSPECT HILL ROAD
WINDSOR CT 06095
USA

W. H. CULLEN
MATERIALS ENGINEERING ASSOCIATES, INC.
9700-B MARTIN LUTHER KING HWY
LANHAM MD 20706
USA

G. E. CUMMINGS
LAWRENCE LIVERMORE NATIONAL LAB
P.O. BOX 808, L-198
LIVERMORE CA 94550
USA

R. A. CUSHMAN
NIAGARA MOHAWK POWER CO.
301 PLAINFIELD ROAD
SYRACUSE NY 13212
USA

D. A. DAHLGREN
SANDIA NATIONAL LABORATORY
P.O. BOX 5800
ALBUQUERQUE NM 87185
USA

P. M. DALING
BATTELLE PACIFIC NORTHWEST LAB
P.O. BOX 999
RICHLAND WA 99352
USA

P. S. DAMERELL
MPR ASSOCIATES, INC.
1050 CONNECTICUT AVE N.W.
WASHINGTON DC 20036
USA

J. DARLASTON
BERKELEY NUCLEAR LABS
C.E.G.B.
BERKELEY GLOS GL139PB
UK

G. DAVIS
COMBUSTION ENGINEERING
1000 PROSPECT HILL ROAD
WINDSOR CT 06095
USA

G. DeGRASSI
BROOKHAVEN NATIONAL LAB
BLDG. 129
UPTON NY 11973
USA

R. S. DENNING
BATTELLE COLUMBUS
505 KING AVENUE
COLUMBUS OH 43201
USA

V. DEVITA
ROCKETDYNE (ETEC)
DESOTO AND NORDHOFF
CANOGA PARK CA 91304
USA

R. deWIT
NATIONAL BUREAU OF STANDARDS
RM A113, MATERIALS BLDG
GAITHERSBURG MD 20854
USA

D. R. DIERCKS
ARGONNE NATIONAL LAB
9700 S. CASS AVE
ARGONNE IL 60439
USA

M. diMARZO
UNIVERSITY OF MD.
MECH. ENG. DEPT.
COLLEGE PARK MD 20742
USA

S. R. DOCTOR
BATTELLE PACIFIC NORTHWEST LAB.
P.O. BOX 999
RICHLAND WA 99352
USA

C. V. DODD
OAK RIDGE NATIONAL LAB
P.O. BOX X, 4500S, MS-151
OAK RIDGE TN 37831
USA

P. K. DOHERTY
COMBUSTION ENGINEERING
WINDSOR
CT 1000 PROSPECT HILL ROAD 06095
USA

B. J. DOLAN
DUKE POWER
422 SOUTH CHURCH ST.
CHARLOTTE NC 28242
USA

J. DRCEC
NUCLEAR POWER PLANT KRSKO
VRBINA 12, 68270 KRSKO
KRSKO 68270
YUGOSLAVIA

S. S. DUA
GENERAL ELECTRIC COMPANY
175 CURTNER AVE.
SAN JOSE CA 925125
USA

S. W. DUCE
EG&G IDAHO, INC.
P.O. BOX 1625
IDAHO FALLS ID 83415
USA

J. J. DUCO
CEA FRENCH ATOMIC ENERGY COMMISSION
DAS/SASC,CEN/FAR,BP NO 6
FONTENAY-AUX-ROSES CEDEX CEDEX 92265
FRANCE

R. DUFFEY
EG&G IDAHO, INC.
P.O. BOX 1625
IDAHO FALLS ID 83415
USA

S. R. DUGAN
UNIVERSITY OF MARYLAND
RT. 1
COLLEGE PARK MD 21093
USA

K. DWIVEDY
VIGINIA POWER
5000 DOMINION BLVD.
GLEN ALLEN VA 23060
USA

D. B. EBELING-KOMING
WESTINGHOUSE
P.O. BOX 355, M/S E 4-12A
PITTSBURGH PA 15230
USA

J. L. EDSON
EG&G IDAHO, INC.
P.O. BOX 1625
IDAHO FALLS ID 83415
USA

G. R. EIDAM
BECHTEL
P. O. BOX 72
MIDDLETOWN PA 17057
USA

D. M. EISSENBERG
OAK RIDGE NATIONAL LAB
P.O. BOX Y, BLDG.9104-1 MS-1
OAK RIDGE TN 37831
USA

J. EKMAN
ROLLS ROYCE & ASSOCIATES LTD.
P. O. BOX 31
DERBY DE2 8BJ
UK

Z. J. ELAWAR
ARIZONA NUCLEAR POWER PROJECT
11226 NORTH 23RD AVE.
PHOENIX AZ 85029
USA

T. W. ELLISON
GENERAL ELECTRIC COMPANY
P.O. BOX 1072
SCHENECTADY NY 12301
USA

G. T. EMBLEY
KNOLLS ATOMIC POWER LABORATORY
BOX 1072
SCHENECTADY NY 12301
USA

D. ERB
DEPARTMENT OF ENERGY
WASHINGTON DC 20545
USA

H. A. ERNST
GEORGIA INSTUTUTE OF TECHNOLOGY
ATLANTA GA 30332
USA

M. ERVE
SIEMENS/KWU
HAMMERBACHERSTRASSE 12 + 14
ERLANGEN D-8520
FRG

H. FABIAN
SIEMENS/KWU
HAMMERBACHERSTRASSE 12 + 14
ERLANGEN D-8520
FRG

A. M. FABRY
SCK-CEN
200 BOERETANG
2400 MOL
BELGIUM

C. R. FARRAR
LOS ALAMOS NATIONAL LAB.
MS 5576
LOS ALAMOS NM 87545
USA

J. FELL
UKAEA/AEE WINFRITH
DORCHESRER
DORSET DT28DH
UK

D. FIGLHUBER
UTL
1000 ABERNATHY RD.
ATLANTA GA 30328
USA

H. E. FLORA
UNITED ENGINEERS
305 17TH STREET
PHILADELPHIA PA 19101
USA

E. FOTOPOULOS
BECHTEL
15740 SHADY GROVE ROAD
GAITHERSBURG MD 20877
USA

E. C. FOX
OAK RIDGE NATIONAL LAB
P. O. BOX X
OAK RIDGE TN 37831
USA

M. D. FRESHLEY
BATTELLE PACIFIC NORTHWEST LAB.
P.O. BOX 999
RICHLAND WA 99352
USA

B. C. FRYER
ADVANCED NUCLEAR FUELS CORP.
2101 HORN RAPIDS RD., P.O. BOX 130
RICHLAND WA 99352
USA

E. L. FULLER
ELECTRIC POWER RESEARCH INSTITUTE
3412 HILLVIEW AVE, P.O. BOX 10412
PALO ALTO CA 94303
USA

S. FURUKAWA
TOSHIBA
8 SHINSUGITA-ISOGO-KU
YOKOHAMA KANAGAWA-KEN 235
JAPAN

J. L. GANDRILLE
FRAMATOME
TOUR FIAT CEDEX 16
PARIS FR 92084
FRANCE

F. J. GARDNER
BECHTEL POWER COMPANY
GAITHERSBURG
MD 15740 SHADY GROVE RD. 20878
USA

P. T. GEORGE
CENTRAL ELECTRICITY GENERATING BOARD
BOOTHS HALL
KNUTSFORD CHESHIRE
UK

J. A. GIESEKE
BATTELLE COLUMBUS
505 KING AVENUE
COLUMBUS OH 43201
USA

P. A. GILLES
FRAMATOME
505 KING AVENUE
COLUMBUS OH 43201
USA

T. GINSBERG
BROOKHAVEN NATIONAL LAB
BLDG 820M
UPTON NY 11973
USA

B. GITNICK
ENSA, INC.
P.O. BOX 5537
ROCKVILLE MD 20855
USA

M. W. GOLAY
MASS. INSTITUTE OF TECHNOLOGY
77 MASS. AVE
CAMBRIDGE MA 02139
USA

M. GOMOLINSKI
CEA FRENCH ATOMIC ENERGY COMMISSION
CEN-FAR, IPSN
FONTENAY-AUX-ROSES CEDEX 92265
FRANCE

R. L. GOODMAN
BATTELLE PACIFIC NORTHWEST LAB
P.O. BOX 999
RICHLAND WA 99352
USA

N. GOTOH
HITACHI, LTD.
3-1-1, SAIWAI-CHO
HIYACHI IBARAKI 317
JAPAN

S. R. GREENE
OAK RIDGE NATIONAL LAB
P.O. BOX Y, BLDG.9104-1
OAK RIDGE TN 37831
USA

G. A. GREENE
BROOKHAVEN NATIONAL LAB
BLDG 820M
UPTON NY 11973
USA

W. L. GREENSTREET
OAK RIDGE NATIONAL LAB
P.O. BOX Y, BLDG.9201-3, MS 2
OAK RIDGE TN 37831
USA

M. V. GREGORY
SAVANNAH RIVER LABORATORY
773-41A
AIKEN SC 29808
USA

E. F. GRIER
LAUREL INDUSTRIES
SUITE 1001, 16 11 N. KENT ST.
ARLINGTON VA 22209
USA

P. GRIFFITH
MASSACHUSETTS INST. OF TECH.
ROOM 7-044
CAMBRIDGE MA 02139
USA

P. GRUBER
KRAFTWERK UNION AG
HAMMERBACHERSTRASSE 12 + 14
ERLANGEN D-8520
FRG

P. GRUNER
GESELLSCHAFT FUR REAKTORSICHERHEIT
SCHWERTNERGASSE 1
COLOGNE 5000
FRG

W. E. GUNTHER
BROOKHAVEN NATIONAL LAB
BLDG 130
UPTON NY 11973
USA

J. G. GUPPY
BROOKHAVEN NATIONAL LAB
BLDG 475B
UPTON NY 11973
USA

D. E. GUYON
WESTINGHOUSE BETTIS ATOMIC PWR LAB
P.O. 79
WEST MIFFLIN PA
USA

G. L. GYOREY
GENERAL ELECTRIC
19941 WINTER LN
SARATOGA CA 015070
USA

F. M. HAGGAG
OAK RIDGE NATIONAL LAB
P.O. BOX X, BLDG 4500-S
OAK RIDGE TN 37831
USA

R. E. HALL
BROOKHAVEN NATIONAL LABORATORY
BLDG. 130
UPTON NY 11973
USA

R. G. HANSON
EG&G IDAHO, INC.
P.O. BOX 1625
IDAHO FALLS ID 83415
USA

D. J. HANSON
EG&G IDAHO, INC.
P.O. BOS 1625
IDAHO FALLS ID 83415
USA

Y. A. HASSAN
TEXAS A & M, DEPT. OF NUCLEAR ENGR.
COLLEGE STATION TX 77843
USA

J. R. HAWTHORNE
MATERIALS ENGINEERING ASSOCIATES, INC.
9700-B MARTIN LUTHER KING HWY
LANHAM MD 20706
USA

M. HAYASHI
JAPAN NUS
875 FUTOCHO KOUHOKUKU
YOKOHAMA
JAPAN

Y. HAYASHI
KANSAI ELECTRIC POWER CO., INC.
1100 17TH STREET N.W. SUITE 500
WASHINGTON DC 20036
USA

M. R. HAYNS
UKAEA/SRD
WIGSHAW LANE, CULCHETH
WARRINGTON WA37NB
UK

T. J. HEAMES
SAIC
2109 AIR PARK RD. SE
ALBUQUERQUE NM 87106
USA

R. A. HEDRICK
TECHNOLOGY FOR ENERGY CORP.
P.O. BOX 22996
KNOXVILLE TN 37933
USA

J. A. HEIL
NETHERLANDS ENERGY RES FOUNDATION
POSTBOX 1
PETTEN NH 175520
NETHERLANDS

J. C. HELTON
ARIZONA STATE UNIVERSITY
TEMPE AZ 85287
USA

F. P. HENNESSY
E.I. DUPONT
117 COUNTRY PLACE DR.
N. AGUSTA SC 29841
USA

H. K. HERKENRATH
COMMISSION OF EUROPEAN COMMUNITIES
J.R.C. ISPRA
ISPRA VA 21020
ITALY

R. J. HERTLEIN
KRAFTWERK UNION AG
HAMMERBACHERSTRASSE 12 + 14
ERLANGEN D-8520
FRG

R. T. HESSIAN
STONE & WEBSTER
3 EXECUTIVE CAMPUS
CHERRY HILL NJ 08053
USA

G. F. HEWITT
UKAEA/WRPD
B.392, HARWELL LABORATORY
OXFORDSHIRE OX10 ODY
UK

E. F. HICKEN
GESELLSCHAFT FUR REAKTORSICHERHEIT
FORSCHUNGSGELAENDE
GARCHING 8046
FRG

D. HICKS
UKAEA/WRPD
B.329, HARWELL LABORATORY
OXFORDSHIRE OX11 ORA
UK

L. J. HIGGINBOTHAM
UNIVERSITY OF MARYLAND
1200 FALLS ROAD
BALTIMORE MD 21011
USA

J. C. HIGGINS
BROOKHAVEN NATIONAL LABORATORY
BLDG. 130, 32 LEWIS
UPTON NY 11973
USA

P. R. HILL
PENNSYLVANIA PWR & LIGHT CO.
2 NORTH NINTH STREET
ALLENTOWN PA 18101
USA

J. H. HINTON
SAVANNAH RIVER LABORATORY
707-C RM. 329
AIKEN SC 29808
USA

T. J. HIRONS
LOS ALAMOS NATIONAL LAB
P.O. BOX 1663, MS E561
LOS ALAMOS NM 87545
USA

A. L. HISER
MATERIALS ENGINEERING ASSOCIATES, INC.
9700-B MARTIN LUTHER KING HWY
LANHAM MD 20706
USA

N. HOBSON
NATIONAL NUCLEAR CORP.
BOOTHS HALL, CHELFORD ROAD
KNUTSFORD CHESHIRE
UK

S. A. HODGE
OAK RIDGE NATIONAL LAB
P.O. BOX Y, BLDG.9104-1
OAK RIDGE TN 37831
USA

L. G. HOEGBERG
SWEDISH NUCLEAR POWER INSPECTORATE
SEHLSTEDTSGATAN 11, BOX 27106
STOCKHOLM S10252
SWEDEN

P. HOFMANN
KERNFORSCHUNGSZENTRUM (KfK)
P.O. BOX 3640
D-7500 KARLSRUHE1
FRG

C. HOFMAYER
BROOKHAVEN NATIONAL LAB
BLDG. 129
UPTON NY 11973
USA

G. S. HOLMAN
LAWRENCE LIVERMORE NATIONAL LAB
P. O. BOX 808, L-197
LIVERMORE CA 94550
USA

H. L.O. HOLMSTROM
TECHNICAL RESEARCH CENTRE OF FINLAND
P. O. BOX 169
HELSINKI SF00181
FINLAND

K. W. HOLTZCLAW
GENERAL ELECTRIC COMPANY
175 CURTNER AVENUE, M/C 754
SAN JOSE CA 95125
USA

R. G. HOPPE
WESTINGHOUSE BETTIS ATOMIC PWR LAB
P.O. BOX 79
WEST MIFFLIN PA 15122
USA

J. HORTAL
BROOKHAVEN NATIONAL LAB
BLDG 475B
UPTON NY 11973
USA

P. Y. HOSEMANN
EIR-EIDG. INST. FUR REAKTORFORSCHUNG
WURENLINGEN CH5303
SWITZERLAND

T. W. HSU
VIRGINIA POWER
5000 DOMINION BLVD.
GLEN ALLEN VA 23060
USA

Y. Y. HSU
UNIVERSITY OF MARYLAND
RT. 1
COLLEGE PARK MD 20742
USA

J. M. HU
UNIVERSITY OF MARYLAND
DEPT. OF CIVIL ENGINEERING,
COLLEGE PARK MD 20742
USA

E. W. HUNT, JR.
SAVANNAH RIVER LABORATORY
773-41A, 182
AIKEN SC 29808
USA

P. H. HUTTON
BATTELLE PACIFIC NORTHWEST LAB
P.O. BOX 999
RICHLAND WA 99352
USA

J. G. HWANG
ENSA, INC.
P.O. BOX 20130
SAN JOSE CA 95160
USA

M. L. HYDER
SAVANNAH RIVER LABORATORY
773-41A
AIKEN SC 29808
USA

T. IGUCHI
JAPAN ATOMIC ENERGY RES. INSTITUTE
TOKAI-MURA
IBARAKI 319-11
JAPAN

H. INHABER
NUS CORPORATION
910 CLOPPER ROAD
GAITHERSBURG MD 20878
USA

G. R. IRWIN
UNIVERSITY OF MD., DEPT. OF MECH. ENG.
COLLEGE PARK MD 20742
USA

T. ISHIDA
JAPAN INSTITUTE OF NUCLEAR SAFETY
MITA KOKUSAI BLDG.,1-4-28,MITA
MINATO-KU,TOKYO 108
JAPAN

M. ISHII
ARGONNE NATIONAL LABORATORY
9700 S. CASS AVENUE
ARGONNE IL 60439
USA

S. K. ISKANDER
OAK RIDGE NATIONAL LAB
P. O. BOX X
OAK RIDGE TN 37831
USA

K. ITOH
JAPAN NUS COMPANY
2864-3 NARACHO MIDORIKU
YOKOHAMA JAPAN
JAPAN

R. IVANY
COMBUSTION ENGINEERING
1000 PROSPECT HILL ROAD
WINDSOR CT 06095-500
USA

T. IWAMURA
JAPAN ATOMIC ENERGY RES. INSTITUTE
TOKAI-MURA
IBARAKI 319-11
JAPAN

J. L. JACOBSON
EG&G IDAHO, INC.
P.O. BOX 1625
IDAHO FALLS ID 83415
USA

P. JAMET
CEA FRENCH ATOMIC ENERGY COMMISSION
DEMT/SMTS/EMSI
GIF S/YVETTE 91191
FRANCE

J. F. JANSKY
BTB-LEONBERG
TONWEG-3
LEONBERG
FRG

D. B. JARRELL
BATTELLE PACIFIC NORTHWEST LAB
510 SIGMA 3 3160 G. W. WAY
RICHLAND WA 99352
USA

L. JARRIEL
INTERNATIONAL TECHNOLOGY INC.
575 OAK RIDGE TURNPIKE
OAK RIDGE TN 37830
USA

R. P. JENKS
LOS ALAMOS NATIONAL LAB
P.O. BOX 1663, MS K555
LOS ALAMOS NM 87545
USA

G. W. JOHNSEN
EG&G IDAHO, INC.
P.O. BOX 1625
IDAHO FALLS ID 83415
USA

E. R. JOHNSON
WESTINGHOUSE ELECTRIC CORP.
P. O. BOX 2728
PITTSBURGH PA 15230
USA

W. R. JOHNSON
U. OF VIRGINIA
NUCLEAR ENERGY DEPT-REACTOR BLDG
CHARLOTTESVILLE VA 22903
USA

A. B. JOHNSON
BATTELLE PACIFIC NORTHWEST LAB
P.O. BOX 999
RICHLAND WA 99352
USA

E. R. JOHNSON
WESTINGHOUSE
P O. 355
PITTSBURGH PA 15230
USA

R. JOO
CNSNS
INSURGENTES SUR 1776
MEXICO CITY D.F. 01030
MEXICO

J. A. JOYCE
U.S. NAVAL ACADEMY
MS 11C
ANNAPOLIS MD 21402
USA

S. P. KALRA
ELECTRIC POWER RESEARCH INSTITUTE
P.O. BOX 10412
PALO ALTO CA 94303
USA

F. B.K. KAM
OAK RIDGE NATIONAL LAB
P O. BOX X, 3001
OAK RIDGE TN 37831
USA

L. D. KANNBERG
BATTELLE PACIFIC NORTHWEST LAB
P.O. BOX 999
RICHLAND WA 99352
USA

M. F. KANNINEN
SOUTHWEST RESEARCH INSTITUTE
6220 CULEBRA RD.
SAN ANTONIO TX 78284
USA

H. KANTEE
IMATRON VOIMA OY (IVO)
P.O. BOX 138
HELSINKI SF00101
FINLAND

H. KARWAT
TECHNICAL UNIVERSITAT MUNCHEN
8046 GARSHING FORSCHUNGSGELANDE
GARCHING D8046
FRG

W. Y. KATO
BROOKHAVEN NATIONAL LABORATORY
BLDG. 197C
UPTON NY 11973
USA

K. R. KATSMA
EG&G IDAHO, INC.
P.O. BOX 1625
IDAHO FALLS ID 83415
USA

R. KAWABE
ENERGY RESEARCH LAB., HITACHI, LTD.
1168 MORIYAMA-CHO
HITACHI-SHI IBARAKI-KEN 316
JAPAN

W. KAWAKAMI
JAPAN ATOMIC ENERGY RES. INSTITUTE
1233 WATANUKI-MACHI
TAKASAKI,GUNMA KEN 370-12
JAPAN

J. M. KELLY
BATTELLE PACIFIC NORTHWEST LAB
P.O. BOX 999
RICHLAND WA 99352
USA

R. M. KEMPER
WESTINGHOUSE
4043 W. BENDEN DRIVE
MURRYSVILLE PA 15668
USA

M. F. KENNEDY
ENSA, INC.
4550 N. BAILEY
BUFFALO NY 14226
USA

R. C. KERN
UAI/CDC
6003 EXECUTIVE BLVD.
ROCKVILLE MD 20852
USA

J. G. KEUSENHOFF
GESELLSCHAFT FUR REAKTORSICHERHEIT
SCHWERTNERGASSE 1
COLOGNE 5000
FRG

S. KIM
KOREAN ATOMIC ENERGY RESEARCH INST.
DAEDUK-DANJI, P.O. BOX 7
CHOONG-NAM
KOREA

F. D. KING
SAVANNAH RIVER LABORATORY
773-41A, ROOM 252
AIKEN SC 29808

W. L. KIRK
LOS ALAMOS NATIONAL LAB
P.O. BOX 1663
LOS ALAMOS NM 87545
USA

M. KODA
MITSUBISHI ATOMIC POWER INDUSTRIES
SHIBAKOUEN
MINATO-KU,TOKYO 105
JAPAN

S. J. KOSKI
TVO POWER COMPANY LTD.
SF-27160 OLKILUOTO
SUOMI
FINLAND

C. A. KOT
ARGONNE NATIONAL LAB
9700 S. CASS AVE-BLDG 335
ARGONNE IL 60439
USA

J. J. KOZIOL
COMBUSTION ENGINEERING, INC.
1000 PROSPECT HILL ROAD
WINDSOR CT 06095-0500
USA

B. KUCZERA
KERNFORSCHUNGSZENTRUM (KfK)
P.O. BOX 3640
D-7500 KARLSRUHE 1
FRG

Y. KUKITA
JAPAN ATOMIC ENERGY RES. INSTITUTE
TOKAI-MURA
IBARAKI 319-11
JAPAN

Z. R. KULJIS
COMBUSTION ENGINEERING
1000 PROSPECT HILL ROAD
WINDSOR CT 06095
USA

D. KUPPERMAN
ARGONNE NATIONAL LABORATORY
9700 S. CASS AVENUE
ARGONNE IL 60302
USA

R. J. KURTZ
BATTELLE PACIFIC NORTHWEST LAB
P.O. BOX 999
RICHLAND WA 99352
USA

K. P. KUSSMAUL
UNIVERSITY OF STUTTGART
PFAFFENWALDRING 32
SUTTGART 80 7000
FRG

T. E. LAATS
EG&G IDAHO, INC.
P.O. BOX 1625
IDAHO FALLS ID 83415
USA

F. LAM
ONTARIO HYDRO
700 UNIVERSITY AVE., H-11
TORONTO M5G1X6
CANADA

R. T. LANCET
ROCKWELL INTERNATIONAL
6716 DARYN DR.
WESTHILLS CA 91307
USA

P. M. LANG
U.S. DEPARTMENT OF ENERGY
NE-42
WASHINGTON DC 20545
USA

R. E. LANG
DEPARTMENT OF ENERGY
9800 S. CASS AVE.
ARGONNE IL 60439
USA

B. P. LAUZAU
AMERICAN ELECTRIC POWER SERVICE CORP
1 RIVERSIDE PLAZA
COLUMBUS OH 43215
USA

S. Y. LEE
ARGONNE NATIONAL LABORATORY
9700 S. CASS AVENUE
ARGONNE IL 60439
USA

M. LEE
BROOKHAVEN NATIONAL LABORATORY
BUILDING 130
UPTON NY 11973
USA

J. R. LEHNER
BROOKHAVEN NATIONAL LABORATORY
BUILDING 130
UPTON NR 11973
USA

I. S. LEVY
BATTELLE PACIFIC NORTHWEST LAB
P.O. BOX 999
RICHLAND WA 99352
USA

C. K. LEWE
NUS CORPORATION
910 CLOPPER ROAD
GAITHERSBURG MD 20878
USA

K. J. LIESCH
GESELLSCHAFT FUR REAKTORSICHERHEIT
FORSCHUNGSGELAENDE
GARCHING 8046
FRG

T.-K. LIN
INSTITUTE OF NUCLEAR ENERGY RESEARCH
P.O. BOX 3
LUNG-TAN TAIWAN
ROC

C. W. LIN
ROBERT L. CLOUD ASSOCIATES
125 UNIVERSITY AVENUE
BERKLEY CA 94710
USA

F. W. LINCOLN
WESTINGHOUSE
W. MIFFLIN PA
USA

W. B. LOEWENSTEIN
ELECTRIC POWER RESEARCH INSTITUTE
3412 HILLVIEW AVE., P.O. BOX 10412
PALO ALTO CA 94303
USA

R. J. LOFARO
BROOKHAVEN NATIONAL LAB
BLDG 130
UPTON NY 11973
USA

J. V. LOPEZ
ETSII CATEDRA DE TECHNOLOGIA NUCLEAR
JOSE GUTIERREZ ABASCAL, 2
MADRID 28006
SPAIN

F. J. LOSS
MATERIALS ENGINEERING ASSOCIATES, INC.
9700-B MARTIN LUTHER KING HWY
LANHAM MD 20706
USA

A. L. LOWE
BABCOCK & WILCOX
P.O. BOX 10935
LYNCHBURG VA 24506
USA

R. J. LUTZ, JR.
WESTINGHOUSE ELECTRIC
P. O. BOX 355
PITTSBURGH PA 15230
USA

P. E. MacDONALD
EG&G IDAHO, INC.
P O. BOX 1625
IDAHO FALLS ID 83415
USA

I. K. MADNI
BROOKHAVEN NATIONAL LAB
BLDG 130
UPTON NY 11973
USA

J. MALHERBE
CEA FRENCH ATOMIC ENERGY COMMISSION
DEMT/SMTS/RDMS
GIF S/YVETTE 91191
FRANCE

A. P. MALINAUSKAS
OAK RIDGE NATIONAL LAB
P.O. BOX X, BLDG 4500S MS-135
OAK RIDGE TN 37831
USA

A. N. MALLEN
BROOKHAVEN NATIONAL LAB
BLDG 475B
UPTON NY 11973
USA

P. MARSILI
ENEA/DISP
VIA VITALIANO BRANGATI 48
ROME 00144
ITALY

J. MARTIN
MASS. INST. OF TECHNOLOGY
77 MASSACHUSETTS AVE, RM 24-210
CAMBRIDGE MA 02139
USA

A. MARVRAY
TEXAS UTILITIES ELECTRIC
400 NORTH OLIVE STREET, L. B. 81
DALLAS TX 75201
USA

F. MASUDA
TOSHIBA CORP.
9-3-104, 5-CHOME ISOGO
YOKOHAMA
JAPAN

M. J. MATSUBARA
CEN. RES. INST. OF ELEC. POWER INDUSTRY
11-1 IWATO-KITA, 2-CHOME
KOMAE TOKYO 157
JAPAN

B. MAVKO
J. STEFAN INSTITUTE
JAMOVA 39
LJUBLJANA 6111
YUGOSLAVIA

R. K. McCARDELL
EG&G IDAHO, INC.
P.O. BOX 1625
IDAHO FALLS ID 83415
USA

D. J. McCLOSKEY
SANDIA NATIONAL LABORATORY
P.O. BOX 5800
ALBUQUERQUE NM 87185
USA

G. E. McCREERY
EG&G IDAHO, INC.
P.O. BOX 1625
IDAHO FALLS ID 83415
USA

W. N. McELROY
BATTELLE PACIFIC NORTHWEST LAB.
P.O. BOX 999
RICHLAND WA 99352
USA

M. McGUIRK
BABCOCK & WILCOX
P.O. BOX 10935, 3315 OLD FOREST RD.
LYNCHBURG VA 24506-0935
USA

R. N. H. McMILLAN
UKAEA/SRD
WIGSHAW LANE, CULCHETH
WARRINGTON WA34NE
UK

D. M. MEARS
BABCOCK & WILCOX
P.O. BOX 10935, 3315 OLD FOREST RD.
LYNCHBURG VA 24506-0935
USA

C. MEDICH
VIA NINO BIXIO
PIACENZA
ITALY

J. A. MEINCKE
CONSUMER POWER CO.
1945 W. PARNALL RD.
JACKSON MI
USA

G. M. MELIN
CEA FRENCH ATOMIC ENERGY COMMISSION
SETH/LES - C.E.N.G - 85X
GRENOBLE CEDEX 38041
FRANCE

B. MERCER
UNIVERSITY OF MARYLAND
COLLEGE PARK MD 20742
USA

O. M. MERCIER
EIR-EIDG. INST. FUR REAKTORFORSCHUNG
WURENLINGEN CH5303
SWITZERLAND

Y. MEYZAUD
FRAMATOME
TOUR FIAT CEDEX 16
PARIS FR 92084
FRANCE

J. S. MILLER
GULF STATES UTILITIES CO.
P. O. BOX 220
ST. FRANCISVILLE LA 70775
USA

C. S. MILLER
EG&G IDAHO, INC.
P.O. BOX 1625
IDAHO FALLS ID 83415
USA

R. L. MILLER
WESTINGHOUSE HANFORD COMPANY
P.O. BOX 1970
RICHLAND WA 99352
USA

H. A. MITCHELL
INTERNATIONAL TECHNOLOGY CORP.
575 OAK RIDGE TURNPIKE
OAK RIDGE TN 37830
USA

S. M. MODRO
EG&G IDAHO, INC.
P.O. BOX 1625
IDAHO FALLS ID 83415
USA

C. L. MOHR
MOHR & ASSOCIATES
1440 AGNES
RICHLAND WA 99352
USA

R. O. MONTGOMERY
TEXAS A&M UNIVERSITY
NUCLEAR ENGINEERING DEPT.
COLLEGE STATE TX 77843
USA

B. S. MONTY
WESTINGHOUSE ELECTRIC
P.O. BOX 355
PITTSBURGH PA 15235
USA

J. MORIN
SAVANNAH RIVER LABORATORY
773-41A
AIKEN SC 29808
USA

G. A. MORTENSEN
EG&G IDAHO, INC.
P O. BOX 1625
IDAHO FALLS ID 83415
USA

F. E. MOTLEY
LOS ALAMOS NATIONAL LAB
P.O. BOX 1663
LOS ALAMOS NM 87545
USA

L. D. MUHLSTEIN
WESTINGHOUSE HANFORD COMPANY
P.O. BOX 1970
RICHLAND WA 99352
USA

Y. MURAO
JAPAN ATOMIC ENERGY RESEARCH INST.
TOKAI-MURA
IBARAKI 319-11
JAPAN

R. C. MURRAY
LAWRENCE LIVERMORE NATIONAL LAB
P. O. BOX 808,L-197
LIVERMORE CA 94550
USA

S. A. NAFF
KRAFTWERK UNION AG
HAMMERBACHERSTRASSE 12 + 14
ERLANGEN D-8520
FRG

R. K. NANSTAD
OAK RIDGE NATIONAL LAB
P.O. BOX X, BLDG 4500-S
OAK RIDGE TN 37831
USA

D. J. NAUS
OAK RIDGE NATIONAL LAB
P.O. BOX Y, BLDG. 9204-1
OAK RIDGE TN 37831
USA

H. H. NEELY
ROCKWELL INTERNATIONAL
6633 CANOGA AVENUE
CANOGA PARK CA 91304
USA

L. A. NEIMARK
ARGONNE NATIONAL LABORATORY
9700 S. CASS AVENUE
ARGONNE IL 60302
USA

L. Y. NEYMOTIN
BROOKHAVEN NATIONAL LAB
BLDG 475B
UPTON NY 11973
USA

S. J. NIEMCZYK
GULL ASSOCIATES
1545 18TH ST. NW #112
WASHINGTON DC 20036
USA

M. V. NIKITIN
SCUAE, INTERNATIONAL RELATIONS DEPT
STAROMONETNYI, 26
MOSCOW 109180
USSR

S. NISHINO
ELECTRIC POWER RESEARCH INSTITUTE
3412 HILLVIEW AVE, P.O. BOX 10412
PALO ALTO CA 94303
USA

C. K. NITHIANANDAN
BABCOCK & WILCOX
LYNCHBURG VA 24503
USA

K. K. NIYOGI
UNITED ENGINEERS & CONST. INC.
30 S. 17TH STREET
PHILADELPHIA PA 19101
USA

Y. NOGUCHI
CHUBU ELECTRIC POWER CO. INC
900 17TH ST. N.W., SUITE 714
WASHINGTON DC 20006
USA

P. NORTH
EG&G IDAHO, INC.
P. O. BOX 1625
IDAHO FALLS ID 83415
USA

J. G. O'BRIEN
UNIVERSITY OF MARYLAND
RT. 1
COLLEGE PARK MD 21093
USA

C. F. OBENCHAIN
EG&G IDAHO, INC.
P.O. BOX 1625
IDAHO FALLS ID 83415
USA

K. OKABE
MITSUBISHI ATOMIC POWER INDUSTRIES
4-1, SHIBAKOUEN 2-CHOME
MINATO-KU TOKYO
JAPAN

R. C. OLSON
BALTIMORE GAS & ELECTRIC
CALVERT CLIFFS - P.O. BOX 1535
LUSBY MD 20657
USA

H. P. OLSON
SAVANNAH RIVER LABORATORY
AIKEN SC 29808
USA

A. M. OMAR
ATOMIC ENERGY CONTROL BOARD
270 ALBERT STREET
OTTAWA KIPSS9
CANADA

A. OMOTO
TOKYO ELECTRIC POWER
POTOMAC
MD 8605 TIMBER HILL LANE 20854
USA

A. T. ONESTO
ETEC
P.O. BOX 1449
CANOGA PARK CA 91304
USA

D. J. OSETEK
EG&G IDAHO, INC.
P.O. BOX 1625
IDAHO FALLS ID 83415
USA

L. J. OTT
OAK RIDGE NATIONAL LAB
P.O. BOX Y, BLDG.9104-1
OAK RIDGE TN 37831
USA

J. PAN
UNIVERSITY OF MICHIGAN
2250 G. G. BROWN
ANN ARBOR MI 48109
USA

B. PANELLA
POLITECNICO DI TORINO
CORSO DUCA DEGLI ABRUZZI, 24
TORINO 10100
ITALY

M. V. PARECE
BABCOCK & WILCOX
P.O. BOX 10935, 3315 OLD FOREST RD
LYNCHBURG VA 24506-0935
USA

A. C. PAYNE, JR.
SANDIA NATIONAL LABORATORY
P.O. BOX 5800
ALBUQUERQUE MN 87185
USA

G. PETRANGELI
ENEA/DISP
VIA VITALIANO BRANCATI, 48
ROME 00144
ITALY

L. PETRUSHA
BABCOCK & WILCOX
P.O. BOX 10935, 3315 OLD FOREST ROD.
LYNCHBURG VA 24506-0935
USA

D. A. PETTI
EG&G IDAHO, INC.
P.O. BOX 1625
IDAHO FALLS ID 83415
USA

L. K. PIPLIES
COMMISSION OF EUROPEAN COMMUNITIES
I-21020
ISPRA I-21020 ISPRA
ITALY

M. P. PLESSINGER
EG&G IDAHO, INC.
P.O. BOX 1625
IDAHO FALLS ID 83415
USA

M. G. PLYS
FAUSKE & ASSOCIATES, INC
16W070 W. 83RD STREET
BURR RIDGE IL 60521
USA

M. Z. PODOWSKI
RENSSELAER POLYTECHNIC INST.
TROY NY 12180
USA

G. J. POSAKONY
BATTELLE PACIFIC NORTHWEST LAB.
P.O. BOX 999
RICHLAND WA 99352
USA

T. PRATT
BROOKHAVEN NATIONAL LABORATORY
BUILDING 130
UPTON NY 11973
USA

D. A. PRELEWICZ
ENSA, INC.
P.O. BOX 5537
ROCKVILLE MD 20855
USA

J. G. PRUETT
OAK RIDGE NATIONAL LAB
P.O. BOX X, BLDG 4500S MS-135
OAK RIDGE TN 37831
USA

C. E. PUGH
OAK RIDGE NATIONAL LAB
P.O. BOX Y
OAK RIDGE TN 37831
USA

W. R. QUEALY
HM NUCLEAR ISTALLATIONS INSPECTORATE
ST. PETERS HOUSE, BALLIOL ROAD
BOOTLE MERSEYSIDE L203LZ
UK

K. RAES
BATTELLE FRANKFURT
AM ROMERHOF 35
FRANKFORT
FRG

F. RAHN
ELECTRIC POWER RESEARCH INSTITUTE
3412 HILLVIEW AVE.
PALO ALTO CA 94303
USA

N. C. RASMUSSEN
MASS. INSTITUTE OF TECHNOLOGY
ROOM 24-205
CAMBRIDGE MA 02139
USA

M. REICH
BROOKHAVEN NATIONAL LAB
BLDG. 129
UPTON NY 11973
USA

H. RENNER
NUS CORPORATION
910 CLOPPER ROAD
GAITHERSBURG MD 20878
USA

L. N. RIB
LNR ASSOCIATES
8605 GRIMSBY COURT
POTOMAS MD 20854
USA

D. R. RILEY
ELECTRIC POWER RESEARCH INST.
501 FOREST AVE # 601
PALO ALTO CA 94301
USA

C. L. RITCHEY
BABCOCK & WILCOX
P.O. BOX 10935, 3315 OLD FOREST RD.
LYNCHBURG VA 24506-0935
USA

C. M. ROBERTS
UNIVERSITY OF MARYLAND
COLLEGE PARK MD 20742
USA

D. E. ROBERTSON
BATTELLE PACIFIC NORTHWEST LAB
P.O. BOX 999
RICHLAND WA 99352
USA

G. E. ROBINSON
PENN STATE UNIVERSITY
231 SACKETT BLDG
UNIVERSITY PARK PA 16902
USA

U. S. ROHATGI
BROOKHAVEN NATIONAL LAB
BLDG 475B
UPTON NY 11973
USA

J. V. ROTZ
BECHTEL
15740 SHADY GROVE RD.
AITHERSBURG MD 20877
USA

J. C. ROUSSEAU
CEA FRENCH ATOMIC ENERGY COMMISSION
CENTRE D'ETUDES NUCLEAIRES
GRENOBLE 38041
FRANCE

D. RUBIO
ELECTRIC POWER RESEARCH INSTITUTE
3412 HILLVIEW AVE.
PALO ALTO CA 94303
USA

K. D. RUSSEL
EG&G IDAHO, INC.
P.O. BOX 1625
IDAHO FALLS ID 83415
USA

B. SAFFELL
BATTELLE COLUMBUS DIVISION
505 KING AVENUE
COLUMBUS OH 43201
USA

H. SAKAMOTO
NUCLEAR POWER ENGINEERING TEST CENTER
3-13, 4-CHOME, TORANOMON
MINATO-KU, TOKYO 105
JAPAN

H. SAKURAGI
JAPAN INSTITUTE OF NUCLEAR SAFETY
MITA KOKUSAI BLDG., 1-4-28, MITA
MINATO-KU, TOKYO 108
JAPAN

J. SALUJA
VIKING SYSTEMS INTERNATIONAL
121 N. HIGHLAND AVE.
PITTSBURG PA 15206
USA

L. E. SALYARDS
BALTIMORE GAS & ELECTRIC
CALVERT CLIFFS - P.O. BOX 1535
LUSBY MD 20657
USA

M. SARRAM
UNITED ENGINEERS & CONST. INC.
30 S. 17TH ST., P.O. BOX 8223
PHILADELPHIA PA 19101
USA

I. SATO
JAPAN STEEL WORKS
4 CHATSU-MACHI
MURORAN HOKKAIDO
JAPAN

D. G. SATTERWHITE
EG&G IDAHO, INC.
P.O. BOX 1625
IDAHO FALLS ID 83415
USA

M. B. SATTISON
EG&G IDAHO, INC.
P.O. BOX 1625
IDAHO FALLS ID 83415
USA

J. C. SCARBOROUGH
JCS LIMITED
6936 RACE NORSE LANE
ROCKVILLE MD 20852
USA

P. J. SCHALLY
GESELLSCHAFT FUR REAKTORSICHERHEIT
SCHWERTNERGASSE 1
KOELN 5060
FRG

A. P. SCHMITT
CEA FRENCH ATOMIC ENERGY COMMISSION
CEN-FAR, IPSN
FONTENAY-AUX-ROSES CEDEX 92265
FRANCE

R. R. SCHULTZ
EG&G IDAHO, INC.
P.O. BOX 1625
IDAHO FALLS ID 83415
USA

C. W. SCHWARTZ
UNIVERSITY OF MD., DEPT. OF CIVIL ENG.
COLLEGE PARK MD 20742
USA

J. H. SCOBEL
WESTINGHOUSE
MEC E 3-21
PITTSBURGH PA 15230
USA

F. SEARS
NORTHEAST UTILITIES
P. O. BOX 270
HARTFORD CT 06141-0270
USA

S. S. SETH
THE MITRE CORPORATION
7525 COLSHIRE DRIVE, MAIL - W721
McLEAN VA 22102
USA

R. T. SEWELL
RISK ENGINEERING INC.
5255 PINE RIDGE ROAD
GOLDEN CO 80403
USA

W. J. SHACK
ARGONNE NATIONAL LABORATORY
BUILDING 212
ARGONNE IL 60302
USA

VIK SHAH
EG&G IDAHO, INC.
11428 ROCKVILLE PIKE, SUITE 410
ROCKVILLE MD 20852
USA

R. H. SHANNON
CONSULTANT
P.O.BOX 2264
ROCKVILLE MD 20852
USA

R. SHARMA
AMERICAN ELECTRIC POWER SERVICE CORP
1 RIVERSIDE PLAZA
COLUMBUS OH 43216
USA

R. A. SHAW
EG&G IDAHO, INC.
P.O. BOX 1625
IDAHO FALLS ID 83415
USA

J. M. SHEA
NORTHEAST UTILITIES
107 SELDEN ST., W-1S
BERLIN CT 06037
USA

L. SHEN
ATOMIC ENERGY COUNCIL,EXECUTIVE YUAN
67, LANE144, KEELUNG RD., SEC.4
TAIPEI TAIWAN 107
ROC

G. L. SHERWOOD, JR.
U.S. DEPARTMENT OF ENERGY
GERMANTOWN MD 20767
USA

P. SHEWMON
ADVISORY COMM. ON REACTOR SAFEGUARDS
2477 LYTHAM ROAD
COLUMBUS OH 43220
USA

D. J. SHIMECK
WESTINGHOUSE
RD2, BOX 194
EXPORT PA 15632
USA

M. SHIMIZU
JAPAN ATOMIC ENERGY RES. INSTITUTE
TOKAI-MURA IBARAKI-KEN 319-11
JAPAN

M. S. SHINKO
EMERGENCY RESPONSE TEAM
P.O. BOX 129
WASHINGTON GROVE MD 20880
USA

E. G. SILVER
OAK RIDGE NATIONAL LAB
P.O. BOX Y, BLDG.9201-3, MS 5
OAK RIDGE TN 37831
USA

F. A. SIMONEN
BATTELLE PACIFIC NORTHWEST LAB
P.O. BOX 999
RICHLAND WA 99352
USA

G. M. SLAUGHTER
OAK RIDGE NATIONAL LAB
P.O. BOX X, BLDG 4500-S
OAK RIDGE TN 37831
USA

M. K. SMITH
BABCOCK & WILCOX
P.O. BOX 10935, 3315 OLD FOREST RD.
LYNCHBURG VA 24506-0935
USA

A. W. SNYDER
SANDIA NATIONAL LABORATORY
P O BOX 5800, DIVISION 6500
ALBUQUERQUE NM 87185
USA

K. SODA
JAPAN ATOMIC ENERGY RES. INSTITUTE
TOKAI-MURA IBARAKI-KEN 319-11
JAPAN

H. G. SONNENBURG
GESELLSCHAFT FUR REAKTORSICHERHEIT
FORSCHUNGSGELAENDE
GARCHING 8046
FRG

P. SOO
BROOKHAVEN NATIONAL LAB
BLDG 830
UPTON NY 11973
USA

J. L. SPRUNG
SANDIA NATIONAL LABORATORY
P.O. BOX 5800
ALBUQUERQUE NM 87185
USA

D. SQUARER
WESTINGHOUSE R&D
1310 BEULAH RD.
PITTSBURGH PA 15235
USA

M. G. SRINIVASAN
ARGONNE NATIONAL LAB
9700 S. CASS AVE-BLDG 335
ARGONNE IL 60439
USA

K. E. ST. JOHN
YANKEE ATOMIC ELECTRIC COMPANY
1671 WORCESTER RD.
FRAMINGHAM MA 01701
USA

H. STADTKE
COMMISSION OF EUROPEAN COMMUNITIES
121020, ISPRA
ISPRA
ITALY

R. STEELE
EG&G IDAHO, INC.
P.O. BOX 1625
IDAHO FALLS ID 83415
USA

J. P. STEELMAN
BALTIMORE GAS & ELECTRIC
LUSBY POST OFFICE
LUSBY MD 20657
USA

N. PONOMAREV- STEPNOI
I. V. KURCHATOV INST. OF ATOMIC ENERGY
KURCHATOV SQUARE
MOSCOW 123182
USSR

P. M. STOOP
NETHERLANDS ENERGY RES FOUNDATION ECN
3 WESTERDUINWEG, P.O. BOX 1
PETTEN (NH) 1755 ZG
NETHERLANDS

E. STUBBE
TRACTEBEL
31 RUE DE LA SCIENCE
BRUSSELS 1040
BELGIUM

M. SUBUDHI
BROOKHAVEN NATIONAL LAB
BLDG 130
UPTON NY 11973
USA

W. SUGNET
ELECTRIC POWER RESEARCH INSTITUTE
3412 HILLVIEW AVE.
PALO ALTO CA 94303
USA

R. M. SUMMERS
SANDIA NATIONAL LABORATORY
P.O. BOX 5800, DIVISION 6418
ALBUQUERQUE NM 87185
USA

B. SUN
ELECTRIC POWER RESEARCH INSTITUTE
3412 HILLVIEW AVE.
PALO ALTO CA 94303
USA

R. K. SUNDARAM
YANKEE ATOMIC ELECTRIC COMPANY
1671 WORCESTER ROAD
FRAMINGHAM MA 01519
USA

D. G. SWANSON
PDI TECHNOLOGY
246 VIKING AVE.
BREA CA 92621
USA

H. TAKAHASHI
MITSUBISHI ATOMIC POWER INDUSTRIES
4-1, SHIBAKOUEN 2-CHOME
MINATO-KU TOKYO
JAPAN

Y. K. TANG
ELECTRIC POWER RESEARCH INSTITUTE
3412 HILLVIEW AVE.
PALO ALTO CA 94303
USA

H. T. TANG
ELECTRIC POWER RESEARCH INST.
3412 HILLVIEW AVE.
PALO ALTO CA 94303
USA

K. TASAKA
JAPAN ATOMIC ENERGY RES. INSTITUTE
TOKAI-MURA IBARAKI-KEN 319-11
JAPAN

J. H. TAYLOR
BROOKHAVEN NATIONAL LAB
BLDG 130
UPTON NY 11973
USA

T. A. THEOFANOUS
UNIV. OF CALIF., SANTA BARBARA
817 SEA RANCH DRIVE
SANTA BARBARA CA 93109
USA

E. W. THOMAS
BECHTEL EASTERN POWER
SHADY GOVE ROAD
GAITHERSBURG MD
USA

B. J. TOLLEY
COMMISSION OF THE EUROPEAN COMM
200, RUE DE LA LOI
BRUSSELS 1049
BELGIUM

B. TOLMAN
EG&G IDAHO, INC.
2355 TASMAN
IDAHO FALLS ID 83401
USA

K. TOMOMURA
CENTURY RESEARCH CENTER CORPORATION
3-6-2 NIHONBASHI- HONCHO 3-CHOME
CHUO-KU, TOKYO 103
JAPAN

L. S. TONG
TAI
9733 LOOKOUT PLACE
GAITHERSBURG MD 20879
USA

F. TOTSUKA
ENERGY RESEARCH LAB., HITACHI, LTD.
1-29-4 HANAYAMA-CHO
HITACHI-SHI IBARAKI-KEN 316
JAPAN

T. M. TRAN
TENNESEE VALLEY AUTHORITY
400 SUMMIT HILL
KNOXVILLE TN 37902
USA

J. R. TRAVIS
LOS ALAMOS NATIONAL LAB.
GROUP T-3, M/S B216
LOS ALAMOS NM 87545
USA

D. E. TRUE
ERIN ENGINEERING
1850 MT. DIABLO BLVD., SUITE 600
WALNUT CREEK CA 94596
USA

A. A. TUDOR
SAVANNAH RIVER LABORATORY
773-41A
AIKEN SC 29808
USA

N. K. TUTU
BROOKHAVEN NATIONAL LABORATORY
BUILDING 820M
UPTON NY 11973
USA

T. UESHIMA
ELECTRIC POWER RESEARCH INSTITUTE
3412 HILLVIEW AVE., P.O. BOX 10412
PALO ALTO CA 94303
USA

T. UMEMOTO
ISHIKAWAJIMA-HARIMA HEAVY INDUSTRIES
1-SHIN-NAKARA,ISOGO-KU
YOKAHAMA 235
JAPAN

K. D. UNDERWOOD
UNIVERSITY OF MARYLAND
COLLEGE PARK MD 20742
USA

S. UNWIN
BROOKHAVEN NATIONAL LABORATORY
BLDG. 130
UPTON NY 11973
USA

R. A. VALENTIN
ARGONNE NATIONAL LAB
9700 S. CASS AVE-BLDG 208
ARGONNE IL 60439
USA

R. M. VAN KUIJK
N. V. KEMA
POSTBUS 9035, UTRECHTSEWEG 310
6800 ET ARNHEM
NETHERLANDS

N. VASUDEVAN
BABCOCK & WILCOX
P.O. BOX 10935, 3315 OLD FOREST ROAD
LYNCHBURG VA 24506-0935
USA

C. M. VERTES
WESTINGHOUSE
NORTHERN PIKE RD.
MONROEVILLE PA 15146
USA

G. VESCOVI
SIET
NINO BIXIO 27
PIACENZA
ITALY

W. E. VESELY
SAIC
SUITE 245, 2929 KENNY ROAD
COLUMBUS OH 43221
USA

J. L. VON HERRMANN
IT-DELIAN
2011 EYE STREET
WASHINGTON DC 20006
USA

W. A. VON RIESEMANN
SANDIA NATIONAL LABORATORY
P.O. BOX 5800, DIVISION 6442
ALBUQUERQUE NM 87185
USA

M. WALTER
UNIVERSITY OF MARYLAND
663 W. FAYETTE STREET
BALTIMORE MD 21201
USA

S. F. WANG
INSTITUTE OF NUCLEAR ENERGY RESEARCH
P.O. BOX 3-13
LUNG-TAN TAIWAN 32500
ROC

M. E. WATERMAN
EG&G IDAHO, INC.
11428 ROCKVILLE PIKE, #410
ROCKVILLE MD 20852
USA

W. L. WEAVER
EG&G IDAHO, INC.
P.O. BOX 1625
IDAHO FALLS ID 83415
USA

E. T. WEBER
WESTINGHOUSE HANFORD COMPANY
P.O. BOX 1970
RICHLAND WA 99352
USA

J. R. WEEKS
BROOKHAVEN NATIONAL LAB
BLDG 130
UPTON NY 11973
USA

P. A. WEISS
SIEMENS-KWU
HAMMERBACHERSTRASSE 12 + 14
ERLANGEN D-8520
FRG

A. J. WEISS
BROOKHAVEN NATIONAL LAB
BLDG 197C
UPTON NY 11973
USA

E. WENZINGER
MPR ASSOCIATES, INC.
1050 CONNECTICUT AVE N.W.
WASHINGTON DC 20036
USA

E. T. WESSEL
EDWARD T. WESSEL, CONSULTING ENG.
316 WOLVERINE STREET
HAINES CITY FL 33844
USA

R. A. WESTON
COMBUSTION ENGINEERING
1000 PROSPECT HILL RD.
WINDSOR CT 06095
USA

H. WESTPHAL
GESELLSCHAFT FUR REAKTORSICHERHEIT
SCHWERTNERGASSE 1
COLOGNE 5000
FRG

D. L. WHITCOMB
WASHINGTON PUBLIC POWER SUPPLY SYS.
3000 G. WASH. WAY-P O. BOX 968
RICHLAND WA 99352
USA

T. J. WHITEHEAD
SAIC
101 S. PARK AVE.
IDAHO FALLS ID 83402
USA

P. G. WHITKOP
SAVANNAH RIVER LABORATORY
773-41A
AIKEN SC 29808
USA

G. M. WILKOWSKI
BATTELLE-COLUMBUS DIVISION
505 KING AVENUE
COLUMBUS OH 43201
USA

K. A. WILLIAMS
SAIC
2109 AIR PARK RD. SE
ALBUQUERQUE NM 87106
USA

K. WINEGARDNER
BATTELLE PACIFIC NORTHWEST LAB
P.O. BOX 999
RICHLAND WA 99352
USA

F. WINKLER
KRAFTWERK UNION AG
HAMMERBACHERSTRASSE 12 + 14
ERLANGEN D-8520
FRG

L. WOLF
PROJECT HDR/KERNFORSCHUNGSZENTRUM
POSTFACH 3640
7500 KARLSRUHE 1
FRG

K. WOLFERT
GESELLSCHAFT FUR REAKTORSICHERHEIT
FORSCHUNGSGELAENDE
GARCHING 8046
FRG

Y. C. WONG
CEGB, GENERATION DEV. & CONST. DIV.
BARNETT WAY
BARNWOOD GLOUCESTER GL4 7RS
UK

G. WONG
GENERAL PUBLIC UTILITIES
1 UPPER POND ROAD
PARSIPPANY NJ 07054
USA

L. R. WOOD
GENERAL ELECTRIC COMPANY
P.O. BOX 1072, BUILDING P-1, ROOM 111
SCHENECTADY NY 12301
USA

W. WULFF
BROOKHAVEN NATIONAL LAB
BLDG 475B
UPTON NY 11973
USA

G. YAGAWA
UNIVERSITY OF TOKYO
HONGO, BUNKYOKU
TOKYO 113
JAPAN

K. K. YOON
BABCOCK & WILCOX
P.O. BOX 10935, 3315 OLD FOREST ROAD
LYNCHBURG VA 24506-0935
USA

E. YOSHIKOWA
NUCLEAR POWER ENGINEERING TEST CENTEI
NO. 2 AKIYAMA BLDG., 6-2, 3-CHOME, MIN
TOKYO 105
JAPAN

R. YOUNG
UKAEA\SRD
WIGSHAW LANE
CULCHETH WARRINGTON WA3 4NE
UK

J. ZDAREK
CZECHOSLOVAK EMBASSY
3900 LINNEAN AVE. N.W.
WASHINGTON DC 20008
CZECHESLOVAKIA

K. ZIEGLOWSKI
KWU-OFFENBACH
6050 OFFENBACH BERLINER STR.
FRG

R. ZIPPER
GESELLSCHAFT FUR REAKTORSICHERHEIT
SCHWERTNERGASSE 1
COLOGNE
FRG

R. ZOGRAN
MPR ASSOCIATES, INC.
1050 CONNECTICUT AVE N.W.
WASHINGTON DC 20036
USA

PROCEEDINGS OF THE
FIFTEENTH WATER REACTOR SAFETY INFORMATION MEETING

October 26-29, 1987

TABLE OF CONTENTS - VOLUME 6

TMI-2

Chairperson: R. B. Foulds (NRC)

EFFECTIVENESS AND SAFETY ASPECTS OF SELECTED DECONTAMINATION METHODS FOR LWRs "THE RECONTAMINATION EXPERIENCE"

S. W. Duce
Idaho National Engineering Laboratory, EG&G Idaho Inc.*

During the years 1983 to 1986 chemical decontaminations of primary recirculation system piping was performed at many boiling water reactors in the United States. At most facilities the recirculation piping was replaced following the chemical decontamination. At a few facilities the piping was inspected for cracks and weld overlays were applied to any identified cracks. This paper presents information on the recontamination of these recirculation systems following one to two fuel cycles.

INTRODUCTION

During the years 1983 to 1986 many utilities operating BWRs (boiling water reactors) in the United States performed chemical decontaminations of primary coolant recirculation system (PCRS) piping. These chemical decontaminations were performed as part of an ALARA (As Low As Reasonably Achievable) dose savings program for personnel working on the PCRS piping. There were two main thrusts for PCRS piping work: in-service inspection with weld overlays on discovered cracks, or complete PCRS replacement. Interest within the NRC in the effectiveness of these chemical decontamination processes resulted in the funding of a program "Effectiveness and Safety Aspects of Selected Decontamination Processes" which was instituted in the fall of 1983 by EG&G Idaho at the Idaho National Engineering Laboratory (INEL). The purpose of this program was to obtain information on both chemical decontamination processes and recontamination of decontaminated systems in light water reactors. During the years 1984 to 1986 observations of the various chemical decontamination processes, as they were applied at BWRs, and measurements to determine the effectiveness of the processes were made. A final report, "Effectiveness and Safety Aspects of Selected Decontamination Process", NUREG/CR-4445,[1] was written and published in August 1986 which described the results of the program.

The recontamination determination aspect of the program started during the summer of 1985, where measurements to determine the recontamination of PCRS piping began, and continued through to the summer of 1987. Initial measurements were made on BWR recirculation piping that had been chemically decontaminated for the purpose of inspection and/or weld overlay. Later measurements were on PCRS piping that had either been replaced with new piping or had operated for a second fuel cycle past a chemical decontamination. Measurements made consisted of dose rate determinations using either TLDs (thermoluminescent dosimeters) or an Eberline E530-N with a "peanut" GM detector, and gamma spectral measurements to determine the internal PCRS piping surface concentration of radionuclides in the oxide film.

*Work supported by the U. S. Nuclear Regulatory Commission, Office of Nuclear Regulatory Research, under DOE Contract No. DE-AC07-76ID0570.

METHODS

During the course of the recontamination study seven BWRs were visited: Quad Cities Nuclear Power Station Units 1 and 2, Pilgrim Nuclear Power Station, Millstone Nuclear Power Station Unit 1, Peach Bottom Atomic Power Station Unit 2, Hatch Generating Station Unit 2, and Limerick Atomic Power Station Unit 1. In addition to the seven facilities visited, information for Cooper Nuclear Station and Monticello Nuclear Generating Plant were obtained from Radiological and Chemical Technology Inc. (RCT).[1,2] These facilities represent two different models and two different types of containment. All of the facilities, with the exception of Cooper, Hatch Unit 2, Peach Bottom Unit 2, and Limerick Unit 1, are BWR Model 3s with a Mark I containment. Cooper, Hatch and Peach Bottom are BWR 4s with Mark 1 containments, and Limerick is a BWR 4 with a Mark II containment.

At each facility information on power history, reactor chemistry, and reactor coolant activation product concentrations were obtained. Information on soluble zinc was also requested but not frequently obtained. Pre-chemical decontamination dose rates on the PCRS piping were obtained if the information was not available from the previous efforts of the Effectiveness and Safety Aspects of Chemical Decontamination Methods program.

Measurements of dose rate and gamma spectral emissions were made at similar locations at all facilities to allow for comparison of the measurement data. At each facility dose rate measurements were made on the PCRS piping using TLDs and/or an Eberline E530-N GM. Dose rate measurements were made on the risers, suction and discharge piping, and on the inlet and outlet pipe elbows for the recirculation pumps. When TLDs were used to determine the dose rates a "cheerio" TLD, which contained two TLD chips, was placed in a plastic bag. The bag was taped to a location and left for a period of two to three hours before being removed. All TLDs were then returned to the INEL for analysis. In all cases "trip" TLDs were used to subtract dose that resulted from air shipment and the transit time within the drywell. The Eberline E530-N used a "peanut" GM tube (i.e., an approximately 1/4" long GM tube), which was shielded in a two pi geometry by a tungsten hemisphere.

Gamma spectral measurements were made on the vertical run of the four suction and discharge pipes using an Ortec CPD-1 germanium detector to acquire the spectra at each location. The detector was placed in a collimated tungsten shield which was attached to a pipe. The shield and collimator reduced the gamma spectral interference of other sources in the drywell while maximizing the gamma fluence from the measured pipe. A 200-foot signal, preamplifier, and high voltage cable connected the detector to a Davidson Multichannel Analyzer which acquired the spectral data in 4096 channels and stored the results on cassette tapes. Two spectra were acquired at each location, a collimated spectrum and a background spectrum. The background spectrum was used to adjust the collimated spectrum for unattenuated gamma rays from other drywell sources. Spectral tapes were returned to the INEL for analysis of peak energy and radionuclide identification by a VAX 11/750 computer using a sophisticated gamma-ray analysis package termed GAP which uses nonlinear least squares fitting of a gaussion function to define peaks.

RESULTS AND DISCUSSION

The following discussion presents and summarizes the results of the recontamination measurements of PCRS piping that was either chemically decontaminated or replaced at BWRs. In this discussion and throughout the rest of this report the words new and old pipe are used to indicate pipe that were either replaced or chemically decontaminated, respectively, during a previous refueling outage.

Dose rate measurement results tended to vary between the TLD and E530-N GM. In those cases where disagreement was noted, the TLD results were normally used as these results represented a time weighted average over several hours. In most cases the disagreement occurred when the dose rates were <100 mR/h. At the low dose rates meter variation of the E530-N increased significantly, wavering $\pm$10 to $\pm$15 mR/h about a central value, making it difficult to obtain an accurate reading. Table 1 lists calculated average values for the measured dose rates from various components. The listed values have been supplemented with measurement data from facility personnel, from vendor reports,[2,3] and from General Electric.[4] Data for Quad Cities Units 1 and 2 appear several times in Table 1. The reason for this is that both units underwent successive decontaminations, making the post-decontamination measurements for the prior decontamination the pre-decontamination measurements (after a number of fuel cycles) for the latter decontamination. In all cases, with the exception of Millstone Unit 1 risers, the average one to two year recontamination values were at least a factor of two lower than the pre-decontamination average values.

Average component dose rate data from Table 1 were used to calculate recontamination factors (shown in Table 2) for each component and for the total system. A recontamination factor is defined as the ratio of a measurement performed one to two years after a decontamination to the corresponding measurement performed prior to a decontamination. Overall recontamination factors average 0.49, 0.47, and 0.43 for risers, suction/discharge, and elbows, respectively, but vary from 0.16 to 1.2 for the risers, from 0.15 to 0.78 for the suction/discharge pipe, and 0.15 to 0.58 for the pump elbows. For new pipe the averages are 0.29, 0.29, and 0.20 for risers, suction/discharge, and elbows, respectively; while for old pipe that was decontaminated, the averages are 0.70, 0.65, and 0.55, respectively for the same locations.

Total system recontamination factors for the two BWR models studied are plotted in Figure 1. With the exception of Pilgrim, there appears to be a definite trend in the recontamination rates of the PCRS piping where the older facilities (i.e., BWR 3s), as measured by dose rate, are higher than the recontamination rates for the newer facilities. This observation concurs with the findings of an Electric Power Research Institute (EPRI) program on BWR radiation assessment,[5] where it was found that the older model BWRs had higher dose rates than the newer facilities. However, the EPRI researchers could not find any correlation to facility parameters that could explain the difference. A second but less pronounced trend in Figure 1 indicates the recontamination factor for old pipe is higher than that for new pipe. The first four data points in

TABLE 1. AVERAGE COMPONENT DOSE RATE DATA (mR/h)

AVERAGE PRE-DECONTAMINATION VALUES

LOCATION:	PILGRIM	MILLSTONE-1	MONTICELLO	PEACH BOTTOM-2	COOPER
RISERS	800	383	638	825	730
SUCT/DISCH	400	210	463	391	444
ELBOWS	306	120	ND	614	688

LOCATION:	QUAD CITY-1	QUAD CITY-1	QUAD CITY-2	QUAD CITY-2
RISERS	1230	714	1394	785
SUCT/DISCH	483	230	433	283
ELBOWS	427	248	690	320

AVERAGE ONE TO TWO YEAR RECONTAMINATION VALUES

LOCATION:	PILGRIM	MILLSTONE-1	MONTICELLO	PEACH BOTTOM-2	COOPER
RISERS	125	447	383	198	138
SUCT/DISCH	121	164	199	101	69
ELBOWS	77	67	ND	93	ND

LOCATION:	QUAD CITY-1	QUAD CITY-2	QUAD CITY-2	HATCH	LIMERICK-1
RISERS	714	785	683	94	133
SUCT/DISCH	230	283	303	44	55
ELBOWS	248	320	400	168	216

LOCATION:	SUSQUEHANNA-2
RISERS	156
SUCT/DISCH	101
ELBOWS	ND

ND = No Data.

Table 2. RECONTAMINATION FACTORS BASED ON DOSE RATES

COMPONENT:	PILGRIM	MILLSTONE-1	MONTICELLO	PEACH BOTTOM-2
RISERS	0.156	1.17	0.600	0.210
SUCT/DISCH	0.302	0.781	0.430	0.279
ELBOWS	0.252	0.558	ND	0.151

COMPONENT:	COOPER	QUAD CITY-1	QUAD CITY-2	QUAD CITY-2
RISERS	0.189	0.580	0.563	0.490
SUCT/DISCH	0.155	0.476	0.654	0.700
ELBOWS	ND	0.581	0.464	0.580

COMPONENT AVERAGES:	ALL PLANTS	NEW PIPE PLANTS	OLD PIPE PLANTS
RISERS	0.495	0.289	0.700
SUCT/DISCH	0.472	0.291	0.653
ELBOWS	0.431	0.201	0.546

ND = No Data.

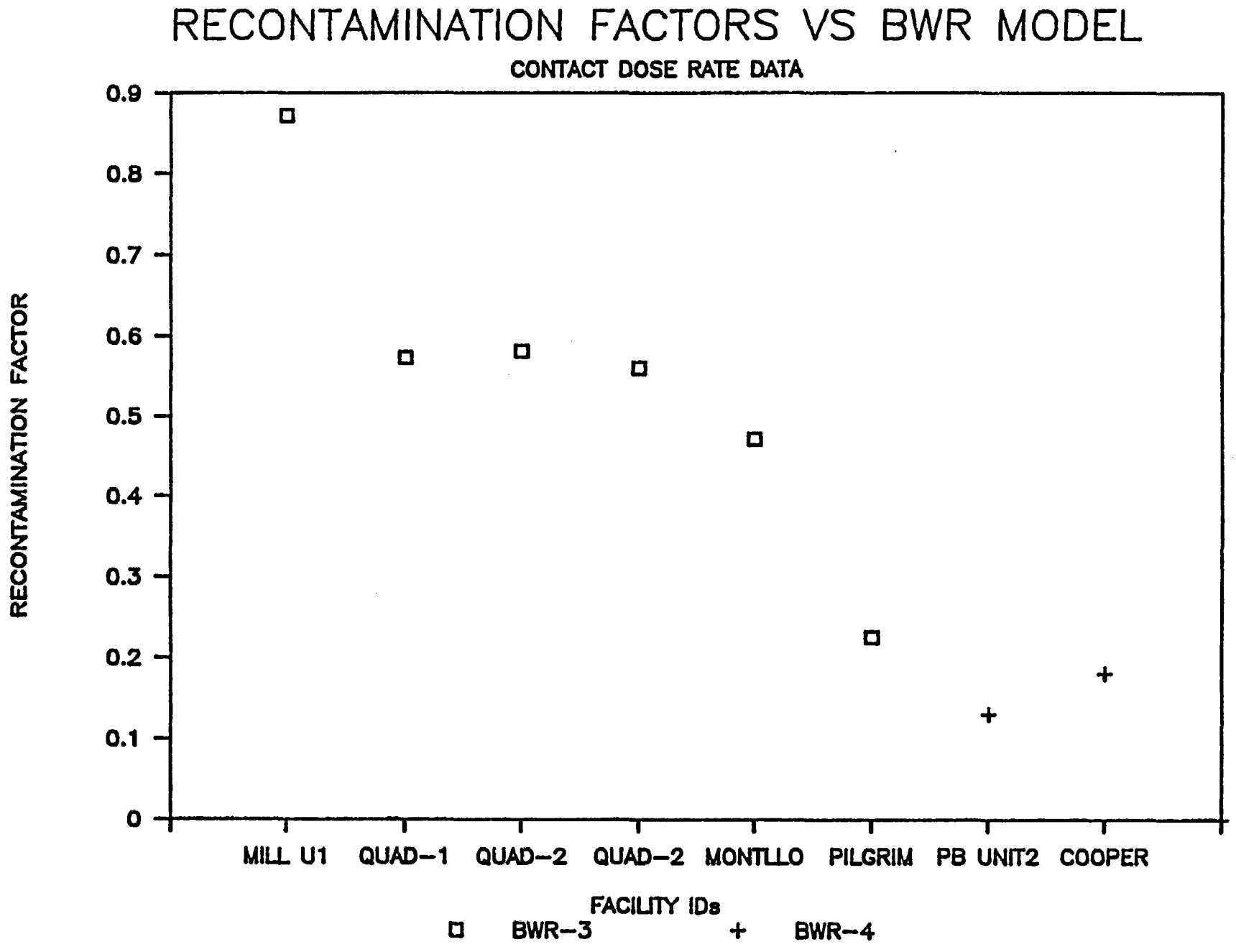
RECONTAMINATION FACTORS VS BWR MODEL
CONTACT DOSE RATE DATA
RECONTAMINATION FACTOR
0.9
0.8
0.7
0.6
0.5
0.4
0.3
0.2
0.1
0
MILL U1
QUAD-1
QUAD-2
QUAD-2
MONTLLO
PILGRIM
PB UNIT2
COOPER
FACILITY IDs
BWR-3
BWR-4

FIGURE 1

Figure 1 (which are for old pipe) are higher than the fifth through eighth data points (which are for new pipe). This trend for higher recontamination factors in decontaminated systems can also be seen in the data in Table 2, where recontamination factors for old pipe are shown to be slightly more than twice the corresponding values for new pipe.

An effort was made to find correlations between dose rate data and physical plant parameters that were acquired during the study. Both effective full power hours (EFPHs) and reactor coolant Co-60 concentrations were tested for correlations. The only correlation that was observed was one in which the dose rates on the elbows decreased with EFPHs. The reduced dose rates of the elbows may be a function of abrasion of the oxide film on the outer pipe walls due to the flow of water as it makes the 90° bends before and after the recirculation pump. Other than this correlation neither of these two parameters resulted in any further positive correlations to the dose rates.

Gamma spectral data acquired pre-decontamination, post-decontamination, or following the first or second fuel cycle(s) either by EG&G Idaho or by RCT[2,3] are listed in Table 3. Error values listed are for counting statistics only; total measurement error is estimated to be less than 30%. With the exception of Limerick, Co-60 accounted for $\geq$85% of the activity in the oxide films at all facilities, which was expected. The low Co-60 film concentrations at Limerick are approximately equal to the Co-58 concentrations which is also expected as this is the first fuel cycle for Limerick. As time goes on, the longer half-life Co-60 will dominate all other radionuclides as reactor coolant and surface film activities reach equilibrium while the shorter half-life Co-58 will remain approximately the same as it already reached equilibrium in the coolant and on pipe surfaces.

Recontamination factors for each radionuclide were calculated for those plants where pre- and post-decontamination spectral information were available. These recontamination factors (listed in Table 4) were calculated by dividing the surface film concentrations measured after the first or second fuel cycle following pipe decontamination or pipe replacement by the concentrations obtained prior to decontamination. For Quad Cities Unit 1 and Millstone Unit 1, where pre-decontamination results were not available, the pre-decontamination surface film values were estimated by multiplying the post-decontamination surface concentrations by the average decontamination factor for the suction/discharge piping for each facility respectively.

The results indicate that, in general, the old pipe systems tended to have higher recontamination factors than the new pipe systems. For example, for Co-60, the average recontamination factor was approximately 1.5 times higher for the decontaminated PCRS pipe than is was for replaced pipe. It is interesting to note that the average Co-58 surface activities after the first or second fuel cycle following a decontamination or pipe replacement were nearly a factor of three higher than the pre-decontamination activities. In addition, the recontamination rates for Mn-54 were much higher at Millstone Unit 1 and Cooper (where they

TABLE 3. MEASURED RADIONUCLIDE SURFACE FILM CONCENTRATIONS IN PCRS PIPING (uCi/cm^2)

QUAD CITIES UNIT 1	DATE: 8-15-84		STATUS: Post-decontamination	
NUCLIDE	A SUCTION	A DISCHARGE	B SUCTION	B DISCHARGE
Co-60	2.4± 0.1	0.96 ± 0.08	1.2 ± 0.1	1.6 ± 0.1
mR/h	29	31	16	73

QUAD CITIES UNIT 1	DATE: 1-15-86		STATUS: 1st Fuel Cycle	
NUCLIDE	A SUCTION	A DISCHARGE	B SUCTION	B DISCHARGE
Co-58	1.08 ± 0.02	1.10 ± 0.06	0.82 ± 0.05	1.04 ± 0.06
Mn-54	0.94 ± 0.06	0.84 ± 0.06	0.62 ± 0.05	0.84 ± 0.05
Zn-65	0.49 ± 0.06	0.47 ± 0.06	ND	1.5 ± 0.2
Co-60	10.2 ± 0.1	7.1 ± 0.1	6.84 ± 0.08	8.0 ± 0.1
mR/h	276	281	EV	287

QUAD CITIES UNIT 2	DATE: 4-13-85		STATUS: 1st Fuel Cycle	
NUCLIDE	A SUCTION	A DISCHARGE	B SUCTION	B DISCHARGE
Co-58	1.7 ± 0.1	1.4 ± 0.1	NM	1.4 ± 0.1
Mn-54	1.6 ± 0.1	1.7 ± 0.1	NM	1.1 ± 0.1
Zn-65	1.0 ± 0.1	0.9 ± 0.1	NM	1.0 ± 0.1
Fe-59	0.38 ± 0.06	0.44 ± 0.06	NM	ND
Co-60	20.7 ± 0.1	17.9 ± 0.1	NM	18.1 ± 0.1
mR/h	347	333	475	354

MILLSTONE UNIT 1	DATE: 6-15-84		STATUS: Post decontamination	
NUCLIDE	A SUCTION	A DISCHARGE	B SUCTION	B DISCHARGE
Co-58	0.03 ± 0.01	0.02 ± 0.01	0.04 ± 0.01	0.04 ± 0.01
Mn-54	0.03 ± 0.01	0.05 ± 0.01	0.02 ± 0.01	0.03 ± 0.01
Co=60	0.8 ± 0.01	0.65 ± 0.07	0.94 ± 0.01	0.78 ± 0.01
mR/h	12	20	20	14

MILLSTONE UNIT 1	DATE: 10-30-85		STATUS: 1st Fuel Cycle	
NUCLIDE	A SUCTION	A DISCHARGE	B SUCTION	B DISCHARGE
Co-58	1.8 ± 0.1	1.9 ± 0.1	1.9 ± 0.1	2.1 ± 0.1
Mn-54	4.1 ± 0.1	4.5 ± 0.1	4.1 ± 0.1	4.0 ± 0.1
Fe-59	0.43 ± 0.05	0.51 ± 0.05	0.40 ± 0.05	0.52 ± 0.05
Co-60	7.0 ± 0.1	8.6 ± 0.1	7.5 ± 0.1	9.1 ± 0.1
mR/h	167	166	142	182

PILGRIM	DATE: 1-8-87		STATUS: 1st Fuel Cycle	
NUCLIDE	A SUCTION	A DISCHARGE	B SUCTION	B DISCHARGE
Co-58	0.05 ± 0.02	0.05 ± 0.01	0.06 ± 0.01	0.05 ± 0.01
Mn-54	0.63 ± 0.04	0.49 ± 0.01	0.62 ± 0.01	0.51 ± 0.01
Zn-65	0.05 ± 0.03	0.06 ± 0.01	0.06 ± 0.01	0.04 ± 0.01
Co-60	2.95 ± 0.08	3.10 ± 0.05	4.0 ± 0.1	3.20 ± 0.06
mR/h	149	89	155	92

TABLE 3. MEASURED RADIONUCLIDE SURFACE FILM CONCENTRATIONS IN PCRS PIPING (uCi/cm^2) (Contd)

HATCH UNIT 2 DATE: 11-7-86 STATUS: 2nd Fuel Cycle

NUCLIDE	A SUCTION	A DISCHARGE	B SUCTION	B DISCHARGE
Nb-95	0.06 ± 0.01	NM	NM	0.06 ± 0.01
Co-58	0.27 ± 0.01	NM	NM	0.18 ± 0.01
Mn-54	1.13 ± 0.01	NM	NM	0.77 ± 0.01
Zn-65	1.34 ± 0.02	NM	NM	1.11 ± 0.03
Fe-59	0.16 ± 0.01	NM	NM	0.13 ± 0.02
Co=60	2.64 ± 0.06	NM	NM	2.22 ± 0.08
mR/h	43	50	55	38

COOPER* DATE: 11-84 STATUS: Pre-decontamination

NUCLIDE	A SUCTION	A DISCHARGE	B SUCTION	B DISCHARGE
Co-58	0.87	0.92	0.56	0.74
Mn-54	0.17	0.17	0.14	0.16
Co-60	6.17	5.91	7.07	5.16
mR/h	450	425	500	400

COOPER DATE: 11-84 STATUS: Post-decontamination

NUCLIDE	A SUCTION*	A DISCHARGE	B SUCTION	B DISCHARGE
Co-58	0.12	0.03 ± 0.01	0.02 ± 0.01	0.4+ ± 0.01
Mn-54	0.56	0.13 ± 0.01	0.11 ± 0.01	0.19 ± 0.1
Co-60	1.22	0.93 ± 0.01	0.98 ± 0.01	1.33 ± 0.05
mR/h	61	74	42	43

COOPER* DATE: 10-86 STATUS: 1st Fuel Cycle

NUCLIDE	A SUCTION	A DISCHARGE	B SUCTION	B DISCHARGE
Co-58	1.56	2.45	1.96	2.35
Mn-54	1.81	1.81	1.61	1.82
Co-60	2.97	2.89	3.56	4.74

MONTICELLO* DATE: 2-6-84 STATUS: Pre-decontamination

NUCLIDE	A SUCTION*	A DISCHARGE	B SUCTION	B DISCHARGE
Co-58	1.08	0.63	0.95	0.8
Mn-54	1.79	1.84	2.03	1.91
Zn-65	2.89	2.28	3.34	2.35
Fe-59	0.75	0.87	0.97	0.7
Co-60	14.42	13.98	15.5	10.46
mR/h	600	400	450	400

MONTICELLO* DATE: 2-84 STATUS: Post-decontamination

NUCLIDE	A SUCTION	A DISCHARGE	B SUCTION	B DISCHARGE
Zn-65	0.15	0.04	NM	<0.01
Co-60	0.20	<0.01	NM	0.07
mR/h	10	7	7	10

TABLE 3. MEASURED RADIONUCLIDE SURFACE FILM CONCENTRATIONS IN PCRS PIPING (uCi/cm^2) (Contd)

MONTICELLO* DATE: 4-86 STATUS: 1st Fuel Cycle

NUCLIDE	A SUCTION	A DISCHARGE	B SUCTION	B DISCHARGE
Co-58	0.74	0.81	1.1	1.16
Mn-54	0.74	1.33	1.22	1.24
Zn-65	1.31	1.26	1.58	1.02
Fe-59	0.26	ND	0.37	0.36
Co-60	5.64	6.1	6.48	6.18
mR/h	185	200	210	200

PEACH BOTTOM UNIT 2 DATE: 7-84 STATUS: Pre-decontamination

NUCLIDE	A SUCTION	A DISCHARGE	B SUCTION	B DISCHARGE
Co-58	0.42 ± 0.05	0.33 ± 0.04	0.36 ± 0.03	NM
Mn-54	0.3 ± 0.2	ND	ND	NM
Zn-65	3.9 ± 0.1	3.2 ± 0.1	3.7 ± 0.1	NM
Co-60	17.0 ± 0.1	13.0 ± 0.1	15.0 ± 0.1	NM
mR/h	370	350	458	384

PEACH BOTTOM UNIT 2 DATE: 8-84 STATUS: Post-decontamination

NUCLIDE	A SUCTION	A DISCHARGE	B SUCTION	B DISCHARGE
Co-58	0.04 ± 0.01	0.03 ± 0.01	0.02 ± 0.01	NM
Zn-65	0.40 ± 0.01	0.32 ± 0.01	0.83 ± 0.07	NM
Co-60	1.30 ± 0.01	0.93 ± 0.08	0.83 ± 0.07	NM
mR/h	20	22	24	17

PEACH BOTTOM UNIT 2 DATE: 3-87 STATUS: 1st Fuel Cycle

NUCLIDE	A SUCTION	A DISCHARGE	B SUCTION	B DISCHARGE
Co-58	1.42 ± 0.05	1.19 ± 0.03	1.60 ± 0.06	1.21 ± 0.05
Mn-54	0.08 ± 0.01	0.07 ± 0.01	0.08 ± 0.01	0.06 ± 0.01
Zn-65	1.65 ± 0.02	1.5 ± 0.2	1.81 ± 0.03	1.52 ± 0.02
Fe-59	0.06 ± 0.01	0.07 ± 0.01	0.07 ± 0.01	0.05 ± 0.01
Co-60	5.5 ± 0.1	4.8 ± 0.1	5.9 ± 0.1	4.9 ± 0.1
mR/h	98	NM	126	103

LIMERICK UNIT 1 DATE: 6-11-87 STATUS: 1st Fuel Cycle

NUCLIDE	A SUCTION	A DISCHARGE	B SUCTION	B DISCHARGE
Co-58	1.93 ± 0.04	1.87 ± 0.01	2.38 ± 0.06	1.10 ± 0.01
Mn-54	0.19 ± 0.01	0.15 ± 0.01	0.21 ± 0.01	0.08 ± 0.01
Zn-65	2.75 ± 0.03	2.76 ± 0.04	3.64 ± 0.05	1.74 ± 0.02
Fe-59	0.13 ± 0.01	0.11 ± 0.01	0.31 ± 0.01	0.07 ± 0.01
Co-60	1.69 ± 0.03	1.61 ± 0.01	2.09 ± 0.06	0.99 ± 0.09
Cr-51	0.49 ± 0.07	0.7 ± 0.1	0.7 ± 0.1	0.3 ± 0.1
mR/h	50	44	56	39

NM = location not measured
ND = nuclide not detected
* = RCT's data

TABLE 4. RECONTAMINATION FACTORS FOR RADIONUCLIDES IN BWR PCRS SUCTION DISCHARGE PIPING

QUAD CITIES UNIT 1

NUCLIDE	A SUCTION	A DISCHARGE	B SUCTION	B DISCHARGE	AVERAGE
Co-60	0.61	1.1	0.81	0.71	0.81

MILLSTONE UNIT 1

NUCLIDE	A SUCTION	A DISCHARGE	B SUCTION	B DISCHARGE	AVERAGE
Co-58	3.5	5.6	2.8	3.1	3.7
Mn-54	8.0	5.3	12.1	7.8	8.3
Co-60	0.51	0.78	0.47	0.69	0.61

COOPER

NUCLIDE	A SUCTION	A DISCHARGE	B SUCTION	B DISCHARGE	AVERAGE
Co-58	1.79	2.66	3.50	3.18	2.78
Mn-54	10.6	10.6	11.5	11.4	11.0
Co-60	0.48	0.49	0.50	0.92	0.60

MONTICELLO

NUCLIDE	A SUCTION	A DISCHARGE	B SUCTION	B DISCHARGE	AVERAGE
Co-58	0.68	1.28	1.16	1.45	1.14
Mn-54	0.41	0.72	0.60	0.65	0.59
Zn-65	0.45	0.55	0.47	0.43	0.47
Co-60	0.39	0.44	0.42	0.59	0.46

PEACH BOTTOM UNIT 2

NUCLIDE	A SUCTION	A DISCHARGE	B SUCTION	B DISCHARGE	AVERAGE
Co-58	3.38	3.61	4.44	**	3.81
Mn-54	0.27	*	*	**	0.27
Zn-65	0.42	0.47	0.49	**	0.46
Co-60	0.32	0.37	0.39	**	0.36

System Averages For All Facilities

NUCLIDE	QUAD 1	MILL	COOPER	MONT	PEACH	TOTAL AVG	DECONED AVG	NEW AVG
Co-58	*	3.7	2.78	1.14	3.81	2.86	3.7	2.58
Mn-54	*	8.3	11.0	0.59	0.27	5.0	8.3	3.95
Zn-65	*	*	*	0.47	0.46	0.46	*	0.46
Co-60	0.81	0.61	0.60	0.46	0.36	0.57	0.71	0.47

* = nuclide not detected in one spectra
** = location not measured

averaged about 10) than at Monticello and Peach Bottom Unit 2 (where they averaged about 0.4). The reason(s) for the behaviors of Co-58 and Mn-54 are not apparent. Pipe replacement versus pipe decontamination can be ruled out as a cause because Millstone Unit 1 was the only one of the three to have its pipe decontaminated (Cooper, Monticello, and Peach Bottom Unit 2 underwent pipe replacement).

Average surface film concentrations are plotted in Figures 2 through 5 for Co-60, Co-58, Mn-54, and Fe-59, respectively. These plots indicate that the radionuclide concentrations in the inner pipe surface films varied widely for the plants studied. The average Co-60 surface concentration varied from about 1.5 uCi/cm^2 (Limerick) to about 19 uCi/cm^2 (Quad Cities Unit 2); Co-58, from 0.05 uCi/cm^2 (Pilgrim) to about 2 uCi/cm^2 (Cooper); Mn-54, from 0.07 uCi/cm^2 (Peach Bottom Unit 2) to 4.2 uCi/cm^2 (Millstone Unit 1); and Fe-59, from 0.06 uCi/cm^2 (Peach Bottom Unit 2) to 0.44 uCi/cm^2 (Quad Cities Unit 2). For Co-60 and Fe-59, the newer plants generally exhibited a lower surface film concentration than did the older plants. No similar generalization, however, can be made concerning Co-58 and Mn-54. In general the Co-60 surface concentration tended to be higher for BWR 3s with old pipe than it was for BWR 3s with new pipe, a similar trend as was seen with the dose rate data.

In order to remove the effects of the reactor coolant radionuclide concentrations from the comparison of the gamma spectral results from the various plants, the surface film concentrations for Co-60 were normalized to the reactor coolant for each plant by dividing the surface radionuclide concentration by yearly average reactor coolant concentrations. Figure 6 shows the resultant bar graph for Co-60. The most striking difference this normalization makes is that the variation between the lowest and the highest values of Co-60 shows a significant reduction from Figure 2 and, with the exception of Quad Cities Unit 2, all plants exhibited a similar value for Co-60, being within ±25% of a mean value of approximately 16. Dependence of plant-to-power history, noted in Figure 2, for surface film concentrations of Co-60 was no longer apparent after the data were normalized to reactor coolant concentrations, indicating that power history plays at best a minor part in recontamination. In addition, there does not appear to be any significant difference between old pipe and new pipe normalized film concentrations.

General Electric has performed controlled studies on Co-60 deposition in a laboratory environment. The results of their findings were published in an EPRI report.[6] Part of their findings showed that within 2000 hours of exposure to simulated reactor coolant, the Co-60 surface film had come to approximately 95% of equilibrium on "as received" type 304 stainless steel test samples. The lack of correlation between surface film Co-60 concentration and EFPHs found in our study agrees well with this finding by General Electric, since all the plants we studied had been operating much longer than 2000 hours following a chemical decontamination or pipe replacement. A linear correlation between Co-60 surface deposition and the Co-60 concentration in the water flowing through the system

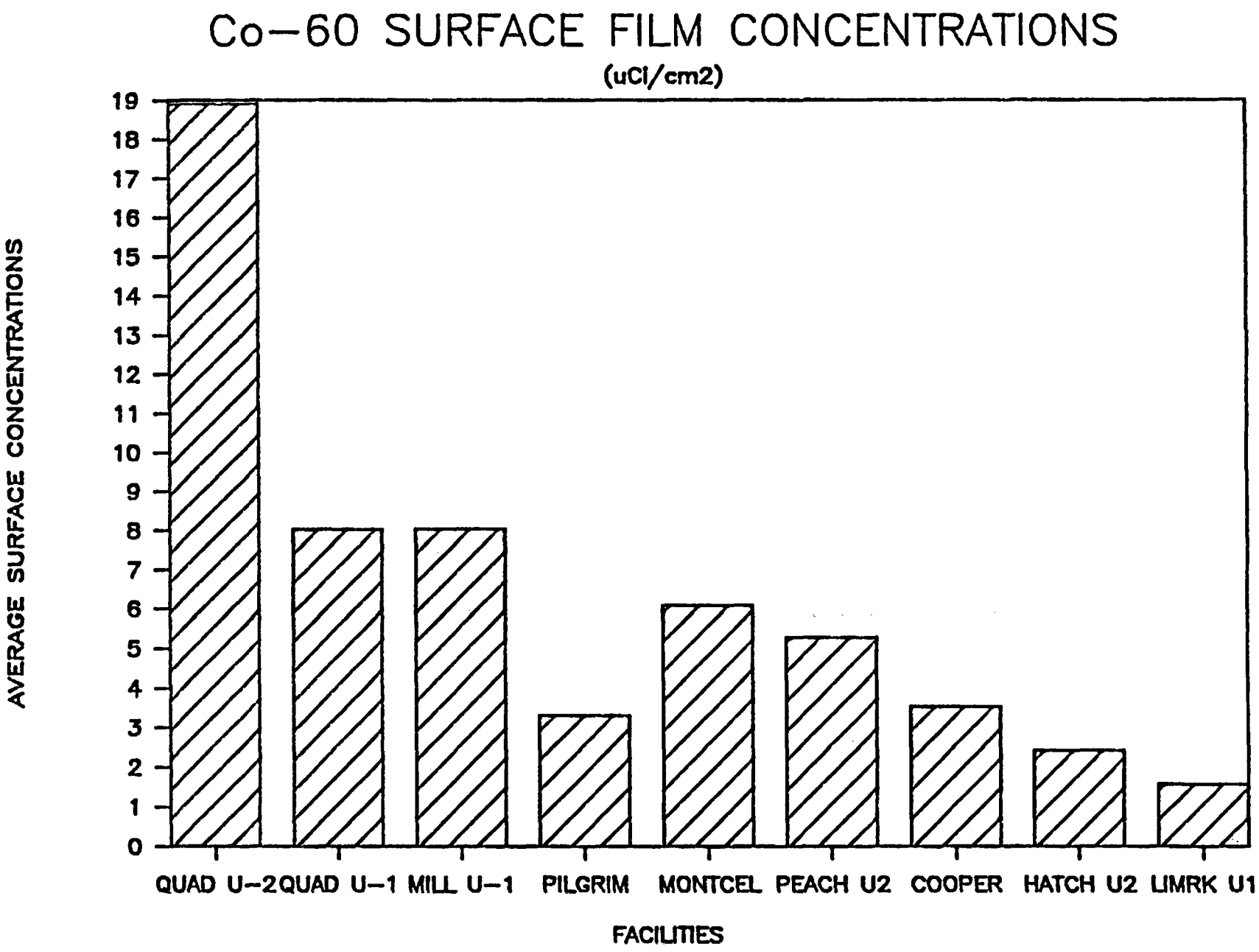
Co–60 SURFACE FILM CONCENTRATIONS
(uCi/cm2)
AVERAGE SURFACE CONCENTRATIONS
19
18
17
16
15
14
13
12
11
10
9
8
7
6
5
4
3
2
1
0
QUAD U–2
QUAD U–1
MILL U–1
PILGRIM
MONTCEL
PEACH U2
COOPER
HATCH U2
LIMRK U1
FACILITIES

FIGURE 2

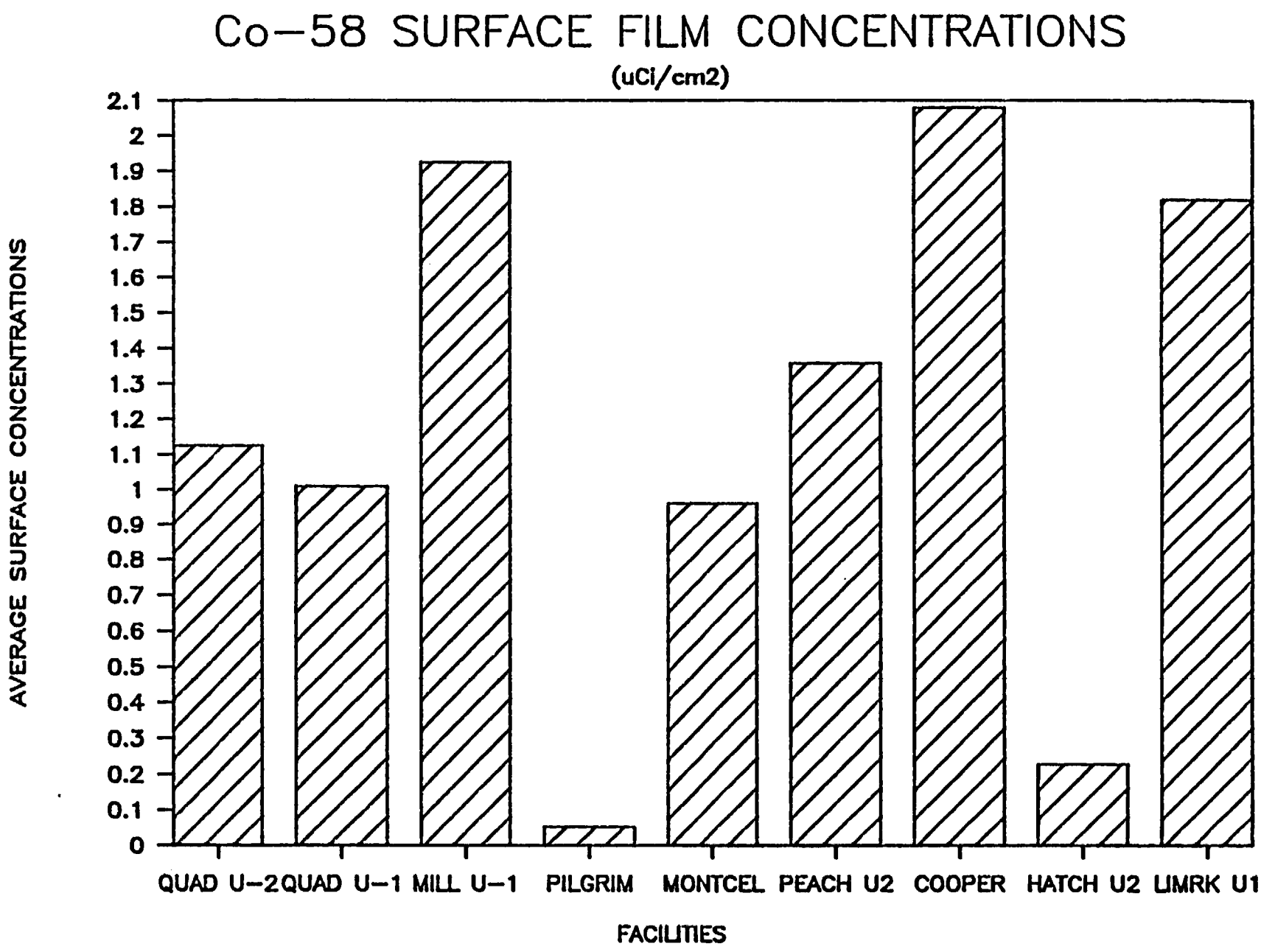
Co–58 SURFACE FILM CONCENTRATIONS
(uCi/cm2)
AVERAGE SURFACE CONCENTRATIONS
2.1
2
1.9
1.8
1.7
1.6
1.5
1.4
1.3
1.2
1.1
1
0.9
0.8
0.7
0.6
0.5
0.4
0.3
0.2
0.1
0
QUAD U–2
QUAD U–1
MILL U–1
PILGRIM
MONTCEL
PEACH U2
COOPER
HATCH U2
LIMRK U1
FACILITIES

FIGURE 3

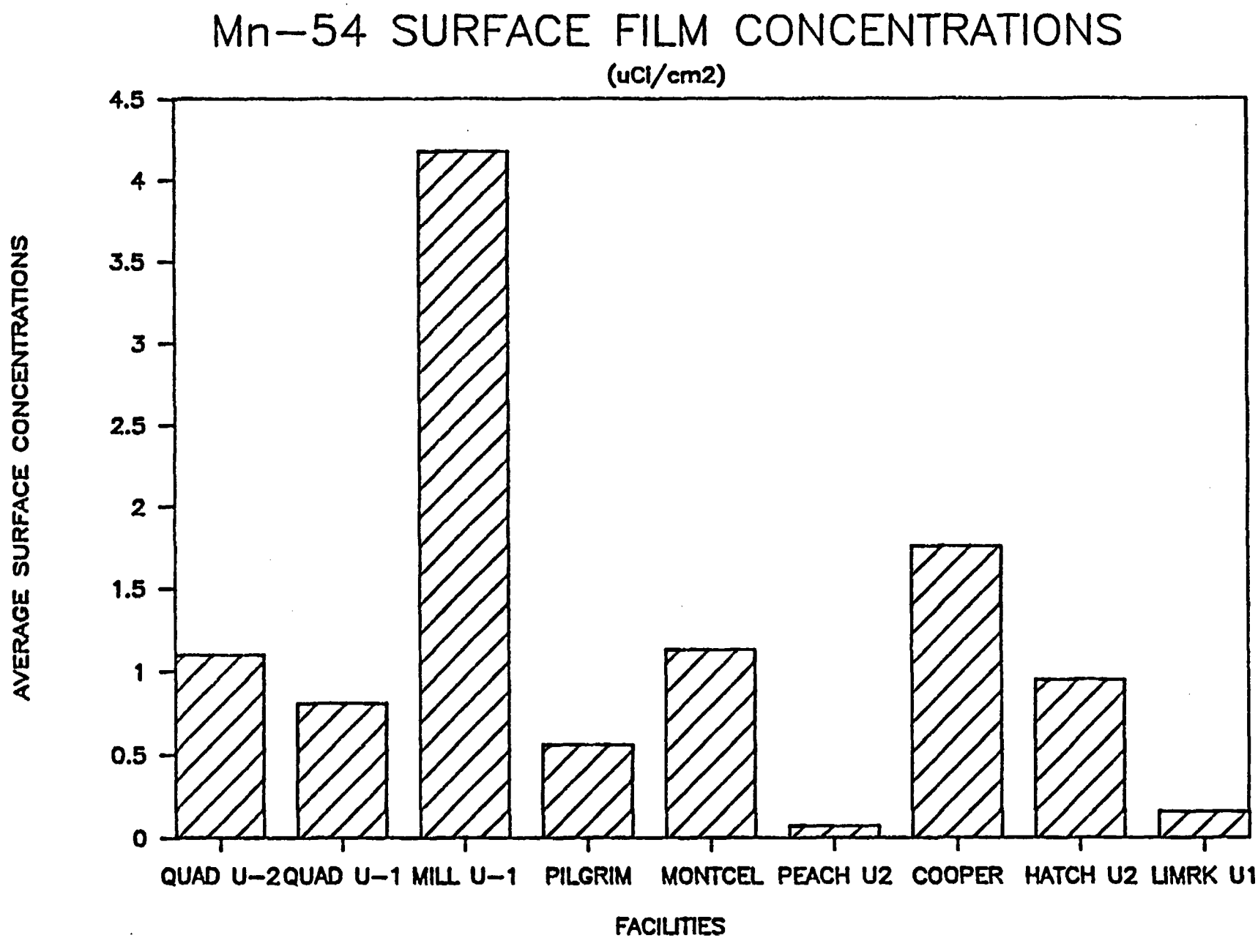
Mn-54 SURFACE FILM CONCENTRATIONS
(uCi/cm2)
AVERAGE SURFACE CONCENTRATIONS
4.5
4
3.5
3
2.5
2
1.5
1
0.5
0
QUAD U-2
QUAD U-1
MILL U-1
PILGRIM
MONTCEL
PEACH U2
COOPER
HATCH U2
LIMRK U1
FACILITIES

FIGURE 4

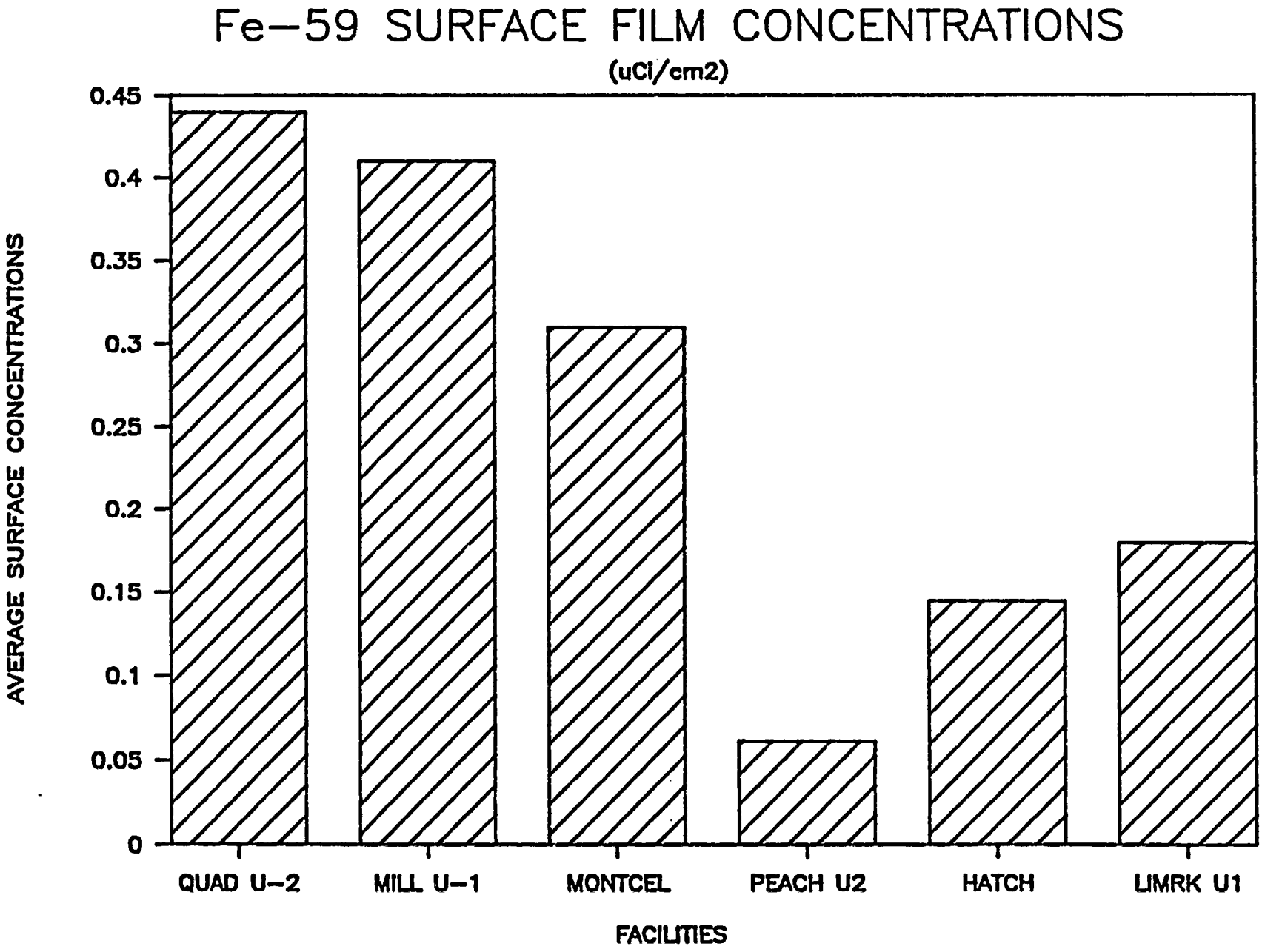
Fe–59 SURFACE FILM CONCENTRATIONS
(uCi/cm2)
AVERAGE SURFACE CONCENTRATIONS
0.45
0.4
0.35
0.3
0.25
0.2
0.15
0.1
0.05
0
QUAD U–2
MILL U–1
MONTCEL
PEACH U2
HATCH
LIMRK U1
FACILITIES

FIGURE 5

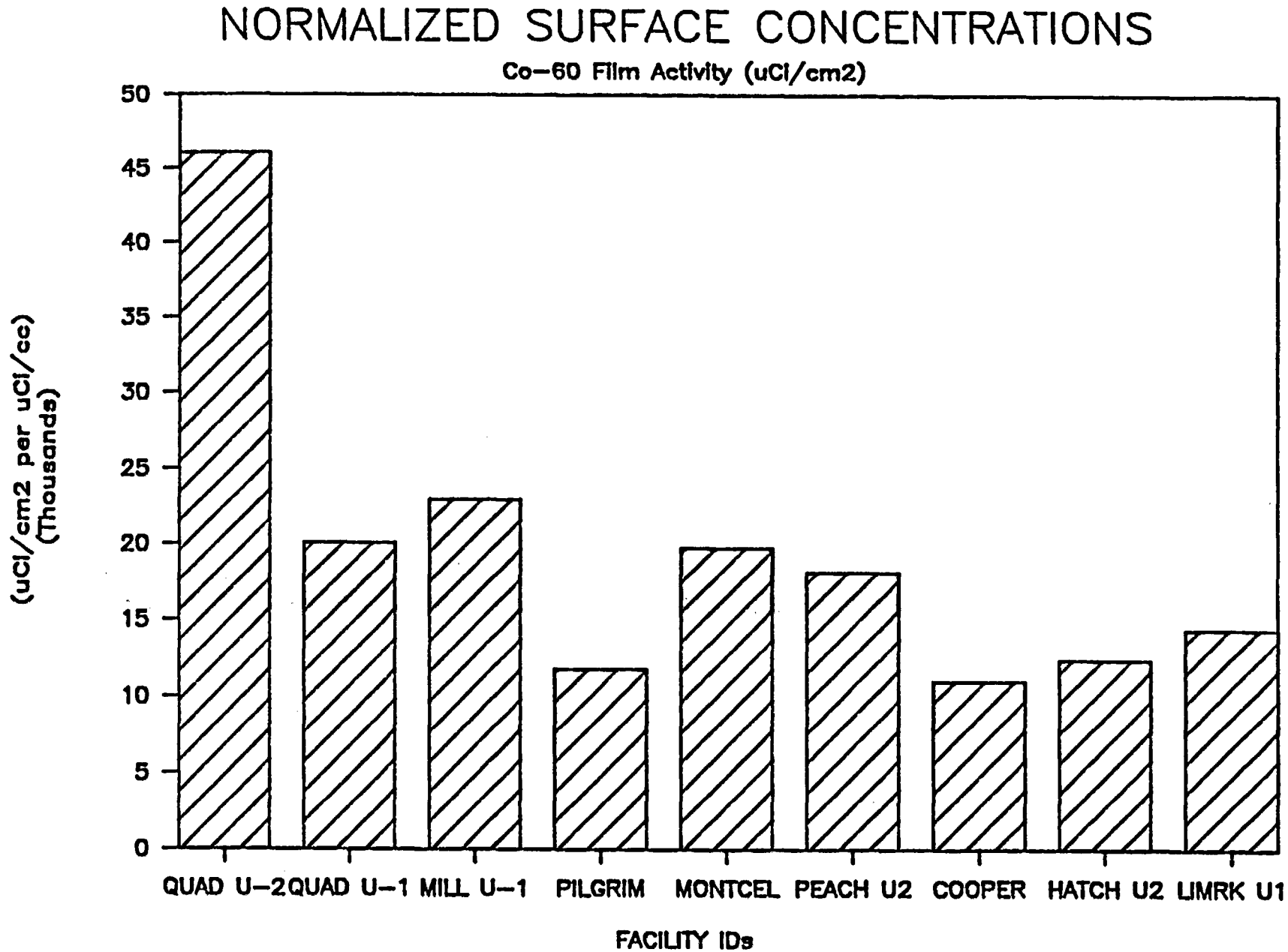
NORMALIZED SURFACE CONCENTRATIONS
Co-60 Film Activity (uCi/cm2)
(uCi/cm2 per uCi/cc)
(Thousands)
50
45
40
35
30
25
20
15
10
5
0
QUAD U-2
QUAD U-1
MILL U-1
PILGRIM
MONTCEL
PEACH U2
COOPER
HATCH U2
LIMRK U1
FACILITY IDs

FIGURE 6

was a second finding by General Electric. This was also found to be true in an earlier General Electric Study[5], where they found ".... the Co-60 levels on high-temperature decontaminated surfaces after several hundred hours were dependent on the soluble Co-60 concentrations in the reactor water during this time period...." The apparent correlation between surface film Co-60 concentration and reactor coolant Co-60 concentration found in our study agrees well with this finding by General Electric.

A mathematical equation for the activity on the pipe surface was determined by C. C. Lin to be:

$$A = RC \ln (kt+1)$$

where A = Co-60 activity on the surface, uCi/cm^2
R = deposition rate constant, kg/cm^2
k = corrosion kinetic constant, h^{-1}
C = Co-60 concentration in water, uCi/kg
t = exposure time, h

General Electric calculated the constants R and k for conductivities $\leq$ 0.1 and approximately 0.5 uS/cm for both type 304 and type 316 stainless steel.

All of the recontamination surface film data listed in Table 3 were tested against the GE equation using the constants for $\leq$0.1 uS/cm^3. The calculated values for $\leq$ 0.1 uS/cm^3 conductivity and the values measured after the first or second fuel cycle after pipe decontamination or replacement, are graphically displayed in Figure 7. There is good agreement (within a factor of two) of the measured data to the calculated values, when tested against the rate constants for $\leq$ 0.1 uS/cm^3 conductivities. This agreement was obtained even though most conductivities ranged from 0.16 to 0.25 uS/cm^3. At a few of the facilities conductivity was high for the first few thousand hours of operation, averaging 0.5 uS/cm^3. However, when these data were compared to calculated values for approximately 0.5 uS/cm^3 conductivity there was poor correlation. The General Electric equation was also tested against the pre-decontamination data. Surface film concentrations were calculated from the average dose rate data using the dose rate to Co-60 uCi/cm^2 factors of 26.09 for new pipe and 22.61 for old pipe. The results are shown in Figure 8. There is not reasonable correlation of the measured data (i.e., the calculated value using the averaged measured dose rates) to the calculated data. However if one allows for the measured values to be high by 50%, which is probably not an unreasonable assumption, then the agreement is quite good.

General Electric also studied the effects of other metal ions in the reactor coolant on the incorporation of Co-60 into the out of core pipe surfaces. Their studies have determined that Zn ions in the reactor coolant tend to inhibit the incorporation of Co-60 into the oxide film in out-of-core pipe surfaces.[6] It was found that Zn concentrations as

CALCULATED–VS–MEASURED PIPE ACTIVITY

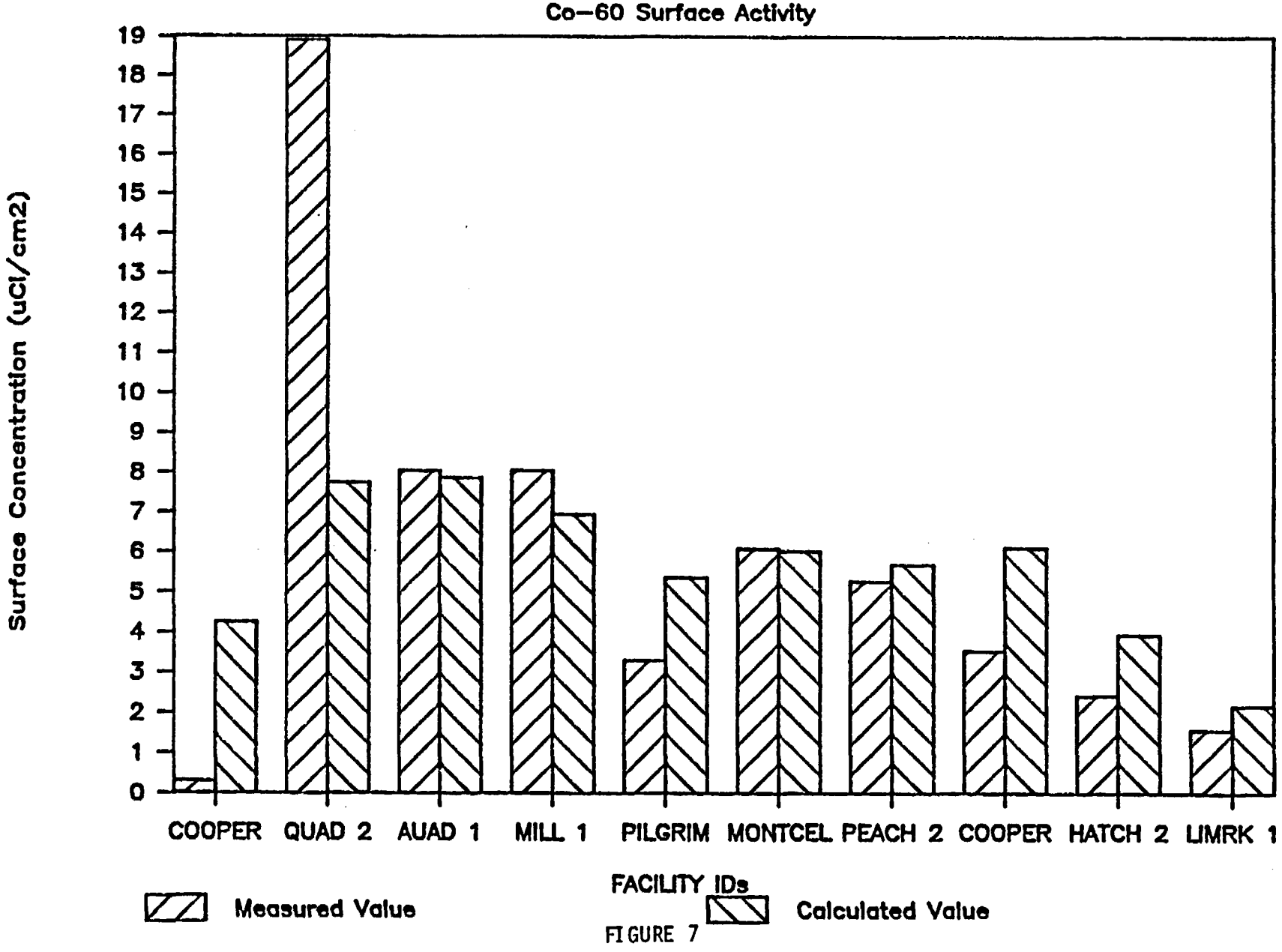

FIGURE 7

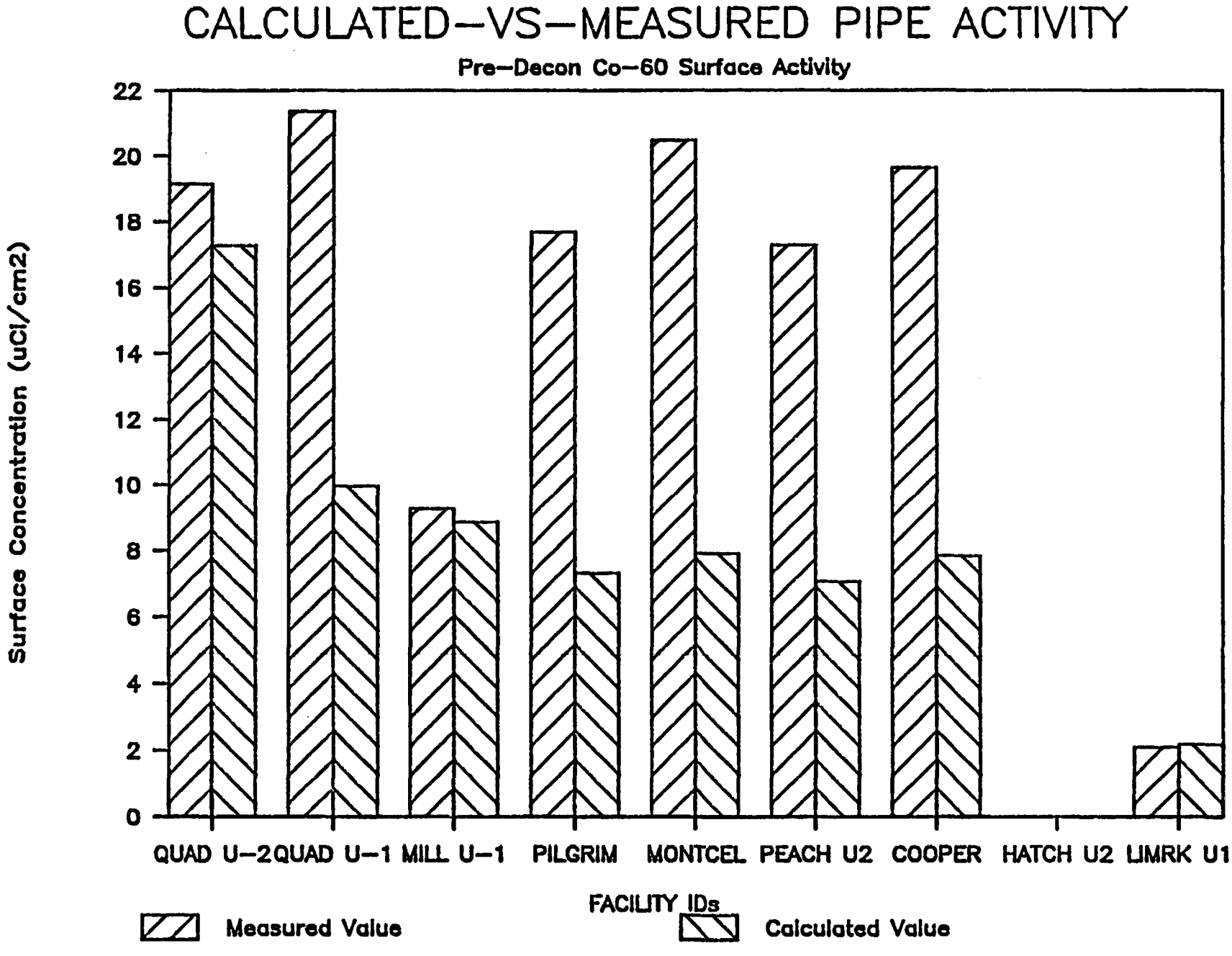
CALCULATED–VS–MEASURED PIPE ACTIVITY
Pre–Decon Co–60 Surface Activity
Surface Concentration (uCi/cm2)
22
20
18
16
14
12
10
8
6
4
2
0
QUAD U–2
QUAD U–1
MILL U–1
PILGRIM
MONTCEL
PEACH U2
COOPER
HATCH U2
LIMRK U1
FACILITY IDs
Measured Value
Calculated Value

FIGURE 8

low as 5 ppb had a positive affect on reducing the incorporation of Co-60. The data acquired as part of the recontamination program as well as data that were acquired as part of a General Electric measurement program on BWR radiation assessment and control program,[5] were used to evaluate if Zn in the reactor coolant did show a trend for reducing the surface film concentrations in the suction/discharge pipe. Table 5 lists the average radioisotopic concentrations (prior to any decontamination or pipe replacement, except where noted) on BWR recirculation lines for both the General Electric data and data obtained in this study. Recontamination data are noted with asterisks. The data indicate that, in general, the trend is for those facilities having Admiralty brass condensers to have lower Co-60 film concentrations for the same equivalent EFPHs than those without brass condensers. The brass condenser tubes contain Zn in the alloyed metal. During normal operation Zn gets into the feedwater, and hence into the reactor coolant, by erosion of the condenser tubing. Note that for Limerick Unit 1, which has measured values of >25 ppb Zn, the data show the same general trend in the contamination rate as Hatch Unit 2 and Brunswick Unit 2, both of which have brass condensers. All three show pipe surface film activities significantly less than the other facilities.

There are two other interesting observations of the data in Table 5. First, for Quad Cities Units 1 and 2, Hatch Unit 2, and Limerick Unit 1, the recontamination data agree well with the initial contamination data time sequence but for Monticello and Millstone the data fit well in the initial contamination data at approximately 3 EFPYs (effective full power years). Secondly, Co-58 approximates the Co-60 film concentrations in the time frame of <1.5 EFPYs, but after that time the Co-60 becomes the dominant nuclide in the pipe surface film. This is due to the equilibrium concentration dependence on the halflife of the radionuclide, where Co-58 has a halflife of 71.4 days and Co-60 has a halflife of 5.26 years. Therefore, the surface film concentration of Co-60 should be much larger than Co-58. Measured data show that Co-60 reaches equilibrium around three to five EFPYs.

Since some of the studied facilities had replaced the PCRS pipes with pre-treated pipe, the measured film concentrations were examined to determine if there was any significant reduction in the out of core surface concentrations of Co-60 caused by any pretreatment of new pipe used in the PCRS replacement. The following lists a brief review of the facilities and pipe treatment received prior to the pipe being installed.

Facility	Pipe Pretreatment
Cooper	Pipe were electropolished and then pre-oxidized using hot moist air ~ 560°F for 150 hours.
Monticello	Pipe were electropolished
Pilgrim	Pipe were electropolished
Hatch	No pipe pretreatment
Peach Bottom	Pipe were electropolished

TABLE 5. RADIOISOTOPIC SURFACE CONCENTRATIONS IN BWR PCRS PIPING

BWR	Concentration (uCi/cm^2)					
	EFPY	Co-60	Co-58	Mn-54	Zn-65	Fe-59
Brunswick-2***	0.32	0.3	0.9	0.2	0.2	ND
	0.96	2.2	1.7	0.9	0.8	ND
	2.19	5.1	2.1	1.1	0.9	ND
Quad Cities-1	1.19**	8.0	1.0	0.8	0.8	ND
	2.79	25.5	1.7	1.4	ND	ND
	4.06	34.7	1.6	2.1	ND	ND
	4.71	38.5	1.5	1.5	ND	ND
	5.27	39.9	1.0	2.1	ND	ND
	6.05	38.3	1.6	1.6	ND	ND
Quad Cities-2	0.90**	14.2	1.1	1.1	1.0	0.4
	2.85	27.9	0.9	1.0	ND	ND
	4.13	34.8	1.5	1.5	ND	ND
	4.63	43.1	1.5	1.6	ND	ND
	5.10	36.9	1.1	1.5	ND	ND
	5.80	39.3	1.3	2.3	ND	ND
Hatch***	0.61	0.5	1.8	0.1	ND	ND
	1.50**	2.4	0.2	0.9	1.2	0.1
Monticello	1.16**	6.1	1.0	1.1	1.3	0.3
	1.31	0.5	0.4	0.1	1.0	ND
	1.88	1.2	1.3	0.3	1.2	ND
	2.35	4.0	1.0	1.0	3.5	ND
	2.83	7.9	1.3	1.1	4.5	ND
	4.41	8.5	0.6	0.5	1.3	ND
	10.26	13.6	0.9	1.9	2.7	0.8
Millstone-1	1.20	3.4	1.8	1.5	0.1	ND
	1.27**	8.1	1.9	4.2	ND	0.5
	1.28	3.3	0.7	1.0	0.1	ND
	2.04	7.1	1.7	3.1	0.6	ND
	2.72	5.8	1.1	1.6	0.1	ND
	3.44	8.9	1.5	2.3	ND	ND
Limerick-1***	1.27	1.6	1.8	0.2	2.7	0.2

ND = not detected in spectra
* = EFPY is effective full power years
** = measured values on pipe that were either removed or decontaminated EFPY is for the next fuel cycle.
***= Admiralty Brass condenser tubes

Figure 9 shows a plot of the reactor coolant normalized Co-60 surface film concentration versus EFPHs. The line is drawn in for an aid to the viewer. Review of Figure 9 shows that there does not appear to be any significant advantage to pretreatment of pipe surfaces to reduce the Co-60 incorporation into the oxide film. Of the facilities that show significant deviation from a linear relationship of normalized surface activity to EFPHs, Hatch and Limerick were lower and Monticello was higher. Hatch did not perform any pipe pretreatment and historically has had low oxide film concentrations as mesured using dose rate. Limerick had measurable Zn at >25 ppb which may have had a greater affect on lowering the Co-60 film concentration than pipe pretreatment. Monticello, which was higher by a factor of 2, replaced the 28 in. PRCS piping with piping that had been formed from stainless steel plate which was rolled and seam welded.[2] This pipe formation process was different than the normal extruded pipe process used for most PCRS replacement piping. The rolled pipe surface was observed to be more rough following electropolishing than the electropolished extruded pipe surfaces, which should, and apparently did, significantly enhance the Co-60 buildup on the pipe surfaces. Our finding agrees with the General Electric finding,[5] where they found that "The prefilming test demonstrated that prefilming of stainless steel surfaces can significantly reduce the initial buildup rate on BWR stainless steel surfaces. However, the longer-term buildup rate appears to be unaffected. Thus, as the exposure time increases, the relative differences between the radioisotopic levels on the prefilmed and non-prefilmed surfaces will decrease." All of the plant data (except that obtained soon after a decontamination) were at facilities that had sufficient operational hours so that any early prefilming advantage would not be apparent with this data. This is borne out by a comparison of Co-60 results obtained from Cooper (see Figure 7). The first set of Cooper data in Figure 7 was obtained after 1104 EFPHs of operation, while the second set was obtained after 8628 EFPHs. At 1104 EFPHs, the calculated value is much larger than the measured value, but this difference is reduced considerably at 8628 EFPHs. This indicates that by 8628 EFPHs the initial advantage of pretreatment of the pipe at Cooper had been lost.

Man-rem savings are a direct result of reduced dose rates in general areas or at contact with equipment components. Chemical decontaminations have been shown to be effective in reducing the dose rates in PCRS piping.[1] However, what about the long term savings of man-rem due to chemical decontaminations? The results of this recontamination study show that for at least the first fuel cycle there will be on average a 43% savings in worker dose for performing a similar task before a chemical decontamination of the PCRS piping. For old pipe systems the savings are not as great averaging 29% but new pipe systems enjoy a greater average savings of 53%. With all facilities the savings are different and are calculated by subtracting the recontamination factor from one. The reader is referred to Table 4 for the recontamination factors for each facility.

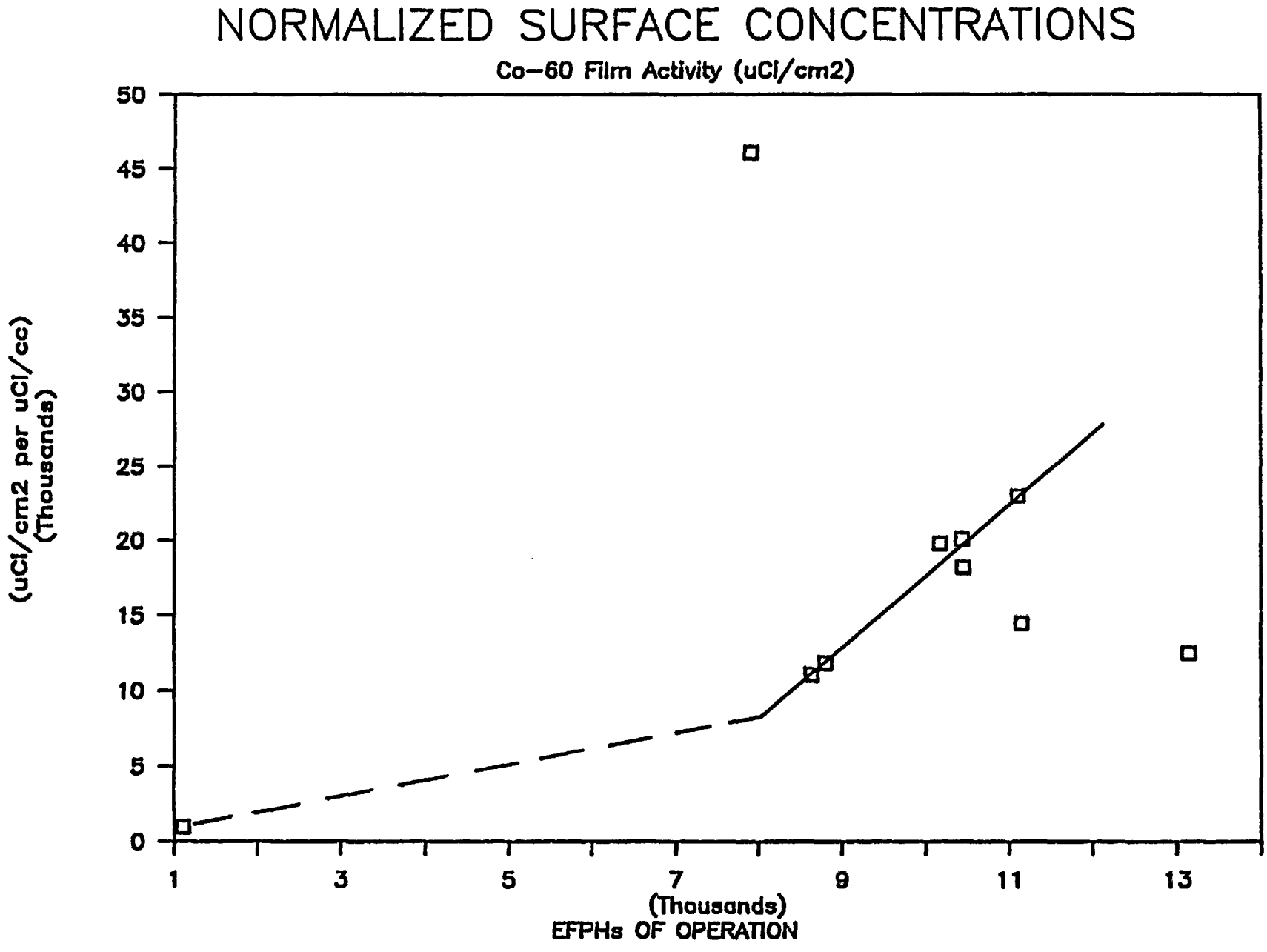
NORMALIZED SURFACE CONCENTRATIONS
Co-60 Film Activity (uCi/cm2)
(uCi/cm2 per uCi/cc)
(Thousands)
50
45
40
35
30
25
20
15
10
5
0
1
3
5
7
9
11
13
(Thousands)
EFPHs OF OPERATION

FIGURE 9

CONCLUSIONS

The results of this study indicate that:

- Dose rates following a decontamination or pipe replacement tend not to be a function of effective full power hours.
- Dose rates following a decontamination or pipe replacement tend to be a function of Co-60 reactor coolant concentrations.
- Surface film concentrations on out of core pipe surfaces tend to be dominated by Co-60 both prior to and following a chemical decontamination or pipe replacement.
- Old pipe systems tend to have higher oxide film radionuclide concentrations than new pipe systems following at least one fuel cycle.
- Co-60 surface film concentrations on out of core pipe surfaces following a decontamination or pipe replacement tend to be a function of reactor coolant Co-60 concentrations.
- Co-60 and Fe-59 surface film concentrations on out of core pipe surfaces tend to be lower in systems where the PCRS pipe were replaced, but Co-58 and Mn-54 tend not to follow this pattern.
- Co-60 surface film concentrations on out of core pipe surfaces following a decontamination or pipe replacement tend not to be a function of effective full power hours.
- Zinc tends to reduce the incorporation rate of Co-60 into the oxide film on out of core pipe surfaces.
- There is little apparent correlation to surface film radionuclide concentrations on out of core pipe surfaces and pre-treatment of pipe surfaces.
- Man-rem savings, following at least one fuel cycle, tend on average to be equal to 43% for all facilities.

REFERENCES

1. S. W. Duce, J. T. Case, "Effectiveness and Safety Aspects of Selected Decontamination Processes," NUREG/CR 4445, EGG-2453, August 1986.

2. R. Asay, et. al., "Primary System Recontamination Following Recirculation Pipe Replacement at Cooper Nuclear Station," RCT-8629-2193, November 12, 1986.

3. T. M. McLachlan, "Radiation Buildup on New Recirculation Piping at the Monticello Nuclear Generating Plant," RCT-8612-2098, May 15, 1986.

4. J. P. Peterson private communication, to S. W. Duce, "Data Collected at BWRs Under BWR Radiation Assessment Program," August 8, 1987.

5. L. D. Anstine, "BWR Radiation Assessment and Control Program: Assessment and Control of BWR Radiation Fields, Vol. 2," EPRI NP-3114, May 1983.

6. C. C. Lin, "BWR Cobalt Deposition Studies - Progress Report 2," EPRI NP-4725, August 1986.

EFFECT OF DECONTAMINATION ON AGING PROCESSES AND CONSIDERATIONS FOR LIFE EXTENSION

D. R. Diercks
Materials and Components Technology Division
Argonne National Laboratory
Argonne, IL 60544

ABSTRACT

The basis for a recently initiated program on the chemical decontamination of nuclear reactor components and the possible impact of decontamination on extended-life service is described. The incentives for extending plant life beyond the present 40-year limit are discussed, and the possible aging degradation processes that may be accentuated in extended-life service are described. Chemical decontamination processes for nuclear plant primary systems are summarized with respect to their corrosive effects on structural alloys, particularly those in the aged condition. Available experience with chemical cleaning processes for the secondary side of PWR steam generators is also briefly considered. Overall, no severe materials corrosion problems have been found that would preclude the use of these chemical processes, but concerns have been raised in several areas, particularly with respect to corrosion-related problems that may develop during extended service.

INTRODUCTION

This paper describes the basis for a recently initiated program on the decontamination of nuclear reactor components and the possible impact of decontamination on extended-life service. This program is being developed in response to the ever-increasing use of chemical decontamination processes in nuclear power plants to reduce worker exposures during repairs and maintenance, and to a growing interest in extending the life of existing nuclear plants beyond their present 40-year licensing period. Concerns about the possible adverse effects of repeated decontaminations on the remaining service life of aged components must be addressed before operating licenses for extended life can be renewed. Although a wide variety of nuclear power plant components are subject to aging effects of one kind or another, the present program is specifically concerned with metallurgical and chemical effects in components that are directly exposed to decontamination solutions, i.e., selected pressure boundary components and reactor internals. In addition, chemical cleaning of steam generators to remove sludge and reduce denting, though not strictly a decontamination process, is also included.

PLANT LIFE EXTENSION AND COMPONENT AGING

The duration of a license for a nuclear power plant was set at a maximum of 40 years by the Atomic Energy Act of 1954, with possible renewal at the end of that time period.[1] Several studies[2-4] to evaluate the technical and economic merits of extending service lives beyond this 40-year limit have found that such life extensions are technically feasible and that the economic incentives are considerable. A 1982 evaluation performed for the Electric Power Research Institute (EPRI) concluded that such life extension could be cost-effective even at a plant refurbishment cost of $300 million to $1 billion.[3] Robert B. Minogue, former Director of the Office of Nuclear Research of the U. S. Nuclear Regulatory Commission (USNRC), has noted that present 40-year operating licenses for nuclear power plants will begin to expire in the year 2001, and by 2015 approximately 85 percent of the licenses granted through 1985 will have expired.[5] It is therefore not surprising that the USNRC has already begun to seriously examine the safety implications associated with nuclear power plant life extension.[6]

The major concern with respect to the possible licensing of nuclear plants for operation beyond 40 years is that of component aging. In terms of metallurgical effects, such aging can take several forms, including low-temperature sensitization of stainless steels, long-term embrittlement of cast duplex stainless steels, and radiation-induced embrittlement of reactor internal components. Each of these aging phenomena will be discussed briefly.

It has been recognized only relatively recently that sensitization of stainless steels can occur after prolonged exposures (of the order of years) to temperatures of 400°C (750°F) or less.[7,8] This process, known as low-temperature sensitization, generally requires an initial brief exposure to higher temperatures (600 to 800°C or 1110 to 1470°F) to nucleate the carbide particles that subsequently grow at lower temperatures. Just as with conventional sensitization, this precipitation process depletes the grain-boundary regions of Cr and leaves them more susceptible to intergranular corrosion. Low-temperature sensitization is of concern in nuclear plant coolant piping and reactor internals operating at temperatures of 250 to 288°C (480 to 550°F), particularly under conditions of extended-life operation.

Another aging phenomenon, sometimes known as 475°C embrittlement, can occur in ferritic and cast duplex stainless stainless steels. When these steels are exposed for extended periods of time to temperatures in the range from 300 to 500°C, the Cr-rich α' phase precipitates within the ferrite, resulting in severe embrittlement. It now appears that a similar series of time-dependent precipitation phenomena may occur at LWR operating temperatures in the ferrite phase of cast duplex stainless steels such as CF-3 and CF-8, which are used to fabricate nuclear plant primary coolant piping as well as valve and pump casings.[9] Again, these very slow aging processes are of greatest concern under conditions of extended-life operation.

The embrittlement of reactor pressure vessels and internal components due to neutron irradiation may also be considered to be an aging phenomenon of sorts. This embrittlement process is generally characterized in terms of an increase in the transition temperature between brittle behavior observed at lower temperatures and ductile fracture at higher temperatures. This transition temperature increases with increasing neutron fluence (and therefore service time), and it has also been found to be strongly influenced by the presence of certain impurities such as Cu and Ni in the steel. Control of these residual element levels has greatly reduced the embrittlement problem in the newer reactor pressure vessels, but older vessels will require careful monitoring, particularly if extended-life operations are attempted.

CHEMICAL DECONTAMINATION

During the operation of a nuclear power plant (BWR or PWR), oxide corrosion films form on the surfaces of piping, pumps, valves, steam generator tubing, and other components in contact with the primary coolant. Some of these corrosion products dissolve or erode in the circulating coolant, are deposited on the fuel cladding, and become activated. The principal radionuclides formed by this activation process are ^{58}Co, ^{60}Co, ^{55}Fe, ^{59}Fe, ^{54}Mn, ^{51}Cr, ^{63}Ni, and ^{65}Zn. These radionuclides, in turn, are released and carried out of the core region by the coolant and are incorporated into the oxide films on the surfaces of the primary coolant system components. The result is a steadily increasing radiation field on these components.

This radiation field is of principal concern during reactor outages for maintenance or repair, since it limits the working time of personnel in the region. In fact, radiation exposure represents a specific cost, commonly quoted as $5000 to $7000 per man-rem,[10,11] that electrical utilities must bear during maintenance and repair procedures. Decontamination of primary loop components to reduce radiation fields and lower the man-rem exposure is therefore of vital economic interest to utilities. For example, based upon experiences with the Dresden 3 and Quad Cities 1 and 2 reactors, Commonwealth Edison Company reports average net savings of $1.25-million from decontamination of recirculation piping preparatory to performing in-service inspection and repair work.[12] Reduction of the radiation exposure of nuclear plant personnel through effective decontamination is also consistent with the NRC objective of maintaining such exposure as low as reasonably achievable (ALARA).

The results of a survey of U. S. experience with the chemical decontamination of commercial nuclear power reactors are summarized in Table I. This tabulation is not necessarily exhaustive, but it does include a large majority of the chemical decontaminations that were performed in this country through the end of 1986. Most of the decontaminations were carried out on BWR primary coolant recirculation systems (PCRS) and reactor water clean-up systems (RWCU). In PWRs, the components most commonly decontaminated have been steam generator channel heads. Almost all of these decontaminations were carried out immediately prior to maintenance

Table I. Summary of Experience with Chemical Decontamination of Commercial Nuclear Power Reactors in the United States.

Date	Plant	Process	Components Decontaminated*	Years Since Startup
		Boiling Water Reactors		
1964	Shippingport	Turco 4502/4521	PCRS	7
6/76	Dresden 1	NS-1 (conc.)	Primary system test loop	16
4/77	Peach Bottom 3	NS-1 (conc.)	RWCS	3
9/77	Peach Bottom 2	NS-1 (conc.)	RWCS	3
10/79	Vermont Yankee	CAN-DECON	RWCS	7
3/80	Brunswick 2	CAN-DECON	RWCS	4
3/81	Nine Mile Point	CAN-DECON	5 primary recirc. pumps	4
4/81	Brunswick 1	CAN-DECON	RWCS	4
10/81	Vermont Yankee	CAN-DECON	RWCS	9
12/81	Brunswick 1	CAN-DECON	aux. steam system	5
4/82	Peach Bottom 2	CAN-DECON	RWCS	8
4/82	Nine Mile Point	CAN-DECON	2 primary recirc. pumps	12
5-8/82	Nine Mile Point	CAN-DECON	PCRS	12
12/82	Hatch 1	CAN-DECON	RWCS	7
4/83	Peach Bottom 3	CAN-DECON	RWCS	8
3-4/83	Vermont Yankee	CAN-DECON	PCRS	10
10/83	Quad Cities 2	CAN-DECON	PCRS	11
10/83	Dresden 3	CAN-DECON	PCRS and RWCS	12
1/84	Pilgrim	NS-1 (dilute)	PCRS	11
3/84	Monticello	LOMI	PCRS and RWCS	13
4/84	Quad Cities 1	CAN-DECON	RWCS	12
4/84	Brunswick 2	Citrox	RWCS	8
5/84	Millstone 1	CAN-DECON	PCRS and RWCS	14
7/84	Peach Bottom 2	CAN-DECON	PCRS	10
7-8/84	Pilgrim	NS-1 (dilute)	PCRS and RWCS	12

Table I. (Cont'd.)

Date	Plant	Process	Components Decontaminated*	Years Since Startup
9/84	Dresden 1	NS-1 (conc.)	PCRS	24
10/84	Dresden 2	NS-1 (dilute)	PCRS	14
12/84	Cooper	Citrox (dilute)	PCRS	10
1984	Quad Cities 2	CAN-DECON	RWCS	12
10/85	Vermont Yankee	LOMI	PCRS and RWCS	13
11/85	Dresden 3	LOMI	PCRS and RWCS	14
1/86	Quad Cities 2	LOMI	PCRS	13
5/86	Quad Cities 1	CAN-DECON/LOMI	2 irrad. fuel assemblies	14
6/86	Oyster Creek	LOMI	PCRS	17
7/86	Brown's Ferry 1,2,&3	7 processes compared	6 RWCS pumps	9-12
12/86	Dresden 2	LOMI	PCRS and RWCS (hot leg)	16
		Pressurized Water Reactors		
1976	Surry	NS-1 (conc.)	Evaporator	3
9/82	Surry 2	CAN-DECON	Channel head (cold leg)	9
11/82	Surry 2	LOMI	Channel head (hot leg)	9
4/83	Ginna	CAN-DECON	Channel heads	13
8/83	Millstone 2	OZOX	Channel heads	8
8/84	Palisades	CAN-DECON	Channel heads	13
5/85	Millstone 2	Citrox A	Channel heads	10
1985	Indian Point 3	LOMI	Channel heads	9
1/86	Connecticut Yankee	CAN-DECON	Channel heads	18
6-8/86	H. B. Robinson	LOMI	Isolated primary pump	15
1986	Millstone 2	OZOX-A	Channel heads	11

* PCRS = Primary Coolant Recirculation System
RWCS = Reactor Water Cleanup System

or repair work to reduce worker exposure. The principal decontamination processes were CAN-DECON, NS-1, and, in more recent years, LOMI. It is apparent from the table that chemical decontamination is becoming an increasingly common practice in this country.

During a nuclear reactor decontamination, the chemical solutions are likely to come in contact with a number of different structural alloys. The more important alloys are listed in Table II along with examples of components in which they are utilized. Although core decontaminations with the fuel in place are not yet being routinely performed in this country, they have been performed in Canada (Douglas Point and Pickering Candu Reactors) and the U. K. (Winfrith SGHWR), and are of growing interest in the U. S. For this reason, Zircaloy cladding material is included in Table II. The high-strength Ni-base Inconel Alloys 718, 625, and X-750, which are used for core structural applications, are included for the same reason.

It should be noted that several of the alloys listed in Table II are susceptible to the long-term metallurgical aging effects previously described. For example, the austenitic stainless steels (SS) and, to a lesser extent, Incoloy 600 are subject to low-temperature sensitization, although Type 316 NG SS has been specifically developed to resist sensitization. Possible aging embrittlement of the cast duplex stainless steels CF-8 and CF-3 has already been discussed, as has the neutron irradiation embrittlement of the low-alloy pressure-vessel materials.

CORROSIVE EFFECTS OF DECONTAMINATION PROCESSES

Table I indicates that the most widely used decontamination processes in this country are CAN-DECON and, more recently, LOMI, and these two processes are of principal interest in the present program. Both processes have been extensively studied for possible corrosive effects on the reactor structural materials with which they come in contact during use. The results of these studies are summarized in this paper.

CAN-DECON Process

The CAN-DECON process is a dilute chemical decontamination process developed by Atomic Energy of Canada Ltd. (AECL) during the early 1970's.[13] The process was first used on a commercial basis in the United States to decontaminate the RWCS of the Vermont Yankee BWR in late 1979. Since that time, more than 20 decontaminations of BWR's and PWR's have been carried out in this country with CAN-DECON.

The principal active chemical reagent used in the CAN-DECON process was originally Nutek L-106, sold by Nuclear Technology Corp. of Amston, CN.[14] Since 1977, when London Nuclear Decontamination Ltd. (now LN Technologies) became the licensee of the AECL for the application of the process, the chemically similar reagent LND-101A has been utilized. This reagent consists of a mixture of organic acids (including oxalic acid) to

Table II. Nuclear Reactor Structural Alloys Likely to be Exposed to Decontaminant Solutions During Chemical Decontamination.

Alloy	Application
Austenitic Stainless Steels	
Type 304	Primary coolant piping
Type 316 NG	Primary coolant piping
Types 308 and 309	Corrosion-resistant cladding on pressure vessels and piping
Cast Duplex Stainless Steels	
CF-8	Primary coolant piping; valve and pump casings
CF-3	
Carbon and Low-alloy Steels	
A106	Primary coolant piping
SA333, Grade B	Primary coolant piping
A516, Grade 70	Primary coolant piping
A508, Grade 2	Reactor pressure vessel
A533, Grade B	Reactor pressure vessel
A302, Grade B	Steam generator shells
A570, Grade 40	Steam generator support plates
Nickel-base Alloys	
Inconel 600	PWR steam generator tubing
Inconel 718	Core structural components
Inconel 625	Core structural components
Inconel X-750	Core structural components
Special Purpose Alloys	
Zircaloy-2 and -4	Nuclear fuel cladding
Haynes Stellite 6B	Control element drives
Haynes Stellite 6	Weld-deposited hard facing on pumps and valves

dissolve the radioactive oxide films present on the components and a chelant to prevent redeposition of dissolved radioactive metal ions. The oxide films formed on PWR steam generator components typically contain more Cr (as much as 40 wt. %) than is present in typical BWR corrosion films.[15] Chromium is present as Cr^{3+} ions, which are insoluble in the LND-101A reagent and its modifications. It is therefore necessary to utilize an alkaline permanganate solution (LND-104) to oxidize the Cr^{3+} ions to the soluble Cr^{6+} state. In decontaminating PWR components, therefore, the reducing LND-101A treatments are typically preceeded by or are alternated with the oxidizing LND-104 treatments.

The CAN-DECON LND-101A solution is typically injected into the circulating reactor coolant in sufficient quantity to achieve a diluted concentration of 0.1 wt. % in solution. A side stream of circulating solution is passed through a filter and cation resin columns to remove particulate and dissolved materials. The normal decontamination temperature is 120°C (248°F), but decontaminations have been carried out successfully at temperatures from approximately 80 to 135°C.[16]

Concerns about the possible detrimental effects of LND-101A on LWR structural alloys were first raised in early 1982 in conjunction with the decontamination of the Nine Mile Point 1 BWR primary coolant recirculation system (PCRS).[17] This decontamination was carried out in order to reduce worker exposure during repairs to safe end-to-pipe welds in the 28-in. diameter coolant lines, which developed through-wall leaks in the heat-affected zones of the welds. A Task Force formed to study the Nine Mile Point 1 failures also considered the question of whether the CAN-DECON decontamination performed immediately prior to component removal contributed to the observed cracking. The Task Force report, issued in September 1982, concluded that "...the 1982 total recirculation system decontamination does not appear to have exacerbated the observed cracking."[17] Its only clear effect, insofar as the cracking was concerned, was "...the increase in sensitivity for inspection of cracks which already existed in the system."[17] However, some of the piping welds were heavily electropolished after decontamination to further reduce radiation levels, and this electropolishing treatment removed some of the original inner surface where intergranular attack (IGA) induced by the decontamination process might have occurred. Furthermore, the failed piping was removed immediately after decontamination and therefore never saw actual reactor service. The Task Force report cautioned that longer term exposures after decontamination might reveal effects related to subsequent crack initiation.[18]

Laboratory tests of the CAN-DECON LND-101A reagent and studies of its possible contribution to the corrosion of reactor structural materials were conducted in 1984 by the General Electric Co. under EPRI sponsorship.[19] Three LWR structural materials, namely sensitized Type 304 stainless steel, Inconel 600, and SA 533 Grade B pressure-vessel low-alloy steel, were evaluated in laboratory tests. Decontamination processing for 48 h at 120°C in a 0.1 wt. % solution of LND-101A produced relatively high corrosion rates of about 0.18 mm/day in the low alloy steel, but the rates for the other two

alloys were of the order of 10^{-3} mm/day. However, the decontamination process was found to have produced IGA to a depth of about 0.2 mm (2 to 3 grain diameters) in the Type 304 stainless steel specimens and 0.09 mm (~3 grain diameters) in the Inconel 600 specimen. In addition, surface pitting was observed in these latter two materials. Subsequent constant extension rate tensile (CERT) tests at 288°C (550°F) in water containing 0.2 ppm dissolved oxygen indicated an increased susceptibility to stress corrosion cracking (SCC) in the sensitized Type 304 stainless steel. In the case of field-decontaminated Type 304 stainless steel BWR pipe welds, shallow IGA was observed in the heat affected zone, and dense shallow pits were found in one specimen. However, neither of these features adversely affected the IGSCC resistance of these specimens as measured by CERT tests.

As a follow-up to the General Electric study, London Nuclear conducted a comprehensive review of general, galvanic, crevice, and pitting corrosion data and SCC test results for the CAN-DECON process obtained by them and others over a number of years.[16,20-23] The alloys evaluated included several carbon steels, austenitic and ferritic stainless steels, nickel-base alloys, Zircaloy-2, and Stellite 6. The LND-101A reagent concentrations in these tests ranged from 0.05 to 0.3 wt. %; solution temperatures ranged from 25 to 135°C; and decontamination times ranged from 6 to 550 h. This study concluded that the LND-101A solution does not, in general, produce any undesirable corrosion effects in the evaluated alloys. The highest corrosion rates were observed in the carbon steels, with a maximum rate of about 0.19 mm/day. However, this rate could be reduced by about a factor of 10 by the addition of suitable corrosion inhibitors. Non-sensitized Type 304 stainless steel and Inconel 600 showed no increase susceptibility to IGSCC. In the sensitized conditions, these two alloys showed a significant susceptibility to IGSCC after a 500-h treatment when the solution contained no ferric ions. The addition of ferric ions at concentrations of ~50 to 80 ppm in the decontaminant solution eliminated the susceptibility to IGA and IGSCC. The enhanced IGA and IGSCC susceptibility previously observed in the General Electric studies was therefore attributed to a lack of ferric ions in solution, a condition that would not normally be present during actual reactor decontamination, except possibly for a brief period near the beginning of the decontamination process. For this reason London Nuclear has introduced a reformulated version of LND-101A, known as Rem-E-D, which contains ferric citrate additions to ensure a sufficiently high concentration of ferric ions during the initial stages of decontamination. In addition, London Nuclear concluded that the presence of oxalic acid in the LND-101A reagent can lead to IGA of certain alloys under severe conditions. Therefore, reagent LND-107, in which the oxalic acid has been removed, was also introduced as an alternative modification of the original LND-101A.[13]

LOMI Process

The LOMI (low oxidation-state metal ion) decontamination process[24] was developed by the Central Felectricity Generating Board in Great Britain, and is currently licensed to several firms for use in the United States. The decontaminating reagent consists of low concentrations of picolinic acid and

vanadium (II) formate plus a chelating agent, and the process works by converting the ferric ions in the oxide layer on the contaminated component surfaces to the more soluble ferrous ions, with the V^{2+} ions serving as the reductant. For PWR oxide films, which typically have a higher Cr concentration, prior alkaline or nitric acid permanganate (AP or NP) oxidation treatments are commonly used. The LOMI reagent is injected into the circulating reactor coolant as with the CAN-DECON process, and a side stream of circulating coolant plus decontamination solution is again passed through a filter and cation exchange resing columns to regenerate the chelant. The normal decontamination temperature of 80 to 90°C (176 to 194°F) for the LOMI process is somewhat lower than the decontamination temperature for the CAN-DECON process.

Both General Electric Company[19] and Pacific Northwest Laboratories (PNL)[25] have conducted studies on the corrosive effects of the LOMI process on LWR structural materials. The General Electric study found the general corrosion rates of SA533 Grade B carbon steel, Type 304 stainless steel, and Inconel 600 to be approximately one order of magnitude lower in the LOMI reagent than in the CAN-DECON reagent, and no IGA or increased susceptibility to SCC was observed. PNL similarly found that both lightly and heavily sensitized Type 304 stainless steel and Inconel 600 specimens exhibited low general corrosion rates in the LOMI solution. The Inconel 600 specimens exhibited some shallow pitting after AP, AP/NP, and AP/NP/LOMI treatments, but the pits repassivated in subsequent post-filming. No IGA or increased susceptibility to SCC was observed under any of the test conditions for either alloy studied by PNL.

Chemical Cleaning of Steam Generators

In the past nine years, the Electric Power Research Institute Steam Generators Owners Group has developed solutions for the chemical cleaning of the secondary side of PWR steam generators to remove Fe and Cu corrosion produce sludge deposits. Because of the large volume of material to be removed, the solutions tend to be more concentrated than those used for primary system decontaminations, and the formulations that have been developed for the Fe and Cu removal steps are somewhat different.[26-28] The principal active ingredient in both cases is ammonium EDTA (ethylene-diaminetetraacetic acid), which is present at a concentration of 10 wt. % in the Fe solvent and 5 wt. % in the Cu solvent. The Fe solvent also contains 1 wt. % hydrazine to reduct Fe^{3+} to Fe^{2+}, which is more easily complexed by EDTA. The two solvents are typically used sequentially, with interspersed rinses, and the application temperatures are 88 to 96°C (190 to 205°F) for the Fe solvent and 32 to 43°C (90 to 110°F) for the Cu solvent. In addition, a stronger solvent containing 20 wt. % ammonium EDTA has been developed for dissolving sludge from crevices.

These concentrated solutions are potentially more corrosive than the dilute solutions used in primary system decontamination, and a series of corrosion tests was carried out during their development.[26,29,30] This series consisted mostly of general corrosion tests, but limited crevice, galvanic,

pitting, and U-bend tests were also conducted. Essentially all of the alloys found in PWR steam generators were tested; weldments and sensitized test specimens were included. Corrosion coupons were also included as a part of the Millstone 2 steam generator cleaning conducted in 1985.[27] For the most part, the general corrosion rates of the carbon and low-alloy steels have typically been found to be less than 0.13 mm (5 mils) per application, and serious galvanic, crevice, or pitting effects were generally not observed. In view of the limited number of steam generator cleanings expected over the life of a PWR, these rates appear to be acceptable. However, unacceptably high localized corrosion rates of carbon and low-alloy steels were observed in some sample weldments, particularly when galvanically coupled to Inconel 600. This effect appears to be influenced most strongly by variations in solvent corrosion inhibitor and weld configuration. Additional site-specific weld region corrosion testing and qualification was recommended before using the chemical cleaning process at a specific plant.

POSSIBLE INTERACTIONS BETWEEN DECONTAMINATION AND AGING

The aging effects discussed above are produced by metallurgical changes that occur throughout the volume of the material, and one would not expect these bulk aging effects to be significantly influenced by decontamination, which is a surface process. However, the microstructural changes produced at the surface of a component by an aging process such as low-temperature sensitization may affect the response of that component to decontamination. Decontamination surface effects can, in turn, greatly influence subsequent corrosion and crack initiation and growth at the component surface. Thus, the principal interaction between decontamination and metallurgical aging is likely to be the effect of aging on decontamination response and the subsequent effect of any surface changes produced by decontamination on corrosion and crack initiation and growth.

An early concern with decontamination was that it might cause IGA and possibly an increased susceptibility to SCC, particularly in sensitized material. This concern has been shown to have some basis in fact for the CAN-DECON process under certain severe conditions, as discussed above. However, the follow-up tests performed by London Nuclear and others provide persuasive evidence that IGA and SCC would not be expected under normal decontamination conditions, and, in addition, the CAN-DECON reagents have been reformulated to further reduce the likelihood of such problems.

The relatively high general corrosion rates observed for carbon and low-alloy steels in the CAN-DECON LND 101A reagent are also of concern. Corrosion rates approaching 0.2 mm/day have been observed, and repeated decontaminations, as during extended-life operation, could lead to corrosion wastages in excess of the corrosion allowances for some components. The presence of cracks through the weld-deposited austenitic stainless steel cladding of the reactor pressure vessel would locally expose the underlying low-alloy steel to these solutions. Corrosion inhibitors have been found effective in reducing corrosion rates, but the sulfur compounds commonly

found in these inhibitors may cause pitting in the austenitic stainless steels. In the case of the LOMI reagent, the general corrosion rates of the carbon and low-alloy steels are about an order of magnitude lower, but excessive corrosion may still occur in PWR decontaminations during the NP oxidizing pretreatment. For both BWR and PWR decontaminations, very little data are available on possible corrosion effects on the high-strength Ni-base alloys used for core structural applications.

The effects of decontamination on aged cast duplex stainless steels have not been evaluated experimentally. The concern here is that, under certain conditions, decontamination might produce microscopically sharp surface irregularities through such localized corrosion processes as IGA, galvanic corrosion at the boundaries between the ferrite and austentite grains, or preferential attack of one of the two phases. These irregularities could, in turn, contribute to reduced impact strength by acting as points of stress concentration. This problem would be aggravated under conditions of extended-life service, since repeated decontaminations would accentuate the surface irregularities and the duplex alloys would have more time to embrittle because of aging effects.

Finally, additional data are needed on the corrosive effects of the more concentrated solutions used to clean the secondary sides of steam generators. The localized corrosion of carbon and low-alloy steel weldments has been discussed above, and the contribution of this wastage to the possible fatigue cracking of secondary feedwater lines owing to cyclic thermal stresses produced by stratified flows must be considered.[31] In addition, further studies are needed on possible IGA and SCC effects in alloys that have been sensitized by long-term aging. It should also be noted that Pacific Nuclear Corporation and KWU are presently developing alternative chemical cleaning solutions, and the possible corrosive effects of these processes will require careful evaluation.

SUMMARY

In summary, the considerable body of data on and experience with the chemical decontamination of nuclear reactor primary systems indicate no severe materials corrosion problems. However, concerns remain in several areas, including (1) the high corrosion rates of carbon and low-alloy steels in the CAN-DECON and possibly in the LOMI NP processes, and the effects of corrosion inhibitors on the pitting of stainless steels; (2) the possible non-uniform corrosion of the cast duplex stainless steels that results in the introduction of microscopic surface features which may accentuate possible aging embrittlement in these materials; and (3) the very limited data available on the high-strength Ni-base alloys used for core structural applications and on materials subjected to long-term aging. Additional data are needed on possible localized corrosion and SCC effects associated with the chemical cleaning of the secondary side of PWR steam generators, particularly on aged and sensitized steam-generator alloys and weldments. These concerns and data needs will be addressed in the experimental portion of the present program.

REFERENCES

1. A. K. Banerjee, C. F. Bergeron, and W. B. Dodson, "An Approach to Nuclear Power Plant Life Extension," Nucl. Saf. 27 (1986), 385-390.

2. C. A. Negin, L. A. Goudarzi, L. U. Kenworthy, and M. E. Lapides, "Planning Study and Economic Feasibility for Extended Life Operation of Light Water Reactor Plants," Report TPS 78-788 (CONF-790923), Electric Power Research Institute (September 1979).

3. C. A. Negin, R. S. Walker, and S. B. Shantzis, "Extended Life Operation of Light Water Reactors: Economic and Technological Review," EPRI NP-2418, Electric Power Research Institute (June 1982).

4. Northern States Power Company, "BWR Pilot Plant Life Extension Study at the Monticello Plant: Phase 1," EPRI NP-5181M, Electric Power Research Institute (May 1987).

5. R. B. Minogue, "Trends in Nuclear Safety Research--Looking Ahead to the 1990's," Proc. Thirteenth Water Reactor Safety Research Information Meeting," NUREG/CP-0072, Vol. 1 (February 1986), pp. 1-8.

6. U. S. Nuclear Regulatory Commission, "Nuclear Plant Aging Research (NPAR) Program Plan," NUREG-1144 (July 1985).

7. M. J. Povich, "Low Temperature Sensitiztion of Type 304 Stainless Steel," Corrosion 34 (1978), 60-65.

8. M. J. Povich and P. Rao, "Low Temperature Sensitiztion of Welded Type 304 Stainless Steel," Corrosion 34 (1978), 269-275.

9. O. K. Chopra and H. M. Chung, "Aging Degradation of Cast Stainless Steel," Proc. Fourteenth Water Reactor Safety Research Information Meeting," NUREG/CP-0082, Vol. 2 (February 1987), pp. 119-142.

10. R. A. Shaw, "Getting at the Source: Reducing Radiation Fields," Nucl. Technol. 44, (1979), 97.

11. J. E. LeSurf and G. D. Weyamn, "Cost-effectiveness of Dilute Chemical Decontamination," Proc. 1981 ANS Winter Mtg., San Francisco, CA, Nov. 29-Dec. 3, 1981; Trans. Am. Nucl. Soc. 39 (1981), 865.

12. C. J. Wood, "Decontamination Helps Control Nuclear-maintenance Costs," Power 129 (January 1985), 29-33.

13. R. Knox, "How Independent Tests Have Eliminated Can-Decon Corrosion Concerns," Nucl. Eng. Int. 32 (March 1987), 48-51.

14. J. F. Remark, "Plant Decontamination Methods Review," EPRI NP-1168, Electric Power Research Institute (March 1981).

15. J. L. Smee, "Decontaminating LWRs with Can-Decon Dilute Processes," Nucl. Eng. Int. 30 (January 1985), 29-33.

16. J. P. Michalko, P. J. Bonnici, and J. L. Smee, "Compilation of Corrosion Data on CAN-DECON™, Volume 1: General, Galvanic, Crevice, and Pitting Corrosion Data from CANDU and BWR Tests," EPRI NP-4222, Vol. 1, Electric Power Research Institute (October 1985).

17. Anon., "Decon Cracking Fears are Allayed," Nucl. Eng. Int. 29 (October 1984), 11.

18. Anon., "Does Can-Decon Encourage Pipe Cracking?," Nucl. Eng. Int. 30 (February 1985), 13.

19. M. T. Wang, "Corrosion Evaluation of Two Processes for Chemical Decontamination of BWR Structural Materials," EPRI NP-4356, Electric Power Research Institute (December 1985).

20. J. P. Michalko and J. L. Smee, "Compilation of Corrosion Data on CAN-DECON™, Volume 2: Influence of CAN-DECON on Stress Corrosion Cracking--Summary of Testing, 1975-1983," EPRI NP-4222, Vol. 2, Electric Power Research Institute (October 1985).

21. P. J. King and B. D. Warr, "Compilation of Corrosion Data on CAN-DECON™, Volume 3: Influence of CAN-DECON Process on Stress Corrosion Cracking--1984 Constant-Extension-Rate Tests," EPRI NP-4222, Vol. 3, Electric Power Research Institute (January 1987).

22. J. L. Smee and V. C. Turner, "Compilation of Corrosion Data on CAN-DECON™, Volume 4: General, Galvanic, Crevice, Pitting, and Stress Corrosion Data From PWR Tests and Applications," EPRI NP-4222, Vol. 4, Electric Power Research Institute (January 1987).

23. J. L. Smee and V. C. Turner, "Compilation of Corrosion Data on CAN-DECON™, Volume 5: Influence of the CAN-DECON™ Process on Stress Corrosion Cracking--Summary of Testing 1984-1985," EPRI NP-4222, Vol. 5, Electric Power Research Institute (January 1987).

24. A. Cruickshank, "Developing Techniques for Decontamination," Nucl. Eng. Int. 28 (November 1983), 41-44.

25. R. L. Clark and R. L. McDowell, "Corrosion Testing of LOMI Decontamination Reagents," EPRI NP-3940, Electric Power Research Institute (March 1985).

26 P. C. Hildebrandt, J. E. Nestell, R. C. Trench, and R. D. Varrin, "Weld Region Corrosion During Chemical Cleaning of PWR Steam Generators, Vol. 1: Overview and Discussion," EPRI NP-5267, Vol. 1, Electric Power Research Institute (July 1987).

27. N. R. Stolzenberg and R. C. Thomas, "Employing a Chemical Method for Tubesheet Sludge Removal," Nucl Eng. Int. 32 (January 1987), 39-41.

28. Anon., "Removing Magnetite from the Oconee Steam Generators," Nucl. Eng. Int. 32 (March 1987), 51-52.

29. E. L. Capener, G. R. Egan, and T. J. Feiersen, "PWR Steam Generator Chemical-Cleaning Data Base," EPRI NP-3477, Vols 1 & 2, Electric Power Research Institute (April 1984).

30. J. L. Barna et al., "Weld Region Corrosion During Chemical Cleaning of PWR Steam Generators, Vol. 2: Tests and Analyses," EPRI NP-5267, Vol. 2, Electric Power Research Institute (July 1987).

31. Investigation and Evaluation of Cracking Incidents in Piping in Pressurized Water Reactors, Report of the USNRC PWR Pipe Crack Study Group, NUREG-0691 (September 1980).

POTENTIAL PROBLEMS ASSOCIATED WITH ION-EXCHANGE RESINS USED IN THE DECONTAMINATION OF LIGHT-WATER REACTOR SYSTEMS*

P. Soo, J.W. Adams, C.R. Kempf
Brookhaven National Laboratory, Upton, NY 11973

ABSTRACT

During a typical decontamination event, ion-exchange resin beds are used to remove corrosion products (radioactive and non-radioactive) and excess decontamination reagents from waste streams. The spent resins may be solidified in a binder, such as cement, or sealed in a high-integrity container (HIC) in order to meet waste stability requirements specified by the Nuclear Regulatory Commission. Lack of stability of low-level waste in a shallow land burial trench may lead to trench subsidence, enhanced water infiltration and waste leaching, which would result in accelerated transport of radionuclides and the complexing agents used for decontamination. The current program is directed at investigating safety problems associated with the handling, solidification and containerization of decontamination resin wastes. The three tasks currently underway include freeze-thaw cycling of cementitious and vinyl ester-styrene forms to determine if mechanical integrity is compromised, a study of the corrosion of container materials by spent decontamination waste resins, and investigations of resin degradation mechanisms.

1. INTRODUCTION

During light-water reactor operation, components in the primary system become radioactive because of the deposition of corrosion products which are transported from the core regions by the coolant. In order to minimize worker exposure to radiation during routine maintenance operations, industrial procedures have been developed to chemically remove the corrosion products and the activity that they contain. After the corrosion products have been removed by organic reagents the waste stream is passed through mixed (anion/cation) resin beds which remove residual reagent and the radioactive and non-radioactive ions in solution. The resins are either sealed in high-integrity containers, or they may be solidified in cement or some other matrix, in order to meet structural stability requirement specified in the NRC Technical Position on Waste Form (NRC, 1983).

* Work performed under the auspices of the U. S. Nuclear Regulatory Commission.

The current program is an effort to evaluate the solidification processes that are being used in industry for decontamination waste, and to determine how the wastes behave during on-site storage and subsequent disposal at a shallow-land burial site. Particularly important are the corrosion of container materials by spent resins, and resin degradation mechanisms which could lead to gas generation and pressurization of sealed containers. Another important consideration involves the potential for the cracking of cement-based decontamination waste forms by alternate freeze-thaw cycling. Such temperature excursions may occur during the storage period prior to disposal when daily temperature excursions could result in the freezing and thawing of water in the cement pore structure, resulting in waste form cracking.

Below are described results to date in the current program. The freeze-thaw cycling effort is close to completion, the container corrosion work will continue for approximately 1 more year to obtain long-term performance data, and the resin degradation effort is currently being initiated.

2. THERMAL-CYCLING OF ION-EXCHANGE-RESIN/BINDER COMPOSITES

2.1 Background

The purpose of this task is to examine the effects of possible temperature variations on solidified ion-exchange resin decontamination wastes during above-ground storage and transportation. Testing, as outlined in the NRC Technical Position on Waste Form, has been completed. The method calls for 30 complete cycles, each with a temperature sequence of -40°C, 20°C, 60°C and 20°C, maintaining a uniform specimen temperature at each step for one hour before proceeding. Following completion of the test, samples were examined for free liquid generation, degradation, and changes in compressive strength with respect to non-cycled controls. In addition, at least one sample was immersion tested in water following thermal cycling. Test specimens included simulated ion-exchange resin decontamination wastes, solidified in cement and vinyl ester-styrene (VES) binders. Test forms were right cylinders, nominally measuring 2 inches in diameter and 4 inches high.

2.2 Test Procedures

The wastes were dewatered mixed-bed resins of four types: 1) one-to-one by volume of polystyrene anion resin (as-received, OH- form) to polystyrene cation resin (fully saturated with Fe^{2+}), 2) one-to-one polystyrene anion resin (fully loaded with LND-101A reagent) to polystyrene cation resin (fully saturated with Fe^{2+}), 3) polyacrylic anion resin (as-received, free base form) and polystyrene cation resin (as-received, H^+ form) in a 2:1 volume ratio, and 4) polyacrylic anion resin (half of which was fully loaded with formic acid, half of which was fully loaded with picolinic acid) and polystyrene cation resin (as-received, H^+ form) in a 2:1 ratio. These wastes will be referred to respectively as PSC, PSL, PAC, and PAL to indicate the type of anion resin and whether it was loaded with decontamination reagent or

Table 1 Ion exchange resin loadings used in simulated decontamination waste streams.

Resin	As-Received Form	Wt. of Resin(g)	Total Exchange Capacity (eq)*	Reagent	Wt. of Reagent in solution (g)	Wt. of Reagent loaded on resin (g)	Loading Efficiency (% of total exchange capacity)
IONAC A-365	NH_2	6000	31.68	Picolinic Acid	3352.0	2830.3	73
IONAC A-365	NH_2	6000	31.68	Formic Acid	1440.4	1171.0	80
IRN-78	OH^-	1200	2.11	LND-101A	141.50	141.50	100
IRN-77	H^+	1200	2.70	$FeSO_4.7H_2O$	380.00	368.2	98
*Based on manufacturer's minimum specification for dewatered resin							

used in the as-received (control) form. In discussing results in the following section, these identifiers will be prefaced by a "C": for wastes solidified in Portland Type I cement or "V" for wastes solidified in VES. Data on the resin loadings are given in Table 1. Formulations for the encapsulation of the resins in cement and VES are given in Table 2.

The cement-based forms were made with a waste (dewatered resin and water) to cement ratio of 0.60 and a water to cement ratio of 0.40 by weight. For the VES forms the waste to binder ratio was 2.24 by weight and the water to binder ratio was 1.12.

Forms for thermal cycling were weighed and measured after removal from the solidification molds. The forms were placed, unsupported, in glass containers measuring about 3 inches in diameter and 6 inches high with a tightly sealed screw cap. Cure times for the forms ranges from 50 to 55 days. Thermal cycling was started at the same time for all forms except picolinate and formate-loaded mixed-bed resins solidified in VES. Four forms of each waste/binder combination were thermally cycled and four were maintained at 20°C over the duration of the test.

Cycling of the samples was carried out according to the following schedule:

Table 2 Formulations used for solidification of simulated mixed-bed resin decontamination wastes.

Code*	Anion Resin (Form)	Wt. Anion Resin (g)	Cation Resin (form)	Wt. Cation Resin (g)	Wt. Water (g)	Wt. Binder (g)**	Waste pH*** before Adjustment	Wt. NaOH Added to Waste (g)	pH of Final Waste
CPSC	IRN-78 (OH^-)	187.5	IRN-77 (Fe^{2+})	187.5	750.0	1875.0	≈6.2	3.2	12.0
CPSL	IRN-78 (LND-101A)	187.5	IRN-77 (Fe^{2+})	187.5	750.0	1875.0	5.3	5.7	12.0
CPAC	IONAC A-365 (NH_2)	250.0	IRN-77 (H^+)	125.0	750.0	1875.0	5.8	0	5.8
CPAL	IONAC A-365 (LOMI)	250.0	IRN-77 (H^+)	125.0	750.0	1875.0	3.3	0	3.3
VPSC	IRN-78 (OH^-)	280.0	IRN-77 (Fe^{2+})	280.0	560.0	500.0	≈7.0	0	≈7.0
VPSL	IRN-78 (LND-101A)	280.0	IRN-77 (Fe^{2+})	280.0	560.0	500.0	5.2	0	5.2
VPAC	IONAC A-365 (NH_2)	373.3	IRN-77 (H^+)	186.7	560.0	500.0	≈5.7	0	≈5.7
VPAL	IONAC A-365 (LOMI)	373.3	IRN-77 (H^+)	186.7	560.0	500.0	3.2	26.9	6.0

* The first letter indicates the binder (C=cement, V=vinyl ester-styrene); the second and third letters indicate the type of anion resin in the waste (PS=IRN-78, PA=IONAC A-365); and the fourth letter indicates whether the anion resin is loaded with decontamination reagent (C=control, L=loaded).

** The binder for cement formulations was Portland I cement. The binder for VES formulation was styrene monomer and does not include the weights of promoter and catalyst added.

*** The term "waste" refers to the slurry of dewatered anion and cation resin plus the water required for batch solidification.

7.5 h at -40°C,
Overnight (≈16.5 h) at 20°C
4.5 h at +60°C,
Overnight (≈19.5 h) at 20°C.

To ensure that uniform temperatures were established through the samples, one waste form for each formulation was drilled and fitted with a Type K thermocouple. Temperatures were maintained to within ± 2°C at the set point temperature. During weekends, temperatures were kept at ambient temperature (≈ 22°C).

2.3 Results

2.3.1 Thermal Cycling of Polyacrylic Anion Resin/Cement Composites

Cement-based control forms containing as-received IONAC A-365 anion resin and IRN-77 cation resin (CPAC) began cracking after two cycles (Figure 1). Cracking occurred in the lower two thirds of the forms and it became more severe with an increasing number of cycles, as can be seen in Figures 1B and 1C. After 30 cycles, almost complete disintegration of the samples occurred. On the other hand, LOMI-loaded polyacrylic resin/cement samples (CPAL) showed no cracking after 13 cycles but, after the full 30 cycles was completed, the specimens showed basically similar but slightly less disintegration than the CPAC controls. The presence of the simulated LOMI reagent on the anion resin apparently minimizes the rate of damage from freeze-thaw cycling.

As expected, uncycled forms, loaded or unloaded with simulated LOMI reagent, showed no tendency to crack.

2.3.2 Thermal Cycling of Polystyrene Anion Resin/Cement Composites

Cement forms containing LND-101A/Fe^{2+} type waste (polystyrene anion and polystyrene cation mixed-bed resins) only began to show effects from thermal cycling after about 20 cycles. Figure 2 shows a typical CPSC form (containing as-received anion and Fe^{2+} loaded cation resin) after 20 cycles, with cracking present near the base of the form. Figure 3 shows the most severe effect of any CPSL form (containing LND-loaded anion and Fe^{2+} loaded cation resin). Near-surface stresses have caused slight spalling on the lower portions of these samples; however, no large structural cracks were noticed.

After the full 30 cycles, cracking of the control and loaded-anion resin forms was still restricted to the lower quarter of the samples. It also appears that the forms containing the LND-101A reagent were less prone to cracking compared to the reagent-free controls.

2.3.3 Thermal Cycling of VES Forms

All VES forms maintained their monolithic structure during the 30 thermal cycles. One form, however, containing polystyrene anion resin loaded

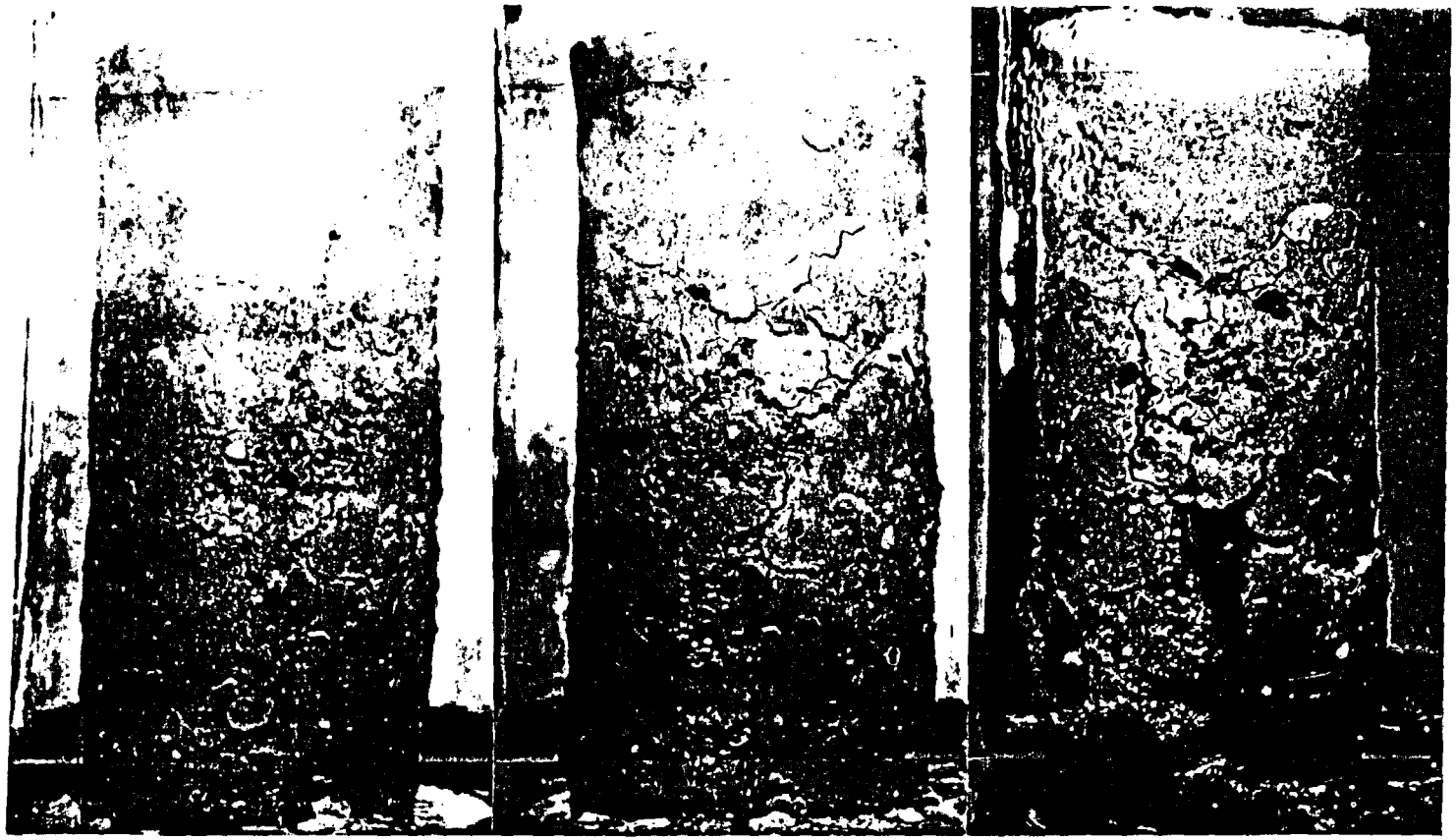

(A) (B) (C)

Figure 1 Cement form containing as-received polyacrylic anion resin (free base form) and as-received polystyrene cation resin (H^+ form) in a 2:1 volume ratio, photographed after (left to right) 2, 5, and 13 thermal cycles. A replicate sample is shown in Figure 4.

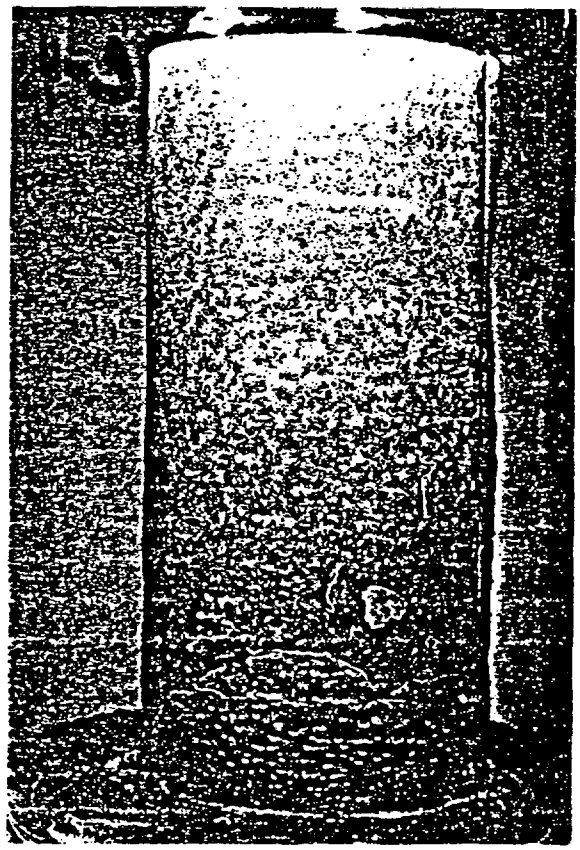

Figure 2 Cement form containing a 1:1 mixture of IRN-78 anion resin (as received, OH^- form) and IRN-77 cation resin (Fe^{2+} form), after 20 thermal cycles.

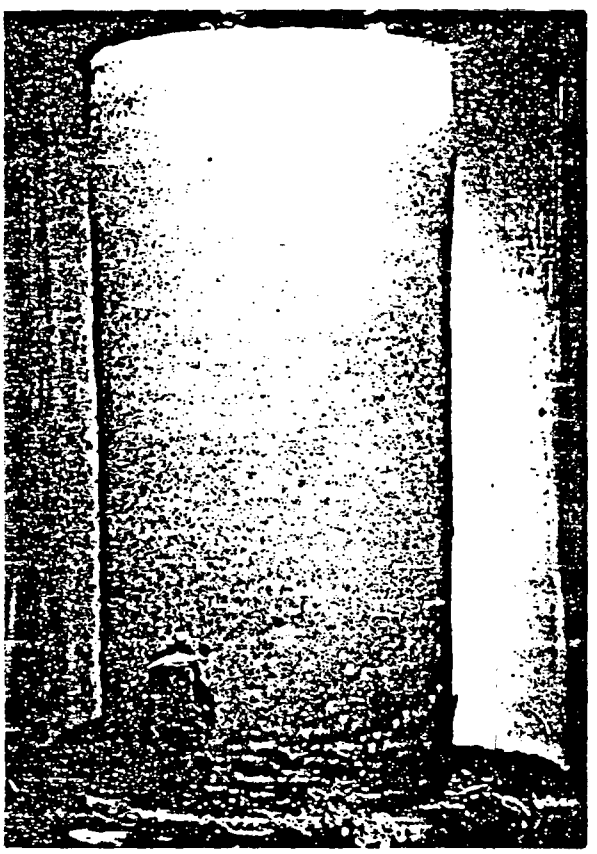

Figure 3 Cement form containing a 1:1 mixture of IRN-78 anion resin (fully loaded with LND-101A reagent) and IRN-77 cation resin (fully loaded with Fe^{2+}), after 20 thermal cycles.

with LND-101A reagent (VPSL type) did develop slight surface irregularities but this was probably a result of its being the last of 9 samples cast from a large batch. It is thought that the VES mixture was less adequately mixed at the bottom of the container resulting in a non-representative composition for this form.

2.3.4 Other Tests on Cement and VES Forms

Table 3 shows compressive strength measurements for the control and loaded forms, together with the amounts of free liquid generated during thermal cycling. The compressive strengths for the cement forms were based on the maximum load attained in the test, whereas for VES forms the strength was based on the load at 10% strain. Usually, forms containing polystyrene anion resin had marginally higher strengths compared to forms containing polyacrylic anion resin, and control forms (as-received resins) were marginally stronger than corresponding forms containing resins loaded with decontamination reagent. No free liquid was observed for any cement samples. However, large amounts of free liquid were generated as cycling of VES samples progressed. One VES form containing LOMI reagent generated about 10.6 g of liquid which, being mainly water, represents a volume of about 10.6 mL. Since a typical 2" diameter x 4" long form has an approximate volume of 206 mL the amount of free liquid in this particular case is about 5.2% by volume. This is far in excess of the maximum 0.5% for solidified wastes recommended in the Technical Position on Waste Form. However, non-cycled VES and cementitious forms, evaluated here, meet this recommendation. Note that all forms easily passed the 50 psi compressive strength recommendation, even cement samples containing large cracks.

Non-cycled cement forms immersed in water appear to show the same relative mechanical integrity as when thermal cycled, i.e., the CPAC form (containing as-received polyacrylic anion and polystyrene cation resin) spalled and cracked within one day after immersion, and the CPAL form (containing LOMI-loaded polyacrylic anion and as-received polystyrene cation resin) spalled after a slightly longer time (about one week). Figure 4 shows an individual CPAC form after immersion times of 2 h and 4 d. Much different behavior was observed for the CPSL and CPSC forms (containing LND-loaded and as-received polystyrene anion resins and Fe^{2+} saturated cation resins) which after about 6 weeks of immersion remain intact.

Immersion tests on the cycled and non-cycled VES forms have been underway for 6 weeks and no loss of integrity is noticeable. However, one of the PSL samples described in Table 3, which gave off a large amount of free liquid during thermal cycling, is actually floating in the water bath.

2.4 Discussion

From these results it is clear that cementitious waste forms containing the polyacrylic-based anion resins are far more susceptible to freeze-thaw cracking compared to those containing polystyrene-based anion resins. Loading of the polyacrylic anion resin with LOMI reagent and the polystyrene

Table 3 Compressive strengths and free-liquid for cement and vinyl-ester styrene decontamination waste forms.

Binder	Resin Type	Compressive Strength (psi)	Free Liquid in Container (g)
Cement (Non-cycled)	PAC	4460±151	0
	PAL	4359±124	0
	PSC	4818±134	0
	PSL	4774±156	0
Cement (Cycled)	PAC	Not tested(1)	0
	PAL	3981(2)	0
	PSC	3374±250(3)	0
	PSC	4414±355(4)	0
	PSL	4538±339(5)	0
VES (Non-cycled)	PAC	1446±10	0.8±0.2
	PAL	To be det.	To be det.
	PSC	1540±11	0.5±0.1
	PSL	1423±17	0.6±0.2
VES (Cycled)	PAC	1645±77	4.9±1.5
	PAL	To be det.	To be det.
	PSC	1570±102	4.3±1.8
	PSL	1689±16	10.6±1.6

1. All four forms were severely cracked during thermal cycling.

2. Only one form was compression tested. Three other forms were severely cracked during thermal cycling.

3. Value is for tests on cracked portion of the forms.

4. Value is for forms which were not cracked or where the cracked portion has been removed prior to compression testing.

5. For one form, cracked portion near bottom of form was removed prior to compression testing.

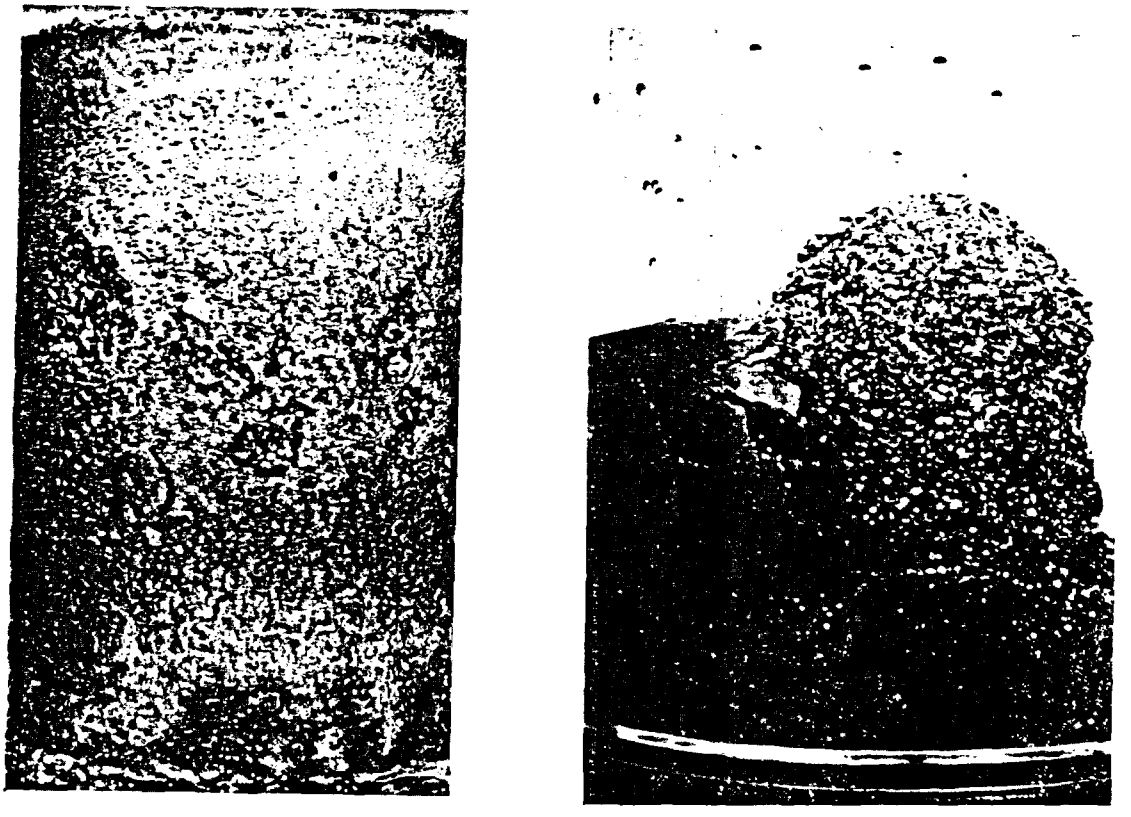

Figure 4 Photograph of cement form containing as-received polyacrylic anion resin and as-received polystyrene cation resin after 2 hours and 4 days immersion in deionized water. The form was a non-cycled control. Magnification 1X.

anion resin with LND-101A reagent appears to retard the tendency of the cement forms to crack when compared with non-loaded controls. However, the reagents only slightly reduce the final severity of the cracking phenomenon.

Three mechanisms may be proposed as contributors to the cracking observed in these cement waste forms:

(i) Free (pore) water, which may accumulate in the lower part of the form during curing by the action of gravity or, during thermal cycling, by means of evaporation, condensation, and resorption. This water freezes during the low temperature part of the cycles and causes volumetric increases which stress the cement structure to failure (Lea, 1971). Horizontal water marks on the cement samples after cycling prove that the lower portions of the forms become loaded with excess water during the cycling process.

(ii) During solidification in the cement paste, the anion and cation resins lose water to the cement hydration process. Upon immersion, water is reabsorbed by the resins and the swelling pressures exert enough stress to cause cracking of the form.

(iii) The cation (IRN-77) resins which are used in the H^+ form undergo ion exchange with constituents, such as Ca^{2+}, from the cement paste during solidification. The effective size of the resin is increased and this, in turn, causes the cement structure to crack.

Severe cracking during immersion of the cementitious forms containing simulated LOMI reagent (CPAL), and the non-loaded controls (CPAC), is probably connected with the presence of cation resins in the as-received H^+ form (mechanism iii). In contrast, forms containing IRN-77 resins loaded with the Fe^{2+} ion (CPSA and CPSL forms, also containing polystyrene-based anion resins) show no evidence of cracking after six weeks of immersion. This could be explained on the basis that the Fe^{2+} loaded cation resins are stable and do not undergo expansion by ion-exchange reactions with the cement components. Further studies are being carried out to fully characterize the immersion test results in this study.

A further contributing factor could be the total amount of water that is used in the formulation. Since resins which are mixed with cement and water during solidification are typically measured in a damp (dewatered) state, the net amount of free water could vary quite widely from one type of cementitious form to another depending on the type of resin used and the ionic loading of the resin. New "control" thermal-cycle tests are currently being performed to determine whether those forms most susceptible to cracking contain the largest amounts of water. However, a definitive correlation between cracking severity and total water content in a form probably cannot be made unless the amount of free (i.e., pore) water available for freezing can be distinguished from the molecules of water present in the hydrated cement and in the resin beads.

3. COMPATIBILITY OF CONTAINER MATERIALS WITH DECONTAMINATION WASTE RESINS

3.1 Background

In some instances, bead resins are not solidified in a matrix, such as cement, to meet the NRC waste stability requirement. Instead, some generators opt to place spent resins in "high integrity containers" (HICs) which

themselves meet the stability requirement. The current task was designed to check the corrosivity of LOMI-loaded mixed-bed resins to selected metallic and polymeric HIC materials. A range of other materials was added to the list of materials studied because of available space in the test vessels. Two different batches of resin were prepared in this study, and they are identical to the control (unloaded) and picolinate/formate loaded resin batches used to prepare the cement forms for the thermal-cycling study, described above. The initial moisture contents of the resin batches were 47.3% by weight for the LOMI-loaded batch and 52.7% for the control batch, based on oven drying of some of the resins.

3.2 Test Procedures

The two HIC materials being studied are high-density polyethylene (HDPE) and Ferralium-255 (a duplex stainless steel). TiCode-12 (a dilute titanium alloy), Type 304 stainless steel, and Type 316 stainless steel were also included. TiCode-12 is very resistant to a wide range of corrosive environments whereas Types 304 and 316 stainless steel are moderately resistant. Carbon steel was added to the test materials later in the program, as some original specimens were deemed surplus, and removed. Ferralium was tested in the as-welded state, and HDPE was prepared in the form of stressed (U-bend) specimens. All other materials were prepared as metallographically polished flat coupons.

Gamma irradiation was incorporated into the test procedure since it is usually present in low-level decontamination wastes. Four separate batches of samples were tested for corrosion while they were in intimate contact with the mixed bed resin. They include:

(i) Specimens exposed to unloaded resins and left unirradiated.

(ii) Specimens exposed to LOMI-loaded anion resin and left unirradiated.

(iii) As for (i) above but irradiated in a gamma field.

(iv) As for (ii) above but irradiated in a gamma field.

The metal specimens were placed in two layers in a vertical resin column contained in a glass cylinder approximately 30 cm tall and 8 cm in diameter. The bottom layer of specimens was laid on the flat bottom of the glass container and covered with resin. A similar layer was placed in the middle of the resin column. Four HDPE U-bend specimens were placed in the column between the layers of metal specimens. Two specimens were prepared such that the oxidized surface layer, formed during high-temperature rotary molding of the container, was on the outer bend of the sample. Since oxidized HDPE is more brittle than non-oxidized material, sharp cracks were formed during the bending process. The other two specimens were bent such that the unoxidized surface was on the outer bend surface. No cracks were present. The two resin/specimen columns to be irradiated were placed in sealed stainless steel vessels and emplaced in the BNL gamma irradiation facility. The irradiation

temperature was about 12°C and the gamma dose rates were in the 1 x 10^4 to 2 x 10^4 rad/h range. The two batches of unirradiated specimens were sealed with "Parafilm" and placed in a refrigerator maintained at about 10°C.

3.3 Results

To date, the irradiated specimens have been examined once, after an accumulated gamma dose of 5 x 10^7 rads. The unirradiated controls have also been examined for comparison purposes. Examination involves carefully removing the resin above the various specimen locations and checking the coupons for evidence of attack.

Figure 5 shows the appearance of the top layer of specimens after removal of the overlying unloaded resin. They had been exposed to a dose of 5 x 10^7 rad at a dose rate of 2.1 x 10^4 rad/h. The long specimens are welded Ferralium, as evidenced by the weld material across their midsections. Figure 6 shows small corrosion spots in a Type 304 stainless steel coupon from the same resin column. Similar spots were also seen in the irradiated specimens exposed to LOMI-loaded resin after the same gamma dose. However, attack in this case was more prominent for the Type 304 stainless steel, and even the more corrosion resistant Type 316 steel also show this type of attack. No other metals showed corrosion effects.

For the unirradiated batches of specimens only Type 304 stainless steel showed any attack. It was in the form of slight staining and was only observed for the LOMI-loaded resin.

For HDPE, cracks were not initiated during the tests on specimens which had the more-ductile non-oxidized layer on the outer U-bend surface. On the other hand cracks formed in the oxidized layer during bending could propagate under some of the test conditions.

3.4 Discussion

Table 4 summarizes results available at this time. Clearly, the attack on Types 304 and 316 stainless steel is enhanced by irradiation and the presence of LOMI-reagent. Cracks can propagate in stressed HDPE and the rate also seems to be accelerated by irradiation and LOMI reagent.

The nature of the corrosion spots was studied and found to be related to contact between individual cation resin beads and the stainless steels. The beads become orange-brown in color, and corrosion spots develop at the points of resin/metal contact where liquid is present as a result of surface tension forces. Apparently, Fe^{2+} ions are removed from the steel, and transferred to the cation resin beads. LOMI reagent may accelerate corrosion by decreasing the pH of residual water in the resin column. The pH of the waste immediately prior to solidification in cement was 3.3 compared to 5.8 for the LOMI-free resins (Table 2).

On the whole, the amount of corrosion was less than expected. This could be influenced by the rapid loss of oxygen in the irradiation vessels by

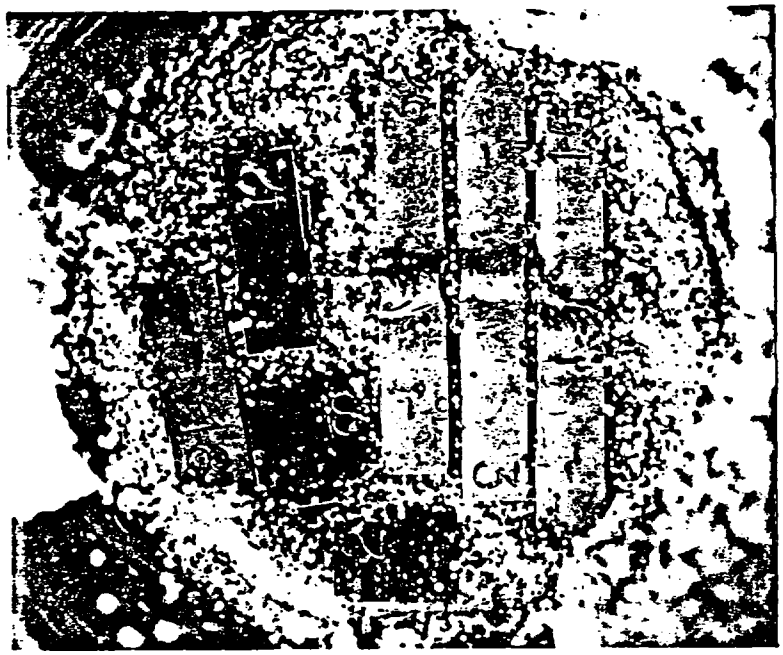

Figure 5 Appearance of top layer of metal specimens after a gamma dose of 5.0×10^7 rad in the presence of LOMI-type as-received mixed-bed resin. Magnification 1.2 X.

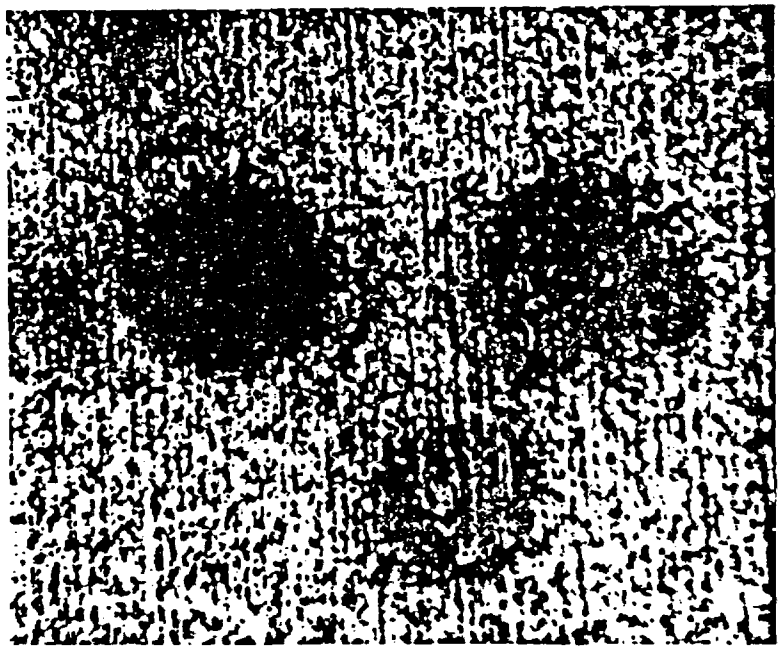

Figure 6 Corrosion spots on Type 304 stainless steel exposed to a gamma dose of 5.0×10^7 rad in the presence of LOMI-type as-received mixed-bed resin. Magnification 50X.

Table 4 The effect of gamma irradiation to 5 x 10^7 rad, and LOMI decontamination reagent, on the corrosion of container materials in contact with mixed-bed ion-exchange resin.

System	Irradiation Dose	Comment
2 parts IONAC A-365 anion resin (as rec.) to 1 part IRN-77 cation resin (as rec.)	0	No corrosion on any metallic specimens. A small crack was initiated at the apex of a bent HDPE specimen.
As above	5 x 10^7 rad	Corrosion spots on T304 SS. No crack propagation in HDPE.
2 part IONAC A-365 anion resin, loaded with LOMI reagent, to 1 part IRN-77 cation resin (as rec.)	0	Slight staining on one T304 SS specimen. Some crack propagation and initiation in HDPE.
As above	5 x 10^7 rad	More prominent corrosion spots on T304 SS compared to un-irradiated control. T316 SS also shows attack but less than T304 SS. Significant crack initiation and propagation in HDPE.

gamma-induced oxidation of the polymeric materials present (Schnabel, W., 1981). Monitoring of the gas pressure within the irradiation vessels showed that there was a rapid loss in pressure of about 20 percent (almost certainly oxygen) during the first 8-10 days, followed by an essentially-linear rise in pressure caused mainly by generation of hydrogen and nitrogen. However, oxygen loss would not be a major factor for unirradiated specimens since significant oxygen should always be present. Factors other than oxygen availability would have to be invoked to explain accelerated attack on irradiated samples.

The experiments are continuing to determine the severity of attack with time. Upon reloading the resin columns, some surplus samples of Ferralium and TiCode-12 were removed and carbon steel specimens substituted.

4. EFFECTS OF OXIDIZING AGENTS ON ION EXCHANGE RESIN WASTES

Test plans are currently being formulated to check the types of oxidizing agents or contaminants which could lead to degradation of ion-exchange

through interaction with the resins and contaminants, will become more concentrated solutions. Current plans include experiments to ascertain which resin/chemical combinations show the greatest potential for exothermic reaction and/or gas generation during dewatering and storage of spent resins.

The objective is to test representative decontamination resin wastes along with typical reactor demineralizer resins, especially those employed where pressurization or thermal excursion incidents were previously observed (Bowerman, B. S., and P. L. Piciulo, 1986). Added to the resin wastes will be chemicals which represent decontamination pretreatments or processes (e.g., EDTA, picolinic acid, HNO_3, or $KMnO_4$), metal ions solubilized in the decontamination processes (e.g. Fe^{2+}, Mn^{2+}, or Cu^{2+}), and chemicals which may be present as a result of biodegradation or radiolytic degradation of a resin bed (e.g. thiols or peroxides). Initially, concentrations and combinations of chemicals will be chosen to try to induce instability in the resin.

Work will be started soon to test the sensitivity of procedures to be used to measure changes in the resins. Of most interest is an oxygen flow-through test which will simulate the oxidation and drying of the resin bed during dewatering. The temperature of the resin bed will be compared to a control with no oxygen flow.

5. ACKNOWLEDGMENT

The authors gratefully acknowledge the assistance of A. Spira and T. Skelaney in the preparation of this manuscript.

6. REFERENCES

Bowerman, B. S. and P. L. Piciulo, "Technical Considerations Affecting Preparation of Ion-Exchange Resins for Disposal," NUREG/CR-4601, 1986.

Lea, F. M., The Chemistry of Cement and Concrete, Chem. Pub. Co. Inc., Third Edition, 1971, p. 611.

NRC, Technical Position on Waste Form, Rev. 0, 1983.

Schnabel, W., Polymer Degradation, Principles and Practical Applications, Hanser International, 1981.

POWER REACTOR DECOMMISSIONING PROJECTS IN THE FEDERAL REPUBLIC OF GERMANY

Robert L. Miller, P.E.

Westinghouse Hanford Company

ABSTRACT

During 1987, three power reactor decommissioning projects in the Federal Republic of Germany (FRG) were visited. The three projects were the Kernkraftwerk Lingen (KWL), the Kernforschungszentrum Karlsruhe Niederaichbach (KKN), and the Kerkraftwerk RWE-Bayernwerk Block A (KRBA). This paper briefly discusses the status of each of these projects and includes some observations on the FRG decommissioning methodology and philosophy.

DISCUSSION

Kernkraftwerk Lingen

The KWL nuclear power station is located near Lingen in lower Saxony in northwest Germany. It was an early prototype boiling-water reactor (BWR) of General Electric design with a 520-MW thermal output. The primary steam heated two steam converters to produce secondary, noncontaminated steam that was lead to the turbine via a fossil-fired super-heater.

In January 1977, the plant was shut-down to check the steam converters. After discovering small cracks in the converters, KWL management decided to replace the converters. The licensing authority defined the replacement as an essential plant modification; thus, the plant would be required to pass through a new licensing procedure.

Because the backfitting required to begin the relicensing procedure would cost 100-200 million Deutsche Marks (DM) with no guarantee of obtaining a new operating license, the parent company decided the financial risk was too great. The decision was made in 1979 to decommission the facility.

Preparations for decommissioning were completed during 1981 and 1982, concurrent with development of documentation required by the licensing authority to place the plant in a "safe enclosure" condition. Figure 1 indicates the safe enclosure portions of the plant. The safe enclosure includes the containment building, the waste treatment building, and the connecting building.

The safe enclosure is designed to have a life of at least 25 years. At the end of the safe enclosure period, the plant will be demolished. Placing the plant in the safe enclosure condition required defueling, considerable

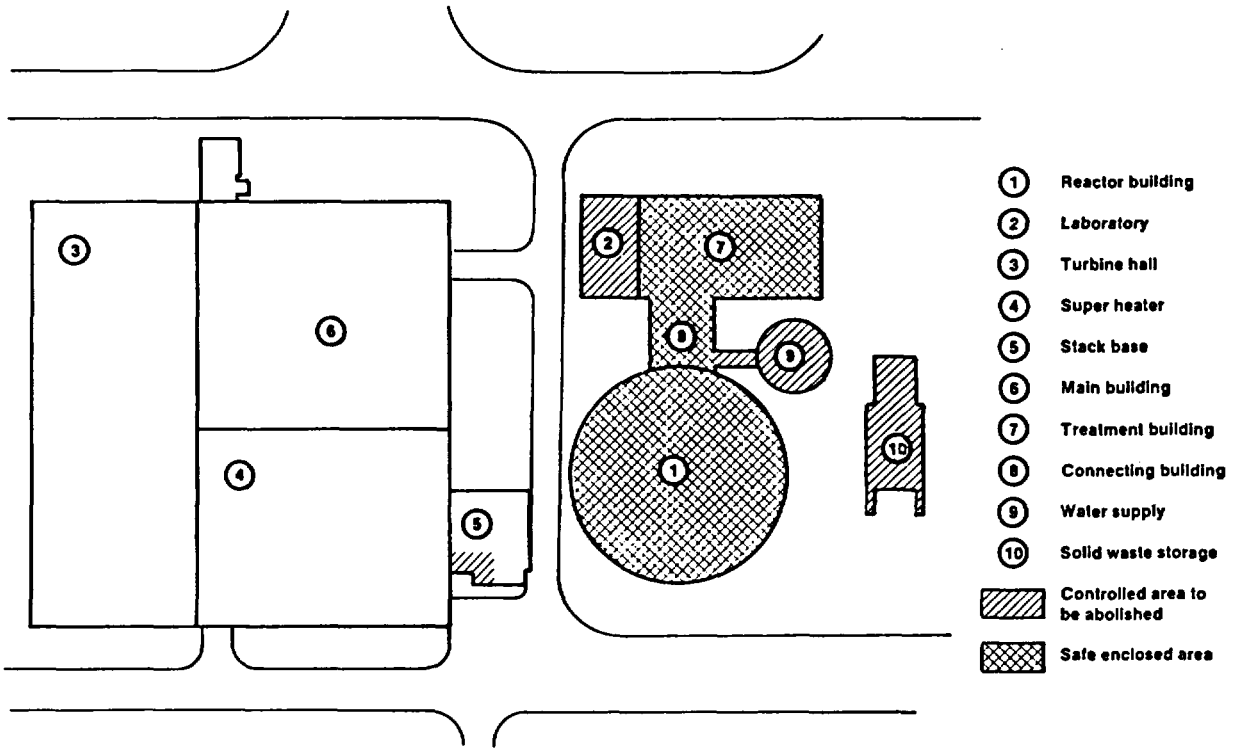

Figure 1. Kernkraftwerk Lingen plant layout.

decontamination, removing all piping penetrations (except one), and sealing all entries into the safe enclosure boundary (except one). A small air circulation system with a drier is being installed to monitor the atmosphere within the enclosure and to maintain the relative humidity at less than approximately 50%.

All wastes generated during the safe enclosure preparations are stored within the containment building. All combustible wastes were sent to a Karlstein facility to be incinerated and the ashes will be returned to KWL for storage. All high dose rate wastes are stored in shielded containers located on the upper floor of the containment building.

Instrumentation will be provided to monitor the access door, the sump levels, and the circulating air system. Alarms will sound in the guard station of the adjacent Lingen-2 power plant if any of the monitored items need attention.

The safe enclosure preparations, scheduled for completion at the end of 1987, cost approximately DM 10-million. The total cost to clear the site to "green field" is estimated to be DM 120-million (1987 DM).

Kernforschungszentrum Karlsruhe Niederaichbach (KKN)

KKN is a 200-MWe gas-cooled (CO_2), heavy-water (D_2O) moderated, pressure-tube type reactor that operated for only an equivalent of 18 full-power days during 1972 to 1974. Leaks in the CO_2/H_2O steam generator were the primary reason for plant shutdown. Due to the unique challenges presented by the KKN, it was decided to decommission the plant as a demonstration project. The plant is in a safe enclosure condition; however, work is actively being pursued to demolish the plant. The machine hall (turbine generator building) is empty and decontaminated. The focus and major challenge now is to remove the pressure-tube calandria (pressure vessel). To accomplish this, a remotely operated manipulator machine has been designed, fabricated, and is being tested by the Noell Company in Wurzburg. This machine will be installed in the space above the pressure vessel and will cut and remove each pressure tube. Work is proceeding at the KKN to prepare for installation of the manipulator machine, following thorough testing at Noell. Some uncertainty exists regarding when the machine will be moved to KKN, but it is likely that it will be done sometime in 1988.

Approximately 1,700 tons of the contaminated steel are expected to be removed during KKN dismantlement; this steel can be recycled by using melting techniques. The melting is part of the total demonstration project and is expected to provide valuable information for future decommissioning projects. A 2-ton induction furnace has been installed in the FR2 reactor building at the Karlsruhe Nuclear Research Center. Current plans are to make three melts/day (i.e. approximately 4-1/2 tons), separate the dross as a low-level waste, and release the metal for reuse.

The activity levels of the melted material are controlled to the levels shown in Table 1 for final disposition.

Table 1. Metallic-Radioactive Levels.

Activity	Disposition
<0.5 Bq/g	Unrestricted
0.5 - 74 Bq/g	Controlled reuse (such as in casks)
>74 Bq/g (averaged over 1kg)	Reuse in controlled areas (as shielding blocks, etc.)
<0.05 Bq/cm^2 (surface contamination)	Unrestricted
0.05 - 0.5 Bq/cm^2	Controlled reuse
>0.5 Bq/cm^2	Reuse in controlled areas

Kerkraftwerk RWE-Bayernwerk Block A

Gundremmingen is the site of the KRBA Reactor. The KRBA is a 250-MWe BWR similar to Dresden in the United States of America and Garigliano in Italy, with the unique feature of having the steam drier inside the pressure vessel. The plant operated well for approximately 10 years. The plant fed an electrical grid that failed, triggering a series of events that caused extensive damage to the plant including fuel pin failures. Plant repairs were made in approximately six months; however, due to findings in other BWRs at that point, it became necessary to check the primary system for intergranular stress corrosion cracking. Lines were cut, cracks were found, and after analysis, the authorities required the piping to be replaced and other changes made. When the estimated cost of repairs reached DM 250 million and there was still no guarantee of approval of long-term operation, it was decided to decommission KRBA to safe enclosure.

The project management method used for the KRBA decommissioning project is described by the project manager, Wolfgang Stang, as the "salami method." That is, small pieces of work are identified and submitted to authorities for approval. After approval, the work is completed, concurrent with submitting another "slice" to the authorities, etc. This management method allows a steady work force of approximately 20 persons to perform all the necessary work from actual dismantling to final survey for release or recycle.

To date, nearly all the piping has been removed from the turbine hall, and the low-pressure section of the turbine itself is nearly removed. Work on the high-pressure turbine section is being started. Small piping and valves that cannot be adequately surveyed are sized and placed in 200-liter drums for future melting. The larger pieces are electropolished for unrestricted release.

All electropolishing is being done in two 5-m^3 tanks. A third 8-m^3 tank was installed to clean the fuel racks. All piping with a sufficient diameter to allow a complete survey is electropolished, and after survey, is released from the site as scrap. The release limit for surface contamination is 0.37 Bq/cm^2. In practice, a value of 0.22 Bq/cm^2 is used. The mass-specific release limit is 3.7 Bq/g. In practice, a value of 0.37 Bq/g is used. Material with a mass-specific activity of up to 1 Bq/g is sold to a smelting company where it is mixed with very "clean" scrap (automobile bodies) in a ratio of three parts clean to one part contaminated. This blended material is used within the nuclear industry for casks and shielding.

To date, approximately 1,200 tons of metal, 50 tons of motors, 30 tons of glasswool, and 50 tons of oil have been removed and released for unrestricted use. The glasswool is still onsite awaiting a decision from the authorities for release levels. An additional 800 tons of metal have been removed and will be used in the nuclear industry for casks and shielding. Approximately 420 tons of concrete have been removed and released.

After completion of the dismantling of the turbine hall and following shipment of the last fuel elements, plans are to begin dismantling

contaminated (not activated) components in the reactor building. The clean turbine hall will be used as a workshop for all future decommissioning.

Dismantling of activated material will await the opening of a final storage facility in 1992. Opening of the final storage facility is a boundary condition for beginning reactor dismantling.

SUMMARY

The FRG has a strong commitment to nuclear power with nearly 35% of their total power generation being nuclear. With this commitment is the recognition that decommissioning of the FRG power plants is a necessary part of the total program. While only KKN dismantling is officially titled a demonstration project, all three projects discussed serve as demonstrations of decommissioning methods. The KWL safe enclosure will demonstrate equipment can be maintained throughout an extended time (25 years) by controlling the relative humidity and providing a nominal air exchange within the enclosure. The KKN project will demonstrate development of remote tooling and waste volume reduction by melting. The KRBA project has already demonstrated that large masses of material can effectively be decontaminated and released for unrestricted use or for controlled use within the industry.

Printed in the United States of America

BD-9300-090 2 (7-87)

RADIONUCLIDE SOURCE TERM MEASUREMENTS FOR POWER REACTOR DECOMMISSIONING ASSESSMENT

D. E. Robertson
C. W. Thomas

Pacific Northwest Laboratory[a]
Richland, Washington 99352

ABSTRACT

Studies are in progress to characterize the residual radionuclide concentrations, distributions, and inventories in materials and components from nuclear power reactors at the time of decommissioning. These studies are providing essential information for assessing the radiological safety, technology, waste disposal, and environmental assurance associated with commercial reactor decommissioning. The decommissioning of Shippingport Station provides the first opportunity, following the establishment of NRC rules on commercial decommissioning and waste disposal, to characterize and assess the residual radiological conditions during the actual decommissioning of a nuclear power station. Through cooperation with the U.S. Department of Energy (DOE), which is conducting the Shippingport Station decommissioning, a detailed examination of residual radionuclide conditions is being performed. Preliminary measurements have indicated that the residual activation product concentrations in primary loop systems at Shippingport Station are, on the average, 5 to 50 times lower than observed at commercial stations. In addition, no significant concentrations of fission products and transuranic radionuclides are present in the residual radioactive materials.

Studies are also in progress to assess the problem associated with decommissioning and disposal of highly neutron activated components from within commercial reactor pressure vessels and spent fuel assembly hardware. This assessment is being accomplished through a sampling and analysis program which examines neutron activation of pressure vessel steel, stainless steel, inconel and zircaloy components of fuel assembly hardware. This assessment will include a comparison of empirical activation product measurements with predicted levels using established codes to evaluate the accuracy and identify any shortcomings in the predictive calculation methodology.

---

[a]Operated for the U.S. Department of Energy (DOE) By Battelle Memorial Institute under contract DE-AC06-76RLO 1830

1.0 INTRODUCTION

The U.S. Nuclear Regulatory Commission (NRC) has recently enacted proposed rules setting forth technical, safety, and financial criteria for decommissioning of licensed nuclear facilities, including commercial nuclear power stations (U.S. N.R.C., 1985). These rules have addressed six major issues, including decommissioning alternatives, timing, planning, financial assurance, residual radioactivity, and environmental review. In addition, the rules governing disposal of low-level radioactive wastes in commercial shallow land burial facilities (U.S. N.R.C., 1981), will be applicable to most of the wastes generated during reactor decommissioning. The appropriate response to each of these issues by the licensee and the NRC depends greatly on an accurate and reliable assessment of the residual radiological conditions existing at the nuclear power stations at the time of decommissioning. Large volumes of data exist which describe the radionuclide concentrations associated with active waste streams generated at nuclear power stations. However, comparatively little information is available that documents the residual radionuclide concentrations, distributions, and inventories residing in contaminated piping, components, and materials of nuclear plant systems and in neutron-activated materials associated with the reactor pressure vessel and biological shield. Especially lacking is a detailed radiological characterization during an actual reactor decommissioning.

This study has been implemented to provide the NRC and licensees with a more comprehensive and defensible data base and regulatory assessment of the radiological factors associated with reactor decommissioning and disposal of wastes generated during these activities. The objectives of this study are being accomplished during a two-phase sampling, measurement, and appraisal program utilizing: 1) the decommissioning of Shippingport Atomic Power Station, and 2) neutron activated materials from commercial reactors. The program is presently in the sample acquisition phase, and radioactive materials are being obtained from Shippingport Station and from a number of commercial stations for comprehensive radionuclide and stable element analyses. These measurements will be utilized to assess the following important aspects of reactor decommissioning:

- radiological safety and technology assessment from an actual reactor decommissioning (Shippingport)
- radiological characterization of intensely radioactive materials (greater than Class-C) associated with the reactor pressure vessel and spent fuel assembly hardware from commercial nuclear power plants
- evaluation of the accuracy of codes for predicting radionuclide inventories in retired reactors and neutron activated components
- assessment of waste disposal options associated with reactor decommissioning.

2.0 SCOPE OF PROJECT

This study comprises two main research areas associated with reactor decommissioning: 1) providing a detailed radiological characterization and assessment from the actual complete decommissioning of Shippingport Atomic Power Station, and 2) conducting a detailed radiological assessment of the highly neutron activated metal components associated with reactor internals and spent fuel assembly hardware.

2.1 RADIOLOGICAL CHARACTERIZATION FROM SHIPPINGPORT DECOMMISSIONING

The complete dismantlement of Shippingport Atomic Power Station and the restoration of the site to unrestricted use provides a unique opportunity to conduct a detailed radiological assessment from an actual reactor decommissioning. Although this reactor station is a Department of Energy (DOE) facility and not subject to the decommissioning and radioactive waste disposal rules provided by the NRC for commercial reactors, the technology, safety, and transportation methods associated with its decommissioning are very similar to that which a commercial licensee would utilize.

Shippingport Station is significantly smaller than most commercial reactors and it is recognized that there are some differences in design, materials and operations. However, the similarities are such that an examination of the residual radioactivity associated with its dismantlement could provide valuable generic information for helping to assess the technology, safety, and costs of decommissioning commercial stations.

The residual radionuclide inventory remaining within nuclear power plants following permanent shutdown is primarily affected by the following parameters:

- composition and purity of construction materials
- general design of the primary and secondary systems
- core design
- operational parameters (water chemistry, corrosion control, fuel integrity, radwaste management, maintenance operations and housekeeping)
- criticality control
- reactor power level (megawatts)
- length of operation.

With regard to all of the above parameters, except reactor power level, and later water chemistry, the Shippingport Station bears many similarities to a modern, commercial pressurized water reactor (PWR) power station. It is quite probable that the inventory and distribution of residual radionuclides would scale up in a generic way to larger light-water reactor (LWR)/PWR stations that have experienced little or no fuel failures. Therefore, it is

expected that a sampling and analysis of the primary and secondary systems during decommissioning would provide a unique opportunity to develop information generically applicable to the eventual decommissioning of larger commercial PWR stations.

The following table gives a comparison of important parameters of the Shippingport Station primary system with that for the Reference PWR used in the conceptual decommissioning assessment by Smith et al. (1978).

TABLE 2.1. Comparison of the Shippingport Primary System with the Primary System in a Reference PWR

Component	Reference PWR	Shippingport
Power	1000 MWe	72 MWe
Pressure vessel size	44' X 15' diam.	33.2' X 10.5' dia.
Piping Systems	80 miles	20 miles
Fuel Cladding	Zircaloy	Zircaloy
Control Rods	Ag-In (ss clad)	Hafnium
Vessel Internals	Stainless and Inconel	Stainless and Inconel
Reactor Vessel	Carbon steel, stainless steel clad, 0.156" min.	Carbon steel, stainless steel clad, 0.125" min.
Heat Exchangers	Carbon steel, inconel and stainless steel clad, U tube type	Stainless tubes, U and straight tube types
Coolant Loops	4	4
Primary Piping	Stainless steel	Stainless steel
pH Control	LiOH, 0.2 to 2 ppm	LiOH (Core 1); NH_4OH (Cores II & III)
Oxygen Control	Hydrogen, 30 ml/kg	Hydrogen, 25 ml/kg
Reactivity Control	Boric acid, 0-2000 ppm	see footnote

(a)Core I controlled with rods only; Core II used control rods and burnable poison inside the fuel rods; Core III was controlled by moveable fuel rods only. $K_2B_4O_7 \cdot 8H_2O$ was used only for defueling criticality control.

The similarity between the two primary systems is striking. The composition of the fuel cladding, reactor vessel internals, and primary loop materials are essentially identical. These materials supply the major and trace elements which are the parent elements of the radionuclides formed by neutron activation of the pressure vessel, vessel internals, and corrosion product impurities in the primary coolant. The important water chemistry parameters, e.g. pH and oxygen control, are also similar. The main difference, other than size, is the composition of the control rods. However, the control rods do not contribute significantly to the residual

radionuclide inventory deposited throughout the primary and secondary systems.

The Shippingport primary loop contains all the components of a typical PWR: a pressurizer, steam generators, coolant pumps, the reactor vessel itself, and a chemical purification system. As shown in the above table, the materials of construction within the primary loop are, stainless steel, carbon steel, zircaloy, and inconel, and are very similar to those used in typical PWR primary systems. The coolant and purification system was also typical of other PWRs, being a combination of regenerative and non-regenerative heat exchangers with filters and ion exchange beds. Likewise, pH and corrosion controls were similar to commercial PWRs. Lithium hydroxide (and later NH_4OH) was utilized for pH control, and hydrogen and hydrazine (at starting only) were used to limit oxygen levels and thus minimize corrosion. Thus, the fact that the Shippingport Station appears to be similar to a scaled-down version of a modern, commercial PWR would permit generic observations and conclusions regarding residual radioactivity considerations during dismantlement and decommissioning of PWRs in general.

To the extent possible, samples from the primary, secondary, and auxiliary systems at Shippingport are being obtained for detailed radiochemical analyses. These measurements will provide the basis for estimating the radionuclide inventory and distribution within the various plant systems, and for assessing the waste disposal options under the assumption that the decommissioning materials are representative of commercial wastes which would come under NRC and U.S. Department of Transportation (DOT) regulations.

2.2 RADIOLOGICAL CHARACTERIZATION OF HIGHLY NEUTRON ACTIVATED METALS ASSOCIATED WITH PRESSURE VESSELS AND FUEL ASSEMBLIES

One of the most significant unanswered problems associated with commercial reactor decommissioning is the disposition of the highly neutron activated metal components associated with the reactor pressure vessel internals and the fuel assembly hardware. As shown in Table 2.2, it has been estimated that some of these materials will have concentrations of long-lived radionuclides (^{14}C, ^{59}Ni, ^{63}Ni, and ^{94}Nb) that will greatly exceed the Class-C limit for disposal in low-level waste shallow land burial facilities (Luksic, 1986). Since provisions have not been made in either the high-level (10CFR72) or the low-level (10CFR61) radioactive waste disposal rules for disposition of these types of materials, there presently no regulations governing their disposal. It is, therefore, essential that a complete characterization of these types of materials and their radionuclide contents at the time of decommissioning be obtained.

TABLE 2.2. Ratio of Calculated Specific Activity to Maximum Allowable Specific Activity for Shallow Land Burial for Selected Components (adapted from Luksic et al., 1986).

	m^3/MTU	^{14}C	^{59}Ni	^{94}Nb	^{63}Ni
Half-Life		5730 yr	8×10^4 yr	2×10^4 yr	100 yr
10 CFR 61 Class C Limit		80 Ci/m^3	220 Ci/m^3	0.2 Ci/m^3	7000 Ci/m^3
PWR Fuel Assembly (33,000 MWd/MTU)					
Total Fuel Assembly Hardware	0.00651	1.1	3.6	990	15
Grids/Springs/Etc. (SS-304 & Inconel-718)	0.00312	2.4	7.4	2100	32
End Fitting (SS-304)	0.00339	0.03	0.02	0.08	0.08
BWR(a) Assembly (28,000 MWd/MTU)					
Total Fuel Assembly Hardware and Channel	0.04526	0.15	0.09	9.8	0.43
Grid/Springs/Etc. (Zircaloy-4 and Inconel X-750)	0.00209	0.41	1.5	86	7.3
End Fittings (SS-304)	0.00461	0.33	0.20	0.94	0.95
Channel (Zircaloy-4)	0.03856	0.12	<0.01	6.8	<0.01

(a)BWR = boiling-water reactor

In order to accomplish this characterization, samples of stainless steel, inconel and zircaloy alloys used in pressure vessel components and fuel assemblies are being acquired for analyses. These measurements will empirically determine the concentrations of all intermediate and long-lived radionuclides of significance in these materials, including ^{3}H, ^{14}C, ^{59}Ni, ^{63}Ni, ^{90}Sr, ^{94}Nb, ^{99}Tc, ^{129}I, ^{137}Cs, and Pu, Am and Cm isotopes. Concurrently with the empirical measurements, estimates of activation product concentrations in these materials will be calculated using existing codes (e.g. ORIGEN-II, ANISN, etc.) and materials compositions. These calculations will allow a direct comparison with the measured radionuclide concentrations and provide an assessment of the accuracy of the calculational methods.

2.3 WASTE DISPOSAL OPTIONS ASSOCIATED WITH REACTOR DECOMMISSIONING

The recent rule governing disposal of low-level radioactive wastes in shallow land burial facilities (10CFR61) will have direct impact on the options available for disposal of decommissioning wastes. Previous studies (Robertson et al., 1984; Abel et al., 1986) have indicated that essentially all primary, secondary, and auxiliary systems in a nuclear power plant would generally have residual radionuclide contamination levels sufficiently low to permit disposal as Class-A waste. The Shippingport Station decommissioning will be an excellent opportunity to test these previous observations. In addition, the pressure vessel is currently being prepared for packaging and shipment as a low specific activity (LSA) package. The radionuclide characterization and compliance procedures for DOT regulations associated with the shipment and disposal of the pressure vessel will provide important information for evaluating disposal options for commercial reactor pressure vessels.

3.0 EXPERIMENTAL

Specimens of surface-contaminated and neutron activated components from Shippingport Station, from three types of spent fuel assembly hardware, and pressure vessel samples from the Gundremmigen KRB-A reactor have been obtained for detailed radiochemical analyses. These materials will provide the basis for evaluating the radiological safety and waste disposal options associated with reactor decommissioning.

3.1 SHIPPINGPORT STATION SAMPLING

The majority of the residual radioactive material residing within a retired nuclear plant (excluding the pressure vessel and internals) is located within the primary coolant loop attached to the surface corrosion film. Five excellent cores of the primary coolant piping were provided for analysis at PNL by the Shippingport Station Decommissioning Project Office for characterization of the contaminated corrosion layer in the primary system. These cores, shown in Figure 3.1, were 7 cm in diameter by 4 cm thick and contained a thin, black, radioactive corrosion product layer on the inside surface which was very hard and retentive. Cores were taken from the "A," "B," and "C" loop primary coolant piping, at the entrance to (cold side) and exit from (hot side) the reactor pressure vessel at the outer surface of the neutron shield tank (see Figure 3.2). The radioactive corrosion film was removed by immersing the contaminated side in hot 6N hydrochloric acid for several minutes and brushing the surface with a stiff nylon brush. The stripped corrosion film was then completely solubilized by heating in a mixture of hydrochloric and nitric acids and the acid solutions were used for direct gamma spectrometric and radiochemical analyses. One of the core specimens ("A" loop-hot side) was saved for special testing and was cut into four equal wedge-shaped pieces for conducting a series of special form tests for radioactive materials.

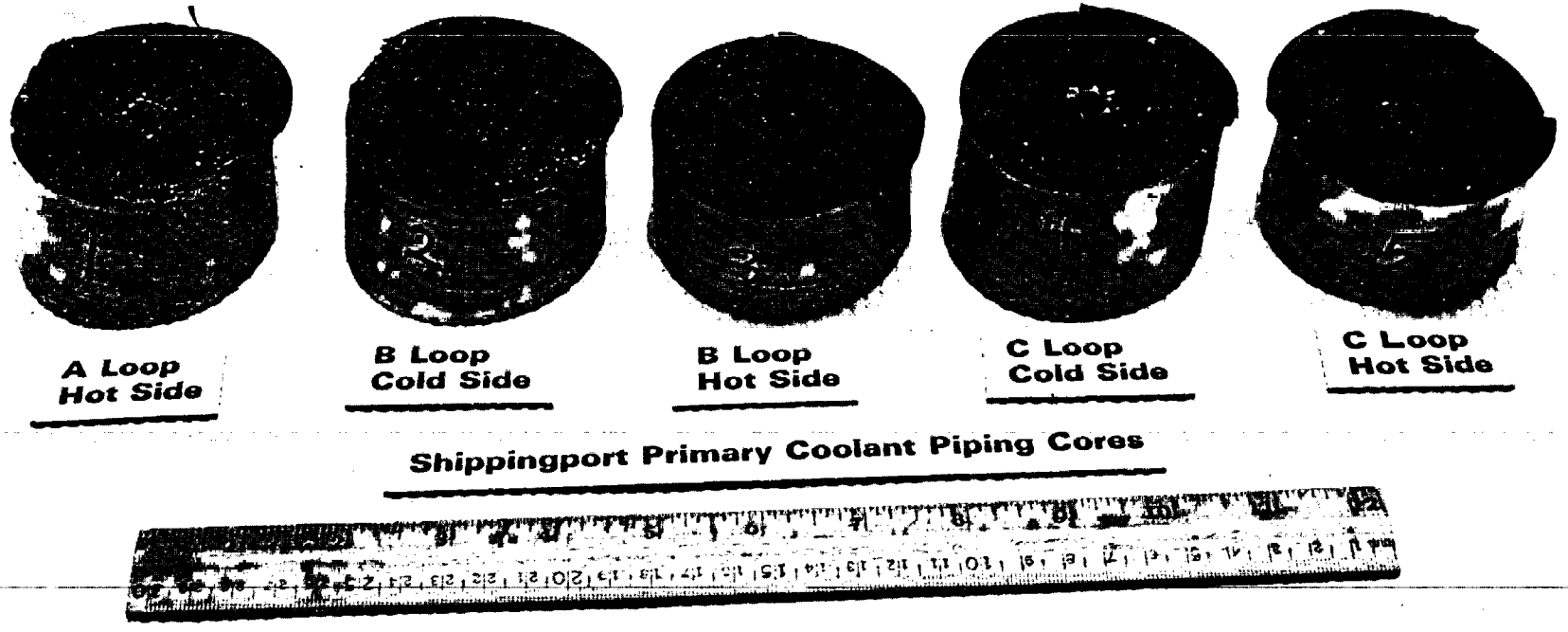

Figure 3.1. Shippingport Station Primary Coolant Piping Cores Showing Contaminated Inner Surface

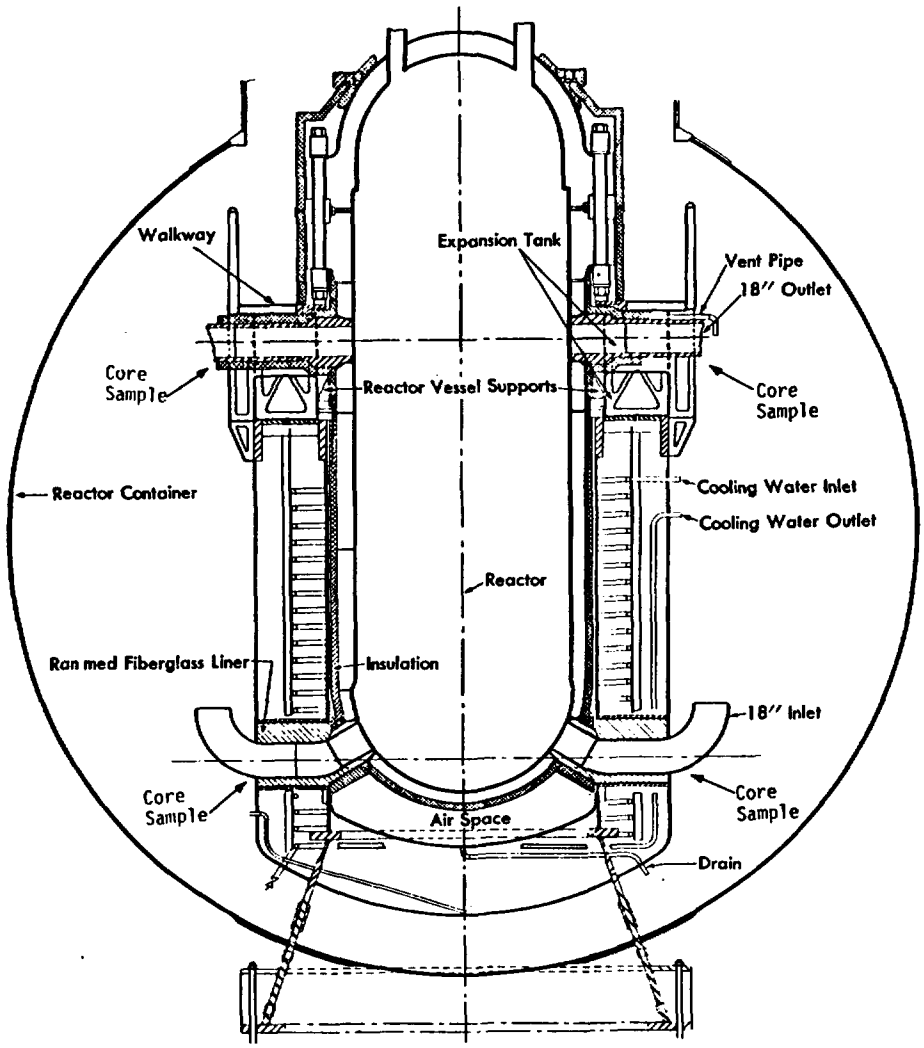

Figure 3.2. Shippingport Reactor Pressure Vessel Surrounded by the Neutron Shield Tank and Reactor Chamber. Sampling Locations for Cores from the Primary Coolant Inlet (Cold) and Outlet (Hot) Piping Are Shown.

Also obtained from several of these cores were small strips of the thin lip of stainless steel around the outer circumference of the contaminated side of the cores. The lip segments were a remnant from the coring operation and were formed when the core prematurely broke free from the piping before the hole saw completely cut through the pipe. These lip segments can be seen still attached to the outer circumference of the cores in Figure 3.1. Pieces of these strips were mounted in epoxy resin and a cross-section was polished for examination by microphotography and scanning electron microscopy (SEM)/x-ray microprobe analysis for chemical composition.

Other samples of primary, secondary, and auxiliary system components were also collected during the dismantling and shipped to Argonne National Laboratory (ANL) where further sub-sampling was conducted for materials characterization studies at ANL and radiological characterization studies at PNL. These samples included the following materials:

- primary coolant check valve ("B" loop)
- primary coolant purification piping
- monitoring/instrumentation system primary coolant piping (BD and AC chambers)
- fuel pool recirculation system piping
- secondary system feedwater piping
- main steam piping.

In addition to the surface-contaminated components, samples from the highly neutron activated fuel assembly hardware from the Core 3 fuel elements are also being obtained. These samples, taken from a blanket rod, a reflector rod, and a seed rod, include pieces of the following components:

- stainless steel grid bolts and lock nuts
- inconel-750 springs
- 348-stainless steel support sleeve
- zircaloy-4 cladding (midplane and upper end).

3.2 GUNDREMMINGEN KRB-A PRESSURE VESSEL

On January 13, 1977, the Gundremmigen KRB-A reactor, a 250-MWe BWR, was permanently shutdown after 10 years of operation at 75% availability. After decommissioning, 15 cores (trepans) of the reactor pressure vessel were taken for radiological and materials characterization. The trepans were taken at different axial and azimuthal positions within the 90 to 135 degree octant of the reactor. Two 8- and 9- gram segments of trepan G (115°), representing depths through the pressure vessel of 5.5 cm (0.41 T) and 9.0 cm (0.67 T) from its inside surface, were sent to PNL for detailed radiochemical and elemental analysis, which are currently in progress. The neutron fluences

for the pressure vessel have been carefully calculated (Prillinger, 1986), and these specimens will provide an excellent opportunity to test the accuracy of computer codes for estimating activation product concentrations in a reactor pressure vessel.

3.3 SAMPLING COMPONENTS FROM COMMERCIAL POWER REACTOR FUEL ASSEMBLIES

A number of well-characterized spent fuel assemblies have become available at PNL for obtaining samples of the various metals of construction. These specimens will be radiochemically analyzed for the long-lived activation products of waste disposal concern. The empirical measurements will then be compared with calculated activation product concentrations using existing codes (e.g., ORIGEN, ANISN, etc.) to determine the accuracy with which calculated estimates can be made. This comparison will lend confidence to calculational methods and/or identify shortcomings in these methods.

Three high-burnup commercial fuel assemblies are currently being sampled. The following materials are being obtained for analysis:

Assembly Type	Reactor Station	Materials Sampled
General Electric (7 X 7)	Cooper	Stainless steel bottom end fittings, and upper tie plate, inconel expansion springs, zircaloy grid spacers
Combustion Engineering (14 X 14)	Calvert Cliffs	Stainless steel bottom end fittings and flow/hold-down plates, zircaloy and inconel grid spacers, inconel hold-down springs
Westinghouse (14 X 14)	Point Beach	Stainless steel bottom and upper end fittings, inconel hold-down springs, zircaloy guide tube and grid spacers

One- to 10- gm specimens of the above materials are being cut from these fuel assemblies. Full hot-cell facilities at PNL are required for this work and individual 10-gm pieces range in dose rate from a few hundred mR/h to over 50 R/h. radiochemical analysis are proceeding in both the hot-cell facilities and in shielded fume hoods.

4.0 RESULTS AND DISCUSSION

Although the radioanalytical analyses are presently in progress, some preliminary results are available for characterizing the residual radionuclides associated with the corrosion film on the Shippingport Station systems exposed to primary coolant.

4.1 RESIDUAL RADIONUCLIDE CONCENTRATION IN SHIPPINGPORT PRIMARY COOLANT PIPING

The primary coolant piping core specimens described in Section 3.1 were analyzed for the long-lived radionuclides of a safety and waste disposal concern. The results are given in Table 4.1. It is immediately obvious that the residual radioactivity at Shippingport Station is somewhat atypical of that observed in a number of commercial nuclear power stations (Robertson, et al. 1984; Abel et al., 1986). First, the gamma-ray spectra of the stripped corrosion layer resembled a pure ^{60}Co spectrum. A careful examination of the spectra could not identify any other gamma-emitting radionuclides. Although the samples contained ^{55}Fe and ^{63}Ni concentrations that were sometimes comparable to the ^{60}Co levels, these radionuclides emit only low-energy x-rays and beta particles and cannot be detected by direct gamma-ray spectrometry. The second unusual feature of the residual radioactivity is the almost complete absence of any fission products or transuranic radionuclides. Although trace amounts of Pu, Am, and Cm isotopes were detectible in the corrosion film samples, their concentrations were so low that their origin appears to have been from traces of tramp uranium on the outer surfaces of the fuel elements, and not due to leakage from failed fuel. These measurements confirm the fact that no measurable fuel failures occurred at Shippingport Station during the entire operating history of the plant - a truly noteworthy operational record.

A comparison of the residual radionuclide concentrations associated with the contaminated surfaces of primary coolant piping at Shippingport Station with that observed at seven commercial nuclear power stations is shown in Figure 4.1. The data from the seven commercial units were taken from Robertson, et al. (1984). Shown is Figure 4.1 are the range and average concentrations of ^{60}Co, ^{63}Ni, ^{55}Fe, ^{94}Nb, ^{137}Cs, and $^{239-240}Pu$ associated with the residual radioactivity at these stations. The average concentrations of the activation product radionuclides ^{60}Co, ^{63}Ni, ^{55}Fe, and ^{94}Nb are lower in the Shippingport samples by factors of about 10, 2.7, 60, and 40, respectively. The $^{239-240}Pu$ and ^{137}Cs are 1000 and greater than 200 times lower, respectively, than the average concentrations for the commercial units.

In addition to the surface contamination, the stainless steel cores from the primary coolant piping had also become slightly neutron activated, and ^{60}Co, ^{55}Fe, and $^{63,59}Ni$ were the main radionuclide constituents in the metal itself. Drill turnings were collected from six locations (shown in Figure 4.2), dissolved in acid, and analyzed for gamma-emitting radionuclides, ^{55}Fe and ^{63}Ni. The ^{60}Co concentrations are given in Table 4.2, and averaged about 1000 pCi/g of steel for the B and C hoop "hot side" (outlet piping) and about 80 to 400 pCi/g of steel for the B and C loop "cold side" (inlet piping) samples. Elemental analyses are currently in progress to provide stable Co, Fe, and Ni concentrations for calculating specific activities from which neutron fluences at these locations can be determined.

TABLE 4.1

Residual Radionuclide Concentrations Associated With
the Corrosion Layer on Shippingport Primary Coolant Piping

Radionuclide Concentration ($\mu Ci/cm^2$) as of Feb., 1987

Radionuclide	Half-Life(yr)	B-Loop, Cold Side	B-Loop, Hot Side	C-Loop, Cold Side	C-Loop, Hot Side
^{60}Co	5.27	0.38 ± 0.011	0.88 ± 0.029	0.57 ± 0.017	0.88 ± 0.029
^{55}Fe	2.7	0.050 ± 0.0002	1.13 ± 0.034	0.100 ± 0.003	0.62 ± 0.019
^{63}Ni	100	0.035 ± 0.0018	0.53 ± 0.029	0.069 ± 0.006	0.74 ± 0.037
^{59}Ni	8.0×10^4	(2.25 ± 0.113)E-4	(4.04 ± 0.121)E-3	(4.40 ± 0.132)E-4	(3.20 ± 0.096)E-3
^{94}Nb	2.0×10^4	(2.40 ± 0.44)E-6	(1.13 ± 0.07)E-5	(6.09 ± 0.53)E-6	(7.85 ± 0.43)E-6
^{14}C	5730	(5.6 ± 7.7)E-5	(4.9 ± 8.8)E-5	(8.1 ± 7.8)E-5	(6.9 ± 6.1)E-5
^{99}Tc	2.13×10^5	(3.4 ± 2.4)E-6	(2.8 ± 0.24)E-5	(8.1 ± 2.2)E-6	(1.29) ± 0.27)E-5
^{3}H	12.33	(1.4 ± 1.6)E-6	(1.7 ± 1.6)E-6	(1.2 ± 1.3)E-6	(1.6 ± 1.8)E-6
$^{239-240}Pu$	2.44×10^4	(1.26 ± 0.06)E-7	(1.88 ± 0.10)E-7	(3.09 ± 0.04)E-6	(2.79 ± 0.09)E-7
^{238}Pu	87.8	(7.51 ± 0.43)E-8	(1.16 ± 0.08)E-7	(5.56 ± 0.18)E-7	(1.31 ± 0.07)E-7
^{241}Am	433	(1.10 ± 0.16)E-7	(1.36 ± 0.14)E-7	(1.16 ± 0.04)E-6	(1.67 ± 0.16)E-7
^{244}Cm	18.1	(9.0 ± 7.9)E-9	(5.9 ± 5.9)E-9	(8.7 ± 3.8)E-9	(5.8 ± 5.8)E-9
^{137}Cs	30.2	<3E-4	<5E-4	<4E-4	<5E-4
Dose Rate @ 1 cm					
w/beta shield (mR/h)		10	32	15	22
w/out beta shield (mRad/h)		230	1000	350	800

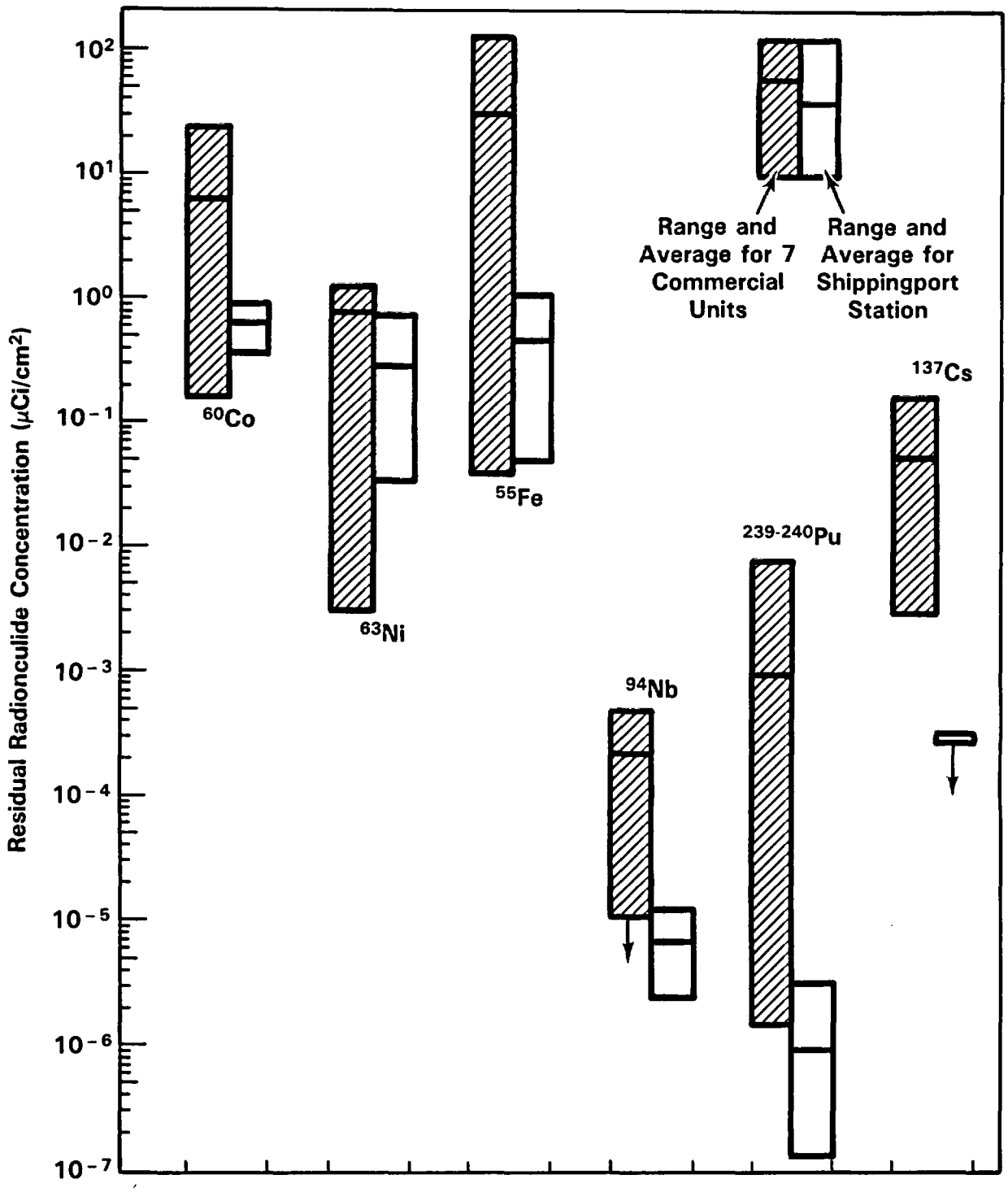

Figure 4.1. Comparison of Residual Radionuclide Concentrations on Primary Coolant Piping from Shippingport Station with Seven Commercial Stations

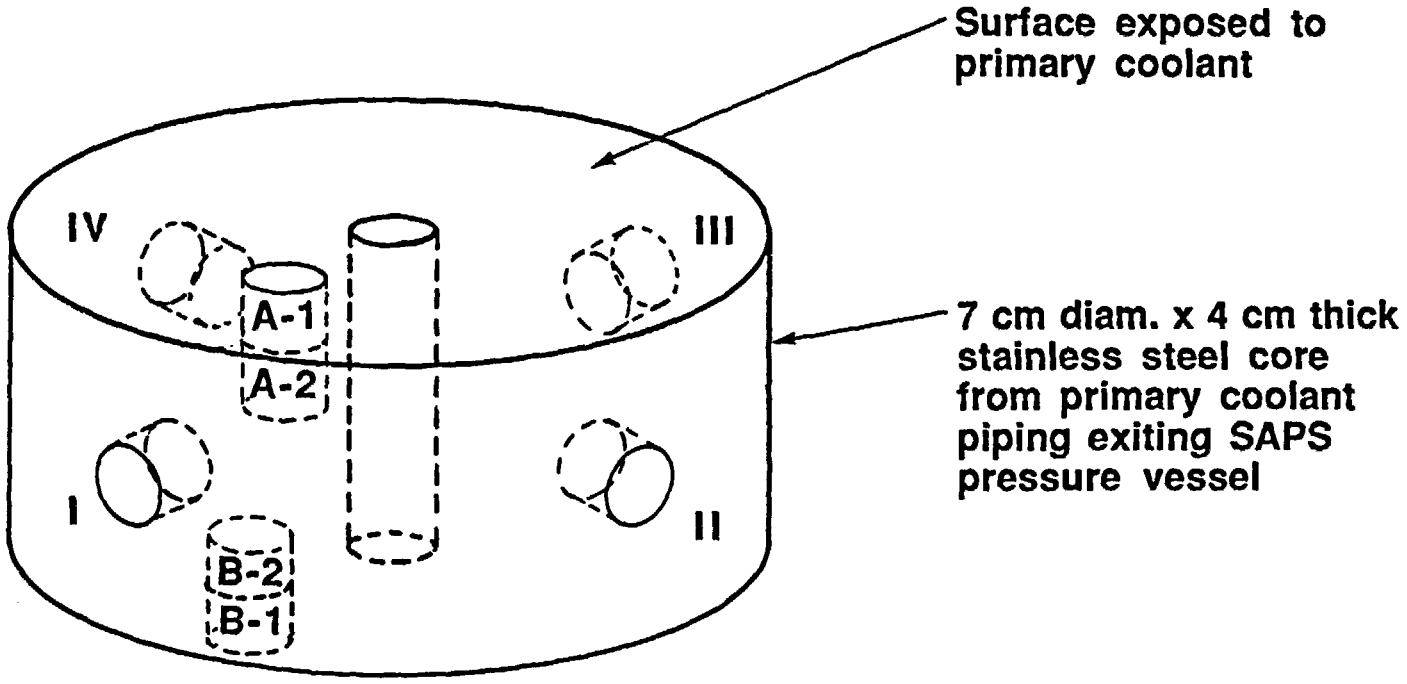

Figure 4.2. Sampling Locations for Obtaining Drill Turnings from Stainless Steel Primary Coolant Piping from Shippingport Station

TABLE 4.2

^{60}Co Concentrations in Stainless Steel Primary Cooling Piping Exiting the Shippingport Reactor Pressure Vessel

Sample	Subsample (Drill Turnings) Location	^{60}Co Concentration (pCi/gm)(A)
B-Loop, Cold Side	I	128
	II	124
	III	119
	IV	59
	B-1	333
	B-2	431
	A-1	482
	A-2	150
B-Loop, Hot Side	I	965
	II	1,061
	III	962
	IV	1,111
	B-1	1,142
	B-2	1,109
	A-1	10,150*
	A-2	1,468
C-Loop, Cold Side	I	77.9
	II	82.9
	III	87.4
	IV	87.4
	B-1	206
	B-2	108
	A-1	793
	A-2	538
C-Loop, Hot Side	I	1,059
	II	975
	III	1,042
	IV	1,040
	B-1	1,237
	B-2	972
	A-1	6,428*
	A-2	6,733*

* Drill turnings appear to be contaminated with surface contamination from the more radioactive corrosion film.
(A) Activity as of May, 1987.

4.2 PHYSICAL/CHEMICAL CHARACTERIZATION OF THE CORROSION FILM ON SHIPPINGPORT STATION PRIMARY COOLANT PIPING

The thin strips of stainless steel removed from the perimeter of the primary coolant piping cores contained an undisturbed layer of corrosion products. These strips were mounted edgewise in epoxy resin, polished, and examined by microphotography and SEM/x-ray microprobe analysis to determine the physical structure of the corrosion layer and its chemical composition.

Photomicrographic cross-sections of the contaminated corrosion layer on B-loop, hot (outlet) and cold (inlet) primary coolant piping are shown in Figure 4.3. The photomicrographs clearly show that the outer corrosion layer on the hot leg (outlet) piping is about three to four times thicker than that observed on the cold leg (inlet) piping. Both specimens show a very thin oxide layer of a uniform thickness of about 1.5 to 2 μm attached directly to the base metal. Attached to this oxide layer is a granular layer of corrosion product particles which range in thickness from about 8 to 15 μm on the hot leg piping to about 3 to 5 μm on the cold leg piping. The corrosion product granules on the hot leg specimen are of a much coarser texture, with individual particles having diameters of up to 1-2 μm.

Figure 4.4 shows two SEM micrographs of the hot leg piping corrosion layer with specific regions selected for chemical analysis by energy dispersive x-ray fluorescence microprobe analysis (EDAX). These micrographs more clearly show the thin (1.5-2 μm) oxide layer attached to the base metal, with the thicker, granular outer layer of corrosion product particles. The chemical analyses for the probe locations are given in Table 4.3. As shown in Table 4.3, the analysis of the base metal (X1) is typical of AISI Type 304 stainless steel. The thin adherent oxide layer (X6) appears to be a multimetal oxide, e.g., MXO_4, M_2O_3, or MO_2. The larger corrosion product metal oxide particles in the outer layer (X3, X4) are enriched in Al, Zr, and Ni, and depleted in Cr and Mn, relative to the base metal. The same analyses conducted on the cold leg piping specimen showed very similar results.

The inner oxide layer and the outer granular layer of corrosion product particles are very adherent to the base metal. Subsequent special form testing (49CFR173.469) of another core specimen (A-loop, hot side) to determine the dispersability of the contaminated corrosion layer showed this layer to be highly resistant to detachment caused by impact, percussion, heating, and leaching with high-purity water and seawater (Robertson, et al. 1987). These tests were conducted to simulate the accidental release of radioactive material from the contaminated inside surfaces of the Shippingport reactor pressure vessel in the event of an accident during transportation for disposal. The pressure vessel is being prepared intact for an LSA shipment for burial at Hanford, Washington (Kea, 1987).

4.3 LOW-LEVEL WASTE DISPOSAL CONSIDERATIONS OF SHIPPINGPORT DECOMMISSIONING MATERIALS

Although the decommissioning wastes generated at Shippingport Station are not subject to the regulations governing shallow land disposal of commercial low-level wastes (10CFR61), an assessment of the radionuclide

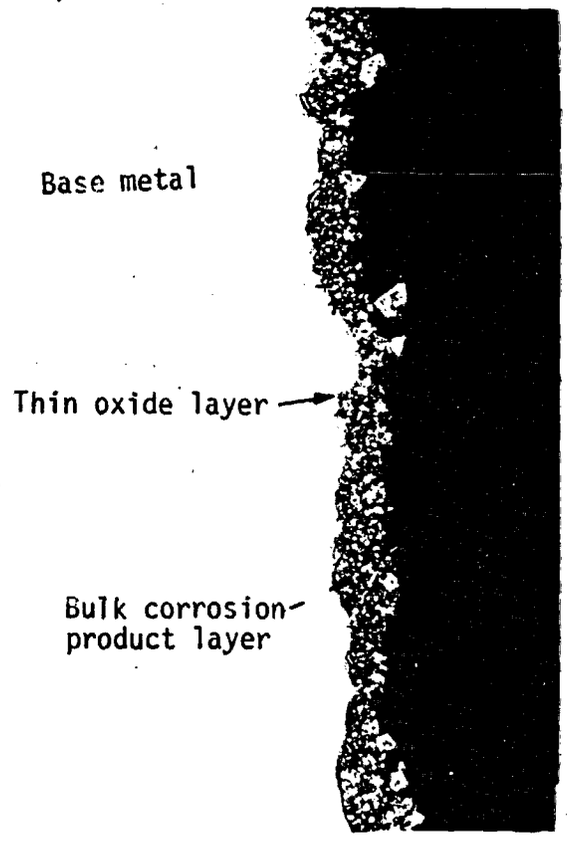

"B" Loop
Hot Let (Outlet) Piping

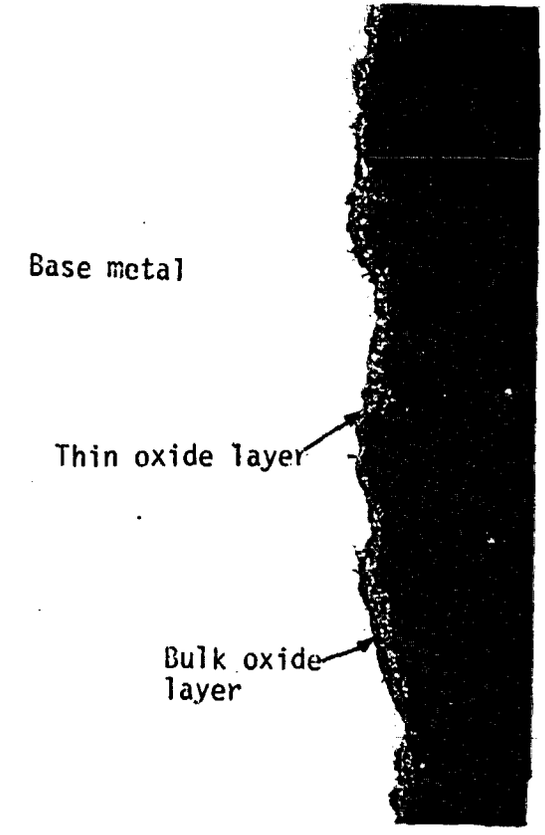

"B" Loop
Cold Leg (Inlet) Piping

Figure 4.3. Photomicrographs of the Contaminated Surface of Primary Coolant Piping Cores from the "B" Loop at Shippingport Station

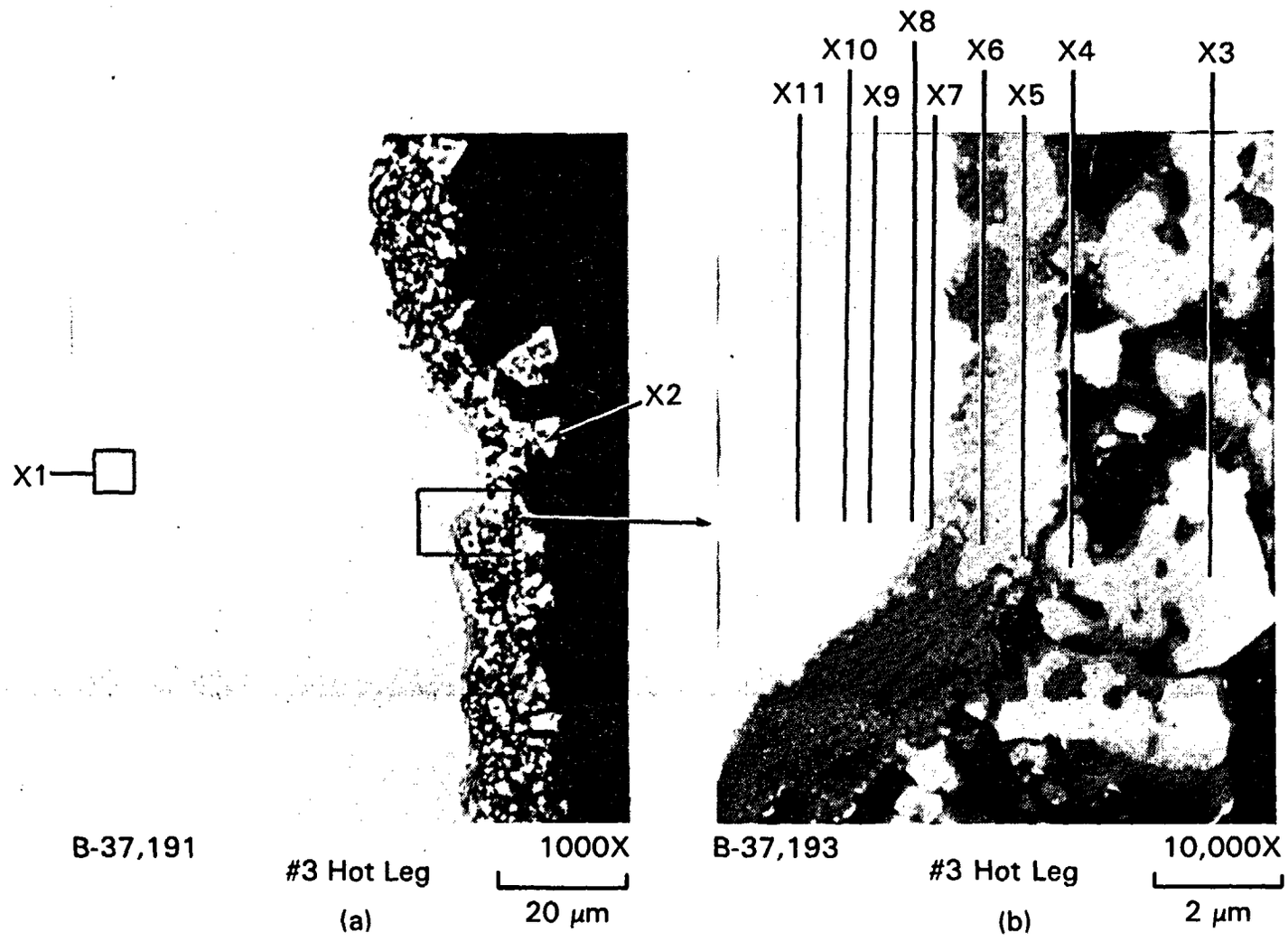

Figure 4.4. SEM Micrographs of Region of Shippingport Station Hot Leg Showing Probe Locations Selected for Chemical Analysis (EDAX). The Chemical Analysis for the Probe Locations Are Given in Table 4.3.

TABLE 4.3. Composition in Weight % and (Atomic %) of the Shippingport Station Primary Coolant Piping Corrosion Film at Hot Leg (Specimen #3). Probe Locations Shown in Figure 4.4.

	LOCATION										
Element	X1	X2	X3	X4	X5	X6	X7	X8	X9	X10	X11
Al	0.7 (1.5)	1.2 (1.3)	1.6 (1.6)	2.2 (2.2)	1.4 (1.4)	0.8 (0.9)	0.8 (0.9)	1.1 (1.5)	0.7 (1.0)	1.1 (1.5)	0.7 (1.0)
Si	1.3 (2.5)	1.4 (1.4)	0.9 (0.9)	1.4 (1.4)	1.3 (1.3)	1.5 (1.5)	1.6 (1.8)	1.6 (2.1)	1.5 (2.1)	1.6 (2.3)	1.4 (2.1)
P	0 (0)	0 (0)	0 (0)	0 (0)	0 (0)	0 (0)	0 (0)	0 (0)	0 (0)	0 (0)	0 (0)
S	0 (0)	0 (0)	0 (0)	0 (0)	0 (0)	0 (0)	0 (0)	0 (0)	0.2 (0.3)	0 (0)	0 (0)
Cr	18.2 (18.9)	0.4 (0.2)	1.3 (0.7)	9.7 (5.0)	17.7 (9.3)	20.4 (10.9)	20.2 (12.1)	17.0 (11.6)	15.9 (12.1)	15.5 (11.8)	15.5 (12.1)
Mn	1.8 (1.8)	0 (0)	0.1 (0.1)	0.6 (0.3)	0.7 (0.3)	1.1 (0.6)	1.3 (0.7)	1.3 (0.8)	1.7 (1.2)	1.6 (1.1)	1.7 (1.3)
Fe	67.6 (65.3)	40.7 (20.4)	39.6 (18.8)	30.5 (14.5)	26.7 (13.0)	27.2 (13.6)	33.4 (18.7)	46.1 (29.3)	55.4 (39.2)	56.1 (39.6)	57.7 (41.9)
Ni	9.9 (9.1)	16.2 (7.7)	12.6 (5.7)	13.2 (6.0)	11.1 (5.2)	9.9 (4.7)	12.2 (6.5)	11.3 (6.8)	9.0 (6.1)	8.9 (6.0)	8.7 (6.0)
Zr	0 (0)	0.7 (0.2)	0.5 (0.1)	0 (0)	0 (0)	0.2 (0.1)	0 (0)	0 (0)	0 (0)	0 (0)	0 (0)
Mo	0 (0)	0 (0)	0 (0)	0 (0)	0.2 (0.5)	0 (0)	0.2 (0.1)	0 (0)	0 (0)	0 (0)	0 (0)
Cs	0.1 (0.05)	0 (0)	0.2 (0.04)	0 (0)	0.2 (0.04)	0 (0)	0 (0)	0 (0)	0.3 (0.1)	0 (0)	0.3 (0.1)
O*	0.3 (0.9)	39.3 (68.8)	43.3 (72.2)	42.5 (70.8)	40.8 (69.5)	38.9 (67.9)	30.3 (59.2)	21.6 (47.9)	15.3 (37.9)	15.3 (37.8)	14.0 (35.5)

* Residual Assumption

contamination associated with the various decommissioning wastes is of interest. Based upon the comprehensive radiochemical analyses of the corrosion film associated with the primary coolant piping (Table 4.1), and assuming that the average concentration and observed range are representative of the contamination level of all plant systems exposed to primary coolant, e.g. steam generators, pressurizer, coolant pumps, primary purification systems, etc., it is possible to classify the waste with respect to the regulations in 10CFR61. Robertson et al. (1984) and Abel et al. (1986) have shown that for commercial power reactor stations having 5 to 50 times higher residual radioactivity levels in the primary systems, all components (excluding the pressure vessel) could be disposed of as Class "A" low-level waste (the least restrictive classification) in shallow land burial facilities. It, therefore, becomes obvious that all primary systems removed during the decommissioning would be well below Class "A" radionuclide concentrations and, therefore, eligible for disposal as Class "A" waste if it were to be disposed of in a commercial facility. These results confirm that for well-maintained power reactors, the residual radionuclide levels associated with the most contaminated systems outside of the pressure vessel can be readily disposed as Class "A" waste during commercial reactor decommissioning.

4.4 NEUTRON ACTIVATED COMPONENTS FROM COMMERCIAL REACTORS

Although a large sampling and radiochemical analysis program is currently underway to determine activation levels in pressure vessel steel and reactor internal components (see Sections 3.2 and 3.3), sufficient data for incorporation in this paper are presently not available. These measurements will, however, firmly document the levels of long-lived activation products produced in spent fuel assembly hardware, pressure vessel internal components, and in the pressure vessel itself. Comparisons will then be made with predicted levels calculated from existing activation codes to test their accuracy.

5.0 SUMMARY AND CONCLUSIONS

Work underway at PNL is carefully documenting the residual radiological conditions in retired nuclear power stations slated for decommissioning. The residual radionuclide conditions observed at Shippingport Station indicate that the average levels of long-lived activation products ^{60}Co, ^{55}Fe, ^{63}Ni, ^{59}Ni, and ^{94}Nb are approximately 5 to 50 times lower than observed in commercial nuclear power stations. In addition, the residual radioactive materials are essentially free of long-lived fission product and transuranic radionuclides (Pu, Am, Cm). These conditions have simplified the dismantling and decommissioning of the Shippingport Station. Had these decommissioning wastes gone to a commercial low-level waste shallow land burial facility, they would all have qualified as Class "A" waste.

6.0 REFERENCES

Abel, K. H., et al. (1986). "Residual Radionuclide Contamination Within and Around Commercial Nuclear Power Plant," NUREG/CR-4289, U.S. Nuclear Regulatory Commission, Washington, D.C.

Kea, K. I. (1987). "Reactor Pressure Vessel Preparation for Shipment and Burial," IN: 1987 International Decommissioning Symposium, October 4-8, 1987, Pittsburgh, PA, CONF-871018-Vol. 1, pp. II-31 to II-47, Gail A. Taft, Ed., Westinghouse Hanford Corporation, Richland, WA.

Luksic, A. T., et al., "Spent Fuel Disassembly Hardware and Other Non-Fuel Bearing Components: Characterization, Disposal Cost Estimates, and Proposed Repository Acceptance Requirements," PNL-6046, Pacific Northwest Laboratory, October, 1986.

Robertson, D. E., et al. (1984). "Residual Radionuclide Contamination Within and Around Nuclear Power Plants: Origin, Distribution, Inventory, and Decommissioning Assessment," Rad. Waste Mgmt. Nucl. Fuel Cycle, 5, pp. 285-310.

Robertson, D. E., K. T. Hara and W. M. Badbada (1987). "Special Form Testing of Shippingport Atomic Power Station outlet Coolant Piping Specimens," report in clearance, Pacific Northwest Laboratory, Richland, WA.

Smith, R. I., G. J. Konek and W. E. Kennedy, Jr. (1978). "Technology, Safety and Costs of Decommissioning a Reference Pressurized Water Reactor Power Station," NUREG/CR-0130, Vols. 1 and 2. Prepared for the U.S. Nuclear Regulatory Commission by Pacific Northwest Laboratory, Richland, Washington, June 1978.

U.S. N.R.C. (1981). "Licensing Requirements for Land Disposal of Radioactive Wastes," 10 CFR 61. Federal Register, 46, No. 142, Friday, July 24, 1981, U.S. Nuclear Regulatory Commission, Washington, D.C.

U.S. N.R.C. (1986). "Licensing Requirements for the Independent Store of Spent Nuclear Fuel and High Level Radioactive Waste, 10 CFR Parts 2, 19, 20, 21, 51, 70, 73, 75, and 150, Federal Register 51, No. 101, Tuesday, May 27, 1986.

SEVERE ACCIDENT MANAGEMENT IN THE UNITED STATES

Presented at the Fifteenth

Water Reactor Safety Information Meeting

October 26-30, 1987

Brian W. Sheron
Director, Division of Reactor and Plant Systems
Office of Nuclear Regulatory Research
U.S. Nuclear Regulatory Commission

Good day. Today I would like to discuss with you the concept of severe accident management, the role it is expected to play if a severe accident were to occur, and the approach the NRC expects to take in ensuring the implementation of severe accident management programs in operating U.S. plants.

First, severe accident management is only part of a larger concept called risk management. Risk management is in essence the underlying philosophy of operation of all U.S. plants, as well as the underlying philosophy of the NRC's entire regulatory program. The major elements of risk management are depicted in Figure 1 and consist of reliability management, accident management, and emergency management. Together these elements form a safety hierarchy.

Reliability management is by far the main focus of both regulatory and industry programs, and strives to achieve safety through ensuring reliable plant

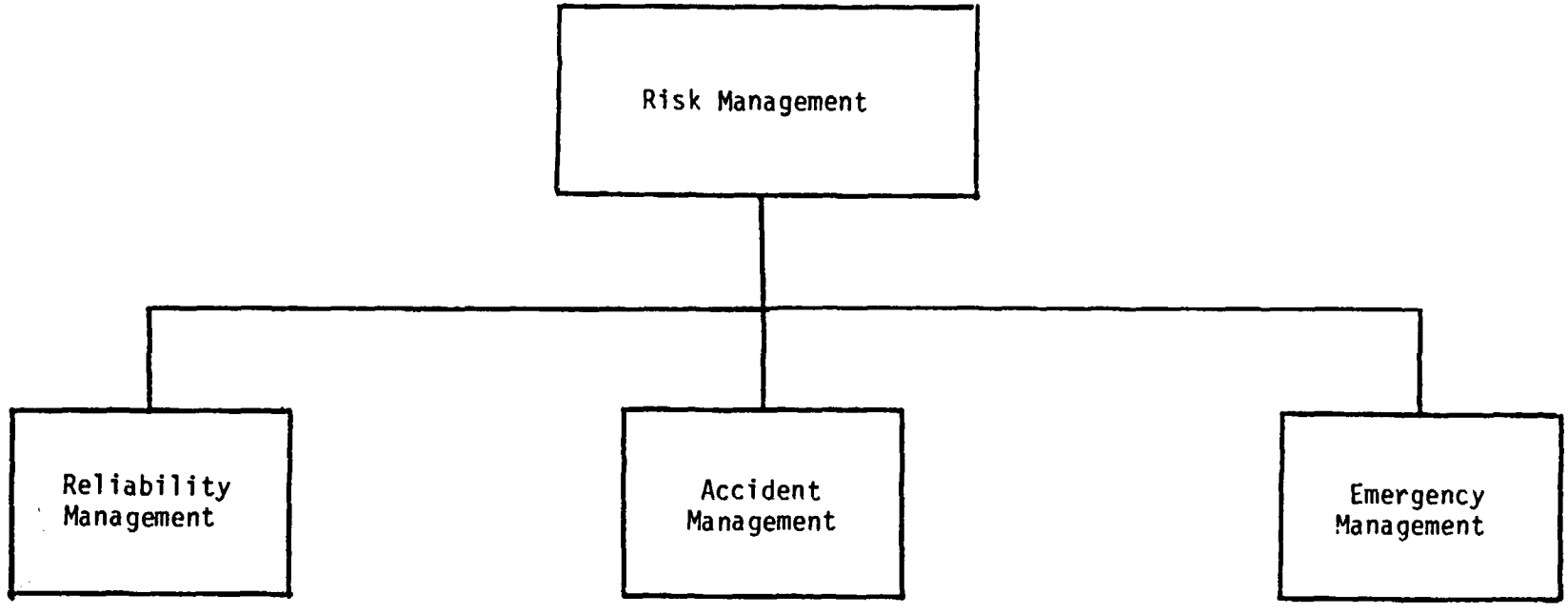

FIGURE 1

Elements of Risk Management

construction and operation. It encompasses quality assurance, quality control, high quality design and construction methods and requirements, and effective operations management, to name a few.

Notwithstanding the objective of ensuring safety through reliable design and operation, it is recognized that, as in any technology, things can go wrong. In recognition of this, precautions are taken to minimize the consequences of failures. For most plants, the extent of the precautions originally taken were primarily derived from the design basis of the plant. For example, the containment design basis is set by postulating a large break loss-of-coolant accident. However, these precautions did not include consideration of core melt accidents. Following TMI-2, the extent of these precautions was expanded to include the ability to accommodate certain aspects of beyond design basis accidents. In the area of design, all U.S. plants were required to accommodate safely the release of 75 percent of the maximum amount of hydrogen that could theoretically be released through complete oxidation of the fuel cladding. Safety parameter display systems were required. In addition, emergency procedures were extensively revised to be symptom rather than event oriented, and were expanded to provide guidance on managing accidents up to inadequate core cooling events.

Recognizing that in the event of certain failures a core melt and potentially containment failure could not be avoided, the Commission also implemented emergency management. This involved requiring all licensees to have offsite emergency plans that provided for evacuation or sheltering of the public in a structured, planned manner in the event of a radiological emergency.

From the following discussions of the concept of risk management, it is evident that a key ingredient that is still missing in the operation of plants is the management of accidents that progress beyond inadequate core cooling. This is the area of severe accident management.

Severe Accident Management Concept

As a concept, severe accident management is new but not unique. Procedures for the management of events that went up to degraded cores were instituted following the TMI-2 accident. The need for these procedures was obvious: operators would not sit idly by when an event occurred, as assumed for the establishment of the design basis. Rather, they could and in all probability would actively intervene in an attempt to mitigate the event. Thus, while the procedurs were designed to aid the operator in making the right decisions, they also were specifically designed to help ensure the operator did not make the wrong decision. In fact, they were so structured so that if a wrong decision was made, the operator would be guided to correct the error and take the right action based on the observed symptoms.

While it has never been accurately quantified, many safety experts from a variety of backgrounds seem to generally agree that the operator can potentially contribute anywhere from 10 to 50 percent of the risk to the health and safety of the public. Although the Commission is conducting a number of research programs aimed at developing human reliability models and data bases in an attempt to quantify the risk contributed by the operator,

this is by far a highly inexact science, and our ability to quantify this risk with reasonable uncertainty bounds is still in the future.

An alternative way to pursue the reduction of uncertainty in risk resulting from operator actions is to concentrate on minimizing the extent to which an operator will have to operate without guidance. Therefore, the basic premise underlying the need for an accident management program is that a much more substantial reduction in not only absolute risk but also in risk uncertainty can be obtained by providing operators with guidance on how to manage severe accidents, rather than relying on a "seat-of-the-pants" decision process that unfolds as a severe accident is occurring.

It must also be pointed out that the need for a severe accident management program becomes obvious from a risk reduction perspective when one considers that severe accidents contribute the largest risk to the health and safety of the public. The concept of accident management, then, is primarily founded on the premise that a substantial reduction in not only risk, but risk uncertainty, can be achieved by ensuring operators are properly instructed in the handling of severe accidents.

The Role of Severe Accident Management

The terms "Severe Accident Management" and "Severe Accident Management Strategies" are frequently used in the abstract. They imply that there is perhaps this complex sequence of actions that operators can take that somehow

will miraculously prevent core melt, or vessel or containment failure. Frequently, rather abstract terms such as "core stabilization" are used. Let me assure you that severe accident management is not a "black art," but rather a process in which potentially effective actions that reduce or mitigate the consequences of a severe accident are identified, evaluated, incorporated into a structured program, implemented at a plant site, and are available to the operators and management in the event of a severe accident. Severe accident management encompasses both technical as well as human factor and organizational (or administrative) areas. All of these are now discussed.

Technical Areas

In Figure 2, the four main technical areas related to severe accident management are shown. These are 1) existing Emergency Operating Procedures (EOPs), 2) preventive measures, 3) in-vessel management, and 4) ex-vessel management. Since I have already discussed the genesis of the current EOPs and their scope (up to inadequate core cooling), I will not address these further.

The area of preventive measures encompasses that wide assortment of programs and efforts designed to identify and correct significant contributors to risk found in plants. Programs such as the Commission's Unresolved and Generic Safety Issue (USI/GSI) programs are designed to examine the risk significance of potential generic deficiencies in design or operation of commercial U.S.

FIGURE 2

Elements of Accident Management

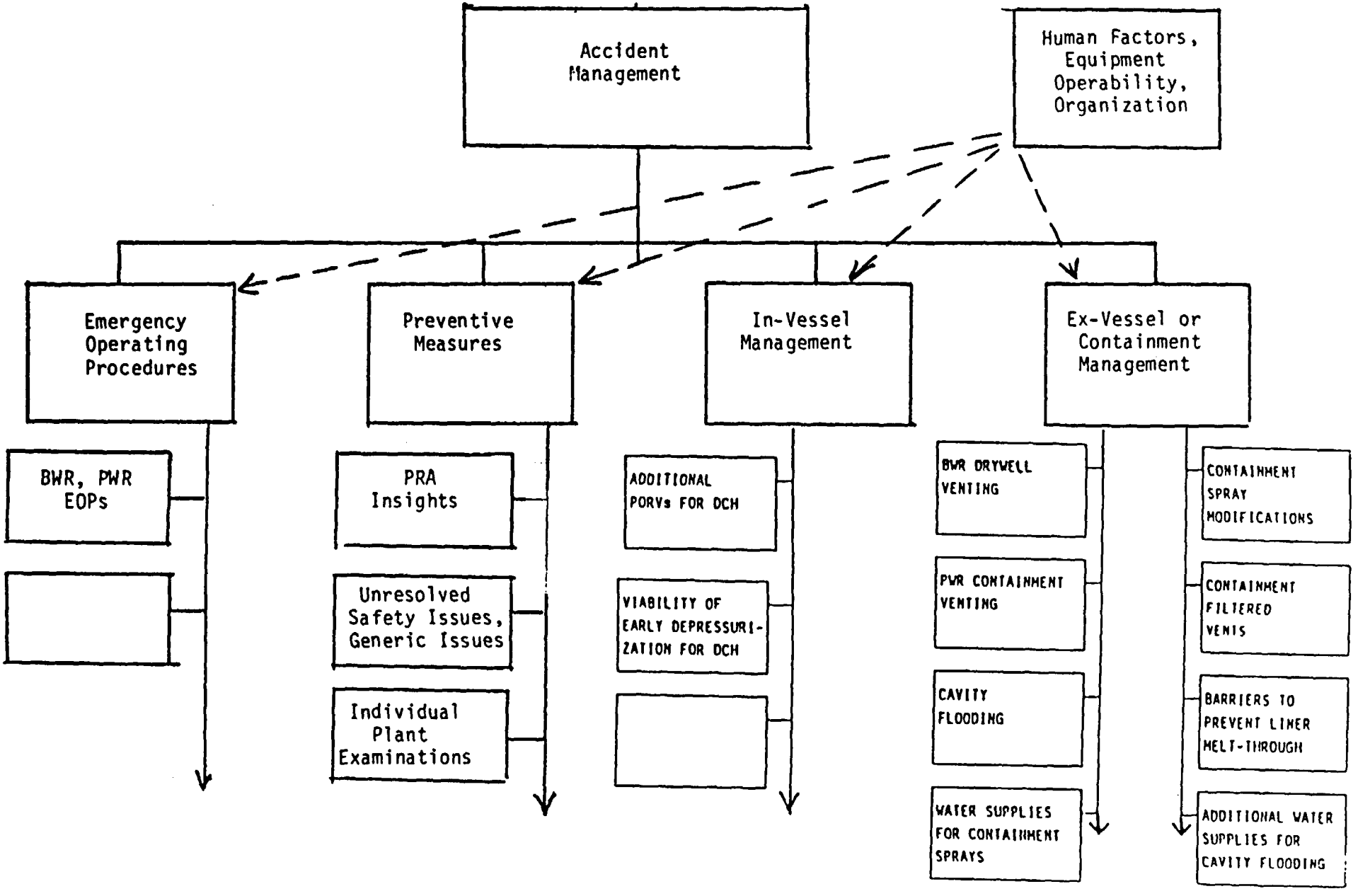

plants, and identify cost-effective means to correct any deficiencies. Probabilistic Risk Assessments, or PRAs, also provide insights into both plant specific and generic risk dominant sequences with the intent to ensure that they do not pose unacceptable risks.

In-vessel Management

The three major barriers to fission product release are the fuel cladding, the primary system pressure boundary, and the containment. In-vessel accident management addresses the maintenance of the first two boundaries. With the possible expection of ATWS, all core melts result from the loss of coolant from the primary system. Thus, there is no secret to in-vessel accident management. The fundamental strategy is to put water in the vessel sufficient to cool the core. Thus, accident management actions are expected to focus on identifying all alternative means for injecting water into the primary system. Considerations include the use of low pressure systems, such as the fire protection system, with suitable connectors available and consideration of the need for locating hoses, etc., at strategic locations. Symptoms that would alert the operators to when core integrity was lost should be predicted. Concerns regarding inappropriate actions must also be evaluated. For example, would the introduction of relatively cool water from a recovered water supply onto a hot molten core that has not yet penetrated the vessel produce a vessel failure due to excessive pressurization from rapid steam production? Are there special procedures an operator should follow to minimize any adverse effects of introducing water onto a molten core? The

following were only a few examples of the considerations that must go into the development of an effective in-vessel severe accident management program.

Ex-vessel Management

Once the cladding and primary system boundary have failed, the containment is the only barrier which prevents the release of fission products to the environment. There are a number of actions an operator may take in an attempt to maintain containment integrity. In particular, the restoration of failed safety systems poses a number of unique questions that an operator should have answers to prior to taking restoration action. A number of examples are listed below:

- Will restoration of igniters in a hydrogen-filled containment result in unacceptable detonation?

- Will restoration of containment sprays in a steam and hydrogen-filled containment condense steam to the extent a detonable mixture of hydrogen results with unacceptable consequences?

- Will initiating containment sprays into a previously vented containment result in implosion?

In addition to actions related to restoration of failed safety systems, the benefits from additional mitigative features must also be explored. In

Europe, for example, all reactors in France, Germany, and Sweden have been or will be fitted with filtered vents for their containments to prevent late overpressure failures. Direct Containment Heating (DCH) is a highly controversial subject related to the early overpressurization failure of PWR containments due to direct heating of the containment atmosphere by the molten core ejected during a vessel melt-through at high pressure. Due to the complex phenomena associated with this scenario, it may not be possible to adequately resolve the issue within the near future. Hence, an alternative approach is to rapidly depressurize the primary system prior to vessel failure to preclude ejecting melt into the upper containment atmosphere. The feasibility of such an approach should be studied to identify a) the ability to depressurize to a suitably low pressure prior to vessel failure, b) the key symptoms an operator must recognize and use to initiate depressurization, c) the desirability of adding additional blowdown valves to better achieve the necessary depressurization, and d) the adverse consequences associated with depressurization.

The preceding discussions and examples of technical issues associated with in-vessel and ex-vessel accident management hopefully illustrate the need for severe accident programs to be developed in a systematic, structured manner, as well as exemplifying the subtle technical issues that must be resolved prior to implementing any severe accident management actions.

Human Factors and Organizational Considerations

Any study of the technical issues associated with developing an effective accident management program must be accompanied by a consideration of the

human factors issues that play a large role in the effectiveness of such a program. It is difficult to distinguish some of the issues between "human factors" and organizational. Whichever way they are categorized is not important, however, provided they are appropriately considered and treated. As such, they will be discussed together here.

One of the first and foremost questions that implementing a severe accident management program raises is the decision-making process. In light of the stress and confusion a severe accident would impose on not only a utility, but also on the numerous other organizations that have response responsibilities, it is imperative that the decision-making process be clearly established and understood by all plant personnel, from each and every operator to the company president. For example, if a decision must be made to depressurize the vessel to prevent DCH, or to vent the containment to prevent overpressure failure, the operators and plant management should know exactly who is authorized to make such a decision. In turn, the decision maker must have available all of the information he or she needs to make such a decision. Needed to be known is the reliability of the information used for the decision-making process. For example, can the sensors being relied upon to establish the states of the core and containment be trusted? Will they work in the environment they are being used to assess?

Will the decision maker have the appropriate technical facts readily available to make informed decisions? For example, the decision maker should know what

the ultimate containment pressure is and at what pressure containment venting must commence to be effective. He or she should be aware, in advance, of all of the ramifications of certain decisions. Examples of these were previously discussed in the technical issues section.

Since the effectiveness of any program is only as good as the people who carry it out, it follows that effective severe accident management can only be accomplished by developing all of the necessary information needed for such a program in advance, and then by training the plant "team" to understand the plan and effectively carry it out. Through the development of the technical basis for severe accident decisions, and then the effective implementation of this technical basis into a severe accident management program in which all key plant personnel are trained, will a substantial reduction in risk arising from human factor considerations be achieved.

NRC's Implementation Program

In August, 1985 the Commission issued its Policy on Severe Accidents. This policy stated that while the Commission believed operation of reactors in the U.S. did not pose an undue risk to the health and safety of the public, they also believed that each commercial U.S. reactor licensee should perform a systematic examination of its plant's design for severe accident vulnerabilities. The staff is currently preparing a generic letter to be sent to each licensee requesting they perform an individual plant examination (IPE) to fulfill the policy's guidance.

It is currently our expectation that the conclusions drawn from the IPEs regarding severe accident vulnerabilities will depend on operators taking beneficial action during or prior to the onset of severe core damage. More importantly, these conclusions will in all likelihood also rely on operators not taking specific action which could have adverse effects. Therefore, in order to justify the assumptions made with respect to operator (and plant management) performance, a logical outcome of the IPEs will be a confirmation of the need for an accident management program for each plant.

It is recognized that a substantial amount of work has already been done on severe accident management, both in the U.S. as well as abroad, most notably in France, Germany and Sweden. Since many severe accident management strategies do not involve significant changes in plant design, but rather can be quickly put in place by appropriate training and procedures, it is believed that substantial safety benefits can be achieved by the early initiation of severe accident management programs at each plant that do not rely on the completion of an IPE.

Various ongoing programs (both government and industry) indicate that information on severe accidents and severe accident management will continually be developed over the next several years. In order to effectively incorporate this information into a severe accident management program in a timely manner, we are encouraging all licensees to structure their programs to be flexible and allow for the periodic incorporation of new information.

The NRC Research Program

The NRC's Office of Nuclear Regulatory Research is initiating a comprehensive Accident Management Research Program starting in FY 88. We are currently developing the detailed program structure, but it will generally follow the structure shown on Figures 1 and 2. The main objectives of this program are:

- to provide a technical basis for staff review of licensee accident management programs submitted with the IPE results

- to explore the benefits and drawbacks of severe accident management strategies and share this information with the public, particularly the operators of nuclear plants

- to identify any additional research that is needed to draw conclusions on accident management strategies.

Direct funding of this program from the Division of Reactor and Plant Systems is currently planned in the neighborhood of $2M in FY 88, which includes efforts to carry out the severe accident policy (IPE implementation). The program is being developed to produce results in the short (several months), intermediate (1-2 years), and long term (3 years and beyond). In particular, our short-term results are focused on developing a compendium of severe accident management information for distribution to the U.S. nuclear industry. The compendium will identify the key phenomena associated with severe accidents and what is known

(and not known) at this time about severe accident management strategies associated with these phenomena. It is the sole intent of this report to inform licensees of the issues (pros, cons, uncertainties) associated with severe accident management, and to neither direct, recommend, nor endorse they be implemented at this time. We intend to update this report periodically as new information becomes available.

Progress to date in developing the research program has focused on establishing the key tasks for the in-vessel and ex-vessel work. Figure 3 depicts the key tasks associated with the in-vessel program, and Figure 4 depicts the key tasks associated with the ex-vessel program. In the coming months, these tasks will be further refined, and individual work elements identified. We anticipate involving substantial university and college expertise along with national laboratory expertise to resolve specialized problems associated with invididual tasks.

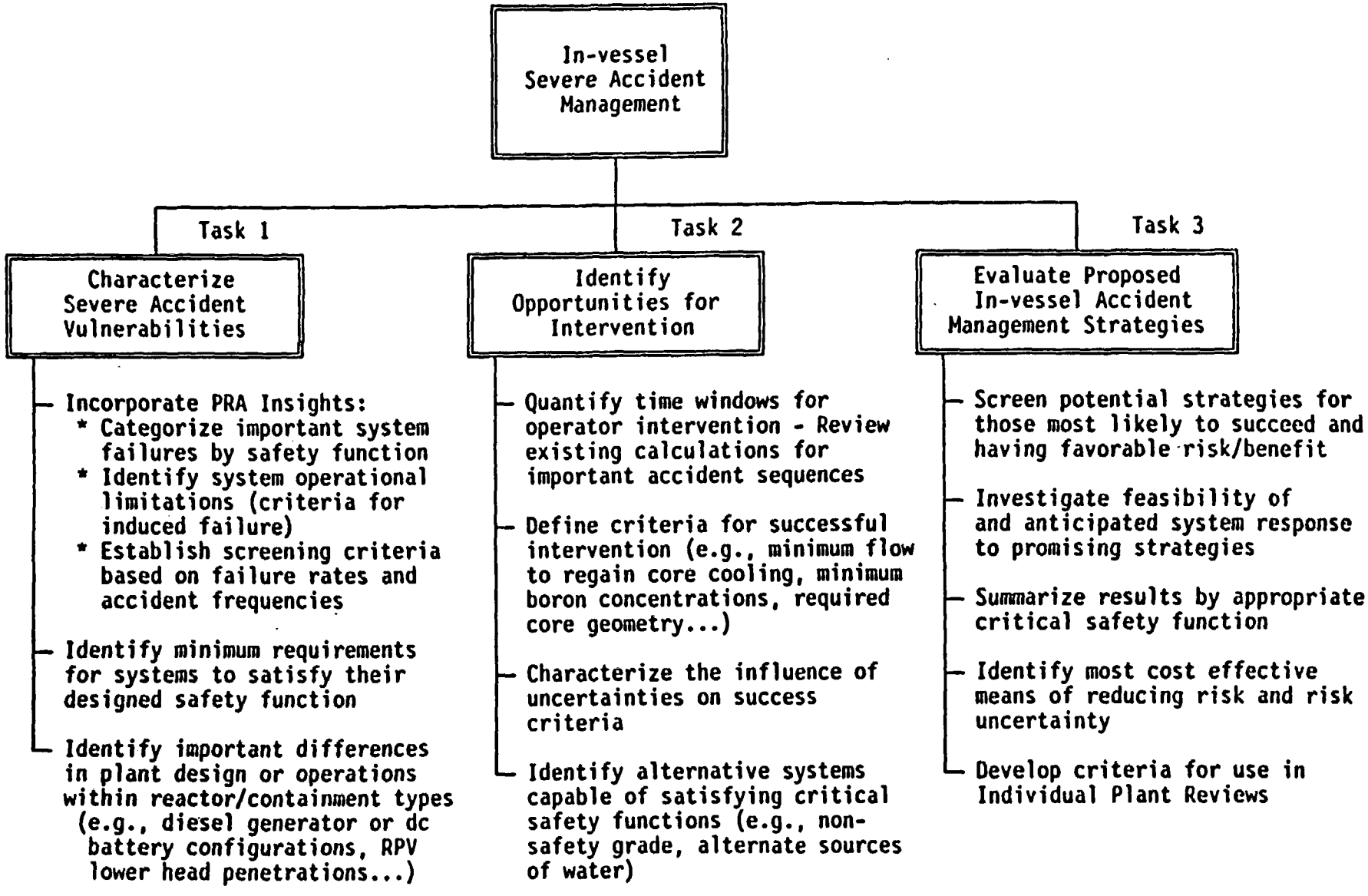
In-vessel Severe Accident Management
Task 1
Characterize Severe Accident Vulnerabilities
Incorporate PRA Insights:
* Categorize important system failures by safety function
* Identify system operational limitations (criteria for induced failure)
* Establish screening criteria based on failure rates and accident frequencies
Identify minimum requirements for systems to satisfy their designed safety function
Identify important differences in plant design or operations within reactor/containment types (e.g., diesel generator or dc battery configurations, RPV lower head penetrations...)
Task 2
Identify Opportunities for Intervention
Quantify time windows for operator intervention - Review existing calculations for important accident sequences
Define criteria for successful intervention (e.g., minimum flow to regain core cooling, minimum boron concentrations, required core geometry...)
Characterize the influence of uncertainties on success criteria
Identify alternative systems capable of satisfying critical safety functions (e.g., non-safety grade, alternate sources of water)
Task 3
Evaluate Proposed In-vessel Accident Management Strategies
Screen potential strategies for those most likely to succeed and having favorable risk/benefit
Investigate feasibility of and anticipated system response to promising strategies
Summarize results by appropriate critical safety function
Identify most cost effective means of reducing risk and risk uncertainty
Develop criteria for use in Individual Plant Reviews

FIGURE 3

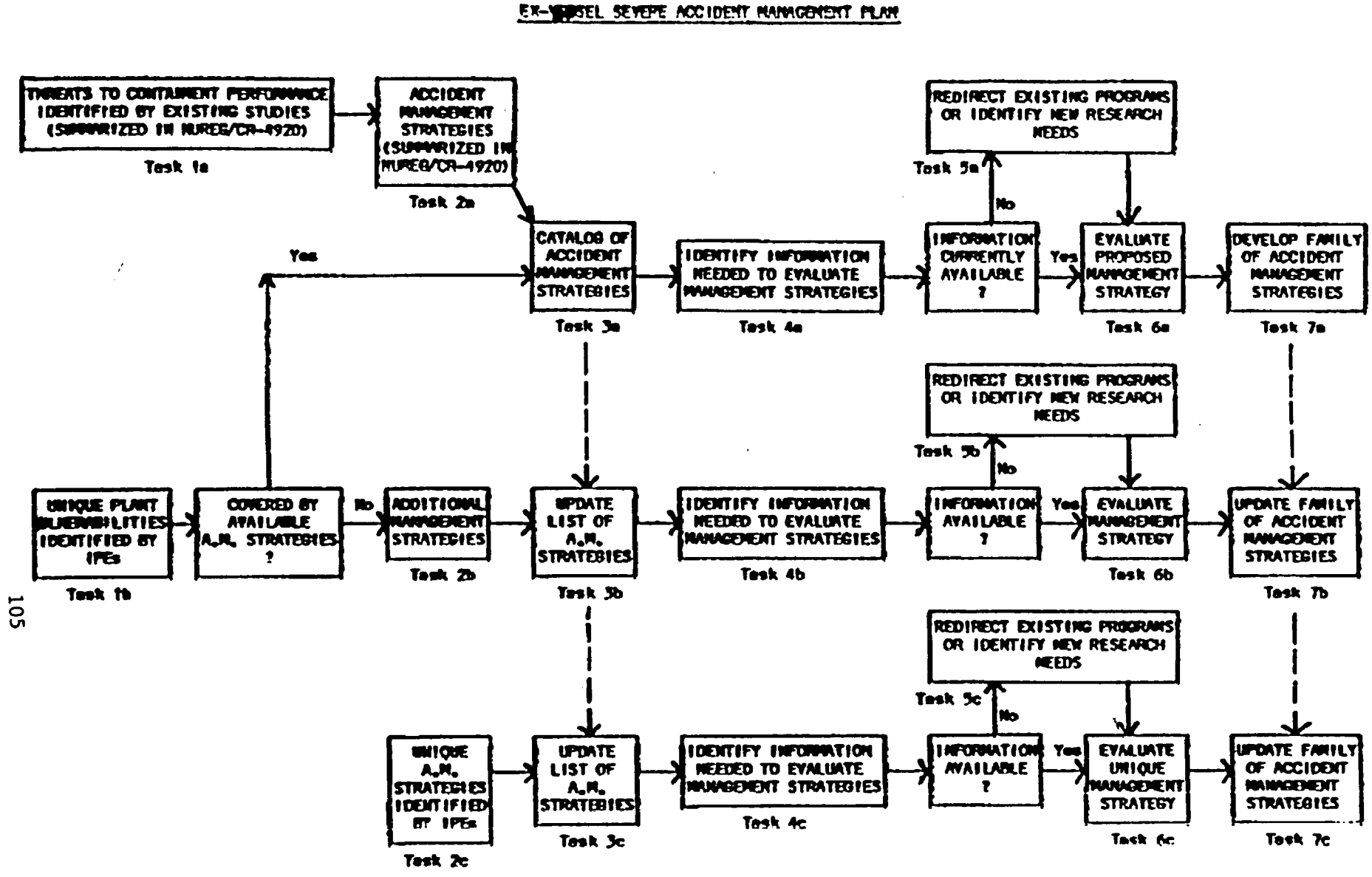
EX-VESSEL SEVERE ACCIDENT MANAGEMENT PLAN
THREATS TO CONTAINMENT PERFORMANCE IDENTIFIED BY EXISTING STUDIES (SUMMARIZED IN NUREG/CR-4920)
Task 1a
ACCIDENT MANAGEMENT STRATEGIES (SUMMARIZED IN NUREG/CR-4920)
Task 2a
REDIRECT EXISTING PROGRAMS OR IDENTIFY NEW RESEARCH NEEDS
Task 5a
No
Yes
CATALOG OF ACCIDENT MANAGEMENT STRATEGIES
Task 3a
IDENTIFY INFORMATION NEEDED TO EVALUATE MANAGEMENT STRATEGIES
Task 4a
INFORMATION CURRENTLY AVAILABLE ?
Yes
EVALUATE PROPOSED MANAGEMENT STRATEGY
Task 6a
DEVELOP FAMILY OF ACCIDENT MANAGEMENT STRATEGIES
Task 7a
REDIRECT EXISTING PROGRAMS OR IDENTIFY NEW RESEARCH NEEDS
Task 5b
No
UNIQUE PLANT VULNERABILITIES IDENTIFIED BY IPEs
Task 1b
COVERED BY AVAILABLE A.M. STRATEGIES ?
No
ADDITIONAL MANAGEMENT STRATEGIES
Task 2b
UPDATE LIST OF A.M. STRATEGIES
Task 3b
IDENTIFY INFORMATION NEEDED TO EVALUATE MANAGEMENT STRATEGIES
Task 4b
INFORMATION AVAILABLE ?
Yes
EVALUATE MANAGEMENT STRATEGY
Task 6b
UPDATE FAMILY OF ACCIDENT MANAGEMENT STRATEGIES
Task 7b
REDIRECT EXISTING PROGRAMS OR IDENTIFY NEW RESEARCH NEEDS
Task 5c
No
UNIQUE A.M. STRATEGIES IDENTIFIED BY IPEs
Task 2c
UPDATE LIST OF A.M. STRATEGIES
Task 3c
IDENTIFY INFORMATION NEEDED TO EVALUATE MANAGEMENT STRATEGIES
Task 4c
INFORMATION AVAILABLE ?
Yes
EVALUATE UNIQUE MANAGEMENT STRATEGY
Task 6c
UPDATE FAMILY OF ACCIDENT MANAGEMENT STRATEGIES
Task 7c

FIGURE 4

SEVERE ACCIDENT MANAGEMENT ON FRENCH PWRs

J. Duco, J. Brisbois, D. Quéniart
Commissariat à l'Energie Atomique, France
Institut de Protection et de Sûreté Nucléaire

1. INTRODUCTION

French PWR power plant design relies basically on a deterministic approach. In such an approach, the consequences of a limited number of conventional situations are assessed, as well as the relevant frequencies of occurrence, which are classed in frequency categories expressed in terms of orders of magnitude. The conventional situations retained are such that their consequences are larger than those of all other situations of the same frequency category. These situations are called the design basis situations.

A probabilistic approach was introduced in France in the early seventies to define safety provisions against external impacts (aircraft crashes and risks related to an industrial environment). In 1977 an overall safety objective - more a target than a mandatory value - was issued by the safety authority in terms of an upper probability limit for having unacceptable consequences. Following that ruling, the utility was required to prove that the loss of the redundant safety-related systems would meet the safety objective. As it did not, additional measures were taken (the "H" operating procedures) to complement the automatic systems normally provided by the initial design, so as to satisfy the safety objective.

The TMI-2 accident enhanced the interest in confused situations in which possible multiple equipment failure and/or unappropriate previous actions of the operators impede the implementation of any of the existing event-oriented procedures. In such situations, the objective becomes to avoid core-melt by any means available : this is the goal of the U1 symptom-oriented procedure.

Whenever a core-melt occurs, the radioactive releases into the environment must be compatible with the feasibility of the off-site emergency plans ; that means that for some hypothetical, but still conceivable scenarios, provisions have to be made to delay and limit the consequences of the loss of the containment : the U2, U4 and U5 ultimate procedures - the latter providing a venting of the containment through a filtration system - have been elaborated for that purpose.

Emergency management procedures, whether event- or symptom-oriented, need a significant R and D effort in order to be elaborated and checked; such an effort resulted in the achievement of the physical code CATHARE and the integral test facility BETHSY, which are both used for adjusting the procedures.
For the case of an emergency, a nationwide organization has been set up to provide the plant operator with a redundant technical expertise, to help him save his plant or mitigate the radiological consequences of a core-melt. Besides, such an organization makes prognoses of possible radioactivity transfers to the environment, aimed at supporting the government representative in charge of protecting the public.

French safety authority / Electricité de France — deterministic

2. FRENCH SAFETY RATIONALE

2.1 Design bases of French PWRs for radioactivity retention in plausible situations

The French Nuclear Power Plant Program is based on the design, construction and operation of identical series of PWRs. The only differences to be found in reactors of the same series involve adaptation to the site.

American reactors under construction were used as the reference for the construction of the first French reactors (Beaver Valley for Fessenheim, North Anna for Bugey). At this stage, Electricité de France and the French safety authority essentially based themselves on American safety regulations (10 CFR 50 and Regulatory Guides) for ensuring and evaluating reactor safety.

The experience gained in the operation of the two Fessenheim and four Bugey units formed the basis for the design of the 900 MWe reactor series (CP1 and then CP2), the 1300 MWe reactor series (P4 then P'4) and then the 1400 MWe reactor series (N4).

Accident prevention relies essentially on a deterministic approach, the objective of which is to demonstrate that, in the situations considered as plausible (normal operation, incident and accident situations), the retention of the radioactive substances is sufficient. Confining radioactivity is provided by "barriers" and the situations to be allowed for result from application of a "defense-in-depth" concept.

The radioactive substances are confined by means of "barriers" placed between them and the plant staff or the general public. In French-built PWRs, three barriers are schematically considered : the cladding of the fuel, the pressure boundary of the primary system and the containment. The integrity of the barriers is checked for normal operation and for the incident and accident situations considered plausible. Radioactive susbstances can only be released if all three barriers fail. (with the exception of containment by-pass)

The "defense-in-depth" concept used to define the situations considered as plausible classically involves three levels.

- Prevention by quality

The design, fabrication and operating range of the equipment are to be such as to provide the installation with sufficient safety margins with regard to specified limits, to ensure its proper behavior.

- Monitoring and protection

The installation is to be equipped with monitoring and protection systems aimed at restoring it to its normal operating range in all foreseeable transient and incident cases.

enveloppe accident

- Safeguarding

Regardless of the above preventive and protective measures, plausible accidents are to be allowed for, and safeguard systems have to be devised to limit the consequences of such accidents.

When applying this concept, the following points must be borne in mind :

1) The fact that a component or system is designed for a given situation does not mean that its failure in that situation can be disregarded. If the consequences of such an event are considered unacceptable, additional provisions must be made to mitigate or prevent them. In this way, appropriate arrangements are made to ensure that the pressure systems can withstand the maximum stress to which they are liable to be subjected, the case of their failure nevertheless being given consideration in accident studies. No exception to this rule is allowed unless the risk is sufficiently minimized by adequate preventive measures. The catastrophic failure of the reactor vessel of a pressurized water reactor is thus excluded in the light of precautions taken during its design and fabrication, and of the tests carried out during the service life of this component to ensure timely detection of any faults which may be forerunners of more serious failures ; in addition, specific regulations apply to this component which is the subject of special scrutiny by the relevant government body.

2) As it is not possible to examine all the accident situations considered plausible, operators and safety authorities have agreed to examine a limited number of them, selected as being representative of the risks. Each situation is chosen and studied in such a manner that its consequences are conservative compared to those of the events of the same nature that are intended to be represented ("envelope accident" approach).

3) It is necessary to identify the failures which can simultaneously jeopardize the arrangements made to prevent the accidents and mitigate their consequences ; provisions have been made to avoid such failures being the origin of unacceptable consequences. In this way, the total failure of the onsite and offsite power supplies can lead to a LOCA (leakage at primary pump seals) which the safeguard systems, having no power, will be unable to compensate for. Similarly, fire can be a source of "common mode" failure. Here the problem is to decide how far to go, and what accident situations are to be allowed for in designing the installation. In the deterministic approach, a conventional list of situations is usually established, such situations being grouped in frequency categories : the lower the probability of occurrence of a category the higher the upper limit for the corresponding consequences.

For each site, French regulations require authorizations for the gaseous and liquid radioactive effluent releases ; these authorizations set the maximum admissible global activities for the releases on a case-by-case basis and specify the limits of activity for some radioactive species. Conversely, French regulations do not set limits on the equivalent doses likely to be received by the public under accident conditions. The radioactive consequences induced by the conventional operating conditions and conditions resulting from external events are calculated without reference to upper limits of dose equivalents, but their assessments are submitted for each unit to the safety authority for approval and are generally deemed acceptable during the licensing procedures in which the agreement of the Ministry of Health has to be obtained. Nonetheless, Electricité de France has proposed the following limits, which have been accepted by the Safety Authorities for PWR design purposes.

Frequency Category	Estimated Frequency (per year)	Maximum Radioactive Consequences
1 Normal operation	1	limited by the radioactive waste release authorizations
2 Minor but frequent incidents	10^{-2} - 1	
3 Unlikely incidents	10^{-4}-10^{-2}	0.5 rem (whole body) or 5m Sv 1.5 rem (thyroid) or 15m Sv
4 Hypothet. accidents	10^{-6}-10^{-4}	15 rem (whole body) or 0.15 Sv 45 rem (thyroid) or 0.45 Sv

Appendix 1 gives the conventional list of operating situations chosen for standardized 1300 MWe nuclear units.

2.2 Complementary probabilistic approach

2.2.1 Safety objectives

The probabilistic approach was first used in France to define safety measures to be taken against external events. This approach was used to establish a relationship between such events which had to be taken into account in the plant design and conventional operating conditions.

For example, on the basis of a probability analysis of an aircraft crashing on a PWR, the French safety authority accepted that the various series of reactors be designed solely to withstand the crash of a general aviation aircraft (based on a 1.5 tonne Cessna 210 as a "hard" projectile and a 5.7 ton Lear Jet 23 as a "soft" projectile), therefore not taking into account the risks deriving from military and commercial aircrafts ; such a policy resulted in deleting some names on the list of candidates for becoming a PWR site.

As early as 1977, an examination of the general technical options for the 1300 MWe PWR series resulted, on the recommendation of the Standing Group ("Groupe Permanent") in charge of the nuclear reactors, in the setting forth of an overall probabilistic objective in the following terms :

"The design of a nuclear unit comprising a PWR should be such that the overall probability that the said unit can induce unacceptable consequences will not exceed 10^{-6} per year".

"From hereon, when a probabilistic approach is to be used to assess whether a group of events should be allowed for in the design of a unit, it should be assumed that this group of events must be allowed for if the probability that it may lead to unacceptable consequences exceeds 10^{-7} per year ; such a threshold cannot be exceeded for the said group unless it can be proved that the calculation of the relevant probabilities is sufficiently conservative".

"Moreover, Electricité de France has to pursue its efforts to extend as early as possible the use of probabilistic approaches for the broadest possible range of events".

"In application of the above, Electricité de France shall examine on a case-by-case basis, whether the simultaneous failure of the redundant files of the systems essential to safety should be taken into account in the design of power units using PWRs ... For these studies "realistic" assumptions and calculations methods may be used".

Such statements have to be supplemented by the following comments for clarification.

1. The overall objective is set forth in terms of "unacceptable consequences" ; in accordance with the above, these "unacceptable consequences" are not defined by any legislative or regulatory text. In fact, such consequences are to be assessed in political terms, taking into account site-related effects and the possible impact of measures aimed at protecting the general public.

2. The probability of 10^{-6} per year is a "target" value for a reactor, and Electricité de France was not required to demonstrate that such a target value had been met ; nevertheless, this objective was considered as reasonable, based on the results of the WASH-1400 Report and on the improvements made in the design of French reactors with respect to the PWR power plant examined in this report. The justification of the design provisions adopted to prevent any unacceptable risk relies heavily on deterministic analyses rather than on an overall probabilistic analysis.

In this regard, in a letter addressed to Electricité de France in 1978, the Ministry of Industry clearly specified the framework for the probabilistic analyses required from Electricité de France :

"I emphasize ... that my concern to extend the use of probabilistic analysis to the greatest possible number of groups of events does not imply the direct use of this approach for the design of pressurized water reactors. Probabilistic evaluation may be run afterwards to show that the assumptions made for the design provisions are well founded, and may furthermore be used, if need be, to improve the definition of the deterministic criteria used for the design of future reactors".

"Neither do the terms of my letter ... (of 1977) ... imply that the safety of a pressurized water reactor be demonstrated today through an exhaustive probabilistic analysis. Conversely, the use of a probabilistic approach should allow a better justification, or even an improvement, of the definition and classification of the events taken into account in the design of a pressurized water reactor".

3. The value of 10^{-7} per year is more directly used in an operational way ; the above-mentioned approach regarding external events does use this value by considering for example several groups of events for aircraft crashes : the probability of a general aviation aircraft crashing on a nuclear power plant in France is such that provisions are made to protect nuclear units systematically, wherever they are located. On the other hand, the probability of a commercial airliner crashing on a reactor in France outside airport approach areas is low enough to obviate the need for protective measures against this type of crash. Regarding military aviation, the matter is examined for each site to make sure the site is indeed suitable for a PWR power plant. The value of 10^{-7} per year can also be used for treating problems involving combinations of external events and conventional operating conditions.

Nonetheless, it should be underlined that the value of 10^{-7} per year is no longer considered as a "cut-off" value, above which design provisions for the occasion must be automatically made. The question of whether or not such design provisions are to be made is examined on a case-by-case basis by making a criticism of the assumptions made, based on the following two major considerations :

a. the overall risk objective : for example, so as to remain within the external event field, greater vulnerability can be attributed to aircraft crashes given a lesser vulnerability to explosions ; in other words, the number of groups of events which lead to unacceptable conditions and have a frequency greater than 10^{-7} per year has to be taken into account.

b. the cost of the extra design provisions envisaged versus the expected benefit as regards safety.

4. In contrast with the conventional deterministic approach, which is based on conservative assumptions and calculations regarding conventional events, the probabilistic approach emphasizes the use of as realistic values as possible for estimating both probabilities and consequences, in order to be fully beneficial and to bring about an improved consistency in the provisions made for preventing the unacceptable from happening.

2.2.2 Implementation of the probabilistic approach on French PWRs

As stated above, in France, the probabilistic approach has been directly applied to the assessment of the measures to be taken regarding external events for which the probability of occurrence can generally be assessed. Such an approach was used for determining the external events to be adopted for the design of the Gravelines nuclear power plant, located close to a large crude oil storage, nearby an oil terminal and not far from a projected LNG terminal. In particular, the probability of the explosion of a drifting gas cloud close to the NPP, resulting in unacceptable consequences, has been assessed for several plant design improvements as regards external explosions.

Moreover, the probabilistic approach has also shown the necessity of complementary provisions to ensure a satisfactory level of safety for some situations which are not included in the list of conventional operating conditions. Upon the proposal of the Standing Group in charge of nuclear reactors, the 1977 letter of the Ministry of Industry to Electricité de France requested thorough examination of the probabilities and the consequences of :

a. anticipated transients without scram
b. total loss of the ultimate heat sink
c. total loss of electrical power supplies (off- and on-site).

On completion of these studies, additional arrangements were effectively implemented on the different series of standardized units, with allowance made for the state of progress of their construction.

More generally, in order to meet the safety objective set forth, the examination of the probabilities and the consequences of the total loss of redundant and safety-related systems is required. Such studies have shown the importance of additional measures to complement the automatic systems normally provided by the initial design.

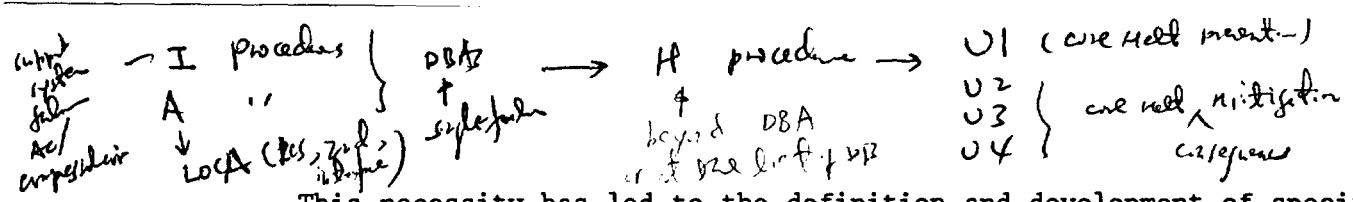

This necessity has led to the definition and development of specific operating procedures designated as the "H Procedures", which will be further examined hereunder.

3. REACTOR OPERATION AND SEVERE ACCIDENT MANAGEMENT

The first domain of application of operating procedures on French PWRs under incident/accident conditions was mainly linked to conventional design basis situations ("I" and "A" procedures) ; this initial domain has been progressively extended to a series of events not allowed for in the original design, but which were identified as requiring consideration under the probabilistic approach ; the procedures addressing this new area are the "H" procedures". All the above event-oriented operating procedures were then supplemented by a symptom-oriented ultimate procedure ("U1" procedure) for preventing core melt and three ultimate procedures ("U2", "U4" and "U5" procedures) to mitigate the consequences of a core melt, each one addressing a preferential containment mode of failure.

3.1 The "I" and "A" operating procedures for conventional incident/accident events

The "I" and "A" operating procedures are essentially related to design basis events ; such accidental events have been defined by considering each failure of active/passive components used in normal operation, liable to jeopardize a major safety function such as :

- the control of the nuclear power
- the evacuation of the core energy
- the confinement of fission products

The consequences of such accidents are limited by the operation of protection/safeguard systems.

The rules for treating these events, in particular the single failure criterion, result in redundant safeguard systems (2 x 100 %), which are emergency power supplied. "A" procedures are linked to breaches (A1 for primary system breaches, A2 for those on the secondary circuit and A3 for breaches at the interface of the two circuits) whereas "I" procedures address partial failures of support systems (electric sources and compressed air). "I" and "A" procedures are event-oriented, which implies that a diagnosis of the accident sequence in course has to be made before any initiation of such procedures.

Event-oriented H procedures H - station Blackout • loss of All FW
• High Flood
• loss of service water

3.2 The "H" and "U3" event-oriented procedures for situations at the limit of the design

The first results of the probabilistic studies performed by EdF in 1978 showed that the probability of unacceptable consequences associated with situations of total loss of redundant and safety-related systems was higher than the safety goal, considering, in this particular case, that the core melt was inducing unacceptable consequences. The safety authorities asked EdF to propose design modifications and adapted procedures to reduce this risk to acceptable values taking into account all normal operating conditions. This resulted in the definition and the development of the five following "H" operating procedures :

H1 for the total loss of the ultimate heat sink loss of service water

H2 for the total loss of steam generator feedwater (normal and auxiliary)

H3 for the total loss of electrical power supplies = station blackout (off- and on-site)

H4-U3 for the mutual back-up of the spray system and emergency low pressure injection system during the recirculation phase

H5 for the protection of sites along rivers against floods exceeding the reference level (millennial flood).

The initial "H" is for "hors dimensionnement", that is "beyond design" : actually, the designation "at the limit of the design" would be more appropriate.

3.2.1 Total loss of the ultimate heat sink : H1 procedure

The H1 procedure specifies the actions to be taken in the event of a failure of the component cooling system, the residual heat removal system or the cold source itself, following the failure of the pumping station or the failure of the four service water pumps. If these events are initiated at full power, there is a risk of damaging the primary pump seals, which induces a small break and leads to a core melt due to the unavailability of the safety injection pumps.

The purpose of the procedure is to bring the plant to a stand-by situation ($T \leq 180°C$, primary pressure ≤ 45 bar), which allows the cooling injection to pump seals to be shut down with no risk of damage. To reach this stage, the operator cools down the primary system using the steam generator, the steam being dumped to the atmosphere.

The water reserves on site and the procedures specified to resupply the auxiliary feedwater tank allow considerable time for repair of the heat sink (one month).

If these events are initiated at shutdown, the loss of heat sink leads to a total loss of reactor cooling and accordingly to core melt. The purpose of the procedure in these situations is also to bring the plant to a standby condition where the reactor cooling is provided by a steam generator (availability of one of two steam generators is required by the technical specifications). When the primary system is open, as in the case of maintenance during shutdown, it may be necessary to start injection by the chemical and volumetric control system, taking water from the refueling water system tank, because the steam generators are not operational. Residual heat is evacuated to the atmosphere by keeping the containment open.
All these actions are described in the H1 procedure which is available on all the 900 MW and 1300 MW plant sites.

3.2.2 Total loss of the steam generator feedwater : H2 procedure

This situation results either from the failure of the main feedwater system, followed by the failure to start the auxiliary feedwater system, or from the failure of the auxiliary feedwater system when it is in operation.

This event leads to the opening of the pressurizer relief valves. Due to the high pressure in the primary system, the safety injection system is inefficient, and this situation would lead to core melting.

H2

The H2 procedure consists of a voluntary opening of the operated valves of the pressurizer before the steam generators are completely dried. The safety injection signal, triggered by depressurisation, is confirmed manually. An estimated time of 40 mn is available to the operators to make such a decision. The standby condition to be reached consists of evacuating residual heat via :

- the auxiliary feedwater system, if it has returned to operation,
- the shutdown cooling system, as soon as permitted by the temperature and pressure of the primary system.

The H2 procedure is available on all 900 MWe and 1300 MWe sites.

3.2.3 Total loss of electrical power supplies : H3 procedure

This situation results either from the loss of external power supply, followed by the loss of the two diesel generators, or from the loss of 6.6 kVolt electric switchboards.

At full power, these events lead to the damage of the primary pump seals due to the loss of cooling and water injection on these seals. This situation results in a small break and leads to core melt due to the unavailability of the safety injection system.

The major objective of the procedure is to maintain the water injection on the pump seals by using another small pump powered by a turbine-generator driven by the steam of the steam generators (Fig. 1). This turbo-generator also produces power for the control of the plant. In addition, one gasturbine is installed on each site, which can be on line three hours after the beginning of the accident.

In reactor shutdown situations where the reactor is cooled by the residual heat removal system, these events lead also to core melt due to the loss of reactor cooling. The procedure consists of cooling the reactor by the steam generators whenever possible.

The processes specified in the H3 procedure for 900 and 1300 MWe PWRs have been justified by a probabilistic study of the risks resulting from a failure of the emergency power supplies ; these studies allowed for the various states of the unit and for failures of power sources and switchboards. The following results were obtained :

	Risk of unacceptable consequences*	
	without H3	with H3
900 MWe Reactor	$1.1.10^{-5}$	$1.3.10^{-7}$
1300 MWe Reactor	$4.7.10^{-6}$	$7.2.10^{-8}$

(*) - The term "unacceptable consequences" in the study means core uncovering.

All the design changes related to the H3 procedure have been taken into account during the construction of the 1300 MWe plants and have been decided upon for the 900 MWe plants, for which their complete implementation is expected shortly.

3.2.4 Loss of the safety injection system in the recirculating phase : H4-U3 procedures

After a LOCA, when the break cannot be isolated and when the residual heat removal system is not available, the long-term decay heat removal is assured by recirculating borated water from the containment sump by means of the low pressure injection pumps ; the heat transferred from the core to the containment is evacuated to the cold source by the containment spray system heat exchanger. Taking into account the fact that this situation can last for months, the probabilistic studies showed that is was necessary to improve the reliability of required functions by increasing the redundancy of the pumping systems after a few days.

The studies showed it was possible, in case of total loss of the containment spray system (CSS) pump, by using connexion sleeves between the low pressure injection system (LPSI) and the CSS, to use LPSI pumps to assure the functions of the two systems and vice versa.

For the 1300 MWe plant, flanges are installed on the pipes of the systems and the connecting sleeves can be installed after a period of 15 days after an accident.
In addition, a mobile unit including one pump and one heat exchanger can be installed 15 days after an accident in case of the loss of all pumps and CSS heat exchangers.

For the 900 MWe plant, the decision to undertake this modification has been made and it will be completed in about one year.

For the N4 plant, the safety authorities asked EdF to demonstrate that the probability of core melt in case of a LOCA followed by a loss of the safety injection system or containment spray system is coherent with the safety goal ($\leq 10^{-7}$/reactor/year).

3.2.5 Protection of the sites along rivers against floods exceeding the millennial flood

This procedure allows for a flood 15 % higher than the millennial flood. Such an event will result in the loss of external power sources and of the heat sink during for about three days. An advance warning of the flood, provided two days before reaching the millennial level, makes it possible to put in place mobile means aimed at protecting necessary material and to bring the NPP to a safe standby state, depending upon its initial state.

3.3 The U1 symptom-oriented ultimate operating procedure for core-melt prevention P use of water level in vessel date

The objective of the measures described in chapter 3.2 is to attempt to fulfill the overall safety goal in the particular case of the loss of redundant systems. However, all the design measures taken at the conception level may be inadequate due either to multiple equipment failures or to the operator's inappropriate previous actions.

In order to attempt to stop the development of potentially serious situations which could lead to core degradation, EdF has proposed a new approach, based on the characterization of every possible cooling state of the core, which will provide an exhaustive coverage of all accident situations. Implementation of such an approach, which necessitates a water level measurement in the vessel, already installed on all 1300 MWe plants, is foreseen in 1989 at the start-up of the Penly plant and will be achieved progressively on all other 1300 MWe plants. This delay is due to the time needed to develop the corresponding set of procedures and to train the operators. Nevertheless a limited application of the state approach has already been implemented on the 900 MWe and 1300 MWe plants where the U1 procedure is used by the safety engineer in all incidental and accidental situations.

U - procedures

Figure 2 gives a description of the organization of the work in the control room between the operator team and the safety engineer. The safety engineer is called to the control room in case of shutdown or loss of subcooled margin. He is in charge of post-incident supervision and carries out monitoring of criticality, primary and secondary parameters, safety injection and containment spray systems and containment activity. The safety engineer, using given criteria, can decide to adopt the U1 procedure, which specifies the actions for each of the nuclear steam supply system (NSSS) states defined by functional and by physical criteria. The U1 actions are performed by the operator team, and during this time the safety engineer is in charge of permanent ultimate supervision to verify the efficiency of the actions.

This procedure will be on line very soon ; computer aids are developped and will be integrated into the safety panel display system.

3.4 The U2, U4 and U5 ultimate procedures for the mitigation of the radiological consequences of a severe accident

The principle of incorporating into French PWRs ultimate procedures devoted to the mitigation of the radiological consequences of severe accidents was accepted in 1981 by the involved parties - the Safety Authority and the utility - in order to meet a requirement which can be summarized as follows :
-in case of a core melting, the third barrier, i.e. the containment and the various systems passing through it, must constitute an ultimate line of defense, which must reduce the radioactive releases to the environment to a level compatible with the feasibility of the off-site emergency plans.

Deriving from the studies made on the basis of the WASH 1400 report, one was led to the definition of three typical source-terms to be used for the assessment of severe accidents. Ultimate procedures were then developped to make the fission product releases compatible with emergency plans.

3.4.1 Reference source terms vs external emergency plan feasibility

In France the expression "source term" is used in a restrictive sense with regard to radioactive releases. A "source term" is a typical release, characteristic of a reactor line and of an accident class. Possible defense against these accidents is sought for in view of the ultimate protection of the population ; they are therefore essentially a reference for defining emergency procedures on the plant and assessing the validity of emergency plans : "Plan d'Urgence Interne" (internal emergency plan), abbreviated PUI, of the power plant and "Plan Particulier d'Intervention", PPI, (off-site particular emergency plan) beyond the site limits. Thus the notion of source term cannot be associated with a specific accident sequence, but rather represents a class of releases.

As shown in Table 1, there are three source terms defined in France for PWR severe accidents, and they all assume a complete core melt-down.

In order of decreasing severity, they are :

- S1, which corresponds to a total and very early loss of containment tightness ; such catastrophic scenarios are difficult to picture physically and thus are currently considered as a part of the residual risk, that is, not requiring, a priori, any specific arrangement ;
- S2, which corresponds to a large and direct release of radioactivity to the atmosphere one day after the beginning of the accident (for example δ mode in the Rasmussen terminology) ;
- S3, which corresponds to an indirect release to the atmosphere, starting one day after the accident onset, through leakpaths between the containment and the atmosphere involving a substantial fission product (F.P.) retention ; S3 also incorporates the minor, normal releases of the containment before its impairment.

These source terms derive from U.S. assessments established more than ten years ago (essentially the WASH-1400 report), which were adapted in the late seventies to PWRs built in France.

Feasibility studies on PPI in France were completed in the early eighties ; they resulted in the following conclusion : for French PWR sites, when using classical operational means, it appears feasible to evacuate the population within a radius of about 5 km around the plant, and to confine it within a radius of about 10 km, provided there is at least a 12-hour advance warning before the postulated releases.

This being considered, in addition to the necessary compliance with ICRP-40 recommendations on doses to the population, it appears that S3 corresponds to release characteristics that can be correctly accommodated by the current PPIs.

This means that steps had to be taken to mitigate the consequences of still conceivable core-melt sequences that could otherwise result in a S2-type release. This is the purpose of procedures U2, U4 and U5.

3.4.2 U2, U4 and U5 procedures for consequence mitigation

3.4.2.1 U2 procedure –

This procedure addresses the search for and processing of abnormal containment tightness defects (β mode).

The U2 procedure must in fact cover a wide range of accident severity, because it is obviously desirable to activate it as soon as any threat of significant release of radioactivity inside the containment has been discovered. It defines :

- the condition of containment surveillance (radioactivity at the stack, in the sumps and inside the containment, state of containment isolation systems),

- the action to be taken to mitigate the radioactive releases (for example : isolation of an unit, reinjection of liquid waste inside the reactor building).

This having been accepted by the Safety Authority, the operating rules are now being written for each PWR standard.

3.4.2.2 U4 procedure (ε mode)

During the studies devoted to the analysis of the consequences of the basemat melt-through by the corium, it appeared that, in the 900 and 1300 MWe standard basemats, direct pathways to the atmosphere of early releases, not filtered by the ground (basemat auscultation, draining systems), were found.

For the N4 standard, these pathways were eliminated at the design stage. For the 900 ad 1300 MWe files of reactors, various arrangements are under study, covered by the general term of U4 procedure, aiming to suppress or to mitigate the presence of these pathways.

3.4.2.3 U5 procedure (δ mode) = containment venting (Flood rx cavity for certain plants)

The U5 procedure uses a device making it possible to effect planned and filtered releases, conceived :

- to reduce the internal pressure of the containment to the design value,

- to decrease significantly the release of some radioactive products to the environment,

- to direct the filtered gases towards the stack, where their radioactivity is counted before dispersion into the environment.

This device includes mainly a tight container, holding a 40 m³ sand bed, 80 cm deep, isolated by valves, connected upstream to the containment atmosphere by a pre-existing penetration (used to perform the containment tightness tests) and downstream to the stack (Fig. 3).

• U3 Procedure – use of Mobile Units to supplement core-injection or containment spray.

• U1 – Last-Resort Measures to prevent core Meltdown.

A research and development programme, called PITEAS filtration, was performed on the sand filtration in the CADARACHE Nuclear Research Center ; it made it possible to define the system, to check the efficiency of the device and its ability to accomplish its task under conditions representative of accidents liable to occur.

The first filters were installed in the Nogent, Cattenom and Chinon plants last summer ; all 900 MWe and 1300 MWe plants will be progressively equipped. This device is included in the N4 standard design (1400 MWe PWRs).

4. R AND D AIMED AT DEVELOPPING ACCIDENT MANAGEMENT PROCEDURES

A joint R and D effort between the utility and CEA/IPSN has been developped in the following three main areas.

4.1 Development of the physical code CATHARE

This code, a version of which is already operational, permits a realistic description of the accident physics and kinetics. Such knowledge is essential to define the criteria for initiating the actions anticipated in the procedures, particularly in the symptom-oriented procedures currently developed. In this type of approach the operator actions are indeed defined at each time on the basis of the actual course of events affecting the NSSS, and not on a supposed sequence resulting from an initiator. Therefore, correlations between the measurable physical parameters and the various states of the NSSS have to be established, so as to define criteria for operator action. Besides, based on the CATHARE code models, the SIPA software is developed as a simulator for studies.

4.2 Construction and operation of the Integral Test Facility Bethsy

The Integral Test Facility Bethsy has been designed for the analysis of PWR accident situations controlled by automatic circuits and/or operator actions.

The main technical objectives are :

- the validation of the physical assumptions made for the definition of operating procedures, whether event-oriented or symptom-oriented ;

- the global validation of the CATHARE code.

The various PWR circuits and systems are modeled, which will provide proper initial conditions and a physical evolution similar to that on the power reactor. Operator actions will be automatically implemented according to the criteria in the procedures, taking into account the time allowed for intervention, which can be adjusted. Such an option eliminates bias that an interface and various operating crews implementing the actions could generate. Besides, the above objectives, the Bethsy facility should provide elements for appreciating the post-accident reactor operation.

FRENCH "U" PROCEDURES

- U1 – LAST-RESORT MEASURES TO PREVENT CORE MELTDOWN
- U2 – ACTIONS IN CASE OF INADEQUATE CONTAINMENT ISOLATION
- U3 – USE OF MOBILE UNITS TO SUPPLEMENT CORE-INJECTION OR CONTAINMENT SPRAY SYSTEMS
- U4 – ACTIONS TO FLOOD THE REACTOR CAVITY (CERTAIN PLANTS ONLY)
- U5 – USE OF CONTROLLED, FILTERED CONTAINMENT VENT

CATHARE code / BETHSY exp

4.3 Achievement of the PITEAS program – filtering

This research program was aimed at examining the feasibility of the filtration device to be used for containment venting under U5 procedure. Laboratory-scale tests were carried out to specify the filtering material under specific conditions representative of the reference accident scenario. These tests were followed by a new series of tests on a loop at a representative scale, to analyze the filter's thermal behavior, particularly its possible clogging by condensates, and to check that the expected efficiency was met for any accident conditions liable to occur. A filtration efficiency of at least a factor 10 can be guaranteed for the aerosols under the above accident conditions. The sand-bed filters currently installed on French PWR power plants derive from the PITEAS program attainments.

4.4 Severe accident management

An EdF-CEA/IPSN joint brainstorming group has been constituted to examine the impact on the course of events of using still available or recovered means during a core-melt sequence : such an analysis is a prerequisite to establishing a strategy for the optimal use of these means.

5. EMERGENCY ORGANIZATION IN FRANCE FOR THE CASE OF A NPP ACCIDENT

Organizations have been set up and are regularly tested to ensure an adequate management of an accident on a NPP. These organizations are based upon a clear definition of responsibilities and roles of the utility and government bodies involved. On each side there is a local organization - the internal emergency plan (PUI, for "plan d'urgence interne") on the utility side, the particular (off-site) emergency plan (PPI, for "plan particulier d'intervention") on the side of the government representative at the "département" level - and a centralised organization at the national level.

5.1 The plant internal emergency plan (PUI)

A three-step PUI exists for each NPP site, which is initiated by the head of the plant whenever an accident occurs : level 1 addresses conventional accidents, whereas levels 2 and 3 correspond to events with actual/potential radiological consequences on- and off-site, respectively. These levels correspond to those of the PPI.

The PUI is initiated at the onset of a series of events requiring the application of a procedure on a pre-established list, so as to provide the operating crew with substantial support for longer term actions : this list comprises, among others, the A1, A2, A3, H1 H2, H3, U1 and U2 procedures previously examined.

After initiating the PUI, the usual plant organization is turned into an emergency organization aimed at :

- making the right decisions and implementing rapidly the relevant actions to bring the NSSS back to a safe state, and mitigate the consequences ;

- collecting any information contributing to diagnosing the accident and making a prognosis for its evolution, with the support of the utility expert groups at the national level ;

- providing information to the administration

Putting in place the PUI results in the constituting of four emergency management teams (PC for "poste de commandement") and one emergency technical team (ELC for "équipe locale de crise") :

- The local emergency management team (PCL for "PC local") is placed in the plant control room ; it controls the actions of the crew on shift so as to save the NSSS.

- The plant emergency management team (plant PCD for plant "PC Direction"), which can be evacuated to an on-site bunker (BdS for "Bloc de Sécurité"), is the only team in charge of plant safety and of the staff protection ; in this prospect, it coordinates the actions of the three other emergency management teams on site. The PCD also ensures the official connections with the local government representative, who is regularly informed of :

  • the plant condition and its anticipated evolution ;
  • the radioactivity transfers to the environment, if any, and their expected evolution.

  The plant PCD is connected, at the national level, with the utility PCD at the "Service de la Production Thermique", or SPT (division of power production by thermal units), the Safety Authority PCD (Service Central de Sûreté des Installations Nucléaires, or SCSIN) and the appropriate body of the Ministry of Health (Service Central de Protection contre les Rayonnements Ionisants, or SCPRI).

- The emergency management team for logistic matters (PCM for "PC Moyens") is in charge of activating on-site intervention means and evacuating the plant staff when appropriate ; the PCM can be withdrawn into the BdS if necessary.

- The emergency management team for measurements (PCC for "PC Contrôles") is responsible for gathering and synthesizing all data regarding local weather conditions and radioactivity, and making previsions of the releases ; the PCC can be sheltered in the BdS.

- The on-site emergency technical team (ELC) is a reflexion group of specialized engineers, the role of which is to assess the real-time situation of the NSSS and its probable evolution, so as to provide the plant PCD with technical recommendations for the short/medium terms accident management actions ; it receives the data from the impaired unit, in particular those of the safety panel. The ELC also transmits the necessary plant-related information to the two national level emergency technical teams, one at the utility SPT, the other at the CEA/IPSN, the latter acting as a technical support of SCSIN ; continuous connections between the three technical assessment teams permits the analyses to be compared and synthesized (Fig. 4).

5.2 The national-level emergency organization

For accidents involving levels 2 or 3 of the PUI, the utility activates a national-level organization at the SPT. The "département"-level government representative (the "Commissaire de la République"), when implementing the PPI, is supported by a national-level organization, coordinated by the "Secrétariat Général du Comité Interministériel de la Sécurité Nucléaire" - SGSN for short- (secretariat of the inter-department committee for nuclear security, at the prime minister level). This organization includes the SCSIN and its technical support, the CEA/IPSN, the SCPRI and the "Direction de la Protection Civile" (civilian protection branch of the department of the interior).

5.2.1 The national-level emergency organization of the utility

This organization comprises an emergency management team and an emergency technical team, both located at the utility headquarters building at Paris.

- The emergency management team (national-level PCD)

Such team, which is in permanent communication with the plant PCD, is the interface with the concerned government bodies, in particular the head of SCSIN (Fig. 4).

- The emergency technical team (ENC for "Equipe Nationale de Crise")

Its role is to supplement the information of the above PCD and give advice and recommendations to it. The ENC is in close contact with the plant ELC which provides information ; it compares its analyses with those of the other emergency technical teams (plant ELC and CEA/IPSN).

The ENC comprises specialized engineers on call, who are expected to arrive at the emergency technical room within an hour. A representative of Framatome also joins the team when the support of the vendor is requested ; his role is to maintain a continuous connection with the Framatome technical support team.

5.2.2 The emergency organization of SCSIN

Three teams are constituted in case of an emergency

- The emergency management team (PCD), chaired by the head of SCSIN, is installed in the emergency center of the Ministry of Industry at Paris.

- The emergency technical team is located on CEA/IPSN premises at Fontenay-aux-Roses, near Paris ; it is chaired by the director of IPSN

- A team is detached locally, partly to the impaired plant, partly to the relevant Prefecture (office of the government representative at the "département"-level).

On the basis of the information gathered on the plant situation and of the analysis elaborated by the CEA/IPSN, the head of SCSIN verifies the adequacy of the actions taken by the utility ; he makes a prognosis regarding the releases of radioactivity and provides assessments of possible radioactive transfers in the environment. Such previsions, as well as those from the utility, should allow the local government representative to take, after the SCPRI advice, the appropriate actions for protecting the public.

About a dozen technical exercices involving at least the utility, SCSIN and CEA/IPSN have been carried out up to now : the lessons learned constitute a major contribution to the improvement of the emergency organization.

TABLE 1

CALCULATED SOURCE TERMS INTO THE ENVIRONMENT (INTEGRATED VALUES IN % OF CORE INVENTORY AT REACTOR SCRAM) FOR ALL PWRs AS BUILT IN FRANCE

Source Term	Noble Gases (1) as Xe 133	Iodine (1) as I 131		Cs (1) as Cs 137	Te (1) as Te 132	Sr (1) as Sr 90	Ru (1) as Ru 106	Lanthanum Actinides as Ce 144
		Inorganic	Organic					
S1	80	60	0.7	40	8	5	2	0,3
S2	75	2.7	0.55	5.5	5.5	0.6	0.5	0.08
S3	75	0.30	0.55	0.35	0.35	0.04	0.03	0.005

(1) - For other isotopes of the same chemical category adequate decay half-lives may be taken into account where appropriate.

Thermal barrier cooling of RC pump is Not needed when no RCPs are Not running?

FIGURE 1

H3 PROCEDURE

Station Blackout

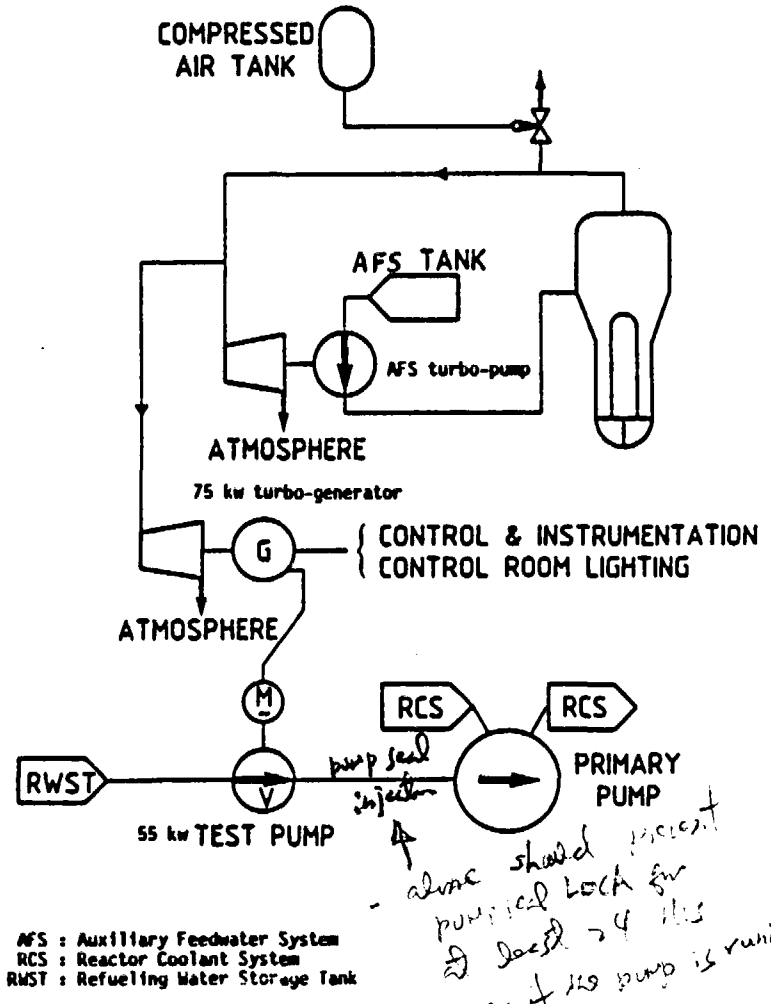

- alone should prevent pumping LOCA for 2 hours + this even if RC pump is running

- It's hard to say the seal leak rate real time during station blackout w/o seal injection or thermal barrier cooling.

(All RCPs have thermal barrier, Not all pumps have seal injection.

FIGURE 2

U1 PROCEDURE

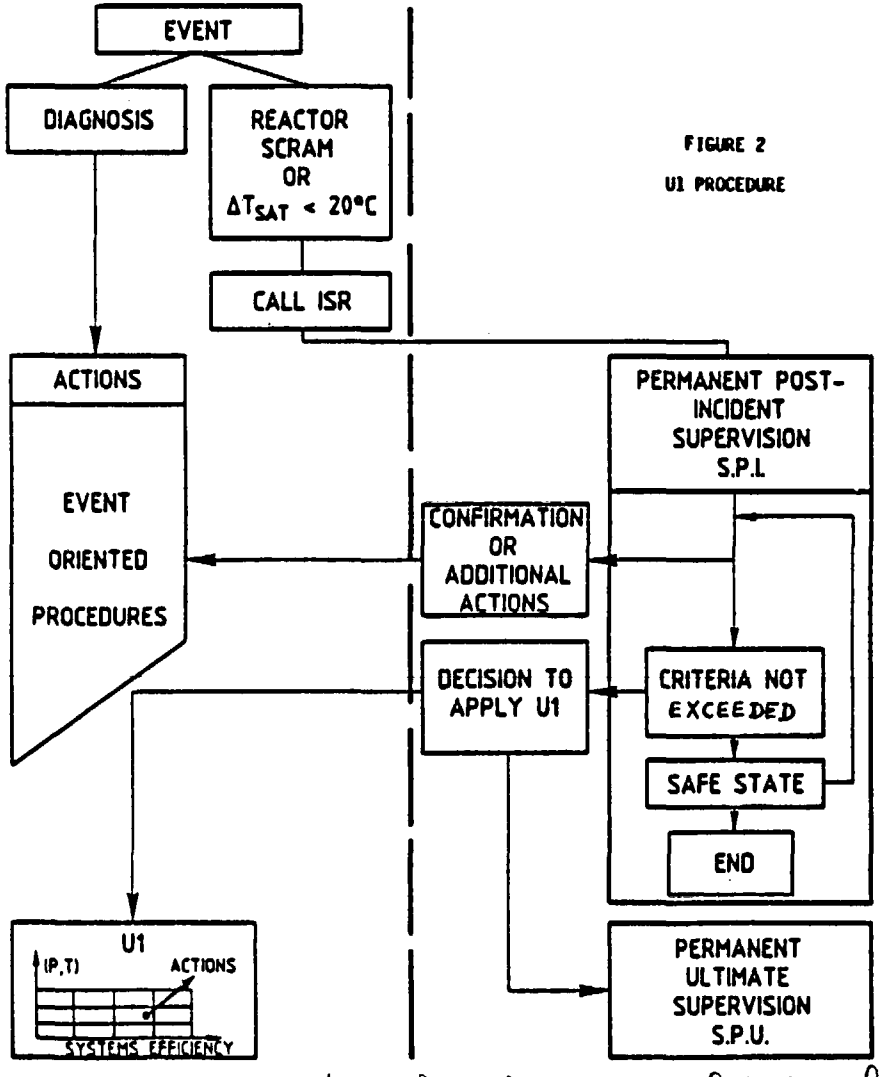

FIGURE 3

U5 - FILTRE A SABLE

U5 SAND BED FILTER

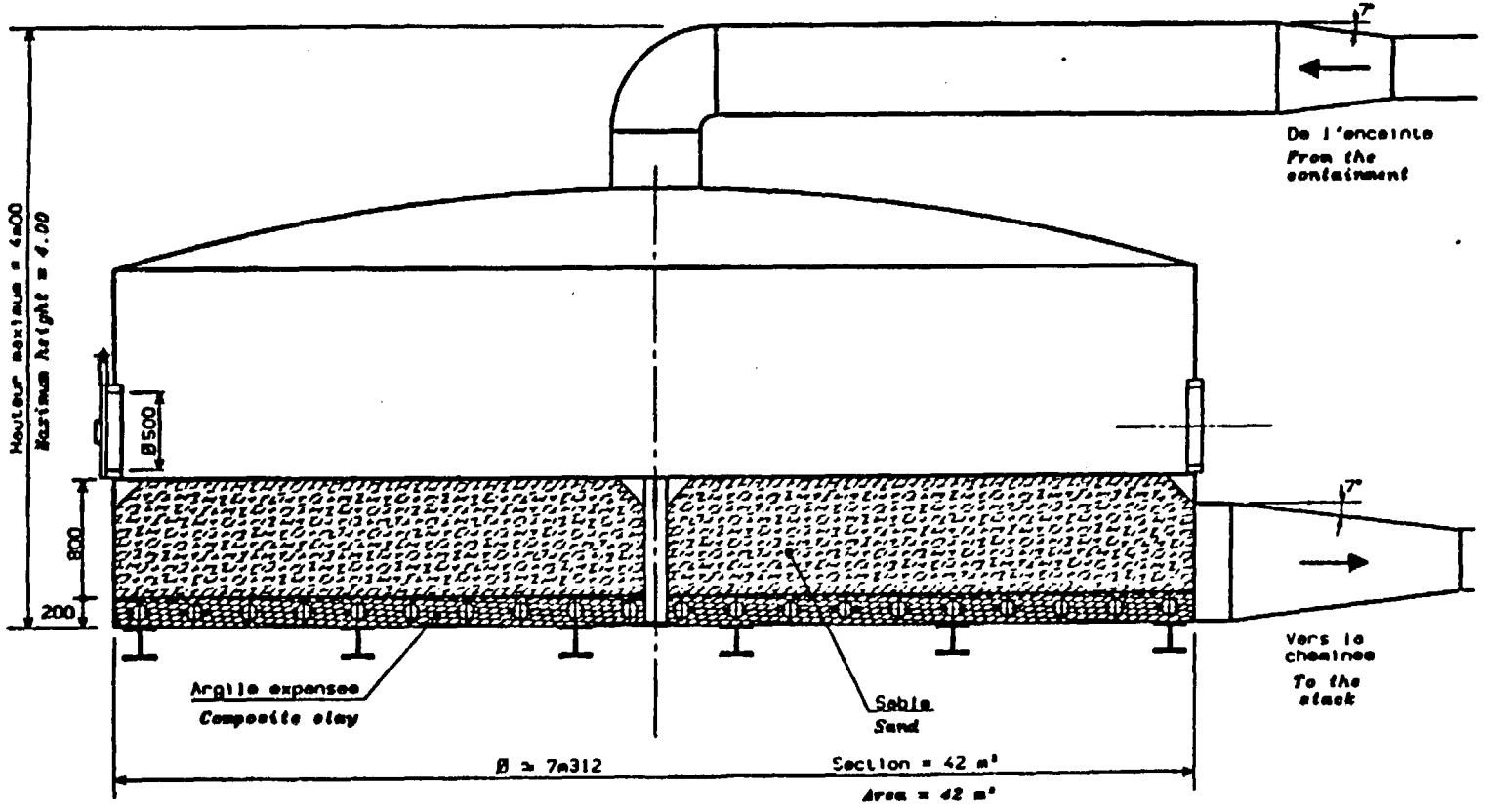

FIGURE 4

ORGANIZATION DURING AN ACCIDENT

IN AN ELECTRICITE DE FRANCE REACTOR

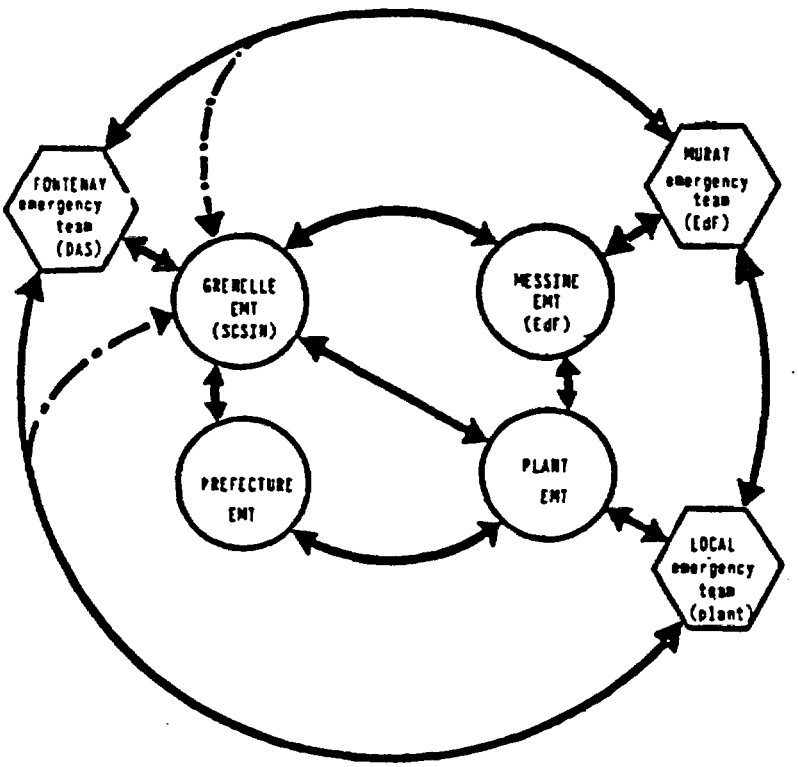

DECISION

ANALYSIS - PROPOSALS

MAIN LINKS

LISTEN-INTO AUDIOCONFERENCES

APPENDIX 1

Incidents of moderate frequency, the consequences of which must be extremely limited :

- Uncontrolled withdrawal of RCC assembly, with reactor subcritical,
- Uncontrolled withdrawal of RCC assembly, with reactor at power,
- Incorrect position, drop of RCC assembly or group of RCC assemblies,
- Uncontrolled dilution of boric acid,
- Partial loss of primary coolant flow,
- Startup of an inactive loop,
- Total load rejection, turbine trip,
- Loss of normal feedwater,
- Malfunction of normal feedwater,
- Loss of offsite power,
- Excessive load increase,
- Inadvertant opening of a pressurizer valve (momentary depressurization of the primary circuit),
- Inadvertant opening of a secondary valve,
- Inadvertant startup of safety injection or emergency borification.

Very infrequent accidents, the consequences of which must be sufficiently limited :

- Loss of primary coolant (small breaks),
- Inadvertant opening of a pressurizer valve (long term depressurization of the primary circuit),
- Small break on secondary piping,
- Total loss of primary coolant,
- Incorrect position of a fuel assembly in the reactor core,
- Withdrawal of an RCC assembly at full power,
- Rupture of chemical and volume control system tank,
- Rupture of gaseous waste treatment system tank.

Severe and hypothetical accidents, the consequences of which must remain acceptable :

- Fuel-handling accident,
- Serious rupture of a secondary circuit (water or steam pipe),
- Motor-driven primary pump rotor blocked,
- RCC assembly ejection,
- Plausible loss of coolant accident,
- Double-ended break of a steam generator tube.

GERMAN ACCIDENT MANAGEMENT PROGRAM

E.F. Hicken, U. Erven, E. Kersting
Gesellschaft für Reaktorsicherheit
Garching, Köln/FRG

Abstract

In the FRG extensive analyses of possible Accident Management measures are performed. The presented results of these analyses show that there is a great potential for the operators to avoid core melt by flexible use of existing or slightly modified systems.

Decisions have been made on Accident Management measures
- to prevent containment failures due to overpressurization of the containment (filtered venting for PWR's and BWR's)
- to prevent containment failures due to hydrogen burn (inerting BWR containments)
- increasing battery capacity for 2-3 hours.

Measures under discussion are e.g.
- catalytic foils to prevent an increase of hydrogen concentration in PWR containments
- secondary and primary "bleed and feed" for PWR's
- diverse use of systems to restore the core coolant inventory and decay heat removal (e.g. by fire fighting system).

The objective of all theses measures is a further decrease of core melt frequency and to limit considerably the consequences in case of a core melt.

The main future activities will be the development and validation of accident management measures as well as a more detailed analysis of the system capabilities. In addition, the appropriateness of instrumentation will be further assessed and diagnostic tools improved. An appropriate procedure description and training will be prepared.

Introduction

Nuclear Power Plants in the Federal Republic of Germany are equipped with comprehensive and reliable safety systems which prevent core damage in case of accidents.

However, beyond this area of accidents (design basis accidents) remains an area with possible sequences against which the plant has not been

designed explicitly, because these sequences have been assessed to be very unlikely.

The causes for these sequences might be

- multiple failures of systems and components
- delayed or missing detection of disturbances
- human error including wrong diagnosis or wrong operator action before or during a sequence
- combinations of different possibilities

Concepts and measures to prevent a core melt or mitigate its consequences which are not explicitly considered in the design are internationally known as Accident Management.

Accident Management includes all measures which are initiated in a plant to identify as early as possible deviations from normal operating or design basis sequences, to diagnose and control them and terminate the disturbances with minimum damage.

In the area of Accident Management we distinguish between "prevention" and "mitigation".

- Prevention includes measures to avoid undue damages to the reactor core.
  Due to the relative slow development from the initiating event to major core degradation (usually hours) there is in principal the possibility for the plant personnel to identify and diagnose the status of the plant and to initiate safety related measures, e.g. reactivating safety or operational or additional systems. These measures are considered to have the highest priority in the Federal Republic of Germany.
  TMI may be an example for the border-line between the "prevention" and "mitigation" area.
- Mitigation includes measures to control and minimize the consequences of core melt sequences.
  If measures to reactivate sufficient core cooling and decay heat removal fail core melt will progressively start. Even in this case measures to control and minimize the consequences should be initiated. The final goal is to keep the integrity of the primary system or at least the containment to avoid an uncontrolled and usually major release of fission products into the environment.

This presentation covers:
- The different nuclear power plant designs in the FRG.
- Objective and elements of the Accident Management Project.
- Basic principles passed by Reactor Safety Commission.
- Analysis of effectiveness (examples).
- System capabilities

- Survey about implemented or decided measures and measures to be studied further
- and future activities.

Fig. 1 shows the two different pressurized water reactor designs, one of them is of an improved B&W type, the other is of KWU design. Differences are as well in the general
design as in the containment design.

In Fig. 2 different designs for BWR's are shown.
Five reactors are of design 69 type and two reactors of the design 72 type. One of the BL 69-plants has external recirculation pumps.
All others have internal pumps. But BL 69 and BL 72 have different containment designs. All BWR's are equipped with a pressure suppression system.

The next two figures show the objective and elements of the Accident Management Project.

An important step in applying accident management measures has been achieved because some basic principles have passed the Reactor Safety Commission

- It is obvious that only symptom or performance goal oriented procedures are applicable instead of event oriented procedures. This is due to the large number of possible sequences.
- It is a tendency now not to incorporate procedures in the frame of Accident Management into the operating manual. Rather it is discussed to specify those in an "emergency operating manual".
- The assessment of the effectiveness of measures should include
  - the system capability to perform the task.
  - disadvantages for operation and design basis accidents
  - Feasibility
  - It is obvious that only realistic assumptions and tools should be used for the analysis to avoid a misleading of operators and to assess past and future sequences.
  - Decision making criterions.
- There is general agreement that redundancy and diversity are usually not required. A decision will be made case by case.
- With conventional engineering design practice the systems should survive earthquakes.

The following chapter covers some analyses of the effectiveness of some measures. A number of sequences and measures have been analysed. The examples shown here are mainly in the preventive area namely for PWR the recovery of secondary side, for PWR the effects of the primary side depressurization and for BWR the coolant supply to the RPV with different measures in case of the "station blackout" respectively "loss of main feedwater". In the mitigation area the effectiveness of containment venting for the PWR will be shown.

In fig. 7 and 8 the pressure in primary and secondary side and the primary water level is shown for a sequence with station blackout and the recovery of the emergency feedwater pumps after 2 hours. In summary: The recovery of the secondary side results in a initial pressure decrease of the secondary and primary side and a decay heat removal from the core by the reflux condenser mode.

In fig. 9 and 10 the same sequence but a recovery of the secondary side with external pumps is shown. In this sequence the operators have to depressurize the secondary side.

Fig. 11 shows the primary side pressure history before and after the initiation of the opening of the relief valves on the pressurizer after 1 1/4 hours. Very soon the pressure is reached where the high pressure injection pumps can start injecting water. If they would be available, the sequence would be stabilizing very soon. In case of a station blackout the pressure has to be decrease below 26 bars to allow an accumulator injection. The pressure minimum is due to the injection of cold water. Depending on the relief valve area the pressure is stabilizing at a specific level. The injection of this water allows a delay of the start of core melt by about 3 hours. The core slump results in a pressure peak. The RPV will fail after about 1000 sec after core slump.

In fig. 12 the flexibility of a BWR is shown. Usually the turbine driven high pressure injection system can cope with transient, and small breaks for hours. After some time the ADS must be delayed. If this system will fail, ADS will be initiated soon. If no low pressure systems would be available (to be identified e.g. through the minimum mass flow rate) ADS should be delayed. In fig. 12 the water level increase is shown in cases where the feedwater tank or fire fighting systems can inject.

In fig. 13 the containment pressure history is shown after initiating filtered venting after two days at a pressure between design and test pressure. if no water would be added to the containment sump a dry out will occur after about 7 days. In case of water injection the pressure decrease is initially steep; the total outflow will be less than in case of no water injection.

The system capabilities to inject water into the RPV are very important for Accident Management. In fig. 14 the injection rates into the primary system are shown with the pressure as a parameter. In addition, the necessary injection rate to compensate for the evaporation of water due to decay heat is included. It is obvious that with decreasing pressure more active and passive systems are available. At a high pressure it can be analyzed that the volume control system is not capable to restore the evaporated water. This can be done with high pressure injection systems only at a pressure level of about 80-90 bars. In case of a station blackout the pressure has to be decreased to less than 26 bars to allow an injection of the accumulators. Below about 10 bars also additional systems can be used.

In fig. 15 a list is given about the existing capabilities for boiling water reactors of BL 69 type. It is obvious that the steam driven high pressure injection system can cope with all transients and small LOCAs. It can also be identified from this figure that there are many systems available which are equipped with emergency power. It should be mentioned that a feed water tank in BWR's, if installed, can be used as a practically passive injection system (this will delay core melt by about 2 hours). One advantage of BWR's is, that it is not necessary to inject borated water. Therefore, fire fighting systems can be used. It's capabilities are similar to one RHR-pump. Because they are usually equipped with additional emergency power this gives the high flexibility to plant personnel.

The next chapter covers implemented measured or those measures which have been decided and will be implemented soon and those measures which have to be studied further. This list is the result of discussions during the last year. It has been decided that all PWRs and BWRs containment will be equipped with a filtered venting system. The design capacity will avoid a catastrophic failure of the containment in case of a slow pressure increase. In our opinion this venting capability will increase the flexibility for the plant personnel with a minimum of electrical power. However, it is also very definite that venting will be the last measure to be undertaken by plant personnel to avoid a major fission product release.

It has also been decided to inert all BWRs of BL 69 type. The specific procedures for the BL 72 type is under discussion.

Battery capacity will be increased for a 2-3 hours operation, at least. An assessment has been performed that offside power will be restored after about 2 hours with high probability.

All plants will be equipped with systems to filter the inlet air to the control room to guarantee the habitability of the control room.

To operate the turbine driven injection system of a BWR also in case of a station blackout all necessary equipment will be connected to a secured battery power supply.

There are still some measures to be discussed further. This is e.g. the functionability of instrumentation under accident conditions. An increase of the range of some instrumentation will mostly satisfy the requirements.

It is evident that the "emergency operating manual" has to be discussed further.

One of the most important issues is the depressurization of the primary system of PWR's. As it has been shown earlier, the flexibility for the plant personnel to react to unforeseen events is increased with decreasing pressure. In addition, from an engineering point of view, the hazards resulting from a highly pressurized vessel with high temperatures and non predictable time and location of the primary cooling system failure should be avoided. On the other hand, an unintended initiation of

depressurization is similar to a small break LOCA, which will contaminate the containment. Discussions are underway to study suitable criteria for initiating the depressurization.

To increase the flexibility for the plant personnel the installation of some connections to the primary side of PWRs is under discussion to allow for an outside injection.

Hydrogen will sooner or later and in one way or the other give the load on the containment. There is a research effort underway in the FRG to further develop catalytic burning. But also electrical (battery powered) ignitors placed at a few specific locations are under discussion.

Flooding of the cavity below the reactor pressure vessel of boiling water reactor is under discussion. Also there is a general feeling that this measure is positive in general but some more research has to be undertaken.

Summarizing the efforts we believe that a lot has been done in the past, but some further work has to be performed. The main activities in the future will be the development and validation of accident management measures as well as a more detailed analysis of the system capabilities. On the other hand some more has to be done to assess instrumentation and to improve diagnostic tools. In addition, an appropriate procedure description and training has to be prepared.

PWRs in the FRG

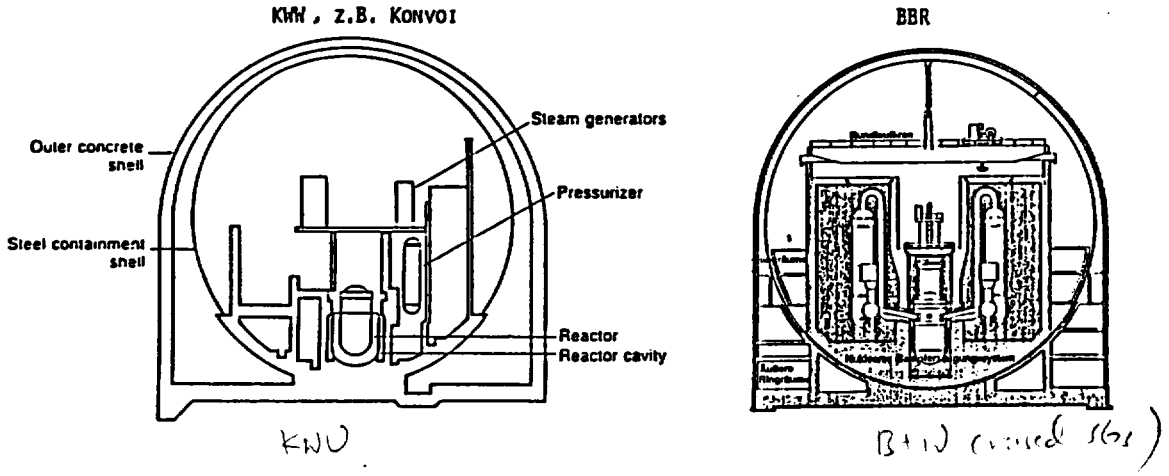

FIG. 1 Differences:
- Primary / Secondary Side
- ECCS
- Containment

BWRs in the FRG

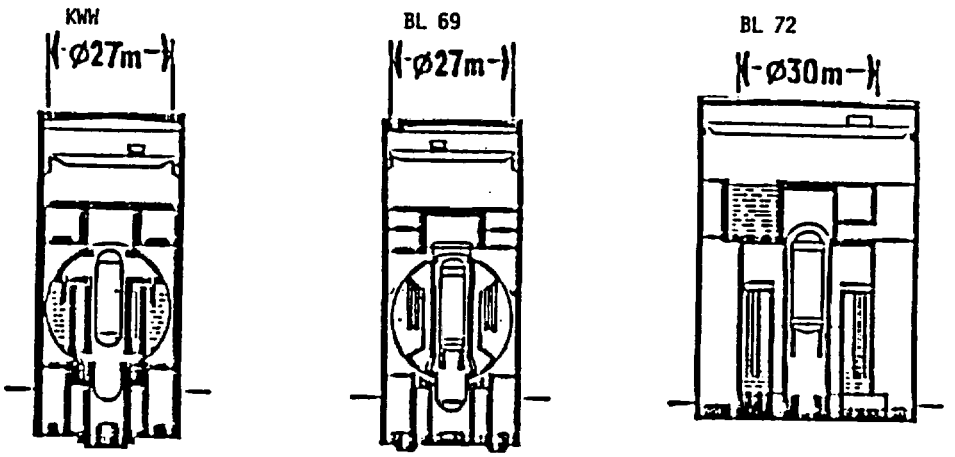

FIG. 2

Differences:
- Coolant Recirculation
- Core Cooling during LOCA
- ECCS
- Containment

2. Objective and Elements of the Accident Management Project

General Objective

Identify the Safety Reserves of Nuclear Power Plants and show optimum Utilization during unexpected Event Sequences without or only slight hardware modifications.

Main Elements

- System Dynamics
- System Analysis
- Accident Information and Decision Aid
- Validation, Verification, Training

Fig. 3

MAIN ITEMS OF ACCIDENT MANAGEMENT PROGRAM

- System Dynamics
  - Realistic Description of Plant Behaviour to define minimum System Requirements Development of Recovery Strategies incl. Assessment of Efficiency
- System Analysis
  - Identification of alternate Recovery Measures
  - Feasibility of Recovery Measures
  - Analysis of necessary technical Provisions and of Information Requirements
- Accident Information and Decision Aids
  - Development of an Information Concept (e.g.: Strategy, Diagnostic Method, State Monitoring)
  - Hard- and Software Development (incl. human Engineering)
  - Development of Accident Procedures
- Validation, Verification, Training
  - Test Procedures
  - Performance Criteria
  - Simulator driven testing
  - Definition of training Requirements
  - organizational Aspects

Fig. 4

3. Basic Principles passed by RSK

- Sympton - or Performance - Oriented Procedures instead of Event-Oriented Procedures
- Plant Internal Emergency Manual in Addition to the Operating Manual
- Evaluation of the Plant Behaviour
  - Assessment of the Effectiveness of Measures should include
    - System Capabilities
    - Disadvantages for Operation and Design Basis Accidents
    - Feasibility
    - the Decision-Making Process
  - Analysis to be based on realistic Assumptions and Tools
- General Design Basis
  - Redundancy/Diversity is usually not required
  - Systems should survive Earthquakes

Fig. 5

4. Analysis of Effectiveness

Examples:

Prevention of core melt

- PWR: Recovery of Secondary Side
- PWR: Primary Side Depressurization
- BWR: Coolant Supply to RPV

Mitigation of Consequences

- PWR: Filtered Containment Venting

Fig. 6

PWR

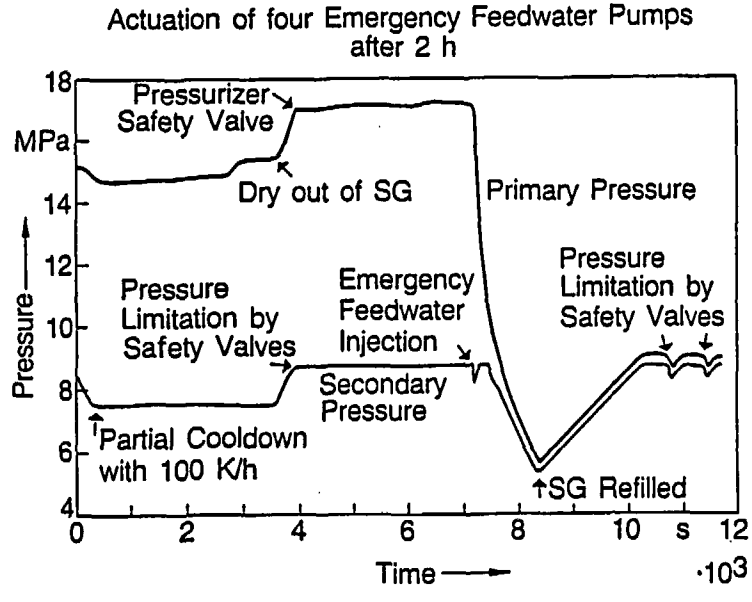

1910K

PRESSURE TIME HISTORY
"STATION BLACK-OUT"
WITH SECONDARY MEASURE

FIG. 7

PWR

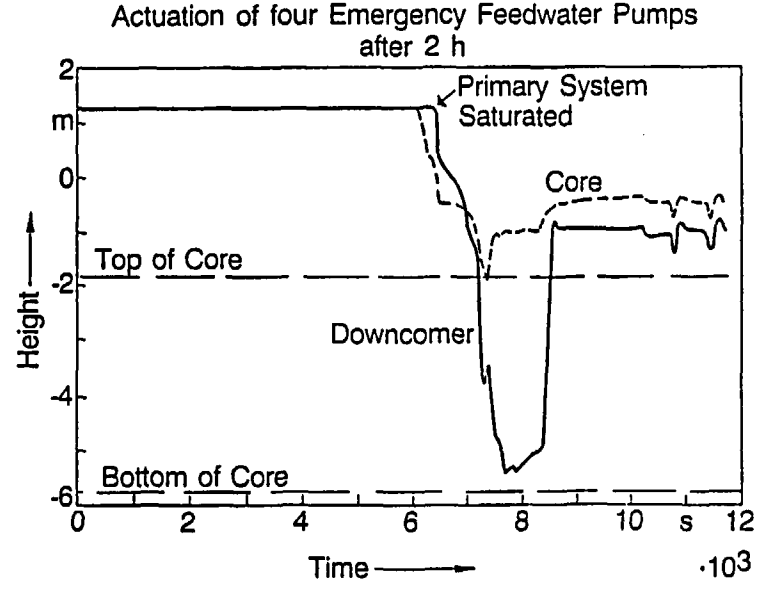

1911K

COLLAPSED LEVEL IN RPV
"STATION BLACK-OUT"
WITH SECONDARY MEASURE

FIG. 8

P W R

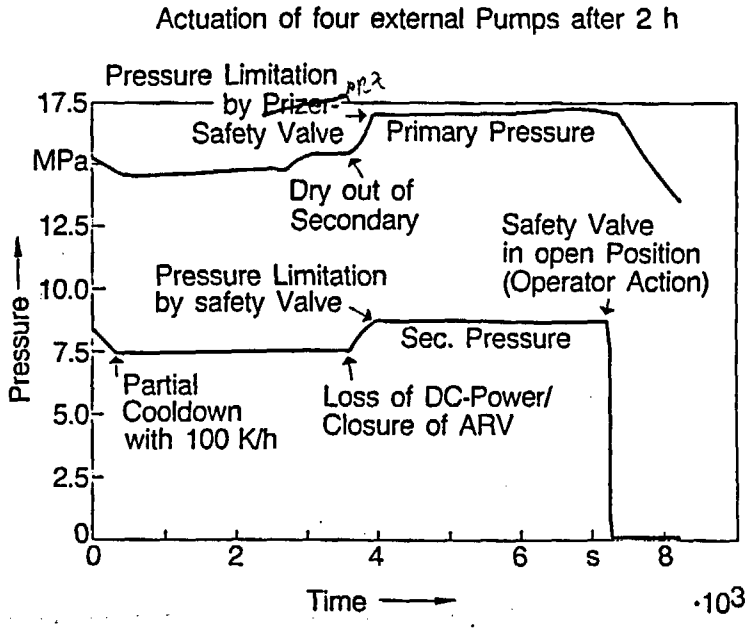

1912K PRESSURE TIME HISTORY
"STATION BLACK-OUT"
WITH SECONDARY MEASURE

FIG. 9

P W R

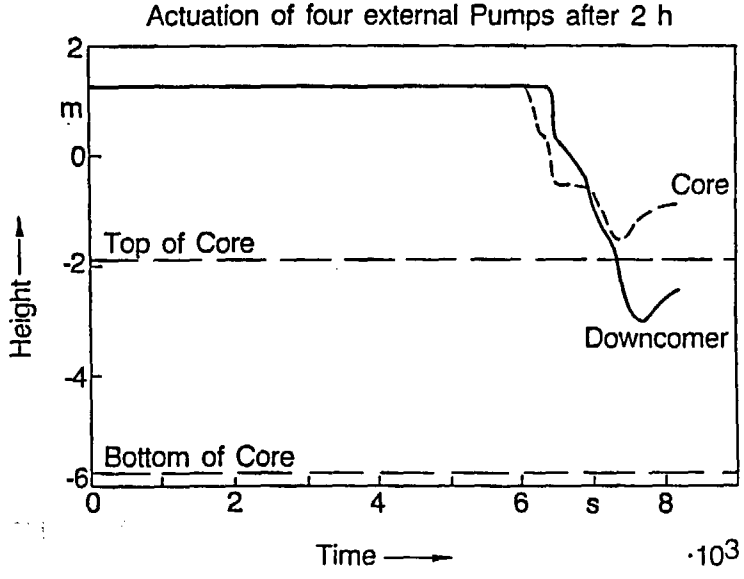

1913K COLLAPSED LEVEL IN RPV
"STATION BLACK-OUT"
WITH SECONDARY MEASURE

FIG. 10

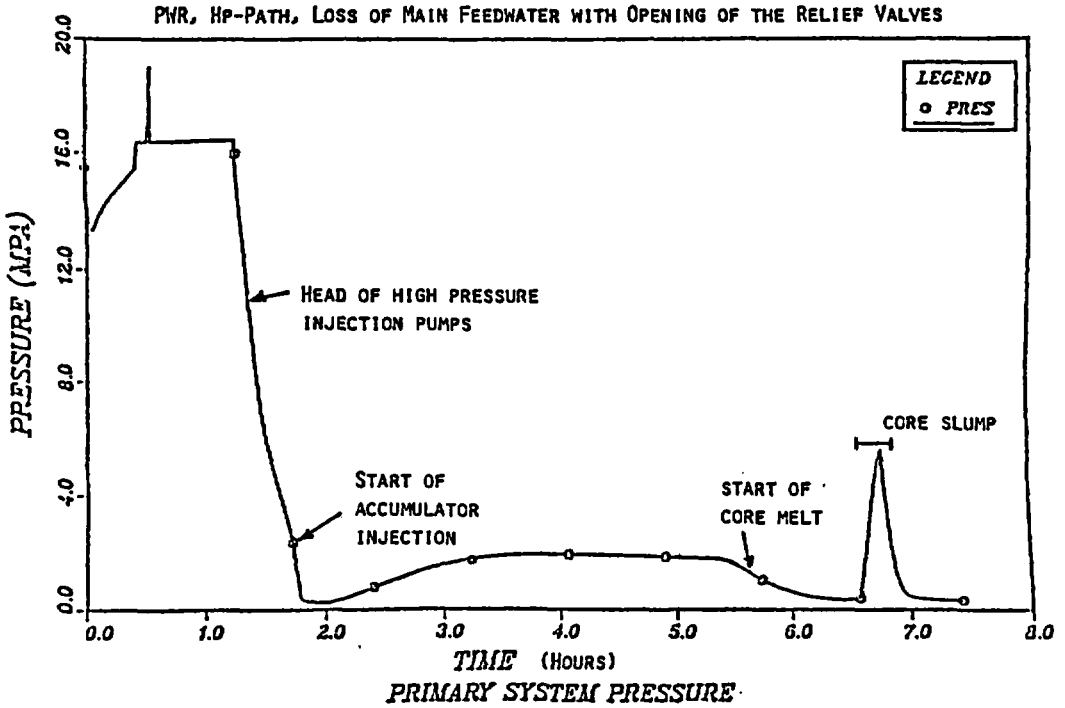
PWR, HP-PATH, LOSS OF MAIN FEEDWATER WITH OPENING OF THE RELIEF VALVES
LEGEND
o PRES
PRESSURE (MPA)
20.0
16.0
12.0
8.0
4.0
0.0
HEAD OF HIGH PRESSURE INJECTION PUMPS
START OF ACCUMULATOR INJECTION
START OF CORE MELT
CORE SLUMP
0.0
1.0
2.0
3.0
4.0
5.0
6.0
7.0
8.0
TIME (HOURS)
PRIMARY SYSTEM PRESSURE

FIG. 11

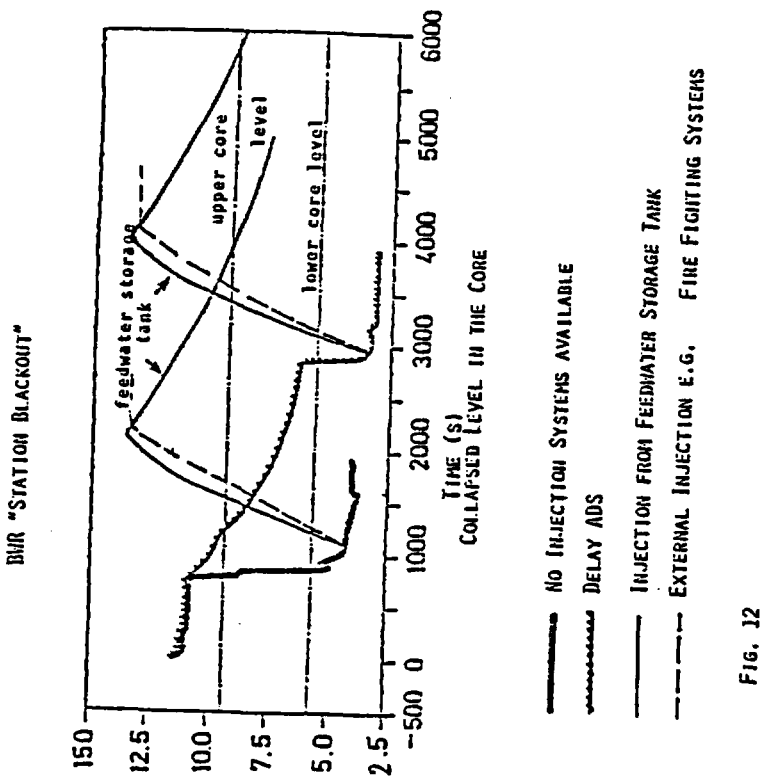
BWR "STATION BLACKOUT"
feedwater storage tank
upper core level
lower core level
TIME (S)
COLLAPSED LEVEL IN THE CORE
6000
5000
4000
3000
2000
1000
0
-500
150
12.5
10.0
7.5
5.0
2.5
NO INJECTION SYSTEMS AVAILABLE
DELAY ADS
INJECTION FROM FEEDWATER STORAGE TANK
EXTERNAL INJECTION E.G. FIRE FIGHTING SYSTEMS

FIG. 12

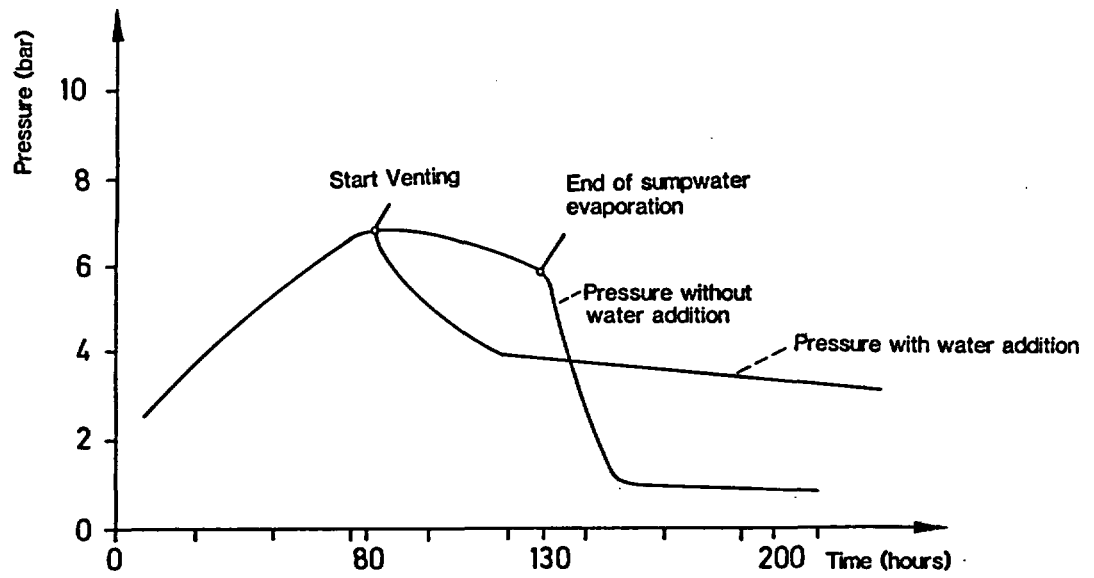

VENTING OF A PWR CONTAINMENT

FIG. 13

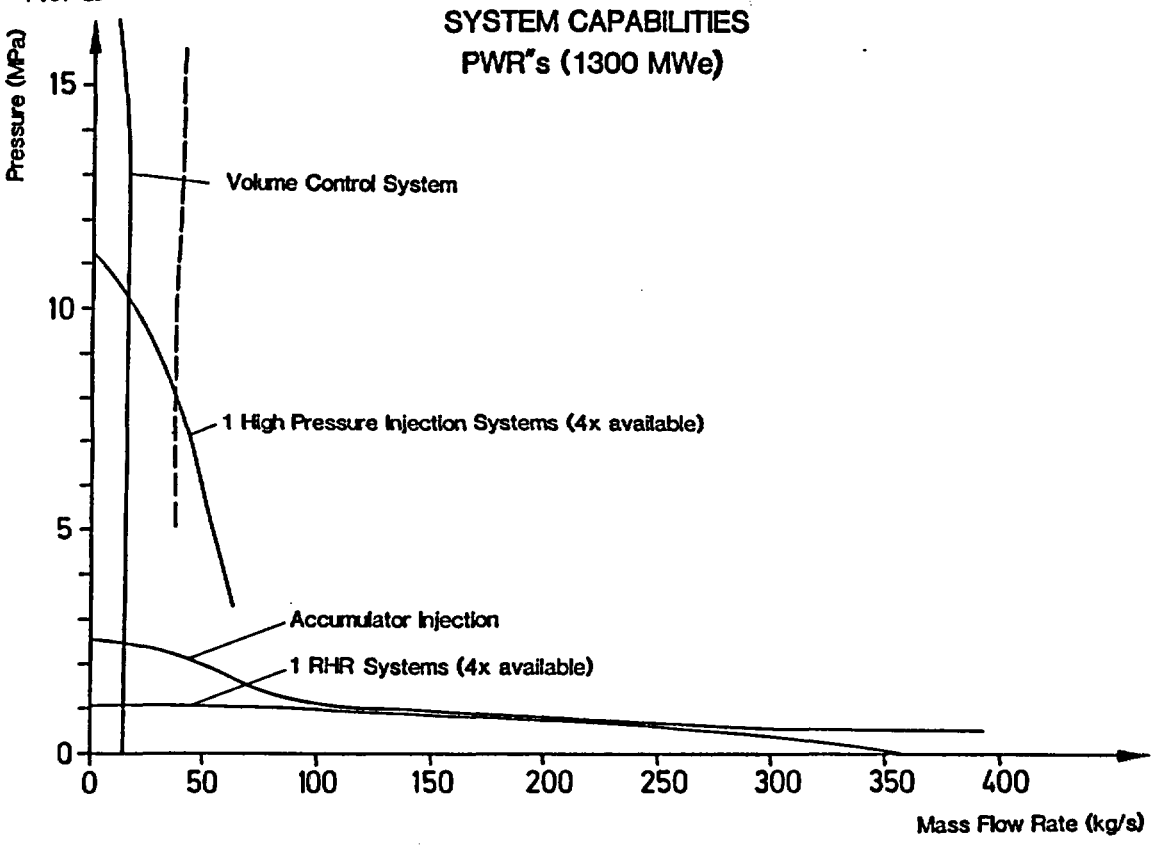

FIG. 14

System Capabilities

BWR 1300 MWe (BL 69)

System	Capacity kg/sec	Pressure bar	Emerg. Power	Storage m^3
High Pressure Injection Steam	1x350	~80	steam driven	cond.pool
High Pressure Coolant Inject. System	1x100	~80	yes	cond.pool
Control Rod Cooling Water System	2x4,2	~80	yes	150(+1080)
Sealing Lubrification Water System	2x6,1	~80	yes	150(+1080)
Feedwater System	25-300	~80	no	150
RHR-Systems	4x130	~15	yes	cond.pool
Reflood System	1x555	~15	yes	cond.pool
Feedback System	3x130	~15	yes	cont.sump
Feedwater Tank		<10	(not needed)	150
1.Fire Fighting System	2x55	12	yes	600
2.Fire Fighting System	3x61	12	yes	River
Mobile Fire Fighting System	2x67	12	yes	River
Drinking Water System	1x55	8		

Fig. 15

6. Implemented (Decided) Measures

- Filtered Venting of BWR and PWR Containments
- Inerting of BWR-Containments (BL 69)
- Battery Capacity for at least 2-3 hours
- Filtering of Control Room Inlet Air
- Turbine driven Injection Systems in BWR's connected to secured Battery Power

Measures to be studied further

- Functionability of Instrumentation under Accident Conditions
- Structure of the Plant Internal Emergency Manual
- Depressurization of the Primary System of PWR's
- Possibilities for Injection into the Primary System of PWR's
- Catalytic Recombination of Hydrogen
- Flooding of Cavity below RPV in BWR's

Fig. 16

7. Future Activities

- Development and validation of additional Accident Management Measures
- Improvement of Instrumentation and Diagnostic Tools
- Preparation of appropriate Procedure Description

Fig. 17

REGULATORY PERSPECTIVE ON ACCIDENT MANAGEMENT ISSUES

Richard J. Barrett
Chief, Risk Applications Branch
Division of Radiation Protection and Emergency Preparedness
Office of Nuclear Reactor Regulation
U.S. Nuclear Regulatory Commission

I appreciate this opportunity to address a topic that is very important to safety and which I believe will be the focus of considerable effort in the near future. Accident management is a subject which has not received the attention it deserves, in spite of the fact that severe accident studies and Probabilistic Risk Assessments continue to highlight its importance.

The schematic shown in Figure 1 outlines the essential functions that are to be accomplished in the event of a reactor accident. At the onset of a transient or LOCA, the plant operational staff switches from a normal operational mode to emergency operations (emergency operating procedures), with the goal of assuring essential safety functions and bringing the plant to a safe state. Most operating events never proceed beyond this stage. However, in cases where multiple plant failures lead to a severely degraded plant configuration and the potential for core damage, two additional functions become important: emergency response and technical support. These two functions are closely related insofar as they involve some of the same people and share the same facilities, but they are oriented toward very different goals. Emergency response involves the implementation of the onsite and offsite emergency plans to minimize the consequences should a radiological release occur. The technical support function provides a backup source of expertise to the licensed operators in their efforts to prevent core damage and minimize the potential for offsite releases.

In recent years a great deal of effort has been expended to improve the emergency operations function. In the area of emergency procedures, generic technical guidelines for each reactor vendor type have been developed by industry and reviewed by NRC, and emergency procedure generation packages, which describe how the generic guidelines are translated into plant-specific emergency operating procedures, are being reviewed for each plant. NRC has reviewed control room design and habitability, operator qualification and training programs. These aspects of emergency operations are routinely the subject of inspections. NRC efforts in this area will continue to be emphasized because of the importance of emergency operations to plant safety.

Similarly, the emergency response activity has received high priority. Emergency plans are carefully reviewed and subjected to periodic drills. NRC also evaluates the utilities' emergency response organizations and facilities. Emergency response will continue to receive priority in the future.

It is in the area of technical support where NRC believes the greatest opportunity exists for significant improvement in our ability to respond to severe accidents. Consequently, my talk this afternoon will deal primarily with NRC's plans for enhancing the industry's technical support capability.

It is important to understand that the technical support function is fundamentally different from the emergency operations function. Table 1 compares the general attributes associated with each. Emergency operations require quick, effective response by trained, licensed operations using well defined procedures based on plant symptoms. Procedures should concentrate on a minimum number of goals and actions because of limitations on the number of tasks an operating crew can effectively carry out. The operators should not be faced with difficult technical decisions. They should have confidence that adherence to procedures will bring the plant to a safe stable condition.

The technical support function is activated when the emergency operating procedures have not been, or are not expected to be, completely successful in bringing the plant under control. In general, there will have been multiple equipment failures, the configuration of safety systems will be seriously degraded, and core cooling may depend on a single train of safeguards. In extreme cases, core damage may be imminent. Under these circumstances, the technical support staff must be prepared to respond based on the accident sequence rather than the specific symptoms. Their focus must be on the fundamental goals of preventing core damage and containment failure by whatever means are at hand. They must work from broadly defined accident management strategies coupled with an in-depth knowledge of plant design and operation. Specifically, the technical support staff should concentrate on four goals:

- Monitoring the effectiveness of strategies attempted or implemented by the control room operators
- Anticipating problems which are likely to further degrade the configuration of safety systems.
- Taking positive action to reestablish the redundancy, diversity and independence of the safety systems, and
- Implementing severe accident management strategies to arrest core damage, prevent containment failure and reduce radiological releases.

Future NRC Initiatives

There have been many operating events in which the control room operators have demonstrated their ability to go beyond the operating procedures and perform "technical support" activities. We rely to a large extent on these "hidden talents" and structure training programs to ensure that they are there. However, the NRC believes we must depend on the technical support staff to

ensure that these functions will be carried out in the event of a severe accident. The utility's technical support staff must have specific guidance, training and periodic drills. The NRC staff hopes to work with the industry in three areas:

1. Review the adequacy of guidance and training for severe accident operations.

The lessons learned about accident recovery actions from over twenty five plant specific PRA's, the NRC Severe Accident Research Program and the industry sponsored IDCOR program will be distilled, disseminated to the technical support staff, and integrated into the utility training programs. NRC wants assurance that adequate training programs will be implemented across the industry.

2. Conduct periodic emergency drills which focus on the technical support function.

The emergency drills currently conducted on a periodic basis for all plants tend to focus primarily on the offsite emergency response function. In the future, the NRC intends to take a more balanced approach to emergency response, including placing a greater emphasis on technical support staff and their relationship to the control room operators.

3. Address severe accident management strategies under development by the NRC Office of Research.

To provide a technical basis for the review of accident management programs submitted by utilities as part of the Individual Plant Examination process, the Office of Research is initiating a study of the effectiveness of various accident management strategies. A set of guidelines on severe accident management strategies will be developed as part of this program. We hope to work with industry to determine the best ways to implement this guidance, as well as future guidance to be developed as a result of ongoing research programs.

Summary

Effective response to reactor accidents requires a combination of emergency operations, technical support and emergency response. The NRC and industry have actively pursued programs to assure the adequacy of emergency operations and emergency response. These programs will continue to receive high priority.

By contrast, the technical support function has received relatively little attention from NRC and the industry. The results from numerous PRA studies and the severe accident programs of NRC and the industry have yielded a wealth of insights on prevention and mitigation of severe accidents. The NRC intends to work with the industry to make these insights available to the technical support staffs through a combination of guidance, training and periodic drills.

ACCIDENT MANAGEMENT FUNCTIONS

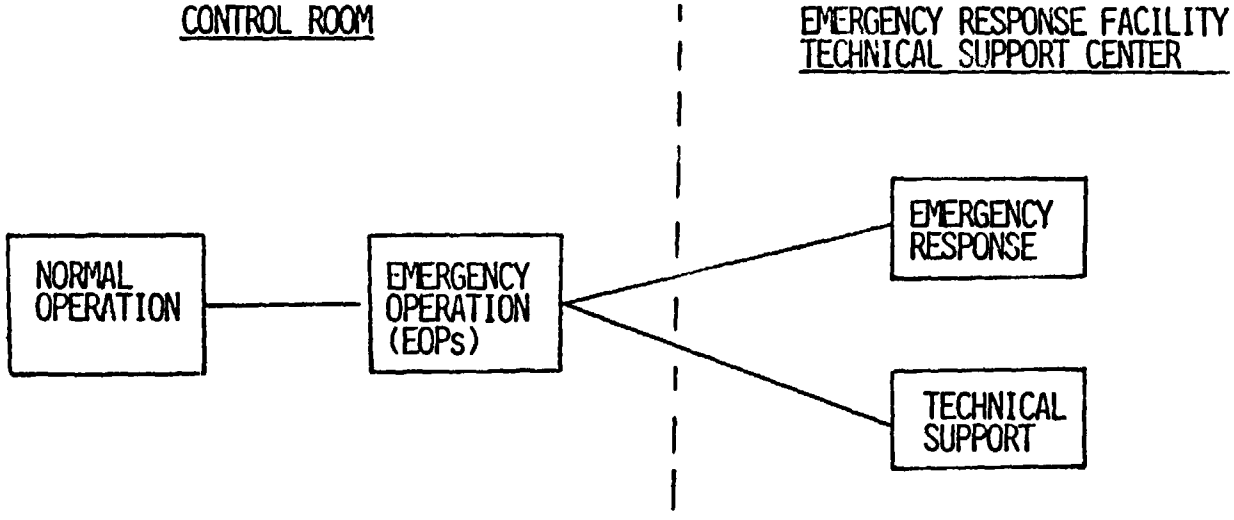

TABLE 1

CHARACTERISTICS OF TECHNICAL SUPPORT VS. EMERGENCY OPERATION

EMERGENCY OPERATIONS	TECHNICAL SUPPORT
o Performed by trained, licensed operators	o Performed by high level engineering and management personnel
o Actions based on:	o Actions based on
- Specific procedures to assure success of safety functions (criticality control, core coverage, heat removal, containment)	- Accident management strategies derived from likely paths to core melt and and containment failure
- Reaction to plant symptoms (flux, flows, pressures, temperatures)	- Anticipation of potential problems or phenomenon
o Success-oriented (goal is to bring plant to a safe stable state)	o Defensive strategy (Do what is necessary to save the core and containment)
o Limited number of options prescribed	o Broad range of options in response to unfolding events
o Strong incentives for adherence to procedures	o Requires authority to overrule established procedures
o Actions should be unambiguously beneficial	o Actions may have negative side effects
o Time for decisionmaking on order of minutes	o Time for decisionmaking on order of hours to days

TMI-2 ACCIDENT SCENARIO DEVELOPMENT[a]

E. L. Tolman, P. Kuan, and J. M. Broughton
Idaho National Engineering Laboratory
EG&G Idaho, Inc.
P.O. Box 1625
Idaho Falls, Idaho 83415

ABSTRACT

A best-estimate accident scenario describing the important mechanisms that controlled the core damage progression during the TMI-2 accident has been described in previous papers and reports. Several important questions were identified in these documents for which additional analysis and/or data are necessary to develop an adequate understanding. This paper summarizes recent analytical work relating to: (a) configuration of the degraded core based on interpreting the source range monitor data, (b) the coolability of the upper core debris bed, (c) potential crust failure mechanisms and the interaction of the molten core material with the reactor vessel coolant, and (d) potential reactor vessel damage.

INTRODUCTION

The TMI-2 accident resulted in extensive damage to the reactor core and significant release of fission products from the fuel. Defueling data has confirmed that approximately 30% of the original core material (50 metric tons) achieved melting temperatures and an estimated 15 metric tons of molten core material relocated to the lower plenum region of the reactor vessel.[1,2] Because of the extensive core damage, the TMI-2 accident offers a unique opportunity to extend our knowledge of important physical mechanisms affecting core damage progression and fission product behavior for a severe accident under achievable reactor system conditions.

The TMI-2 Accident Evaluation Program[3] is being conducted for the U.S. Department of Energy as a severe accident research effort to develop a consistent understanding of the mechanisms controlling the core damage progression and resulting fission product behavior during the TMI-2 accident. This goal is being achieved through:

- Inspection and characterization of the end-state core material distribution and damage state of the core, core support assembly (CSA), and reactor vessel,
- Interpretation and qualification of the TMI-2 data recorded during the accident as it relates to the reactor system thermal hydraulic response, and

---

a. Work supported by the U.S. Department of Energy Assistant Secretary for Nuclear Energy, Office of LWR Safety and Technology under DOE Contract No. DE-AC07-76ID01570.

- Analysis work to integrate these data into a consistent scenario of core damage progression and fission product behavior.

Details of the core damage progression (accident scenario) have been documented in previous papers[4,5] and reports.[6] A summary of the timing and major physical mechanisms hypothesized to have controlled the core damage progression is given in Table 1. Important questions relative to the mechanisms that controlled the core damage progression have been further investigated this year. These include the following:

1. What was the extent of core material relocation before the pump transient (and upper debris formation)?

2. What was the coolability of the upper core debris bed formed as a result of the pump transient at 174 min?

3. What was the mechanism that caused crust failure at 224 min?

4. What was the interaction of the molten core material with the reactor vessel coolant?

5. What was the potential damage to the reactor vessel?

Discussions of recent analytical work relative to each of these areas are provided in the following sections.

TIMING AND EXTENT OF CORE MATERIAL RELOCATION

The available TMI-2 data indicate that severe damage of the core had occurred by between 150-160 min and that a major relocation of core materials occurred between 224-226 min (see Table 1). The source range monitor (SRM) located outside the reactor vessel at the core mid-plane provided a signature of the changing conditions within the reactor vessel. Figure 1 compares the measured SRM response to the normal detector count rate after shutdown. Three features of the SRM response are important relative to the core configuration: (a) the rapid drop in detector count rate coincident with the B-pump transient (174 min), (b) the rapid increase between 224-226 min, and (c) the longer-term response between 400-1500 min showing a slowly increasing and then decreasing trend.

The rapid decrease in the SRM response at 174 min provides a unique benchmark to evaluate the degraded core configuration. Notice, however, that the SRM count rate did not decrease fully to the normal shutdown level. Thus, it can be hypothesized that (a) the core region was not filled with water, and/or (b) the core configuration had changed significantly. The previous interpretation of SRM data[7] assumed that the core was intact, thus giving no insight into the effect of core material relocation on the detector response.

Recent neutronic analysis[8] has been completed to evaluate the effect of core material relocation (both fuel and control rod material) on the SRM

TABLE 1. SUMMARY OF CORE DAMAGE PROGRESSION DURING THE TMI-2 ACCIDENT

Time Period	Summary of Core Damage Progression and Fission Product Behavior
0-100 minutes (Loss-of-coolant Period)	Primary coolant pumps provided cooling to the core. Coolant pump operation was terminated at 100 min.
100-174 minutes (Initial Core Heatup Period)	Core liquid level at pump shutdown was near the top of the active fuel. Core liquid level decreased due to heat transfer (decay heat) from the core. Core temperatures of 1100 K achieved by 140 min. Rapid oxidation of core started near 150 min and resulted in relocation of zircaloy cladding and UO_2 to lower regions of core. Continued core oxidation and subsequent fuel liquefaction and core slumping (melting) of fuel resulted in a large region of consolidated core material in the lower regions of the core. Gaseous fission product release from ruptured cladding occurred by approximately 140 min. Additional release occurred as a result of fuel liquefaction. Fission product release from the consolidated region was minimal because of limited diffusion from the large region.
174-176 minutes (Pump Transient)	The B-pump transient resulted in coolant injection into vessel for a short period (<1 min). Interaction of the coolant with the upper fuel rod remnants resulted in fracturing (thermal/mechanical shock) and in formation of the upper core debris. Cooling of the consolidated core material in the bottom regions of the core was negligible. Little enhanced release from the upper fuel rod remnants during the rod fracturing is estimated based on available examination data. Fission product release from the consolidated region was insignificant.
174-200 minutes (Degraded Core Heatup)	Heatup of the consolidated core material in the bottom of the core continued. Formation and growth of an interior molten region are postulated. Little fission product release from the consolidated region is thought to have occurred due to the limited diffusion through the large region of consolidated material and the solid surrounding crust.

TABLE 1. (contianued)

Time Period	Summary of Core Damage Progression and Fission Product Behavior
200-224 minutes (Degraded Core Heatup)	Continued heatup of the degraded core regions resulted in a large molten region within the consolidated core region. Heat loss from the region was minimal because of the insulating ceramic crust. Fission product behavior within the molten pool was likely dominated by the convective flow and chemistry of the participating materials (fuel, cladding, control rods, and core structure). No significant release from the consolidated region is expected based on the small diffusivity in the ceramic crust.
224-226 minutes (Major Core Relocation)	Localized failure of the core crust in the east quadrant occurred, due to thermal attack or stress induced failure. The upper core debris settled into the molten core zone. Molten core material was displaced from the consolidated core region and flowed downward into the lower plenum region and outward into the core former/baffle plate region. Most of the flow was directed downward into the lower plenum. Fission product release during the molten core material relocation was likely controlled by the interaction between the molten core material and the coolant in the lower core and plenum regions.
Post-226 minutes (Core Cool Down Period)	The relocation of the molten core material resulted in a more coolable geometry. The upper core debris and lower plenum debris were likely cooled in a matter of tens of minutes after the relocation event. The consolidated core region became thermally and mechanically stable after the relocation event, but its complete cooldown could have taken weeks because of its large size, low thermal diffusivity, and continuing decay heat generation. Fission product release was terminated shortly after the relocation event and formation of the lower plenum debris. Examination of the lower plenum debris will provide information to assess the integral release up to the 224 min relocation.

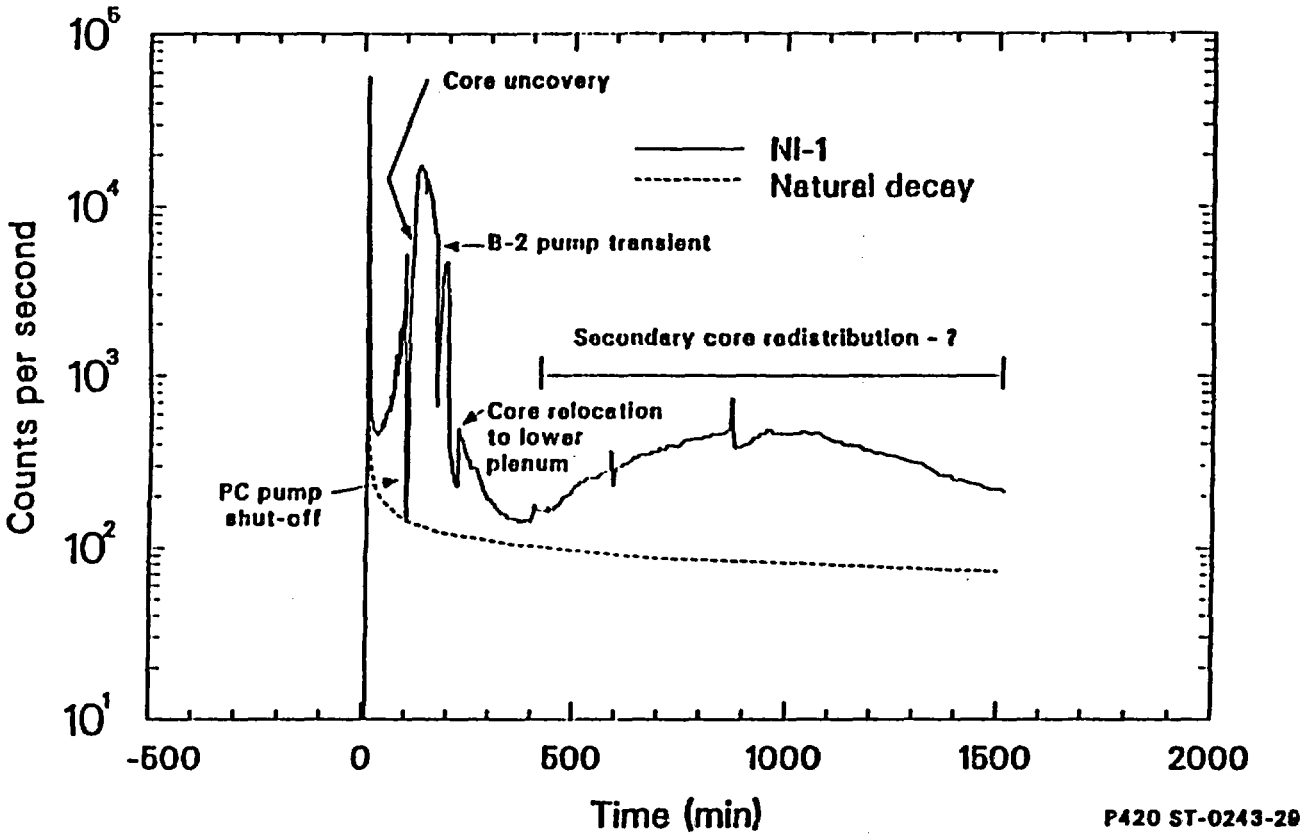

Figure 1. Source range monitor response during the TMI-2 accident.

response. Sensitivity calculations have confirmed that the limited decrease in SRM response at 174 min can be explained by core material relocation and is generally consistent with the core relocation as shown in Fig. 2.

The effect of core material in the lower head region of the reactor vessel was also investigated via two-dimensional neutronic calculations. The end-state degraded core configuration simulated in the neutronic model is shown in Fig. 3. Calculations indicate that relocation of between 10 metric tons of UO_2 and 80% of the core control rod materials is necessary to result in the observed SRM count rate. These calculations generally agree with the known mass of the lower plenum debris[9] and results confirm that a major core relocation occurred between 224-226 min as proposed in the accident scenario.

Additional SRM analysis is now underway to investigate the effect of core material in the core barrel assembly as described in Ref. 1. Also, the sensitivity of the SRM response due to differing configurations of the degraded core material in the lower plenum is being investigated. Possible explanations of the yet unexplained, long term response of the SRM between 400-1500 min are also being evaluated.

UPPER CORE DEBRIS COOLABILITY

The upper core debris study[10] was conducted to evaluate the coolability of the upper debris bed. The debris bed characteristics are summarized below:

- The debris bed axial height varied from 0.75 m to 1.25 m.
- The debris bed mass is estimated to contain from 20-25% of the core materials.
- The debris bed was heterogeneous, containing both Zr and UO_2.
- Approximately 90% of the particles ranged between 1 and 5 mm.

Based on the above data and sample examinations of the debris material[11], the upper core particle bed can be approximated by a right-circular cylinder which has a height of 0.9 m and a diameter of 2.8 m. The bed was modeled with an average particle diameter of 0.9 mm[a] and a porosity of 0.54. Between 3 and 5 hr after reactor scram, the power density in the debris bed is estimated to be about 0.75 MW/m^3. Using these parameters and assuming that all the heat generated in the bed was transferred upwards, the heat flux from the particle bed is compared to the dryout heat flux of the particle bed in Fig. 4. The Lipinski deep bed model[12] is used to calculate the dryout heat flux. Also shown in Fig. 4 is the heat flux from the total debris in the core region if all the heat generated in the debris was transferred upwards through the particle bed. For the particle bed only, the heat flux

---

a. A 0.9 mm particle diameter results in the same effective debris surface area as estimated using the actual particle size distribution.

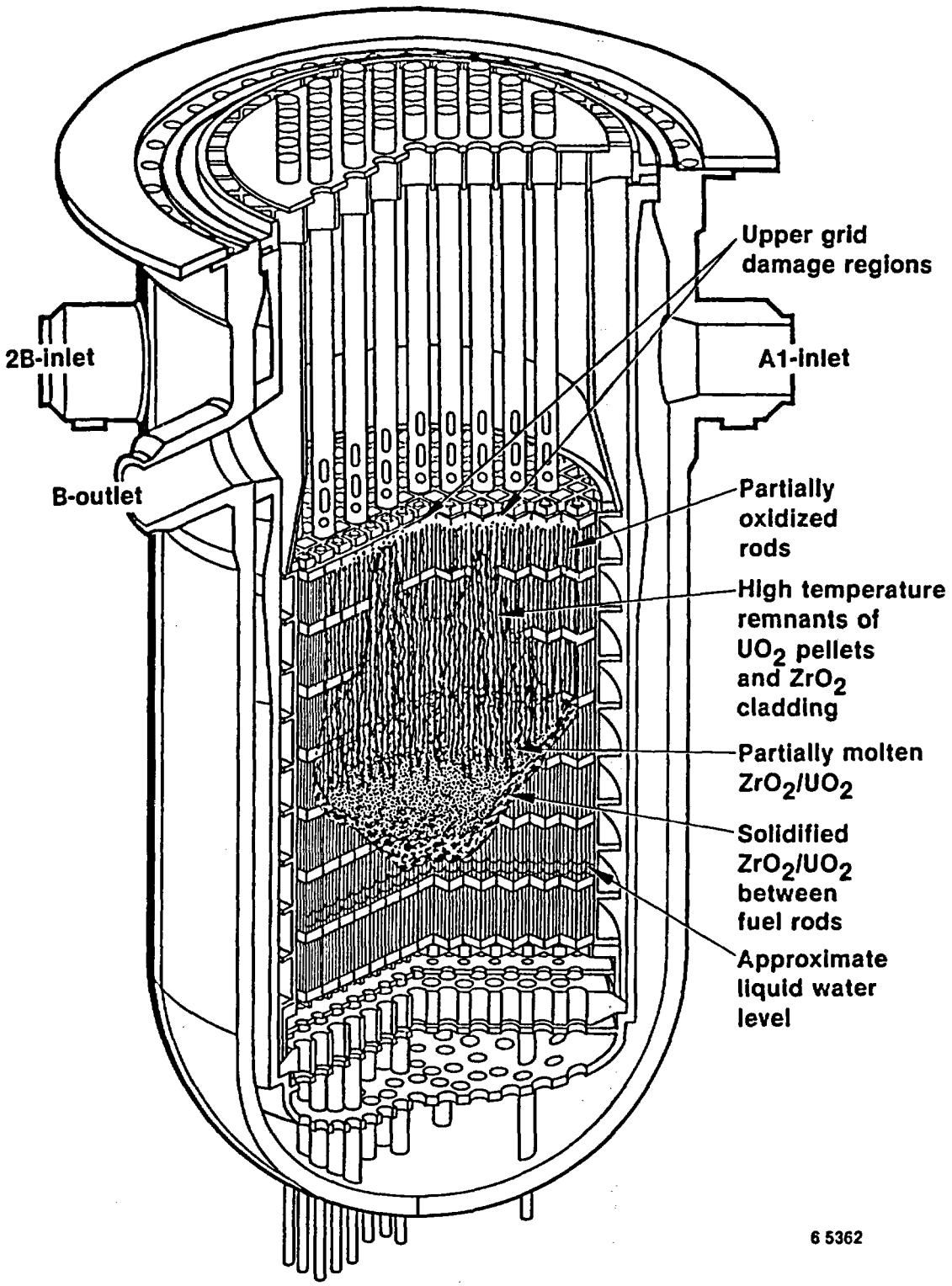

Figure 2. Hypothesized core configuration just prior to 174 m (pump transient).

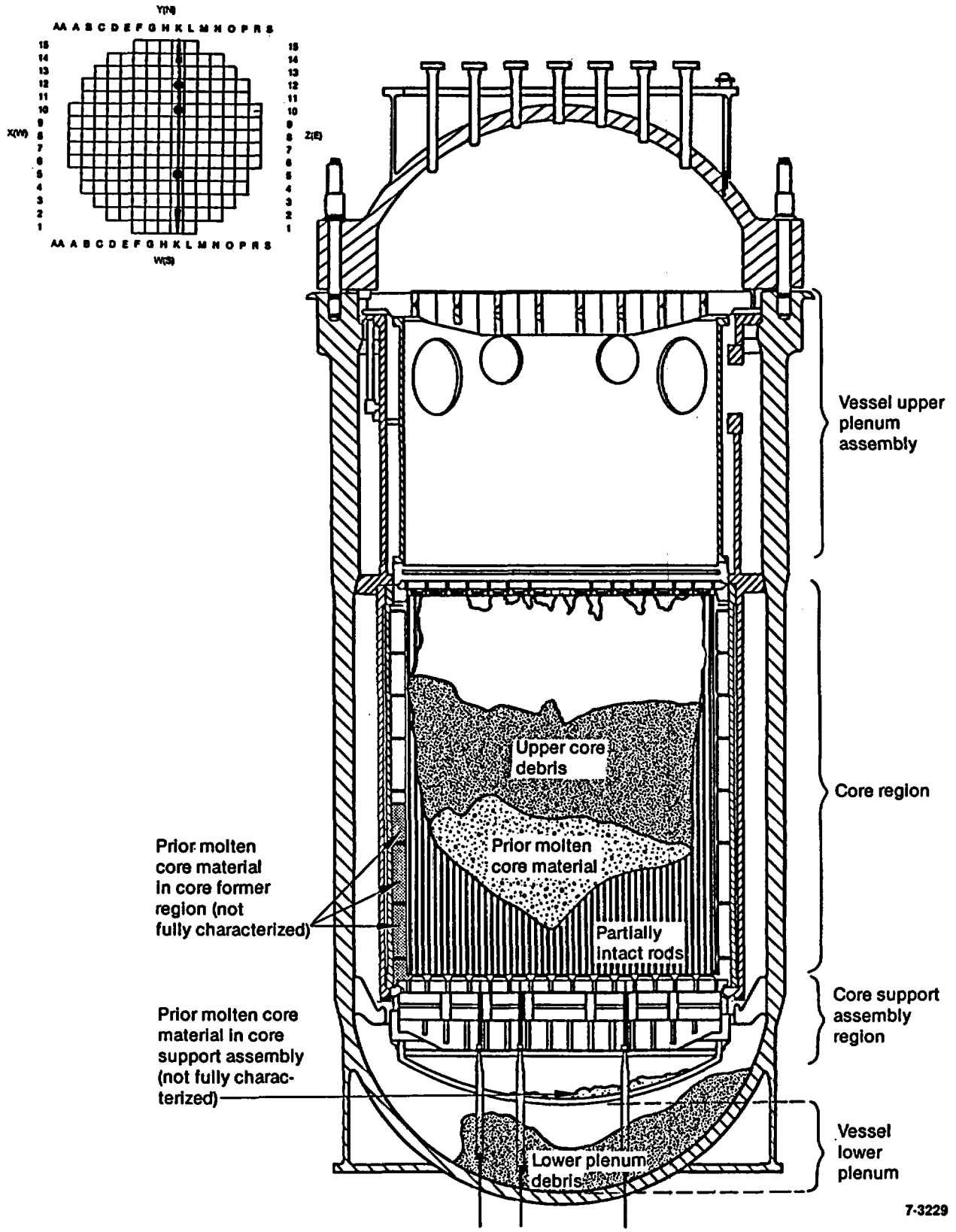

Figure 3. End-state core configuration.

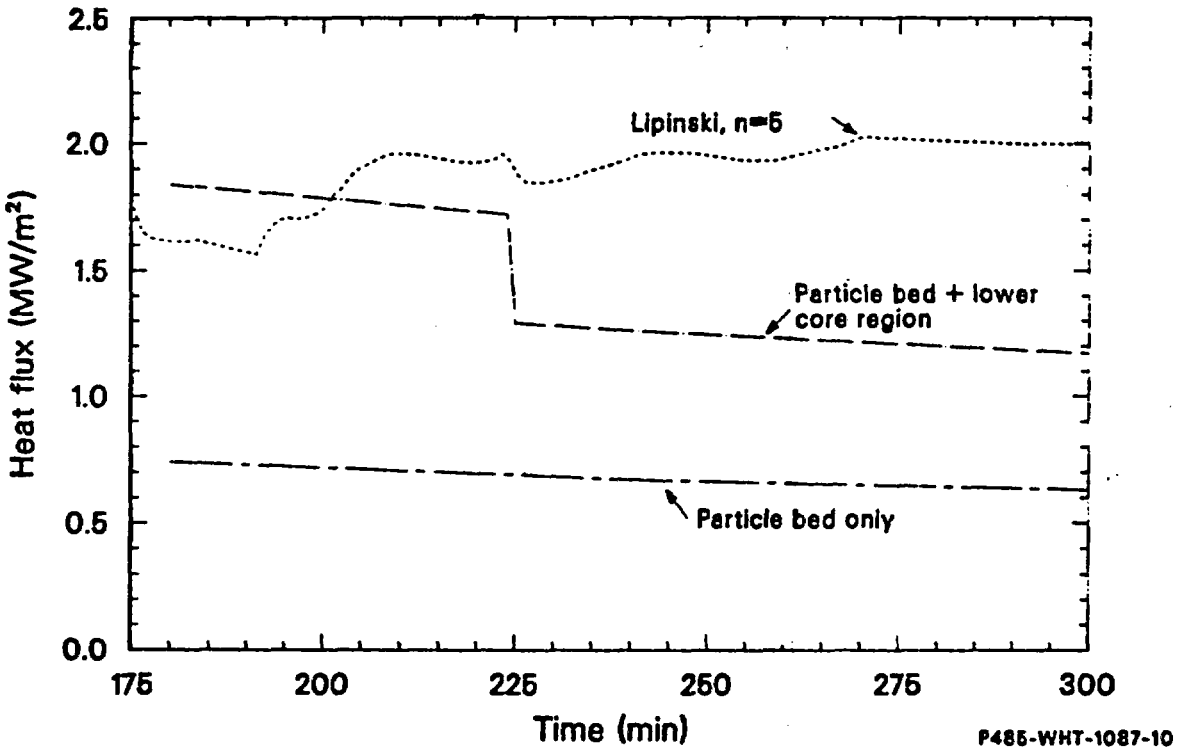

Figure 4. Upper core debris bed - comparison of predicted dryout heat flux to estimated actual bed heat flux for the upper core debris bed.

was much lower than the dryout heat flux and the particle bed was coolable in the presence of water. The debris bed heat flux (assuming most of the heat from the consolidated region was transfered upward into the debris bed) was comparable to the dryout heat flux before the relocation (174-224 min). Thus, the debris bed may not have been cooled appreciably during this time period. After the major core relocation at 224 min, however, the heat flux in the debris dropped due to the removal of fuel and the particle bed became coolable even if all the heat in the lower consolidated region was transferred upward through the particle bed.

Once the particle bed became coolable (i.e. the debris bed heat flux was less than the dryout heat flux), quenching took place in the presence of water. A simple energy balance formulation for the quench time was used to estimate the debris bed quench time. The energy balance model is shown in Fig. 5. It was assumed that heat transfer to the water at the quench front was the same as the dryout heat flux. Thus, the difference between the total dryout heat flux and the internal heat generation rate plus the heat transferred into the debris bed from below, lowered the temperature of the debris bed and led to quenching. Two estimates of the quenching time of the particle bed were carried out. The shortest time was associated with no heat transfer into the bed from below, i.e., only heat generation within the debris bed was considered. The longest time assumed 80% of the heat from the consolidated region was transferred into the upper debris bed. Assuming the emergency core cooling water flooded the core by 207 min and provided the source of cooling and the initial temperature of the debris bed was 2000 K, the earliest predicted quench time was about 18 min, putting the bed quenching time at around 225 min. The latest quench time was predicted to be about 38 min and would have resulted in a final quench time around around 245 min.

POSSIBLE CRUST FAILURE MECHANISMS

Identification of possible crust failure mechanisms is important because the mode of crust failure determines the extent and timing of the molten core relocation and the thermal challenge to the core support structures and reactor vessel. Three possible failure mechanisms were identified in preliminary work to assess crust failure mechanisms.[13,14] The first is melting of the crust. Calculations show that failure of the lower crust is not likely, because in the presence of water the crust thickness is on the order of several inches. However, upper crust melting is possible because of crust thinning due to the predominant upward convective heat transfer from the molten pool.

The second mechanism is structural failure of the crust due to thinning of the upper crust as the molten pool grew. The pressurizer relief valve was opened at approximately 220 min, approximately 4 min before the major core relocation event, causing the reactor system pressure to decrease by about 300 psi. The pressure reduction outside the molten core interior thus increased the pressure differential across the crust and may have led to failure of the crust.

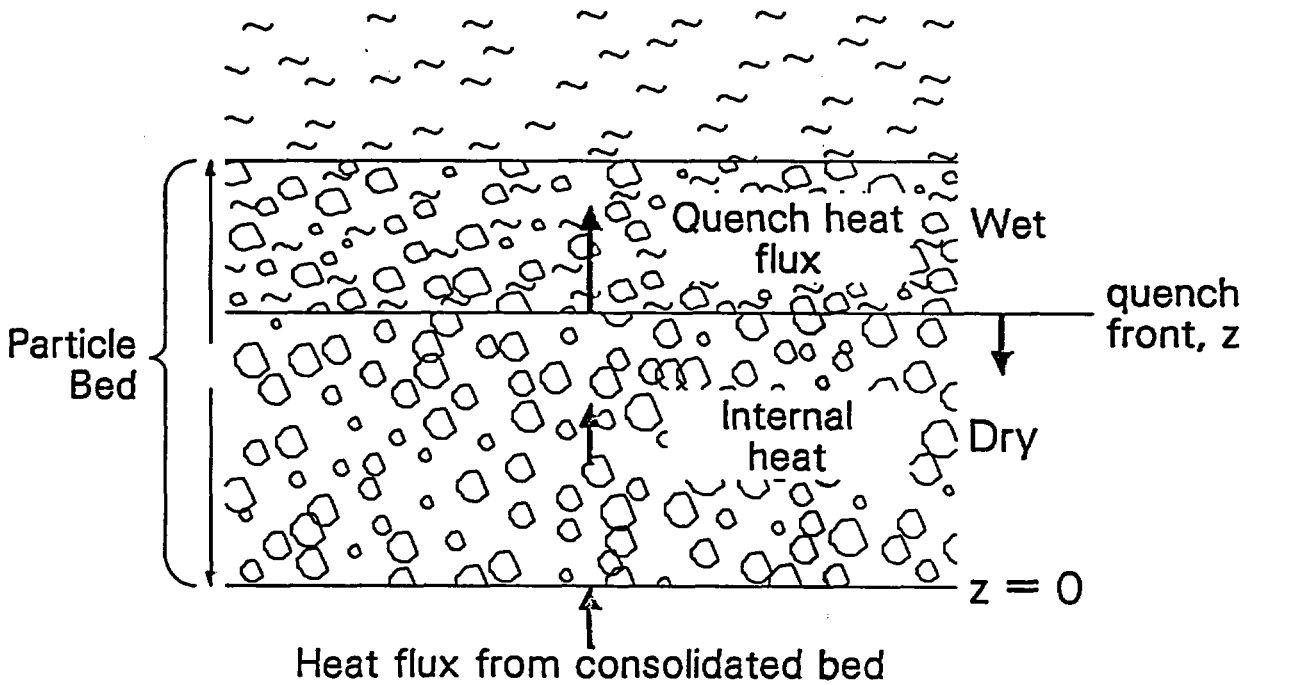

Figure 5. Upper core debris bed quench model.

The third possible mechanism is the potential interaction of the degraded core materials with the core barrel assembly at the core periphery. The degraded core region was skewed to the east side of the vessel and, as the degraded core heated up, it may have caused melting of the core barrel structures which chemically attacked the crust, resulting in crust failure.

Details of a hypothesized crust failure scenario[15] have been proposed based on the thermal properties of the degraded core material as shown in Fig. 6. Because of the ceramic properties of the consolidated material, the temperature profile across the consolidated region would be expected to be relatively constant, as shown in Fig. 6. Significant heat transfer into or out of the consolidated region would occur only at the thermal boundary layer adjacent to the molten region, δ_1, and at the upper coolant interface, δ_2, as shown in Fig. 6. The estimated thickness of these thermal boundary layers is only a few millimeters. Thus, little heat is transferred from the consolidated region, and the internal heat generation results primarily in melting the interior region and formation of a molten pool as shown in Fig. 7(a). As the molten core material regions grows, eventual interaction of the two thermal boundaries shown in Fig. 6 will occur.

Calculations indicate that for a molten pool of 1.25 m radius in equilibrium with the surrounding coolant, the equilibrium crust thickness at the outer surface would be approximately 8 mm. Previous estimates of the crust thickness necessary to support the upper debris bed mass indicate that a crust at least 2.5 cm thick is required. Experiments to measure heat flux variations in convective pools indicate that nonuniform heat fluxes would likely occur in the molten pool, resulting in thinner crusts at the top and at the periphery. These trends, together with a slight skewing of the degraded core region towards the east side of the vessel, are hypothesized to have led to localized failure of the crust near the core periphery as shown conceptually in Fig. 7(b). As the upper crust failed, the upper debris bed would fall into the molten pool, displacing the molten core materials from the core region as shown in Fig. 7(c). Estimates of the time it took to displace the molten core material were made by balancing the drag and gravity forces on the debris particles as they settled into the molten pool. The time required to displace the molten core material in the form of a liquid was calculated to be about 12 s. This is somewhat shorter than the maximum relocating time of about 1 min as inferred from the source range monitor data. The time difference can be explained by considering solidification of the molten ceramic in the interstices of the particles, which is calculated to have prolonged the settling time by an estimated 1 min.

MOLTEN FUEL COOLANT INTERACTION

An evaluation of the interaction of the molten core material with the water in the reactor vessel is also documented in Ref. 15. Breakup of the molten core material stream was analyzed in terms of the growth and detachment of unstable capillary waves or surface ripples on the outer surface of the molten stream or jet. The rate of stream breakup, via the surface wave instability theory, has a square-root dependence on the fluid density surrounding the jet. If the water along the path of jet movement was saturated, the fluid responsible for the breakup of the jet would have been

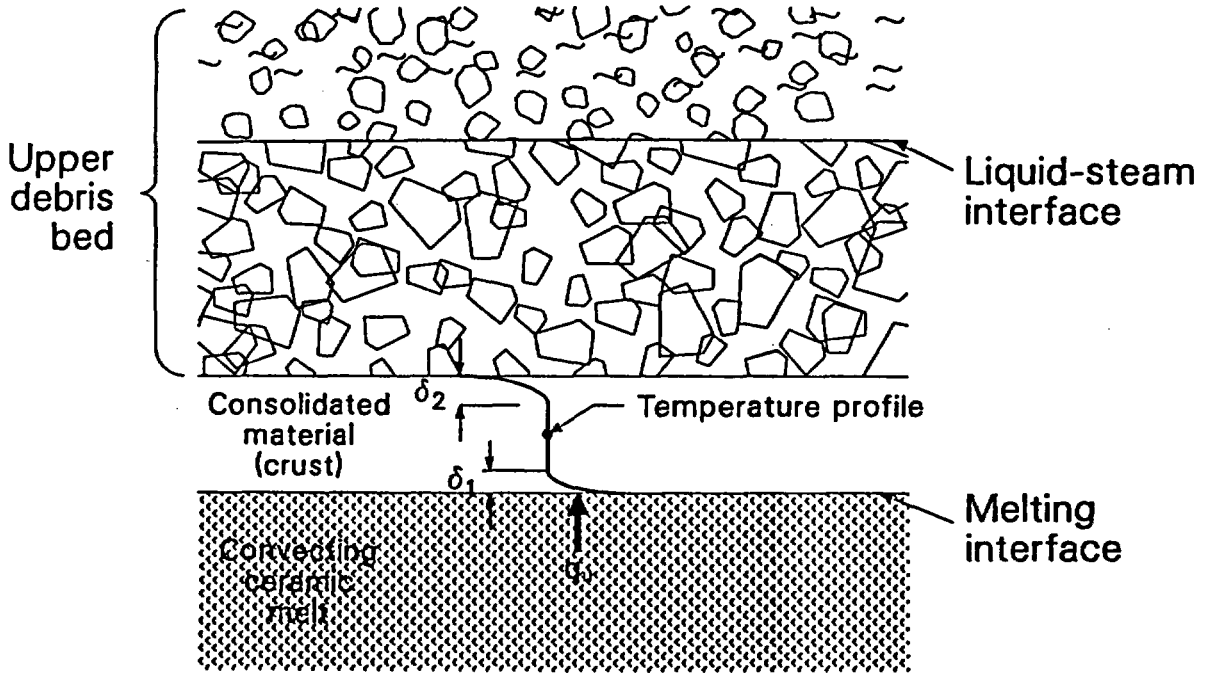

P485-LN87051-3

Figure 6. Degraded core thermal model.

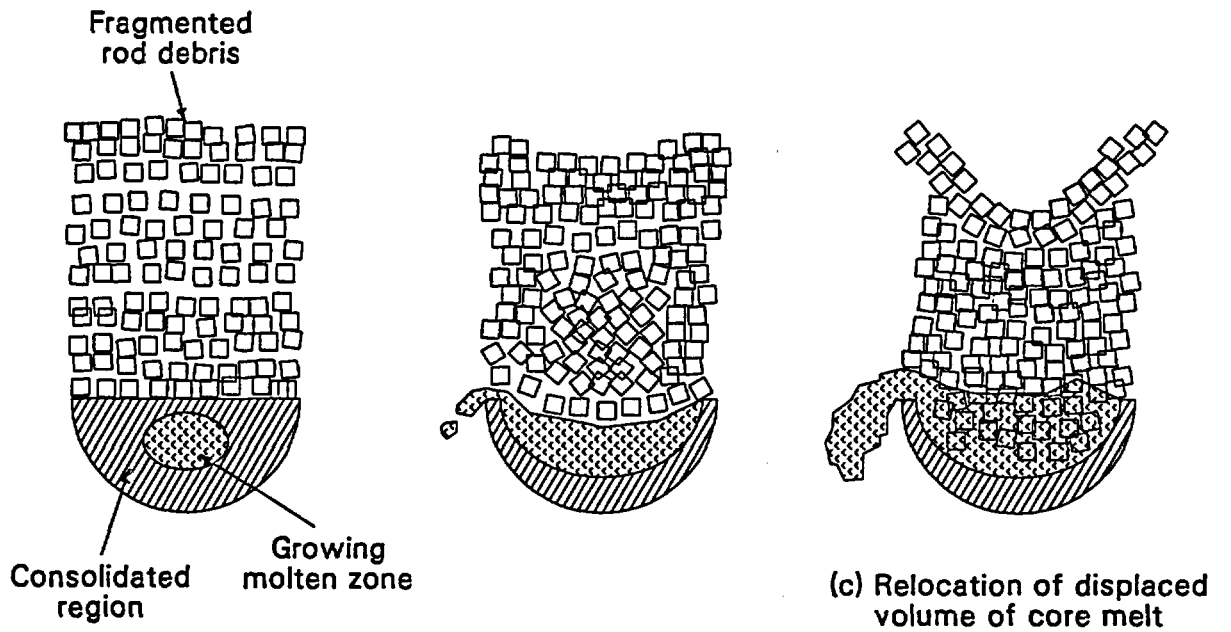

P485-LN87051-2

Figure 7. FAI crust failure scenario.

primarily steam, generated from film-boiling at the surface of the stream. For a stream velocity of 3.7 m/s, and a diameter of 0.08 m (based on an assumed relocation flow pathway of one fuel assembly and a relocation time of 1 min), it would require a distance of about 7 m for complete stream breakup in saturated water. The distance from the mid-core elevation to the bottom of the lower head is about 4 m. Therefore, complete breakup of the jet would not have been possible. In this case, the molten stream may have eroded the vessel head at the point of impingement.

If the water surrounding the jet was subcooled by about 80 K, the steam layer at the jet interface would have been thin, thus allowing interaction of the surrounding water with the jet surface resulting in jet breakup. Due to the square-root dependence of the breakup rate on the fluid density, breakup of the jet is estimated to occur over a traveling distance of about 2 m, which is about half the distance from the core mid-plane to the lower head.

Experiments in which molten core material was dropped into water pools,[16] also show that subcooled water results in particulate debris formation and limited steam generation compared to experiments with saturated water, in which much less molten stream breakup occurred and much higher steam generation was measured.

POTENTIAL VESSEL HEAD DAMAGE

Because a localized crust failure has been hypothesized and 15-20 metric tons of previously molten core material rests on the lower vessel head, two studies were undertaken to evaluate the potential damage to the lower reactor vessel head. The first study is an evaluation of potential localized damage as a result of a highly localized relocation stream.[17] Knowing the amount of lower plenum debris to be about 15 metric tons, and assuming a localized flow area for the relocation stream, a simple gravity flow calculation provides some insight into the flow pathways and timing as illustrated in Fig. 8. The relocation flow times are estimated to be 15 s and 75 s for an assumed flow area associated with the nominal flow area of 4 and 1 fuel assemblies, respectively.

Two cases were considered in evaluating the effect of the molten stream impingement on vessel. These cases are shown in Fig. 9. The first is a relative weak jet, in which the stream turbulence at the vessel wall interface is not maintained. For this case the molten material would freeze at the vessel interface and heat conduction into the vessel wall would be limited by thermal conduction through the frozen layer of core material. The second case assumes a more turbulent stream of core material, in which the stream turbulence at the vessel wall interface is maintained. For this case, the heat conduction from the molten stream is greatly enhanced since molten core material is assumed to be adjacent to the vessel during the relocation time.

For the conduction controlled or weak jet case, damage to the lower head is not predicted. However, for the strong jet case, where turbulence at the vessel interface is maintained, limited damage to the vessel wall may have

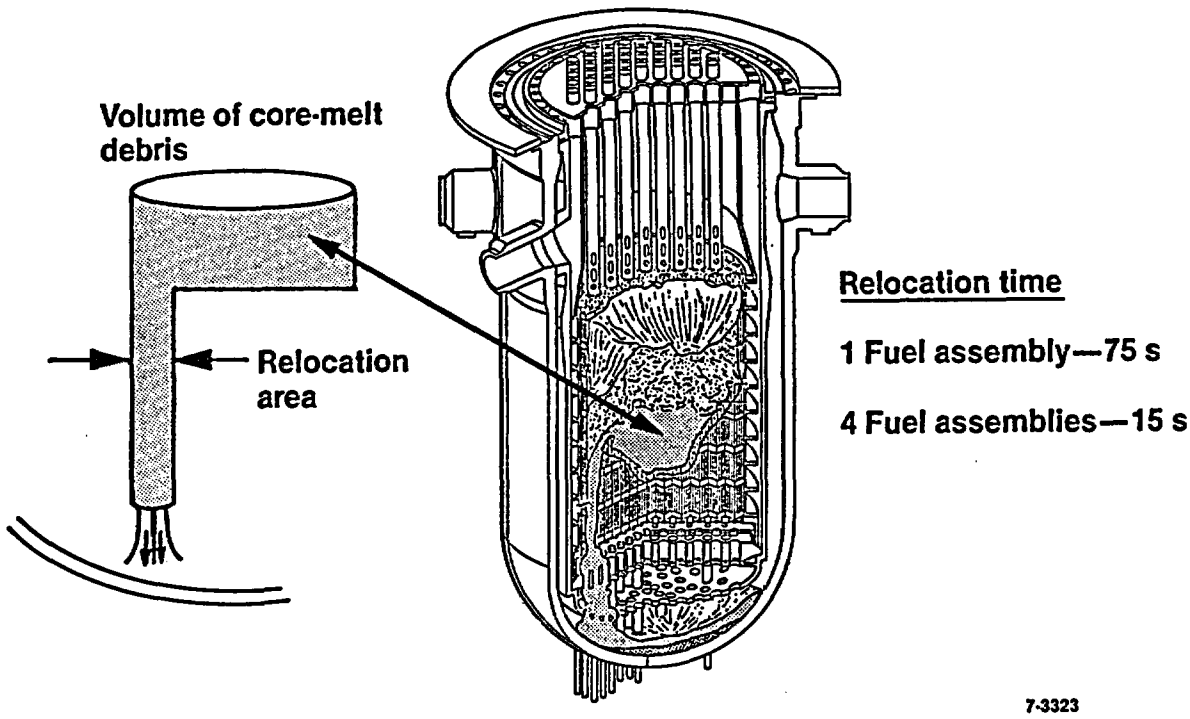

Figure 8. Model for estimating major core relocation timing.

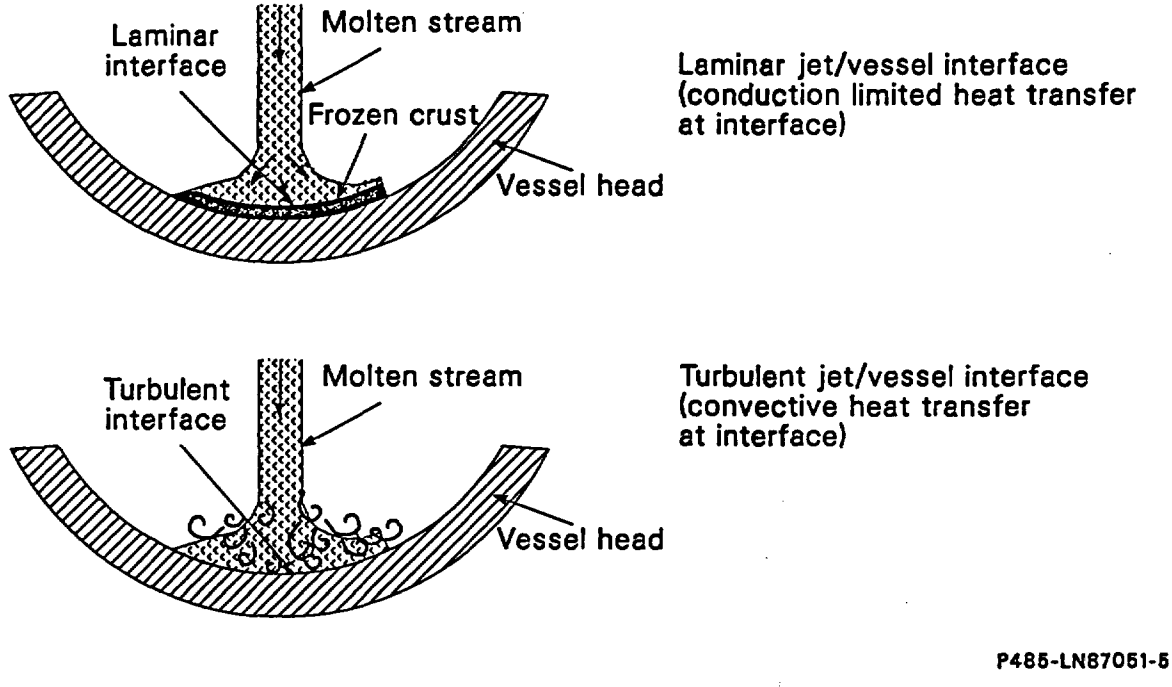

Figure 9. Model assumptions for localized core stream/vessel heat transfer.

occurred. Under these assumptions, limited surface ablation of the vessel liner is calculated. However, the melt front penetration of the vessel wall is estimated to be less than 1 cm. The calculations also indicate a direct jet impingement of 15-20 min is necessary to cause melting of half of the vessel wall thickness. The TMI-2 data clearly do not support relocation times greater than about 1 min.

The second vessel study evaluated the global thermal response of the vessel assuming 15 metric tons of core debris on the vessel head.[18] A two-dimensional (radial, axial) heat conduction model of the TMI-2 lower plenum debris and reactor vessel was utilized to address the vessel margin-to-failure question. Because the debris configuration during the molten core relocation period is somewhat uncertain, two assumed debris configurations were analyzed. The first configureation assumed a porous debris bed resting on the vessel head. The second assumed a porous debris bed supported by a layer of previously molten but consolidated core material adjacent to the vessel head. For each of these cases, two assumptions on debris cooling were made, i.e., (a) no cooling of the debris material, and (b) heat transfer from the debris and consolidated material leading to quenching in a 20 min period. The general lower plenum debris and vessel head model is shown in Fig. 10.

The analyses show that the vessel thermal response is sensitive to both the debris configuration and cooling of the degraded core materials. For the consolidated material configuration, if the upper debris is not cooled, vessel melting is predicted to occur after several hours. However, at temperatures in the range of 1000-1100 K, creep rupture of the vessel becomes an important issue since the reactor system pressures were high (7-10 MPa). Thus, it is expected that vessel failure due to creep rupture would likely occur before vessel melting temperatures are achieved. If cooling of the porous debris on top of the consolidated material is assumed, melting of the vessel is not predicted. However, the vessel temperatures are also predicted to exceed 1100 K for this case. Thus, for the lower plenum configuration with consolidated material adjacent to the vessel, even with debris cooling, vessel creep rupture is an important issue.

For the case in which the lower plenum material is porous debris, vessel melting is not predicted; however, again vessel wall temperatures of 1100 K are predicted, indicating creep rupture of the vessel to be important. However, if cooling of the debris is assumed, vessel wall temperatures are estimated to be less than 800 K. For this case, mechanical challenge to the vessel would be insignificant.

SUMMARY

TMI-2 defueling data to characterize the core damage state and location of the degraded core materials, examination of the degraded core material from the TMI-2 core and lower plenum regions, interpretation of the TMI-2 on-line data recorded during the accident, and supporting analyses are providing a remarkably consistent interpretation of the core damage progression that occurred during the TMI-2 accident. This work has provided a baseline

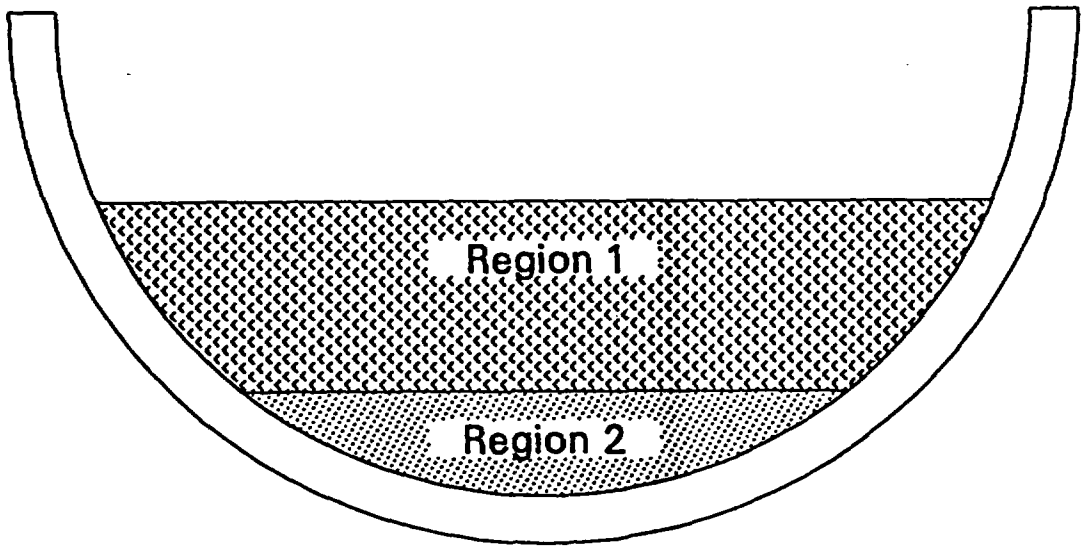

Case 1: Region 1 - porous debris
Region 2 - consolidated material

Case 2: Region 1 - porous debris
Region 2 - porous debris

P486-LN87061-1

Figure 10. Heat conduction model to evaluate vessel heatup.

accident scenario that defines the basic mechanisms that controlled the core damage progression and has provided a baseline from which to interpret the measured fission product distribution. The fission product behavior analysis work based on the core damage progression scenario developed to date is summarized in Ref. 19.

The analytical studies summarized in this paper have significantly improved our understanding of the mechanisms affecting the degraded core heatup, crust failure mechanism, interaction of molten core material with the reactor vessel coolant, and the potential thermal challenge to the reactor vessel. Further analytical work to be completed in the next year will add insight into the earlier phases of the core damage progression, particularly regarding the impact of core flow blockage on the core heat transfer and on hydrogen production. In addition, work is ongoing to establish a better understanding of the mechanisms leading to the damage of the upper grid structures. Work will also be necessary to interpret the most recent observation of very localized melt ablation of the lower fuel assembly grid plate in one of the centrally located fuel assemblies.

Completion of the core and lower vessel region defueling, examination of degraded core materials from these regions, and the necessary supporting analytical work to interpret the data, will complete our understanding of the accident and provide important data to assess more generic technical issues relative to core degradation and fission product behavior during severe accidents in light water reactors.

REFERENCES

1. G. R. Eidam, "GPU Defueling," These proceedings, October 1987.

2. E. Tolman, et al., TMI-2 Core Bore Acquisition Summary Report, EGG-TMI-7385 (Rev. 1), February 1987.

3. E. Tolman, et al., TMI-2 Accident Evaluation Program, EGG-TMI-7048, February 1986.

4. E. Tolman, et al., "Thermal Hydraulic Features of the Accident," ACS Symposium Series 293, April 1985.

5. E. Tolman, et al., "TMI-2 Accident Scenario Update," Proceedings of 14th Water Reactor Safety Information Meeting, October 1986.

6. E. Tolman, et al., TMI-2 Accident Scenario Update, EGG-TMI-7489, December 1986.

7. Interpretation of TMI-2 Instrument Data, NSAC/28, Nuclear Safety Analysis Center (NSAC), Electric Power Research Institute (EPRI), Palo Alto, CA, March 1980.

8. Horng-Yu Wu, et al., Analysis of the TMI-2 Source Range Monitor During the TMI Accident, Pennsylvania State University Report (Nuclear Engineering Department), June 1987.

9. J. P. Adams, et al., TMI-2 Lower Plenum Video Data Summary, EGG-TMI-7429, July 1987.

10. P. Kuan, TMI-2 Upper-Core Particle Bed Thermal Behavior (Draft), EGG-TMI-7757, July 1987.

11. D. Akers, et al., TMI-2-Core Debris Grab Samples--Examination and Analysis (Part 1), GEND-INF-075, September 1986.

12. R. J. Lipinski, "A Coolability Model for Post-Accident Nuclear Reactor Debris," Nuclear Technology, 65, 53, April 1984

13. R. Henry, et al., "Core Relocation Phenomenology," Proceedings of the First International Information Meeting on the TMI-2 Accident, CONF-8510166, Germantown, MD, October 1985.

14. P. Kuan, Core Relocation in the TMI-2 Accident, EGG-TMI-7402, December 1986.

15. M. Epstein, H. Fauske, The TMI-2 Core Relocation - Heat Transfer and Mechanism, Fauske & Associates, Inc. Report FAI/87-49, July 1987.

16. B. Spencer, et al., "Corium Quench in pool mixing Experiments," ANS Proceedings, 1985 NaturalHeat Transfer Conference, ANS 700101, Denver, CO, August 1985.

17. A. Cronenberg, E. Tolman, An Assessment of Damage Potential to the TMI-2 Baffle Plate, Core Former, and Lower Head Assemblies Due to Thermal Attack by Core Debris, EGG-TMI-7790, September 1987.

18. R. Moore, TMI-2 Reactor Vessel Lower Head Heatup Calculations, EGG-TMI-7784, September 1987.

19. D. A. Petti et al., "Analysis of Fission Product Release Behavior During the TMI-2 Accident", This proceeding, October 1987.

TMI-2 Core Bore Examination Results[a]

C. S. Olsen, D. W. Akers, and R. K. McCardell
Idaho National Engineering Laboratory
EG&G Idaho Inc.
Idaho Falls, Idaho 83415

ABSTRACT

Examinations are being performed on samples obtained from the lower portion of the TMI-2 reactor core as part of the TMI-2 Sample Acquisition and Examination Program. This paper presents preliminary results of visual examinations, the gamma spectrometry analyses performed on the intact core bores, and the metallurgical examinations. These examinations indicate significant core damage effects on the distribution of core materials and fission products in the lower reactor core including the substantial relocation and segregation of some fission products (e.g., Sb-125 and Ru-106).

INTRODUCTION

Unit 2 of the Three Mile Island pressurized water reactor underwent a loss-of-coolant accident on March 28, 1979, resulting in severe damage to the reactor core. After the accident, four organizations, General Public Utilities Nuclear Corporation (GPU Nuclear), the Electric Power Research Institute (EPRI), the Nuclear Regulatory Commission (NRC), and the Department of Energy (DOE), collectively known as GEND, cosponsored a postaccident evaluation of the TMI-2 accident. During 1986, a core boring operation was conducted jointly by EG&G Idaho, Inc. and GPU Nuclear to obtain samples of the lower reactor core necessary to spatially characterize the chemical and physical state of this part of the degraded core.[1]. The results of these examinations will be used to provide data on fission product release, interaction between core components, hydrogen generation, and core melt progression.

Previous examinations of the reactor core indicated that the upper reactor core contained a void region almost entirely surrounded by standing peripheral assemblies (Figure 1). Below the void region was a layer of loose debris resting on a hard crust[2]. However, conditions in the region of the core below the debris bed (approximately 50 percent of the core volume) were not known as there were no penetrations through the crust layer. Consequently, to examine this portion of the reactor core, a core boring system capable of penetrating the hard crust was developed to provide access to the lower core region for both examination and defueling purposes. The

a. Work supported by the U.S. Department of Energy, Assistant Secretary for Nuclear Energy, Office of Light Water Reactor Safety and Technology, under DOE contract Number DE-AC07-76-ID01570.

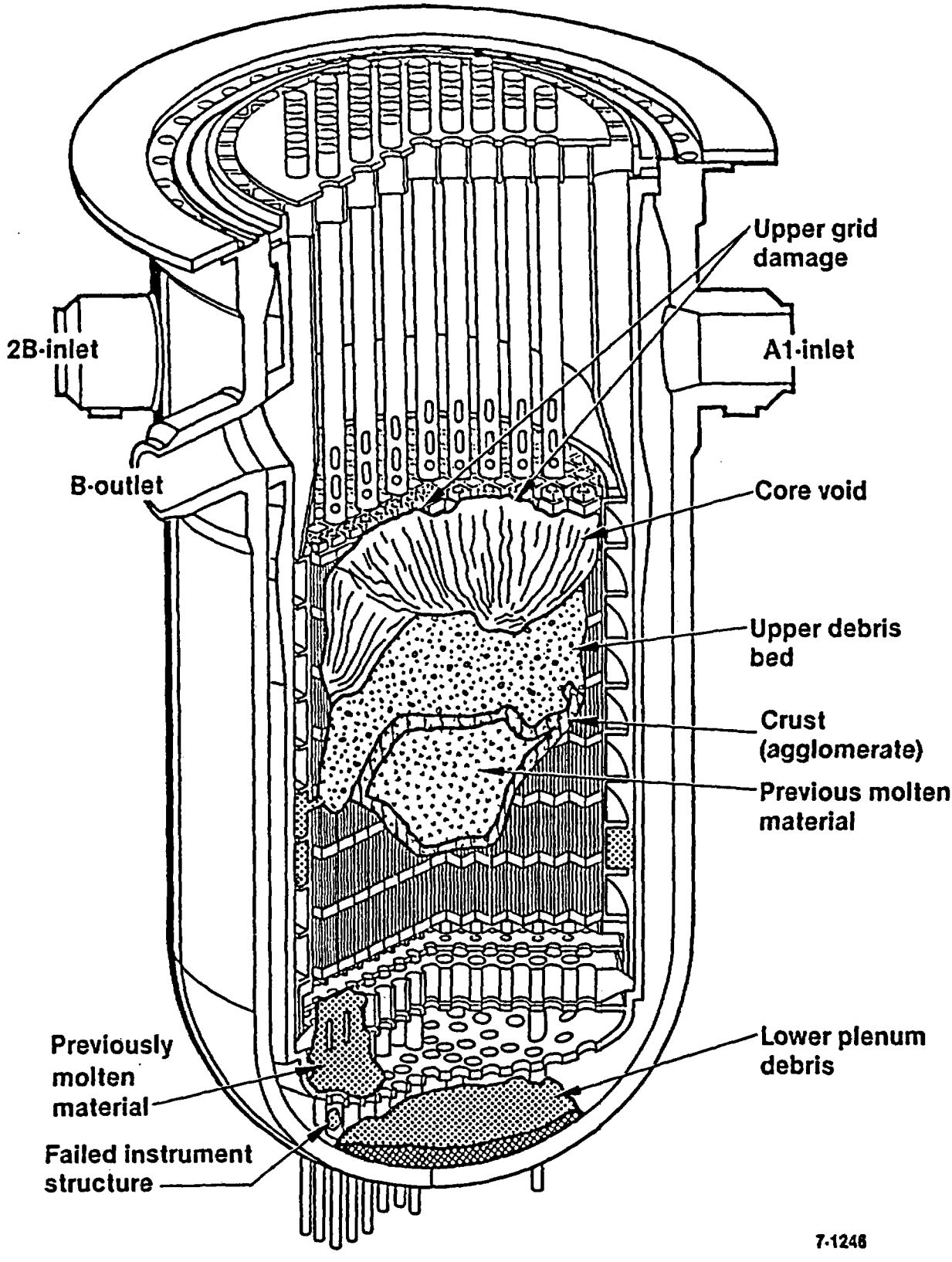

Figure 1. End state condition of the TMI-2 reactor core.

core boring operations were performed during July and August 1986 and the bores acquired were transported to the Idaho National Engineering Laboratory(INEL) for sectioning and distribution of the samples to laboratories participating in the core bore examinations. The initial results of the examinations performed at the INEL are the subject of this paper.

The core bores extracted from the lower core region were obtained from nine pre-selected locations. These core locations were chosen to spatially characterize the current chemical and physical state of the reactor core and to define the distribution of core structural materials within the lower reactor vessel. The samples produced from the coring operation in the reactor vessel were discontinuous bores of fuel material which were approximately 2 m long and 6.4 cm in diameter. Only small amounts of material (i.e., a few grams) were obtained from the lower reactor vessel head cores due to the small particle size of much of the debris located there.

Following the delivery of the cores to the INEL, a series of physical, metallurgical, and radiochemical measurements were begun on specimens from the core bores. The physical measurements which were performed to characterize the general physical characteristics of the debris, include dry weight, immersion density, open porosity, and radiation levels. Metallurgical examinations were performed to characterize the full range of metallurgical properties of the debris (e. g., grain size, composition, oxygen content, etc.) using optical metallography and scanning electron microscopy with energy dispersive x-ray (EDX) analysis and wavelength dispersive x-ray (WDX) analysis. The radiochemical measurements are being performed to determine the chemical composition of the debris and to define the extent of radionuclide retention in the debris. Measurement techniques being used include gamma spectroscopy, neutron activation analysis, liquid scintillation analysis, and mass spectrometry. Results included in this paper are from the visual examinations, the gamma spectrometry analyses performed on the intact core bores and some of the metallurgical analyses. (Not all examinations were complete at the time this paper was prepared.)

VISUAL APPEARANCE AND DENSITY MEASUREMENTS

During the core boring operation, video inspections of the interior of each core bore hole were performed to characterize the lower core and the region immediately below the bottom of the core (the core support assembly region)[3]. These videos indicated that the core below the upper debris bed consisted of two regions: (a) a region of previously molten core materials surrounded by a hard crust, and (b) a region of intact standing fuel rods extending from the bottom of the previously molten region to the bottom of the core.

When the core bores were removed from their split tubes, visual examinations indicated that they contained solid plugs of the upper and lower crusts, previously molten material from between the crusts, and fuel rod stubs (Figure 2). The solid plugs from the upper and lower crusts were generally composed of agglomerated fuel and structural material components.

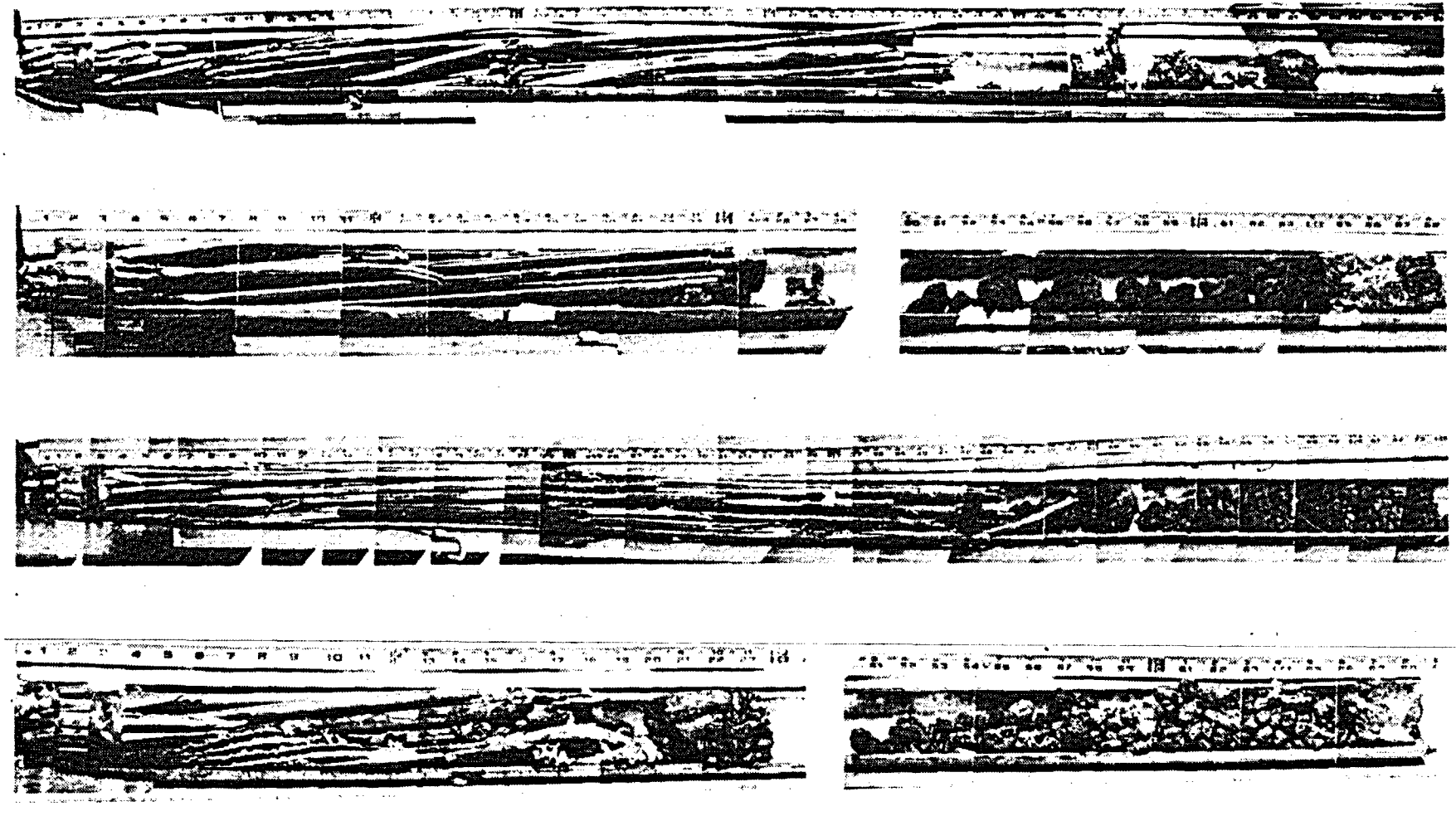

Figure 2. Principle core bore samples--core locations D8, G8, G12, and G9 from the top.

The upper crust samples were composed of a mixture of debris agglomerated with substantial amounts of metallic material, while the lower crust samples were fuel rods surrounded by previously molten material with a different composition than the upper crust. The solid plugs were 6.4 cm in diameter (the size of the core bore) and ranged from 5 to 11.5 cm in length.

The previously molten region between the crusts appeared to be relatively homogeneous and was easily friable. However, the amount of material present between the crust layers was less than the amount expected based on the video inspections of the core holes. The presumed cause of the less than expected quantities of material was that the friable material fragmented and about 80% was flushed out during the core boring operation by the cooling water. The remaining 20% was characterized as "rocks" (large particles of debris) of various sizes. There were some 100 rocks larger than 2.5 cm in diameter present in the core bores.

The fuel rod stubs located in the lower portion of the core bores ranged from 76 cm to 122 cm in length. Shorter stubs were located near the center of the core and longer ones near the periphery. Initial examinations of these rods suggest that the bottom portion of the rods probably remained covered with water during the accident.

The initial examinations performed on the core bore samples included weighing all samples and performing immersion density and open porosity measurements on the eight large plugs of crust material, and 35 of the 100 rock samples. The densities for the 44 samples ranged from 5.44 g/cm^3 to 9.74 g/cm^3 and the open porosity varied from 5.5 to 19%. The densities measured are from 6.5% to 48% less than the density of intact fuel material (10.4 g/cm^3) which suggests that little intact fuel material material is present in the core bore samples. The lower densities are a result of several factors including porosity and the presence of less dense oxidized zirconium and structural materials. The samples with the lowest density were mostly metallic and quite porous, while the samples with the highest density were generally agglomerates of fractured fuel pellets surrounded by previously molten materials.

GAMMA SPECTROSCOPY EXAMINATION OF THE INTACT CORE BORES

This section presents the results of the high resolution gamma ray spectroscopy measurements that were performed on the nine core bores. Initially each core bore was scanned over the entire length to determine the gross gamma ray intensity as a function of position along the axial centerline of each bore. Following the gross gamma analyses, isotopic measurements were performed at intervals of 2.5 cm over the length of each core bore and at additional locations of high activity as indicated by the gross gamma radiation surveys.

Examination of the results of the gross and isotopic surveys of the core bores allow several observations to be made concerning fission product behavior in the lower reactor core:

- The gamma spectroscopy data suggest that the upper and lower crust regions contain significant concentrations (10^1 -10^2 greater than expected) of ^{60}Co, ^{106}Ru, and ^{125}Sb. These radionuclides would be expected to remain as metallic materials and the metallurgical data indicate that they may have segregated and been retained with other metallic components of the core.

- The prior molten material between the crust layers appears to have very low concentrations of the more volatile radionuclides such as ^{137}Cs but has retained significant amounts of the refractory radionuclides (e.g., ^{144}Ce and ^{154}Eu).

- The intact fuel rod sections in the lower core appear to have retained their entire inventories of fission products including the high volatiles (e.g., ^{137}Cs).

METALLURGICAL EXAMINATION RESULTS

Following the initial nondestructive examinations performed on the core bore samples, samples were selected for metallurgical examinations based on appearance, density, and radionuclide content. Samples were obtained from the crust material, the previously molten material from between the crusts, the intact fuel rods, and intact structural components such as control rods, guide tubes, and burnable poison rods. The largest plug samples were sectioned and sampled both transversely and longitudinally to evaluate radial and axial differences in structure and composition. The rock samples were sectioned into either halves or thirds, depending on the size of the particles, to provide samples of the interiors for both metallurgical and radiochemical examinations. For each sample mounted for optical examination, adjacent samples were obtained for radiochemical analyses to allow comparison of the metallurgical results with the corresponding radiochemical composition of the material. The examination results discussed in this paper are from representative samples of the upper, lower, and peripheral crusts, the mixed ceramic and metallic material present in the region between the crusts, and the fuel rod stubs.

Lower Crust

Samples of the lower crust material were obtained at several core bore locations. Figure 3 shows a cross section and the autoradiograph of a representative plug of the lower crust taken from near the center of the core (core location K9). The measured density of this crust sample was 7.2 g/cm^3. The cross section shows the remains of two fuel stack columns surrounded by previously molten material. Molten material apparently flowed down the coolant channels, dissolved the zircaloy cladding, and flowed into the pellet/pellet interfaces and cracks in the pellets.

Several areas of this cross section were examined using optical metallography and back scattered electron (BSE) image analysis. Figure 4 shows an enlarged view of the previously molten material found in the coolant

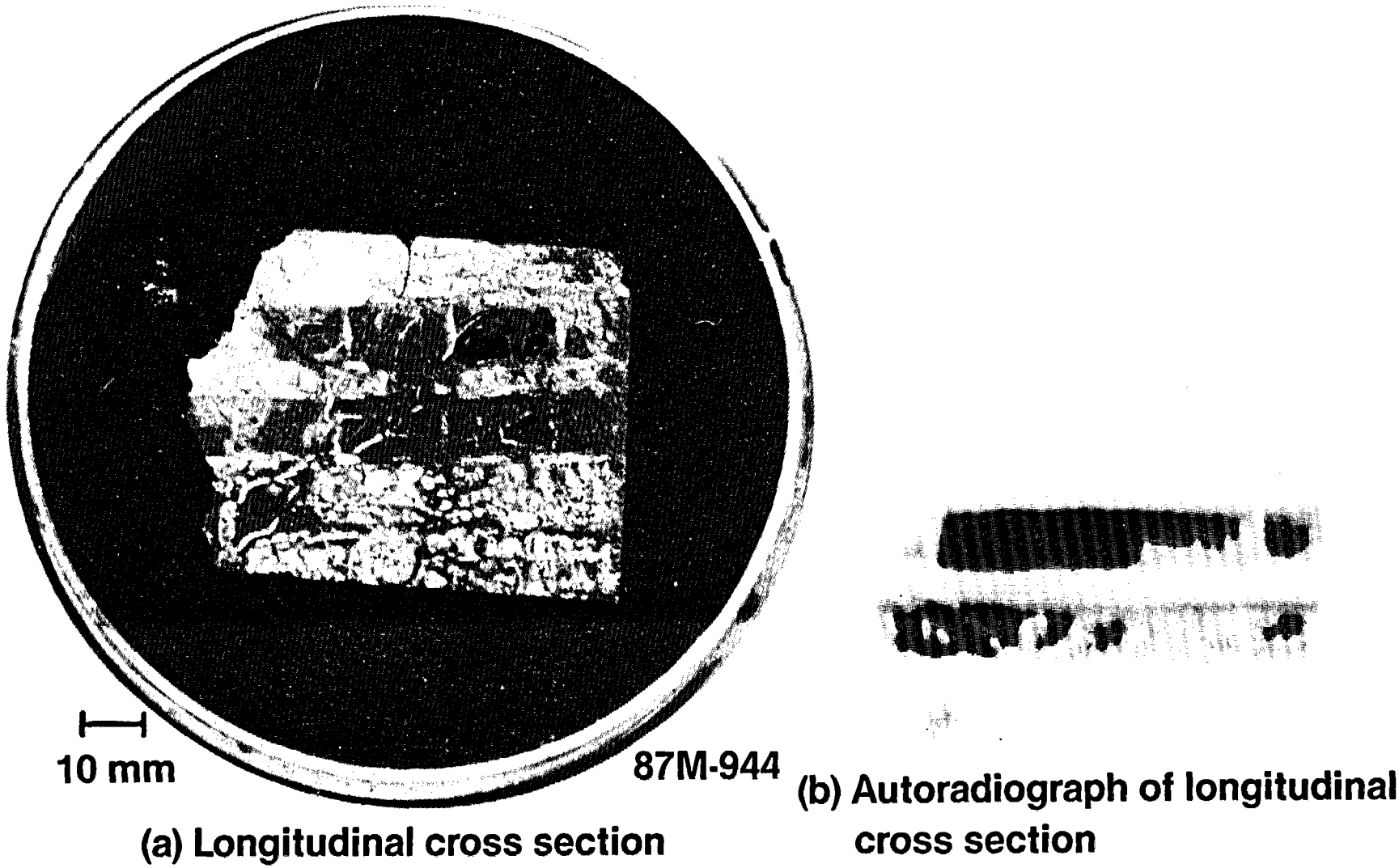

Figure 3. Core location K9--lower crust.

Figure 4. Enlarged view of molten material in the coolant channel.

channels. This material was composed of a mixture of metallic structural and control rod components with relatively small (100 - 200 micron) UO_2 inclusions. Two metallic phases were present as determined from the BSE analysis. The principal phase consisted of zirconium, iron, nickel, and chromium and the secondary phase contained an alloy of silver and indium.

Figure 5 shows an enlarged view of the area at a pellet/pellet interface which is typical of the interfaces in this sample. Figure 6 shows the BSE images for this pellet/pellet interface and the BSE dot maps for U, Zr, and Fe. This figure typifies the method used to identify the composition of the various phases present in a sample. The BSE image represents a composite average of the atomic number of the elements in a particular phase where the degree of brightness is proportional to the atomic number of the element (e.g., the high atomic number uranium is brighter than the lower atomic number iron) and the individual dot maps represent specific elements where the element of interest is brighter than the other elements present in the sample. The uranium and zirconium dot maps in Figure 6 show the presence of a UO_2 pellet above a region in the pellet/pellet interface which contains mostly zirconium with small amounts of uranium.

Other metallic phases are also present in the channel as indicated by the Fe dot map which indicates the interaction of zircaloy with structural and control materials. Several metallic phases were observed which were composed of the following groups of elements (Zr, Sn, Ni, Fe), (Zr, Fe, Cr, Ni, U), (Zr, Ni, In, U), and (Ag, In). Cadmium, a component of the Ag-In-Cd control rods, was found with the Ag and In phases; however, it was present in relatively small amounts. This is probably due to the relatively high volatility of this element (B.p. - 940 K). Also, when Zr was alloyed with In, Fe and Cr were not present. The mechanism resulting in this behavior is not currently understood.

The metallographic examination of the lower vessel plug samples suggest that an interaction occurred between the fuel rods and the structural components (i.e., Fe, Cr, etc.) which resulted in the dissolution of the zircaloy cladding and fuel by the molten structural materials. This interaction would result in a lowering of the melting temperature of the material. Based upon the eutectic temperatures of the binary phases of zirconium with Fe, Ni, or Cr, a minimum possible peak temperature is estimated to be about 1400 K and because there was not an interaction with the unmelted UO_2 fragments, a maximum peak temperature of 2200 K is suggested.

In addition to the metallographic examination of the lower crust autoradiography was performed to evaluate the gross distribution of fission products in the crust. This examination indicated that the fission products in the lower crust were retained within the fuel material and that little activity was present in the metallic debris in the coolant channels.

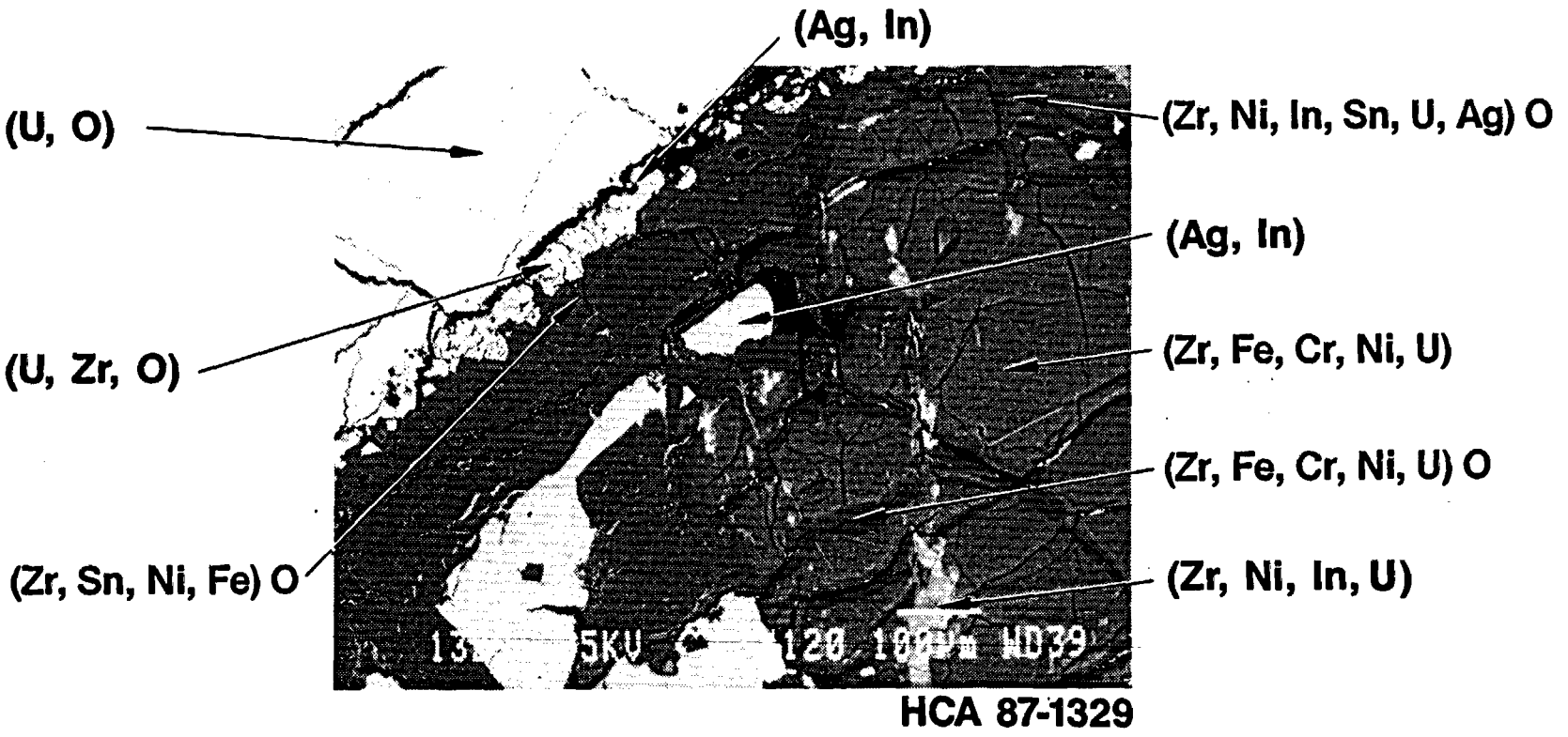

Figure 5. Enlarged view of the pellet/pellet interface.

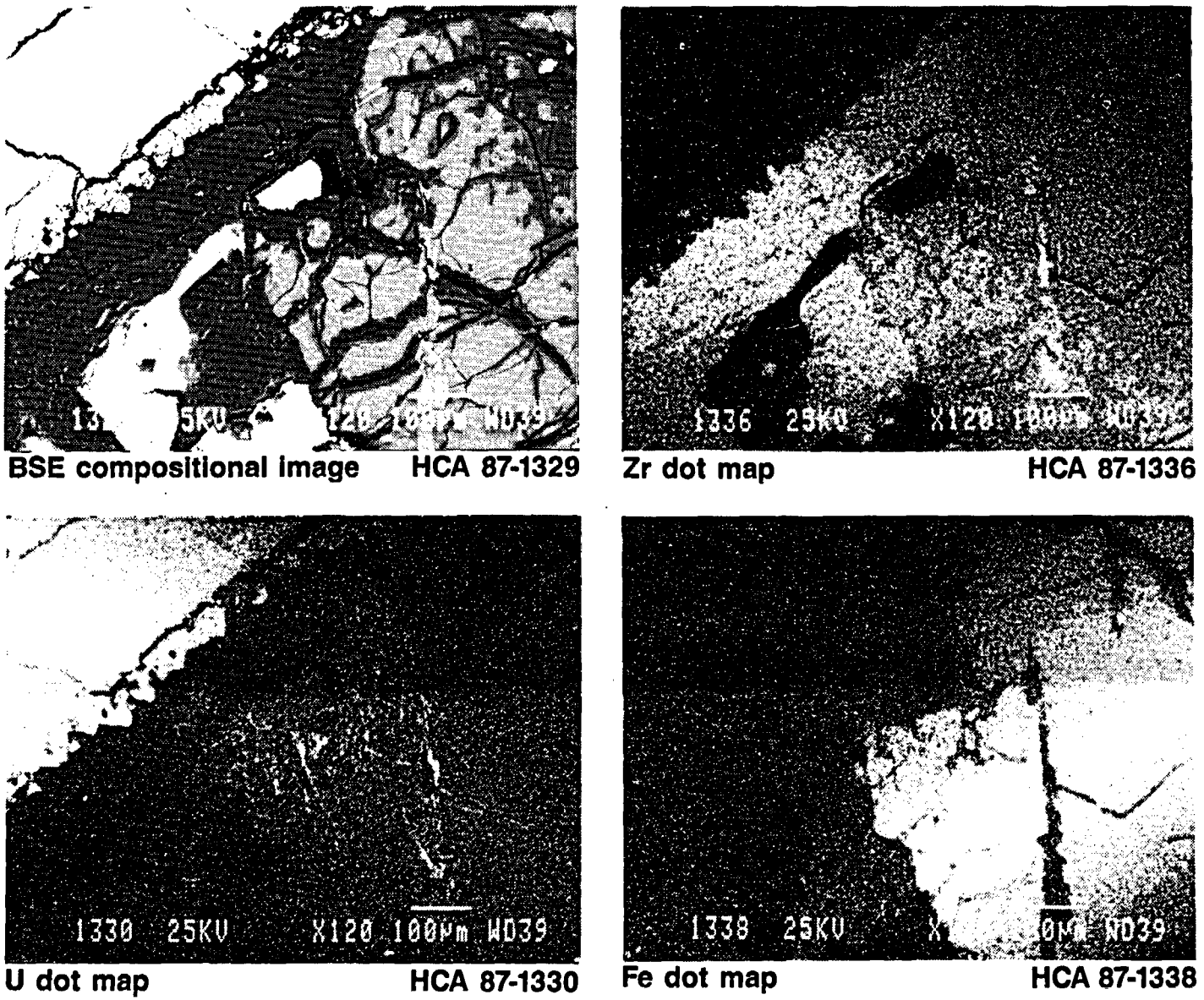

Figure 6. Pellet interface--BSE image and dot maps.

Upper Crust Plug

Figure 7 shows a representative cross section of upper crust material obtained from core bore K9 about 1 meter above the sample discussed in the previous section (Figure 3). The bulk density of this plug section was 7.9 gm/cm^3. Two general types of phases were observed in the upper crust, a ceramic phase containing mostly fuel material components and a metallic phase containing mostly structural components. The composition of the ceramic phase indicated that the interaction between fuel rods and structural/control rod materials was substantially greater than that observed in the lower crust samples. No intact fuel material was present and most structural materials were present as oxides except those which do not oxidize easily (e.g., Ni, Ag and In). The BSE images indicate that the ceramic phase was a mixture of oxides of uranium and zirconium with an average composition of about 56% U and 21% Zr with small amounts (about 1%) of iron, chromium, and nickel in solid solution. Based upon this composition for the ceramic mixture, the peak temperature of this layer was estimated to be about 2800 K.

The metallic phase found in the upper crust was principally composed of iron and nickel; however, as was indicated for the lower crust, a second metallic phase was observed which was principally composed of metallic silver and indium. Unlike the lower crust, however, the upper crust did not contain measurable amounts of Cd, which suggests that the greater degree of materials interaction in this crust allowed most of the relatively volatile Cd to be released.

In contrast to the fission product behavior observed in the lower crust, the autoradiograph of the sample cross section from the upper crust indicated higher concentrations of fission products in the metallic phases rather than in the ceramic phases. The probable identities of the fission products in the metallic crust (i.e., Sb-125 and Ru-106) were indicated by the gamma spectroscopy measurements discussed previously. These radionuclides are expected to be retained as metallic materials in the debris rather than as oxides because of high free energy requirements for oxidation. Other examinations indicate that these fission products are associated with metallic components of the TMI-2 debris[4]. The ceramic phase of the debris is probably depleted in fission products (e.g., Cs-137) which have relatively high volatilities and were released from the ceramic phases during the high temperature portion of the accident.

Peripheral Crust

The peripheral crust is that region of the upper crust that is near the mid-radius of the core. Densities in this part of the crust range from 8-10 g/cm^3 and are generally higher than those observed near the center of the core. A representative cross section from the peripheral crust (core location G8) is shown in Figure 8. Examinations of this cross section and others from the peripheral crust indicate that the materials behavior in this part of the core is different than that observed in the upper and lower crust regions. The presence of substantial amounts of metallic structural components (i.e., Fe, Ni, Ag, and In) is indicated. In Figure 8, the light

Figure 7. Core location K9--upper crust.

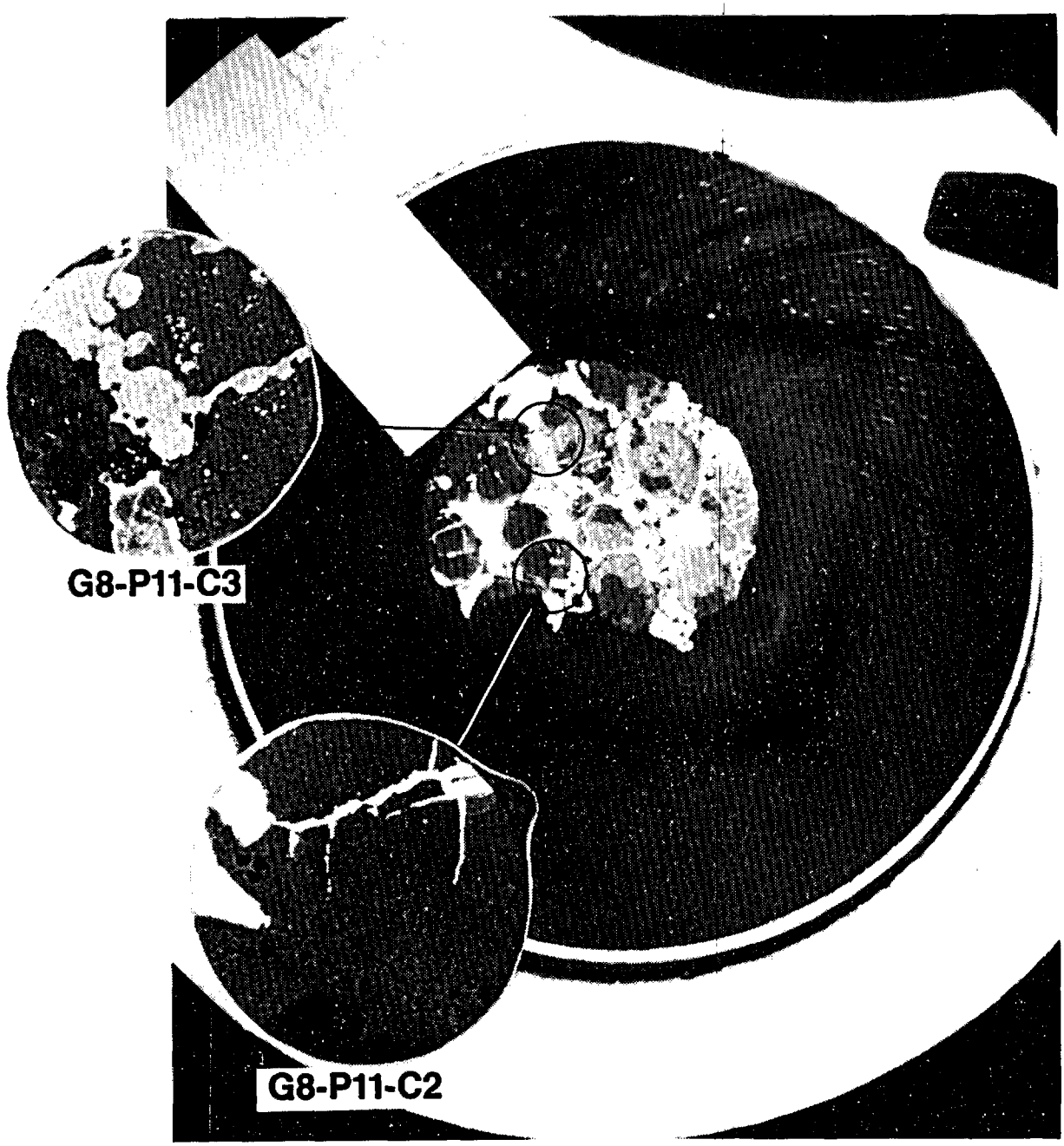

Figure 8. Core location G8--peripheral crust.

areas shown in the enlarged section of G8-P11-C3 are a silver-indium alloy which appears to have flowed into cracks in the ceramic material. Adjacent to this inclusion is a secondary phase containing iron and nickel with a small amount of chromium. The presence of unmelted fuel in the surrounding material suggests that unmelted fuel from the upper debris bed may have slumped into the molten metallics.

A second cross section from the peripheral crust at core location G12 (Figure 9) shows intact fuel pellet remnants encased in a ceramic matrix of mixed oxides of uranium and zirconium. This figure shows an apparent interaction at the fuel pellet/ceramic interface which has resulted in the formation of large (1-4 mm) voids throughout the fuel pellets. This behavior may have been caused by the collapse of relatively intact fuel pellets from the upper debris bed into molten material which then heated the relatively intact material to high temperatures. The actual cause of the porosity is not known.

Autoradiographs of the peripheral plug cross sections were taken. These data indicate the presence of significant accumulations of activity in the metallic phases, similar to the behavior observed in the upper crust samples.

Core Interior Particles

Metallographic examinations were performed on 26 "rock-like" particles from the previously molten material region between the crust layers. The rock samples examined were greater than 25 mm in diameter and were selected based on density, and surface appearance. Although individual particles were relatively homogeneous, the metallographic examinations indicated a diversity of structure and composition between particles. The bulk of the samples examined were determined to be mixtures of both metallic and ceramic phases, however, examples of entirely ceramic and metallic particles were also present. Examples of each of the material types are discussed in this section.

A BSE image of an entirely ceramic particle (K9-P3-F) is shown in Figure 10. Examination of this particle indicated that this was a relatively homogeneous ceramic rock with a number of low atomic number inclusions present. An area at an interface between the light and dark areas was examined using dot maps to evaluate the composition of these phases. The light phases in the examination area were determined to be mixtures of uranium and zirconium and the dark (lower atomic number) regions were determined to be mixtures of iron, chromium, aluminum, and nickel oxides. The presence of nickel oxide in the sample suggests that this sample was subjected to very oxidizing conditions as nickel has a very high oxidation potential and would not be expected to be oxidized by steam oxidation only. Particles of this type resemble rock-like particles of previously molten material obtained from the lower reactor vessel head which contained oxides of uranium and zirconium in the matrix and iron and chromium oxide eutectic mixtures in the grain boundaries[4].

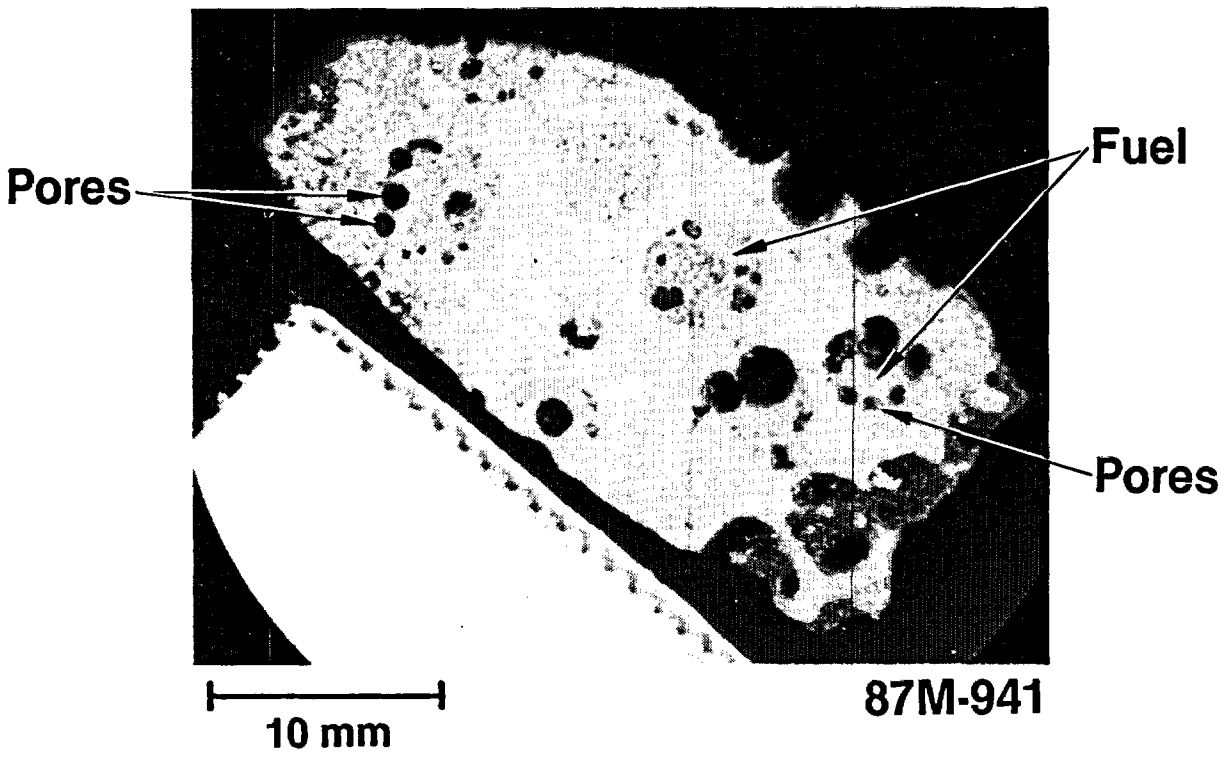

Figure 9. Voids produced in fuel pellets in the peripheral crust.

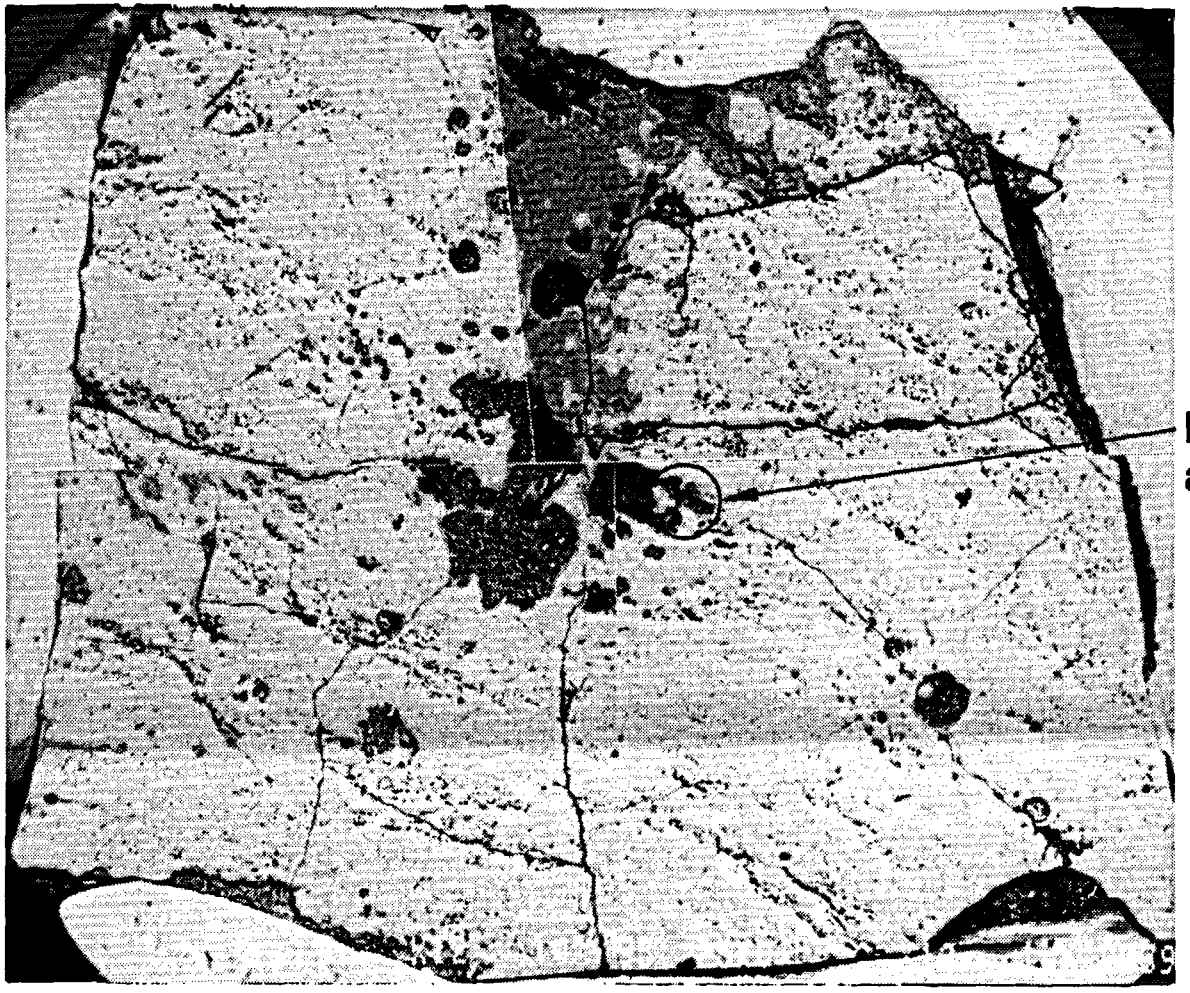

Figure 10. Core location K9--ceramic particle (BSE image).

Figure 11 shows an entirely metallic sample which was obtained from fuel assembly location 09 near the periphery of the core. The metallic matrix of this sample consisted of a nearly dendritic structure of 59% iron, 25% nickel, and 14% chromium with circular inclusions containing silver, indium, and tin (72% Ag, 15% In, and 9% tin). Although some of these Ag-In-Sn inclusions contained voids, many contained a spherical particle of chromium oxide (Cr_2O_3).

A cross section of a particle (core location G12) which contained a ceramic matrix with extensive metallic inclusions is shown in Figure 12. One of these inclusions was examined by SEM to evaluate elemental composition. The BSE image and several associated dot maps are shown in Figure 13. These data indicate that a large degree of segregation of individual elements took place in this sample. The ceramic matrix of the sample is a mixture of the oxides of uranium and zirconium and, at the periphery of the void containing the inclusion, is a layer of iron oxide which contains some oxidized nickel. In the metallic inclusion, there is substantial segregation of the elements. At the bottom of the inclusion relatively pure silver is found with little contamination from other metallic elements (i.e., indium and cadmium). Above this layer, near the particle midpoint, is a nickel-tin layer followed by a zone containing nickel with nickel-tin inclusions. Also in the nickel region, concentrations of the fission product ruthenium were found as a metallic. These data suggest that this fission product, which has a high free energy requirement for oxidation, is released from the fuel and is retained by metallic structures in the core. The materials behavior responsible for the observed structures has not been well defined and additional information will be required to understand this behavior.

The most common fission product measurable in the metallic inclusions of this rock sample was ruthenium; however, technetium, a fission product not found in nature was also measurable. Also, palladium and tellurium, other probable fission products, were measured in association with metallic constituents (i.e., Ag, In, and Fe). These data suggest that the metallic constituents of the core retain fission products with varying chemical characteristics and volatilities that have been released from the fuel material.

A beta/gamma autoradiograph of several different particles is shown in Figure 14. Because the radiograph was performed on all samples with only one exposure time, the intensity of the radiographs may be used as an indicator of the relative activity among the particles. The ceramic particle (G8-P6-B) has the lowest activity which is about the same as the ceramic phase of the mixed ceramic/metallic particle (G8-P10-A). The metallic particle and the fuel remnant surrounded with metallics also have about the same activity as the metallic phase in G8-P10-A. These data again indicate significant release or depletion of the activity in the ceramic phases and suggest similar retentions for all ceramic or metallic components.

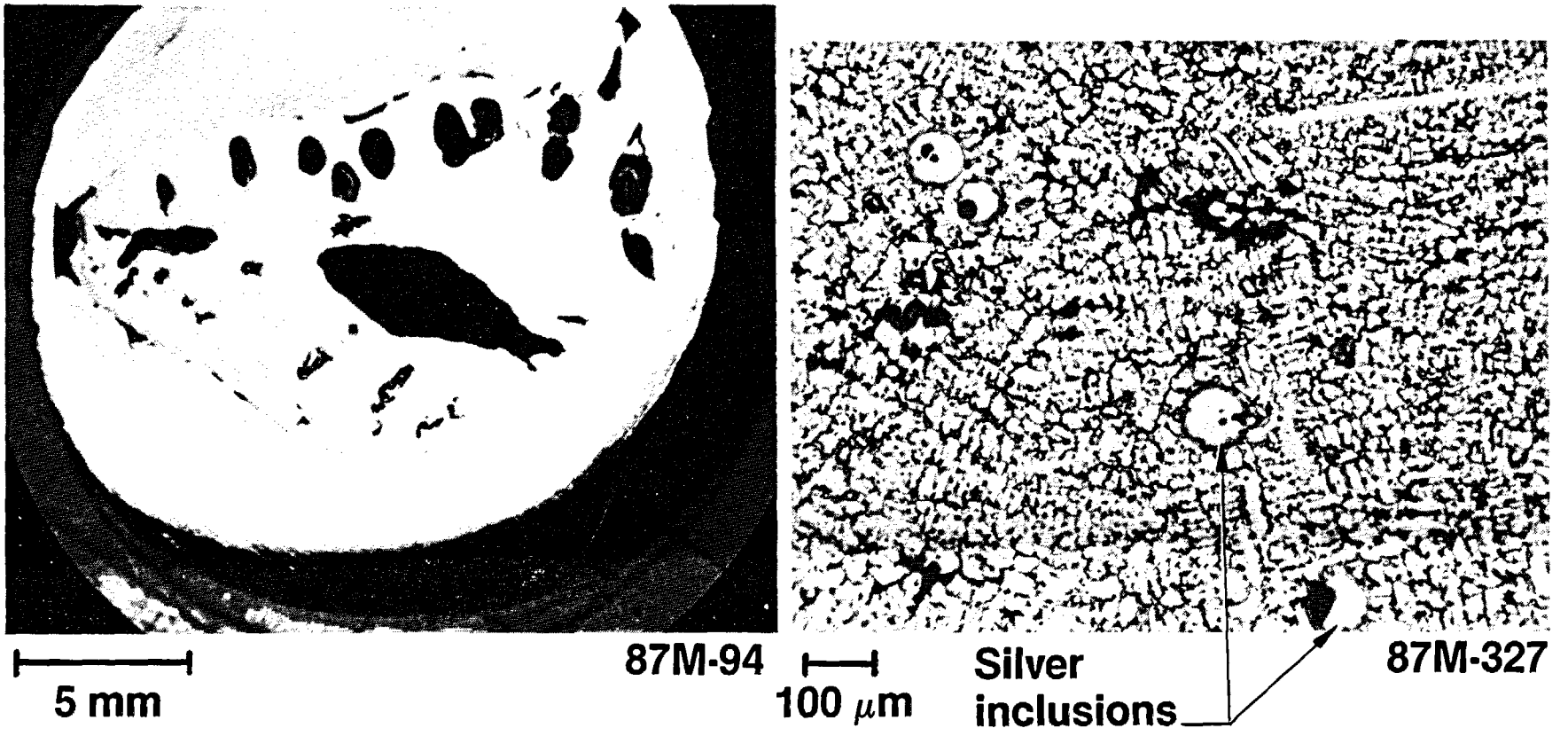

Figure 11. Core location 09--metallic particle.

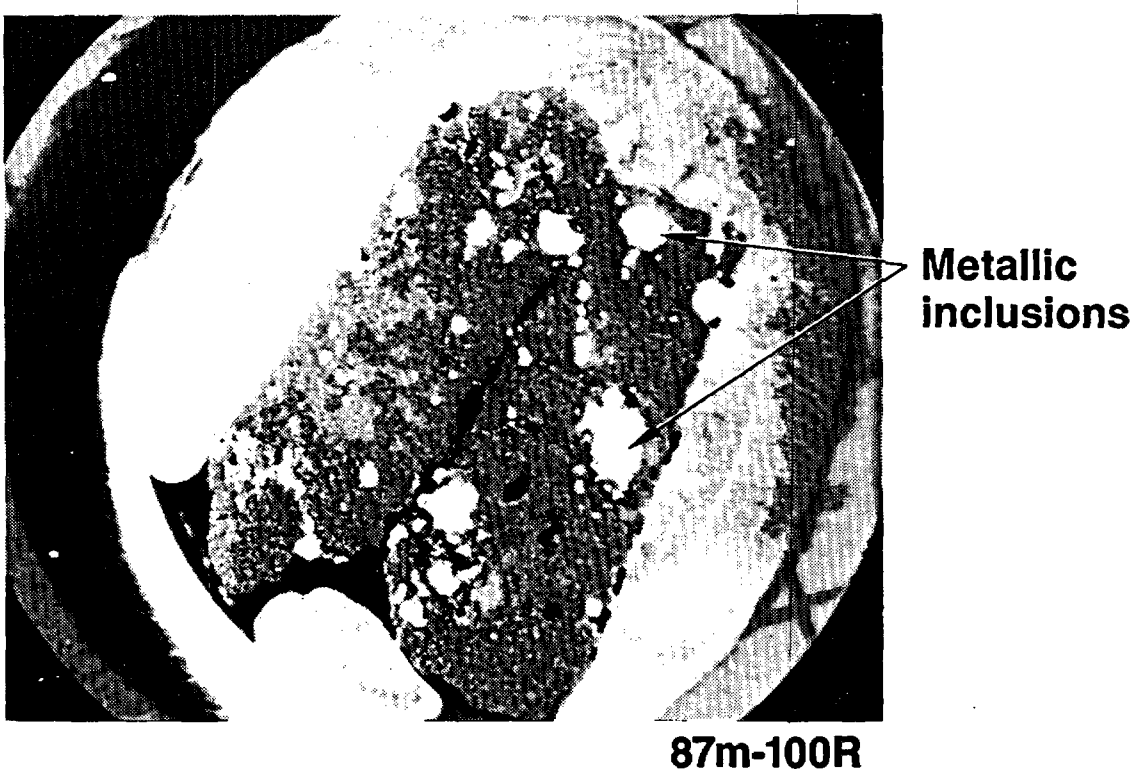

Figure 12. Ceramic particle with metallic inclusions (core location G12).

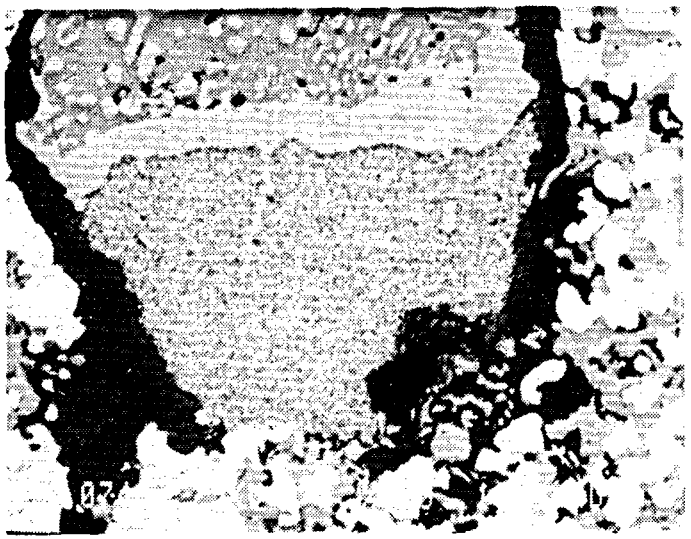

BSE compositional image HCA 87-742

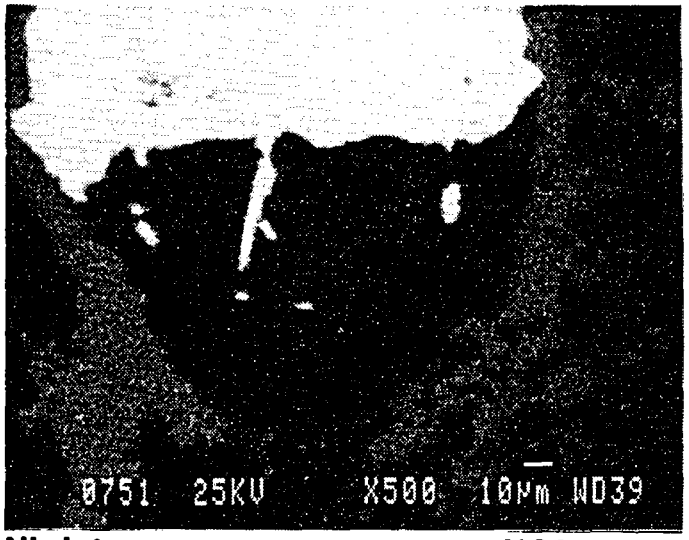

Ni dot map HCA 87-751

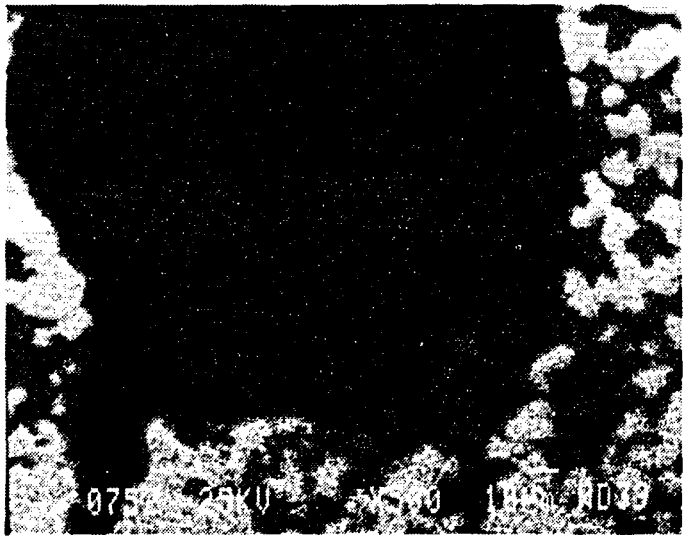

U dot map HCA 87-752

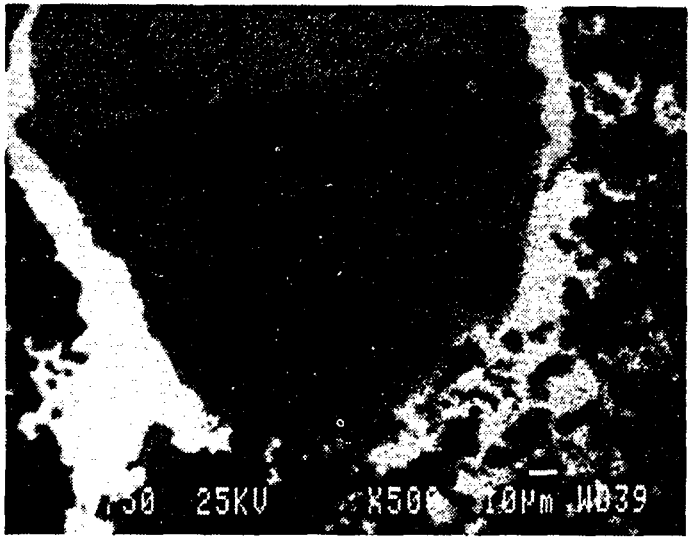

Fe dot map HCA 87-750

Figure 13. Enlarged metallic inclusion from core location G12 (BSE image and dot maps).

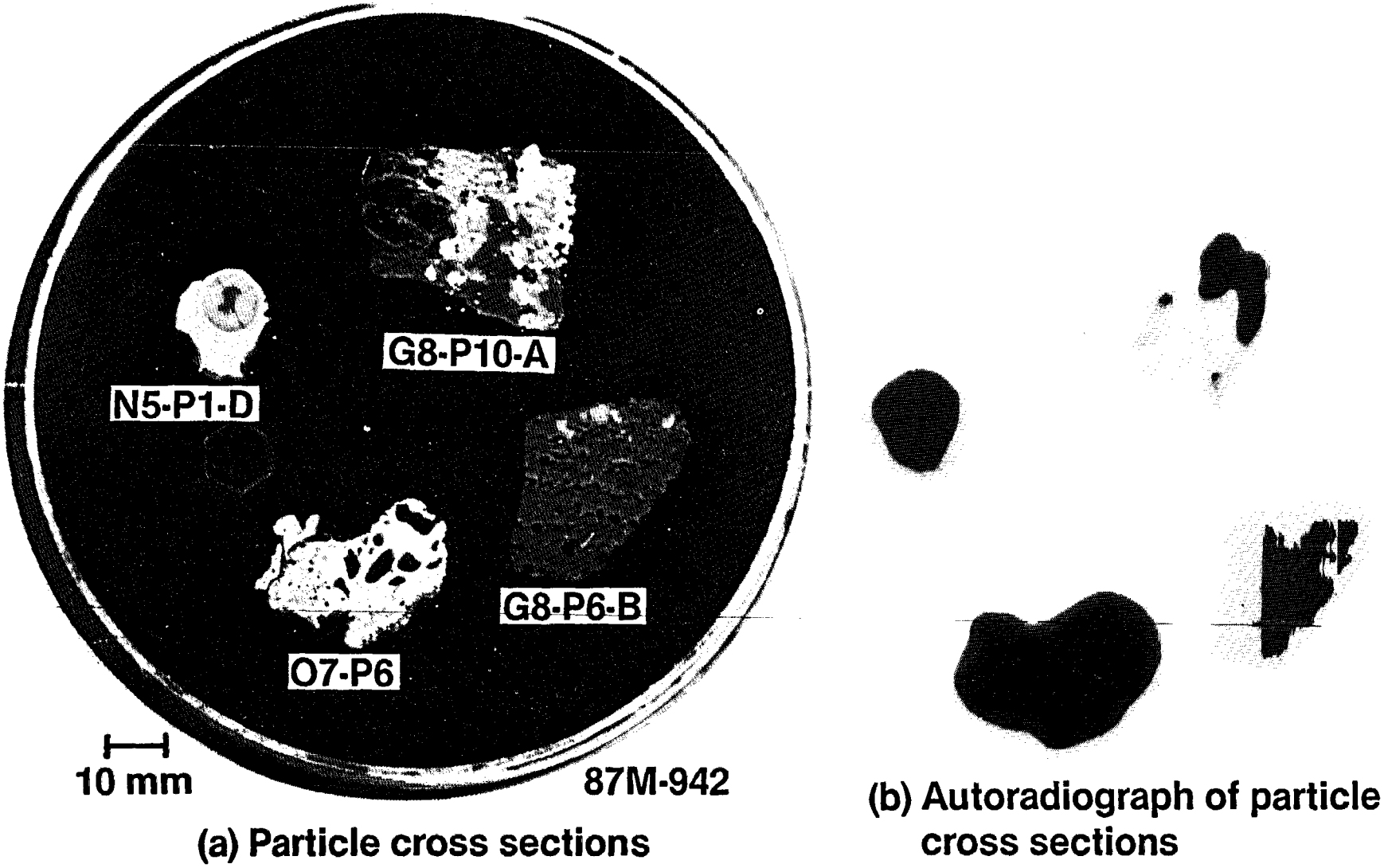

Figure 14. Core locations N5, G8, and O7--particle cross sections and autoradiographs.

Fuel rods and guide tubes

Fuel rods, and guide tubes from the lower portion of the reactor core were examined to evaluate the effects of the accident on the intact rods or tubes. Visual examination of the rods indicated that the rods were generally intact, however, the metallurgical examination indicated that hydriding of the fuel rod and guide tubes had occurred. The hydrides were orientated in the radial direction, which is typical for the cold-work texture of the cladding. Examinations performed on fuel rods at the INEL and at Argonne National Laboratory[5] indicate that the cladding temperature reached temperatures up to 1100 K.

Although no previously molten debris was present between the intact fuel and control rods in the core bores, previously molten material was found in an instrument tube in Assembly G8. The molten material which had apparently flowed down into the zircaloy tube and interacted with the interior surface of the tube was composed mostly of zirconium with some iron and nickel. It also contained relatively small quantities of silver, indium and cadmium from the control rods.

SUMMARY

A summary of the observations and conclusions that have been made from the core bore examinations are listed below. The core bore examination program is not complete and additional information will be provided in the final examination report.

- The lower crust was formed by freezing of relocated molten cladding, structural, and control materials into the fuel assembly coolant channels. Peak temperature of this crust was probably between 1400 K and 2200 K.

- The upper crust is a mixture of previously molten ceramics, metallics, and solid fuel pieces with an estimated maximum temperature of 2800 K.

- The metallic structures in the upper crust are composed primarily of structural (Fe, Cr, and Ni) and control materials (Ag, In, and Cd).

- A range of densities were found in the upper, lower and peripheral crust samples with the higher densities found in the peripheral crust probably due the lower porosity and greater proportion of higher density metallics (e.g., Ag).

- Fission product ruthenium and antimony were retained in the metallic phases of the upper crust and core rocks (mixed ceramic and metallic particles).

- o In the previously molten material region, cesium is at substantially lower concentrations than would be expected for intact fuel material.

- o The radionuclide inventory of the intact fuel rods, including the more volatile radionuclides (e.g., Cs-137) appears to be intact.

- o Cadmium was not detected in the upper crust of the central core region; however, small quantities of Cd were detected in the lower crust.

- o A zircaloy instrument tube at the G8 core location provided a pathway where prior molten fuel flowed down into the tube and interacted with the zircaloy of the tube.

- o Particles of prior molten fuel from the central core region had a wide variety of compositions. Most were a mixture of ceramic and metallic components; however, some were entirely metallic or ceramic.

REFERENCES

1. M. L. Russell et al., TMI-2 Accident Evaluation Program Sample Acquisition and Examination Plan for FY 1987 and Beyond, EGG-TMI-7521,February 1987.

2. D. W. Akers et. al., TMI-2 Core Debris Grab Samples--Examination and Analysis, GEND-075, September 1986.

3. E. L. Tolman et. al., TMI-2 Core Bore Acquisition Summary Report, EGG-TMI-7385, Rev. 1, February 1987.

4. C. S. Olsen et. al., Examination of Debris from the Lower Reactor Head of the TMI-2 Reactor (Draft), EGG-TMI-7573, April 1987.

5. L. A. Neimark et. al., Examination of TMI-2 Core Bore Samples, 15th Water Reactor Safety Research Meeting, October 26-30, 1987 (to be published).

The Microstructural and Microchemical Characterization of Samples from the TMI-2 Core

L. A. Neimark, R. V. Strain, J. E. Sanecki, and W. D. Jackson
Argonne National Laboratory
Argonne, IL 60439

ABSTRACT

Samples of materials from various regions of the TMI-2 reactor core and vessel have been examined at Argonne National Laboratory with a variety of microanalytical techniques. The purpose of these examinations is to characterize the microstructure and microchemistry of the materials so that their origin could be determined, their fission-product content evaluated, and their role in the accident scenario assessed. Macroscopic and microscopic composition inhomogeneities in melted fuel from different reactor locations indicate different cooling rates and solidification temperatures. The mobility of molten fuel could have been enhanced by a low temperature eutectic in the Fe-Cr-O system. Stainless steel-clad Ag-In-Cd control rods could have failed from a eutectic reaction between the Zircaloy guide tubes and the cladding. Significant concentrations of fission-products were not found, but their release from the fuel did not appear to be enhanced by gas-generated channels along grain boundaries.

INTRODUCTION

The TMI-2 accident presents an opportunity to assess the behavior of reactor materials in synergisms never before possible in integral or separate effects testing. While the complexity of the accident scenario and the resulting multitude of materials interactions make a complete interpretation of the interactions virtually impossible, examination of core materials can shed light on some of the materials-related phenomena that did occur and the environment in which they occurred.

Over the past four years Argonne National Laboratory has examined materials taken from a number of locations in the TMI-2 reactor. These samples included filtrate from the makeup water filters, lead screw segments, grab samples from the upper debris bed, debris from the lower plenum, "rocks" and agglomerates from core bores, fuel rod segments from the core periphery and a core bore, a control rod segment from a core bore, and a poison rod (B_4C/Al_2O_3) segment from a core bore. The objectives of these examinations have been to (1) assess the physical states of the materials with respect to their environment, (2) identify safety-related materials interactions, (3) evaluate fission-product behavior with respect to release/retention mechanisms, and (4) contribute to the data base of materials behavior under severe accident conditions. These objectives generally have been fulfilled in the limited number of specimens that have been examined at ANL. However, this

small number of specimens represents only a selective sampling of the core, and this contribution must be viewed together with the other work being conducted at the Idaho National Engineering Laboratory (INEL) and at foreign laboratories in order to obtain a fuller picture of the events that occurred in the TMI-2 core.

Emphasis in this paper will be placed on the microstructural and microchemical aspects of the specimen examinations. The general aspects of sample acquisition and the macroscopic features of TMI-2 core samples is being described elsewhere [1].

SAMPLE LOCATIONS

The samples described in this paper were recovered from the upper debris bed, the lower plenum debris bed, core bores, and peripheral fuel rods. The upper and lower plenum samples were pebble-size, from a fraction of an inch to 1-1/2 in. maximum dimension. The upper bed specimens came from various elevations at locations E9 and H8 and the lower bed specimens from the periphery of the lower plenum. Core bore samples sent to ANL came from a number of locations and in a number of forms. A fuel rod segment came from the 4-16 in. elevation (from the bottom of the core) from central core position K9. A control rod segment came from the 2-20.5 in. elevation from position N12. What is described as a homogeneous rock sample came from position G8 somewhere from the central core region. An agglomerate sample came from the 65 in. elevation from position D8. An agglomerate sample is one that contains both molten material and identifiable rod components.

EXAMINATION METHODS

The principal examination tools have been optical metallography, scanning electron microscopy in the back-scattered electron image mode (BSE), energy-dispersive X-ray spectroscopy (EDS), electron microprobe analysis (EMP), scanning Auger microprobe analysis (SAM), and beta-gamma autoradiography. Gamma spectroscopy has been used to a limited extent.

Because of the multi-component nature of all the samples, optical metallography had limited utility in differentiating the microstructural characteristics. The SEM/BSE images proved to be extremely valuable in delineating phases and their relative atomic numbers. Furthermore, if the specimen activity was low enough, the composition of the phases could be identified immediately by EDS. For specimens of high activity, the compositions were determined by EMP analysis. The SAM was used primarily to confirm the presence of oxygen, a capability the other instruments did not have. Autoradiography was used to locate areas of high activity in the search for fission products. Gamma spectroscopy was used to qualitatively identify the principal activity peaks in a specimen.

RESULTS

Molten Structures

Molten fuel was found in samples examined from all locations: upper debris bed, lower plenum, the core bore rock, and the core bore agglomerate. The microstructures bore both similarities and disimilarities that reflect on the nature and characteristics of the materials.

The upper and lower debris bed samples consisted principally of equiaxed primary grains of U-Zr-O with minor impurities of Fe, Ni, Cr and Al. The grain boundaries consisted of eutectic phases of Fe, Cr, Al and occassionally Ni. Typical microstructures are shown in Fig. 1. A eutectic composition occurs in the $FeO-Cr_2O_3$ system at about 1350°C and 97 a/o FeO [2]. This is some 1200° lower than the solidus temperatures in the UO_2-ZrO_2 system. Such a mixture would retain its fluidity at temperatures significantly below the solidus of the UO_2-ZrO_2 primary grains. This fluidity would have assisted the "melt" in relocating to the lower plenum.

The composition of the primary U-Zr-O grains in the upper and lower plenum samples was not determined quantitatively because of the lack of appropriate standards. However, differences in the U and Zr contents were discerned by the peak height ratios of the EDS analyses and by the shading contrasts in the BSE images. The indicators showed that the lower plenum samples were not homogeneous on either the macroscopic or microscopic levels. The macroscopic areas of slightly differing U and Zr contents were also characterized by their pore morphology as shown in Fig. 2. Higher U-content areas contained pores with a maximum diameter of ~0.2 mm, while higher Zr-content areas contained pores with diameters greater than ~0.5 mm. This difference is attributed to the lower solidus temperature of the higher Zr-content areas leading to gas mobility in molten fuel over a greater temperature range.

On the microscopic level the primary U-Zr-O grains showed a tendency to transform into U-rich and Zr-rich phases beginning at the grain boundaries and moving into the grains as shown in Fig. 3. This transformation was more advanced in the lower plenum specimens than in those from the upper debris bed. Also, the grain size of the lower plenum specimens was significantly larger than that in the upper debris specimens, ~20μ compared to ~100μ (see Fig. 1). Both the grain size and the degree of transformation indicate that the lower plenum material cooled at a slower rate than the upper debris material.

A dendritic structure of U-Zr-O grains in a matrix of Fe-Cr-O eutectic was found surrounding most of the large pores and in one case a small pore area of the lower plenum specimens. These regions were obviously the last to solidify and they were the only areas where non-oxidized metal inclusions of Ag, Ni, Sn, and the fission products Ru and Te were found in these samples. In general, the amount of Ni found in the upper and lower debris samples was considerably less than would be expected from its content in stainless steel and Inconel and the substantial amounts of Fe and Cr that were found. It was

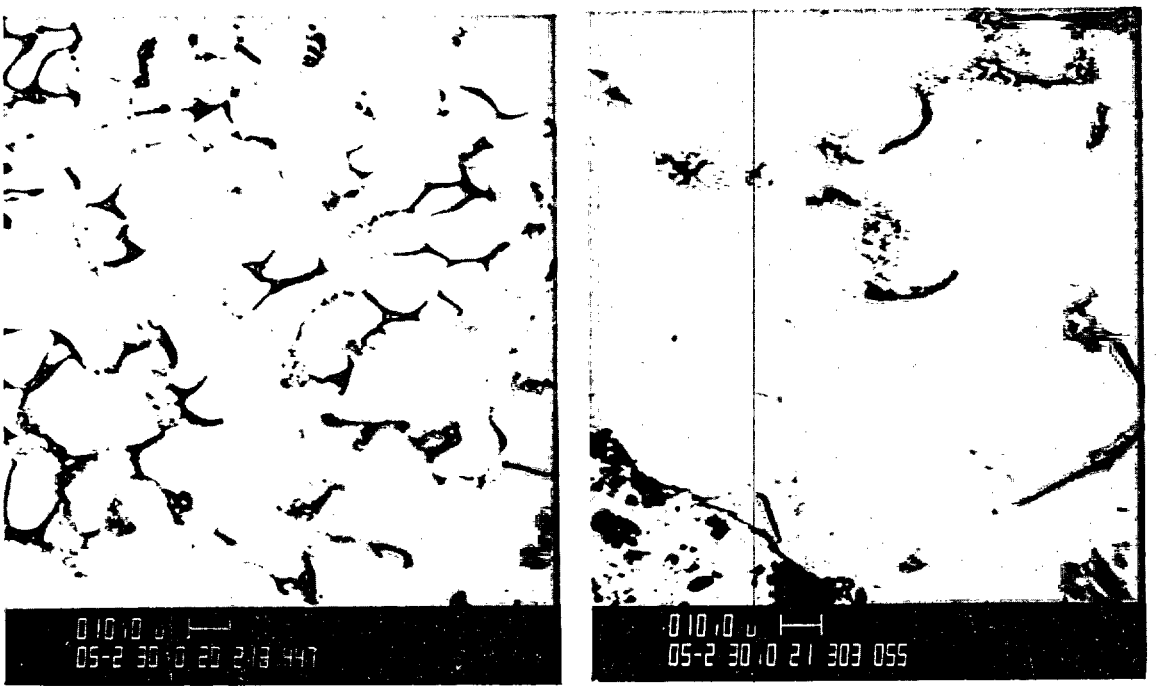

Figure 1. Molten fuel structures (SEM-BSE) from upper debris bed (left) and lower plenum (right). 500X

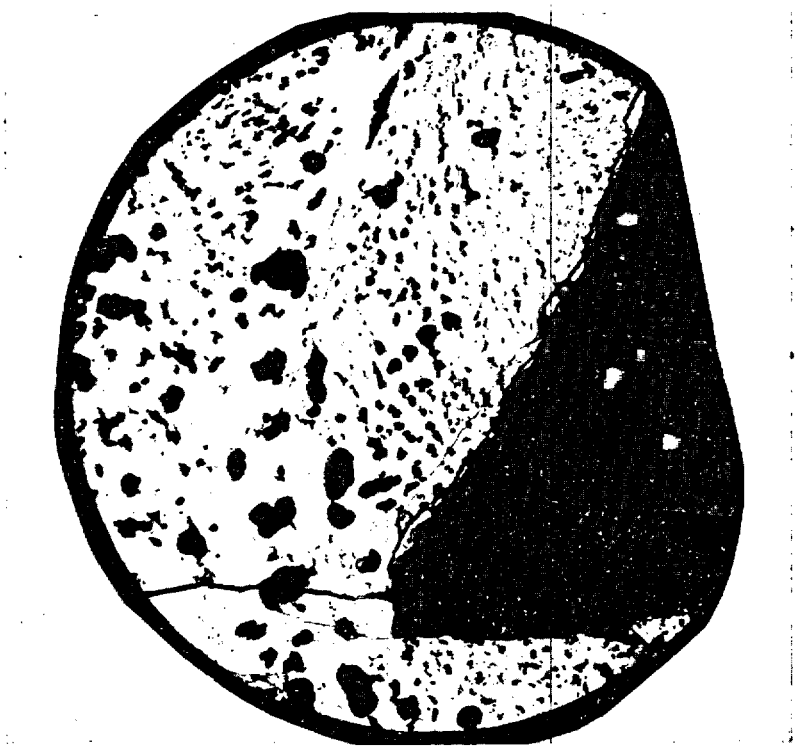

Figure 2. Molten fuel structure of lower plenum debris showing large and small pore regions of somewhat different U and Zr contents. MCT No. 238928A 10X

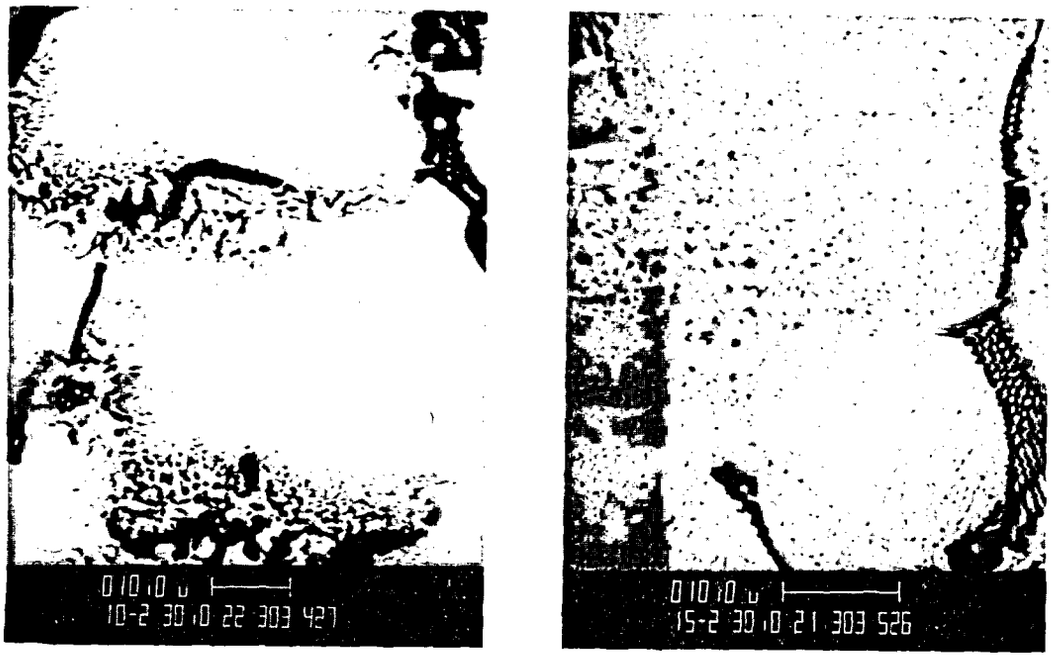

1000X 1500X

Figure 3. SEM-BSE images showing development of U-rich (light) and Zr-rich (gray) phases in structures from lower plenum melt.

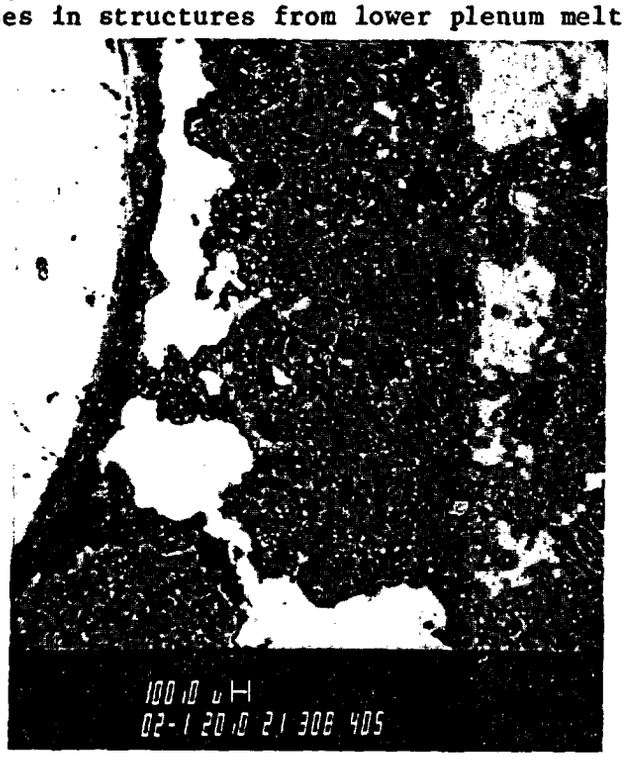

Figure 4. SEM-BSE image of agglomerate structure showing fuel pellet (left), UO_2-Zrc reaction layer, molten Ag-In masses, and dendritic structure of molten structural materials. 15X

concluded that the molten structures of the upper and lower debris beds consist principally of oxidized material with only minor amounts of non-oxidized core materials. These latter elements apparently were fluid at lower temperatures and flowed elsewhere in the reactor structure.

The microstructure of the once-molten core bore rock was homogeneous in its heterogeneity. The structure consisted almost totally of two-phase transformed U-Zr-O grains, 50-100μ diameter pores, and some areas of Fe-Cr-O eutectic. Occasionally, singular metal inclusions of Ag or Ni-Sn were found in the large pores. The most significant differences from the upper and lower debris structures was the larger grains, greater extent of phase transformation, and the absence of the Fe-Cr-O eutectic phase from the grain boundaries of the rock. These differences all indicate a longer time at elevated temperature.

The agglomerate sample that was examined consisted of a fractured UO_2 pellet totally surrounded by a mixture of molten, mainly non-fuel core materials. An area of this structure is shown in Fig. 4. What appears to be cladding in a molten state next to the pellet is actually masses of Ag-In, sans Cd, with some Sn. The thin layer in contact with the fuel is a Zr-UO_2 reaction product. The balance of the molten structure was significantly different from those previously described. The principal grains were dendritic rather than equiaxed and consisted of Fe, Ni, and Cr. The light-colored matrix surrounding the dendrites is made up principally of Ni, Sn, and Zr with lesser amounts of Fe, Cr, U, and In. The amount of Ni in this structure, in excess of its relative amount in stainless steel, constitutes the greatest concentration of Ni found in any of the molten structures examined. It is possible that the high concentration of Ni at this elevation is due to the proximity of a molten Inconel 718 spacer grid. Nonetheless, it would appear that Ni tends to segregate from regions of molten U-Zr-O and concentrates with Sn from the Zircaloy. Because the sample was very high in ^{60}Co activity, EDS analytical data could not be used to identify the phases and the EMP was used instead.

Materials Interactions

The agglomerate sample, described above, exhibited a reaction layer between the UO_2 pellet and the molten Zircaloy cladding. The reaction interaface, shown in Fig. 5, shows a number of different phases indicating the dissolution stages of the reaction. This phase also penetrated the major cracks in the fuel but did not appear to further react with the fuel. Apparently the contact time at the elevated temperatures was short at this elevation.

The fuel rod segment from the central core showed no interaction between the UO_2 and the Zircaloy cladding. The cladding structure clearly showed transformation to the β-phase indicating temperatures on the order of 1000°C. The transformation in the cladding was incomplete around the circumference providing a rather sharp temperature demarcation at about 950°C. The fuel structure in this segment, shown in Fig. 6, was totally fine-grained and contained small metallic inclusions. From SEM-BSE images it was

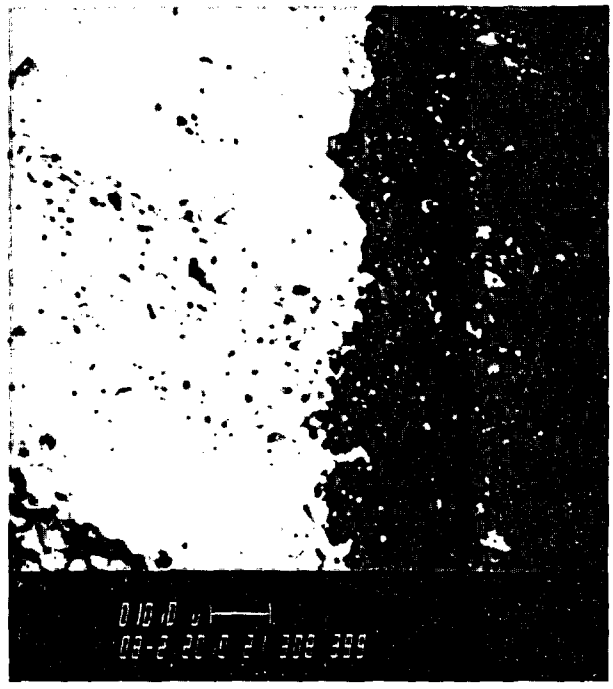

Figure 5. SEM-BSE image of UO_2 pellet (light) and Zircaloy cladding (dark) in agglomerate specimen. Particles of UO_2 are seen in various stages of dissolution in the Zr(O). 800X

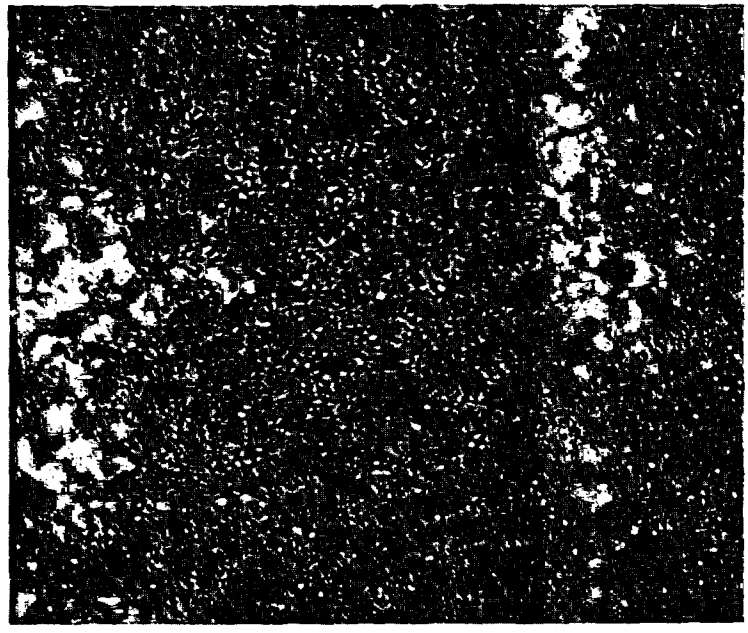

Figure 6. Optical image of etched UO_2 fuel in rod segment from K9. White inclusions are probably non-oxidized Mo.
MCT No. 243861 500X

determined that the inclusions were not free uranium but an element of lower atomic number than UO_2. It is likely that the inclusions are non-oxidized Mo indicating that this particular fuel had an O/M ratio very close to 2.00. (At higher O/M, the Mo would have oxidized and gone into solution with the UO_2. At a lower O/M, free U would have been present.)

The most interesting materials interaction found was between the Zircaloy guide tube and the stainless steel cladding of a Ag-In-Cd control rod. The piece examined, shown in Fig. 7, apparently was at a significant temperature transition boundary. The intact Zircaloy guide tube in the lower part of the segment had transformed to the β-phase (>1000°C) while 0.5 in. above it the Zircaloy formed a eutectic with the stainless steel cladding (935-960°C) as shown in Fig. 8. There was no reaction between the Ag-In-Cd and the stainless steel at either elevation. A molten structure containing Fe, Ni, Cr, Zr, Ag, In, and some Cd was found between the Zircaloy guide tube and the cladding in the lower part of the segment. This material apparently had flowed down from above after the Zr-Fe-Ni eutectics breached the cladding and the Ag-In-Cd had become molten, not necessarily at the same elevation.

Fission-Product Behavior

Based on the qualitative gamma spectroscopy, ^{137}Cs, $^{106}Ru/Rh$, and ^{125}Sb were the only fission products present in detectable quantities, although isolated Ru and Te inclusions were found by EDS. (The principal activity in the samples was ^{60}Co.) Autoradiography indicated that the radioactive species were located principally adjacent to the pores in the molten structures. The finding of Ni inclusions in some of these pores suggests that much of the activity indicated in the autoradiographs is ^{60}Co. However, condensation of Cs-containing species in the pores is possible. (SEM examination of the core bore rock did find small spherical deposits of low atomic number material that could have been vapor-deposited in the pores; an elemental analysis was not possible, however, because of the geometry.)

Both the Ru and Te concentrations were found combined or associated with Ni and Sn in metal inclusions in pores or last-to-freeze dendritic areas. Quantitatively, it is not possible to assess whether such association would significantly retard release of these fission products.

Fractographic examination of one small fuel area in the agglomerate sample, shown in Fig. 9, indicated that there was no significant coalesence of fission-gas bubbles or channel formation on grain boundaries that could have been pathways for fission-product release. Such areas might exist in fuel that was closer to the molten center of the core. However, because of the low fuel burnup and low gas inventory such pathways in what would apparently be a small volume of the core would not be expected to contribute significantly to fission-product release.

CONCLUSIONS

Conclusions drawn from these examinations must obviously be tempered by the meager sampling statistics when generalities are made. However, having

Figure 7. Segment of Ag-In-Cd control rod (top to left) showing remnant of Zircaloy guide tube (right) and surface of reacted stainless steel cladding (left).
MCT No. 243745 2X

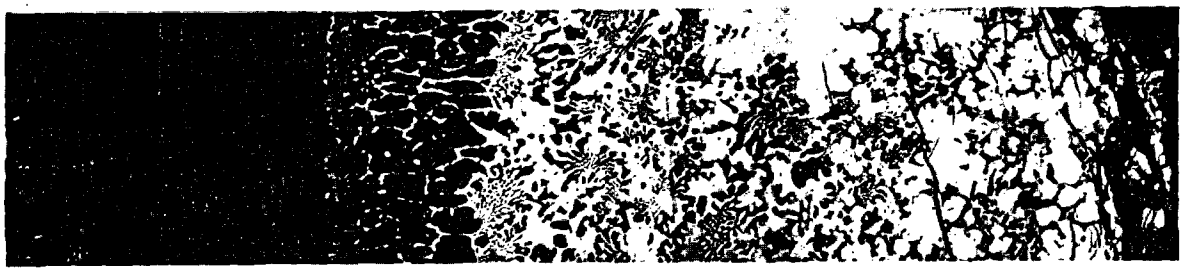

Figure 8. SEM-BSE image of eutectic reaction zones (2) between 304 stainless steel (dark) and Zircaloy (gray). The Ag-In-Cd/SS interface is at the far left and the surface of the "cladding" in Fig. 7 is at the far right.
MCT No. 243798 275X

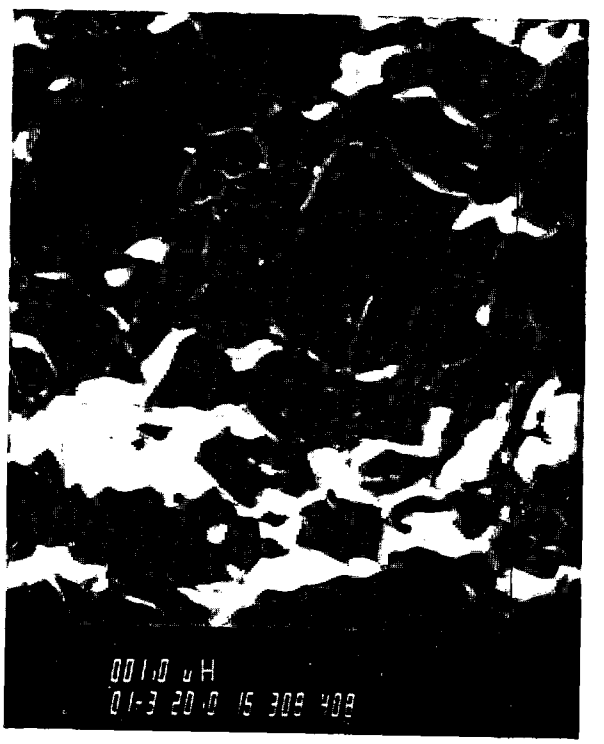

Figure 9. SEM fractograph from UO_2 fuel in agglomerate specimen showing absence of fission gas bubbles or channels on grain boundaries. 1000X

some data is at least a starting point for broadening our knowledge. Therefore, the following is offered in that vein.

1. The microstructures of molten materials examined from different reactor locations indicate different cooling rates and solidification temperatures. This is based on macroscopic and microscopic compositional inhomogeneities in the structures and differing grain sizes and morphologies.

2. Molten material likely reached the lower plenum assisted by a low-melting (~1300°C) eutectic phase of Fe-Cr-Al-O in the melt that provided fluidity.

3. The molten areas basically consist of oxides with random inclusions of non-oxidized materials such as Ni, Sn, Ag, In, some Cd and fission-product Te and Ru.

4. Stainless steel-clad, Ag-In-Cd control rods could have failed from a eutectic reaction between the Zircaloy guide tubes and the cladding at 935-960°C.

5. Fission-product release from unmelted fuel was not enhanced by appreciable pathway development in grain boundaries.

6. Although some metallic Te and Ru were found combined with Ni and Sn inclusions, the effect of this alloying on retarding fission-product release is not readily quantifiable.

ACKNOWLEDGEMENTS

This paper was made possible by the diligent efforts of D. Donahue, F. Pausche, and C. Gebo at ANL's Alpha-Gamma Hot Cell Facility. The work was supported by the U.S. Nuclear Regulatory Commission.

REFERENCES

1. C. S. Olsen, D. W. Akers, and R. McArdell, "TMI-2 Core Bore Examination Results," this conference.

2. E. M. Levin, C. R. Robbins, and H. F. McMurdie, Phase Diagrams for Ceramists, Am. Ceram. Soc., Columbus, OH, Vol. 2, p. 27, 1969.

ANALYSIS OF FISSION PRODUCT RELEASE BEHAVIOR DURING THE TMI-2 ACCIDENT[a]

D. A. Petti, J. P. Adams, J. L. Anderson, and R. R. Hobbins
Idaho National Engineering Laboratory
EG&G Idaho, Inc.
P.O. Box 1625
Idaho Falls, Idaho 83415

ABSTRACT

An analysis of fission product release during the Three Mile Island Unit 2 (TMI-2) accident has been initiated to provide an understanding of fission product behavior that is consistent with both the best estimate accident scenario and fission product results from the ongoing sample acquisition and examination efforts. "First principles" fission product release models are used to describe release from intact, disrupted, and molten fuel. Conclusions relating to fission product release, transport, and chemical form are drawn.

1. INTRODUCTION

The March 1979 accident at Three Mile Island Unit 2 (TMI-2), the most severe core damage accident that has occurred in a U.S. commercial light water reactor, provides a unique opportunity to obtain data about fission product behavior under real accident conditions. A significant fraction of the more volatile fission products was released from the fuel; however, these fission products were confined in the reactor coolant and other plant systems and the containment without significant release to the environment. Examining the dominant physical and chemical processes that affected fission product release behavior during the accident may improve the current understanding of such phenomena as fission product release, transport, and chemical form, an understanding that is currently based largely on separate effects and scaled integral test data. Thus, the accident provides the only full-scale data base with which to study these phenomena. The DOE has sponsored a major program at the INEL to maximize the quantity and quality of this data base. This program is the TMI-2 Accident Evaluation Program and its objective and plan are documented in Reference 1.

The purpose of the work reported here is to analyze fission product release from the core during the accident using "first principles" fission product release models. The results from this study will be used to improve our understanding of the accident scenario and to provide additional insight into the accident. The fission product release and retention estimates developed

---

a. Work supported by the U.S. Department of Energy Assistant Secretary for Nuclear Energy, Office of Light Water Reactor Safety and Technology, under DOE Contract No. DE-AC07-76ID01570.

in this study will be compared, to the extent possible, with retention data from samples that have and will be obtained from TMI.

Brief reviews of the accident scenario and the fission product retention data from TMI-2 are presented in Section 2. Sections 3 through 6 describe the proposed "first principles" analyses that will be used to describe fission product release during the TMI-2 accident. A summary and conclusions from this work are provided in Section 7.

2. REVIEW OF THE TMI-2 ACCIDENT SCENARIO AND FISSION PRODUCT RETENTION DATA

2.1 Accident Scenario

The fission product analysis has been divided into four parts to correspond to the four thermal/hydraulic phases of the accident. Each phase represents a different set of core thermal/hydraulic and fuel conditions. This section will briefly review the five phases of the TMI-2 accident. Additional information about the accident scenario is provided in Reference 2.

Phase 1 is defined as the time from the turbine trip (time zero) until the A-loop reactor coolant pumps (RCPs) were turned off at 100 min. (The B-loop RCPs were turned off earlier at 73 min.) This phase is characterized as a small-break LOCA accompanied by a slow depressurizaton of the reactor coolant system without uncovery or heatup of the core. Hence, no fission product release occurred.

The thermal and hydraulic conditions during Phase 2 (between cessation of forced convection at 100 min and the B-pump transient at 174 min) were characteristic of a slow core boiloff and heatup that started between 114 and 120 min, and continued throughout this phase. Containment radiation monitor signals indicated that some fuel rods had burst between 137 and 142 min. High output currents were observed from the SPNDs in the central upper region. At approximately 150 min, it is believed that rapid oxidation had begun causing cladding temperatures to exceed 1850 K. This exothermic oxidation drove temperatures above clad melting and some fuel dissolution began. Downward relocation of this liquefied material would be expected to occur, resulting in a small blockage of material near the core center. Core heatup analysis indicates that peak core temperatures exceeded 2400 K by 174 min. The upper portions of the core contained partially oxidized rods and high temperature remnants consisting of UO_2 pellets and ZrO_2 cladding. In the central region of the core, a partially molten noncoolable U-Zr-O mixture rested upon a hard pan of ZrO_2/UO_2 ceramic which had solidified between the existing fuel rods.

Phase 3 is defined as the time period between 174 and 224 min. For the purposes of the fission product analysis, this phase is separated into two phases termed Phases 3a and 3b. Phase 3a is termed the "B-pump" transient because the 2B RCP was operated for a short time (several tens of minutes) and introduced about 28 m^3 of water in an effort to cool the core. The

pump transient caused the highly brittle oxidized cladding to fracture, forming a rubble bed of fuel pieces and cladding shards which rested on the molten U-Zr-O mixture.

During Phase 3b between 180 and 224 min, the molten U-Zr-O material and part of the debris bed continued to heat to produce a large molten mass surrounded by a crust. This occurred despite the fact that the liquid level was estimated to be near the top of the core. On top of the crust is a debris bed and a void region formed when the embrittled fuel rods collapsed during Phase 3a. A simplified one-dimensional heatup analysis of the molten mass and the surrounding upper and lower crusts indicates that despite the limited cooling at the periphery the molten material continued to heat up from decay heat due to the high thermal resistance of the oxide and the large thermal capacitance of such a large consolidated mass.

Selected data from the accident substantiate that during the last phase, Phase 4, which lasted from 224 to 230 min, a major relocation of core material occurred. Visual inspection data and crust failure analysis indicate that the crust surrounding the molten pool failed near the top at the southeast core periphery. The molten material then drained through the lower support assembly and into the lower plenum. It is estimated that between 10 and 20 tons of core material relocated to the lower plenum at this time.

As is noted in Reference 2, the accident scenario represents a best-estimate interpretation of the TMI-2 data to date. Work is continuing to define more details, especially from the later phases of the accident. Hence, the understanding of the accident scenario might change.

2.2 Fission Product Retention

The fission product inventory at the time of the accident is needed for the release calculations presented here. Table 1 lists the inventories for various fission products based on a detailed nodal ORIGEN2 inventory calculation.[3]

Small samples from the upper debris bed and the lower plenum have been analyzed for their fission product content.[4] The average fission product retentions for ^{106}Ru, ^{125}Sb, ^{129}I, ^{137}Cs, ^{90}Sr, ^{154}Eu, and ^{144}Ce are presented in Table 2 along with the range found in the various debris samples. One objective of this work is to explain the results in Table 2, especially the high retention of the cesium in the lower plenum samples, the high retention of iodine in the upper debris samples, and the low retention of ruthenium in the lower plenum samples.

3. FISSION PRODUCT RELEASE DURING PHASE 2

During the initial core heatup and degradation, three mechanisms are thought to contribute to fission product release: gap release, diffusional release, and release from liquefied fuel. Because the burnup of fuel in TMI-2 was

TABLE 1. TOTAL CORE ELEMENTAL FISSION PRODUCT INVENTORIES

Element	Inventory[a] (moles)
Kr	42.6
Sr	129.6
Ru	176.1
Sb	2.2
Te	29.2
I	17.3
Xe	314.4
Cs	161.7
Ce	209.9
Eu	3.5

a. Three hours after scram (from Reference 3).

TABLE 2. AVERAGE FISSION PRODUCT RETENTION

	Percent of Inventory Retained[a]			
	Lower Plenum		Upper Plenum	
Radionuclide	Average	Range	Average	Range
I-129	3	3- 24	22	10- 38
Cs-137	14	0- 38	21	6- 32
Ru-106	7	0- 19	55	35- 86
Sb-125	3	0- 17	23	18- 38
Sr-90	114	73-190	93	79-102
Eu-154	86	69-105	90	60-108
Ce-144	110	90-164	114	90-130

a. Compared with core average ORIGEN-2 analysis (μCi/gU).

quite low (<4000 MWd/MTU), very little fission product inventory is expected to have been in the gap. As a result, gap release will not be examined here. This section will discuss models that have been used to describe diffusional release and release from liquefied fuel.

3.1 Booth Diffusion Model

Many out-of-pile postirradiation experiments [5-8] indicate that for temperatures between 1000 and 2180 K prior to fuel dissolution, fission product behavior is dominated by diffusional release of volatile fission products (Xe, Kr, Cs, I, Te) from ruptured fuel rods. Very little release of the medium and low volatile fission products is expected for these temperatures. Many investigators have used the Booth diffusion model [9] has been used successfully to describe the results of fission product release experiments conducted in this temperature range. The Booth diffusion model is based on the solution to the diffusion equation from a sphere of radius a. The fractional release of a fission product is given by

$$FR = 6(Dt/\pi a^2)^{1/2} - 3Dt/a^2 \qquad (1)$$

where

D = diffusion coefficient of the fission product (cm^2/s)

a = "equivalent radius" of the sphere (cm)

t = time (s).

The diffusion coefficient is usually given by an Arrhenius function of the form

$$D = D_0 \exp(-Q/RT) \qquad (2)$$

where

D_0 = pre-exponential factor (cm^2/s)

Q = fission product activation energy (kcal/mole)

R = universal gas constant (kcal/mole K)

T = fuel temperature (K)

and the equivalent radius is derived from the total surface area available for diffusion and the volume of the specimen. In general, this latter parameter is difficult to obtain for specimens that are poly-crystalline. As a result, many researchers correlate their results to an effective diffusion coefficient D' where $D' = D/a^2$.

The Booth model given by Equation (1) is applicable for the case of a constant temperature anneal and releases less than 30%. The temperatures in TMI-2 were not constant during the initial core heatup; hence the diffusion coefficients [Equation (2)] changed with time. As a result, the Booth diffusion model has been modified to account for the transient temperature

response of the core. For a transient temperature, an infinite series form of the solution is used. The fractional retention is given by

$$\text{Fractional retention} = \frac{6}{\pi^2}\sum_{n=1}^{\infty}\frac{1}{n^2}\exp(-n^2\pi^2\tau) \qquad (4)$$

where

$$\tau = \frac{1}{a^2}\int_0^t D[T(t')]\,dt' \quad .$$

The fractional release rate, dFR/dt, is given by

$$\frac{dFR}{dt} = \frac{6D(t)}{a^2}\sum_{n=1}^{\infty}\exp(-n^2\pi^2\tau) \quad . \qquad (5)$$

Thus, for a given node in the TMI-2 core, the release fraction and fractional release rate for the volatile fission products can be calculated once the temperature history has been established and reasonable values of D and a have been chosen.

The core temperature history that was used in this calculation was determined using the SCDAP/RELAP5 computer code.[10] The core was modeled using three representative radial fuel regions, corresponding to the center, middle, and peripheral regions of the core. Six axial nodes were used to model each fuel region resulting in a total of 18 nodes for the entire core. Figure 1 is a schematic representation of the reactor core and vessel nodalization used for this calculation. Cladding temperatures were calculated from accident initiation to the end of Phase 3a, or 180 min. Figure 2 presents the calculated cladding temperatures from 100 to 180 min for the center, middle, and peripheral assemblies in the core. Booth diffusion is a valid representation of fission product behavior only as long as the fuel geometry is preserved. Therefore, the calculation of fission product release was carried out only up to a temperature of 2180 K (temperature at which dissolution of UO_2 by molten zircaloy begins) in the base case calculation.

The expression for the diffusion coefficient, D, was extracted from an extensive study by Lawrence.[11] This study investigated the influence of several environmental conditions on the diffusional release of fission products, including postirradiation anneal versus in-pile testing, stoichiometry, burn-up, fuel density, power rating, and surface vaporization and sublimation. The data base used in determining the best-estimate diffusion coefficient for Xe included data from postirradiation annealling experiments with fuel densities ranging from 58 to 99% of theoretical,

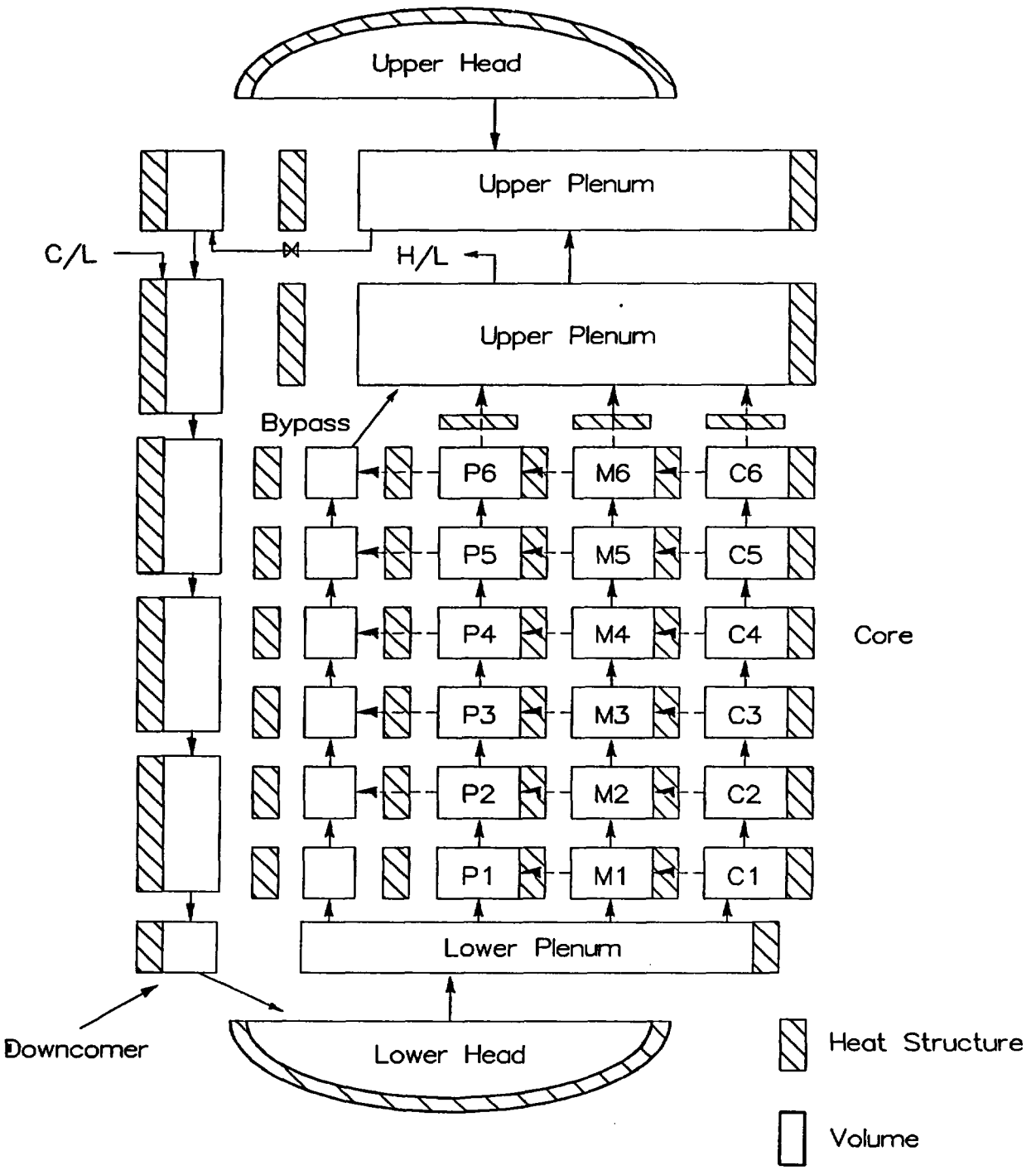

Figure 1. SCDAP/RELAP5 nodalization of the TMI-2 reactor vessel and internals.

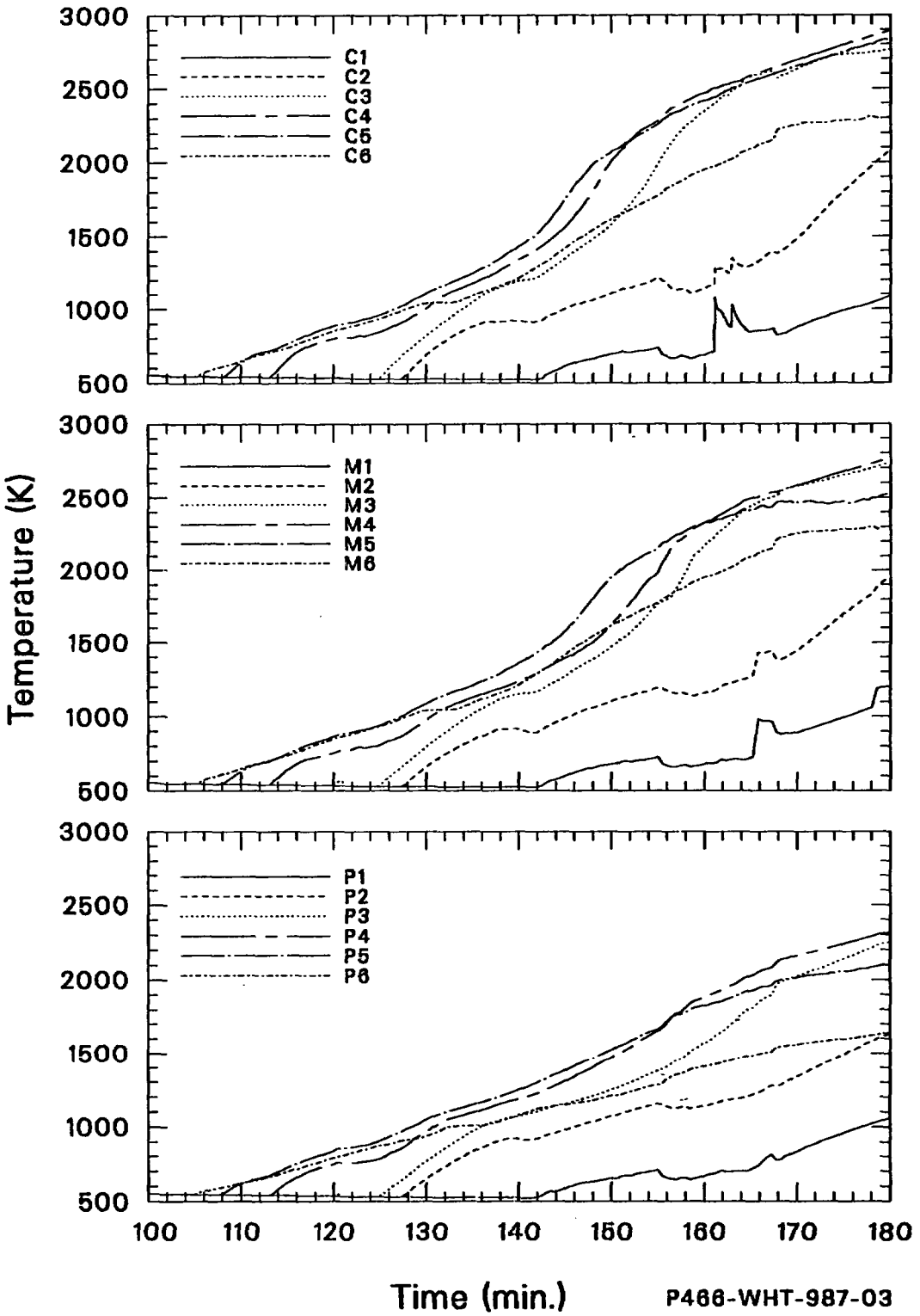

Figure 2. SCDAP/RELAP5 temperature calculations for the TMI-2 accident between 100 and 180 min.

stoichiometry ranging from 1.9 to 2.22, temperatures ranging from 870 to 2470 K, and burnups up to 800 MWd/MTU. The resultant diffusion coefficient for Xe was determined to be

$$D = 7.6\ E\text{-}06\ \exp(-7.0\ E\text{+}04/RT)\ cm^2/s \quad . \tag{6}$$

The sphere radius, a, used in this study was derived from a correlation developed by Belle,[12] illustrated in Figure 3. The least squares fit to the data by Belle, also shown in this figure is [13]

$$a = 3R\ 10^{[20.61\ -\ R(67.9\ -\ 46R)]} \tag{7}$$

where R is the ratio of the fuel density to theoretical density. The density of the fuel used in the TMI-2 core was 92.5% [14] which corresponds to an effective sphere radius of 4.0 E-03 cm. Equation (6) was divided by the square of this effective radius to obtain the fractional release rate versus temperature. This result is plotted in Figure 4.

These three input parameters (calculated core temperatures, diffusion coefficient, and effective sphere radius) were used to estimate Xe release for temperatures up to 2180 K in the base case calculation. In addition, a series of sensitivity studies were made wherein the core temperatures, diffusion coefficient, effective sphere radius, and maximum temperature were varied to bound the expected fission product release. The core temperatures were varied by ±100 K because of uncertainties in the SCDAP/RELAP5 temperature calculation. A second correlation for the diffusion coefficient, developed by Prussin et al.,[8] was used to investigate the sensitivity of the results to this parameter. This correlation is also plotted in Figure 4. The effective sphere radius was varied from 2.0 E-03 (corresponding to the low range of the fuel pellet density) to 2.0 E-02 cm (corresponding to the maximum expected radius in Reference 8). Finally, the maximum temperature up to which the Booth analysis was considered valid was varied between 1700 and 2800 K, the lower temperature corresponding to liquefaction of the steel components in the core and the upper temperature corresponding to the monotectic temperature at which there is an enhanced solubility of UO_2 in molten zircaloy.

Xenon release results for the base case and sensitivity calculations are listed in Table 3. Xenon release was found to be most sensitive to the maximum temperature used in the calculation. As noted, the base case calculation, as well as nearly all of the sensitivity calculations, indicate only minimal (<2%) release of fission product Xe due to diffusion during Phase 2. This low total release is the result of the generally small calculated release rates (on the order of 5 E-03 %/s). The exception is for the upper bound calculation, designated number 9 in Table 3. For this calculation, all of the parameters were set to result in the maximum expected release, including the largest diffusion coefficient, highest maximum temperature, and highest cladding temperatures. The resulting core-average release was 27%. Thus, the core-average release of Xe (and by implication, Kr, I, and Cs) is calculated to be between 0 and 27%.

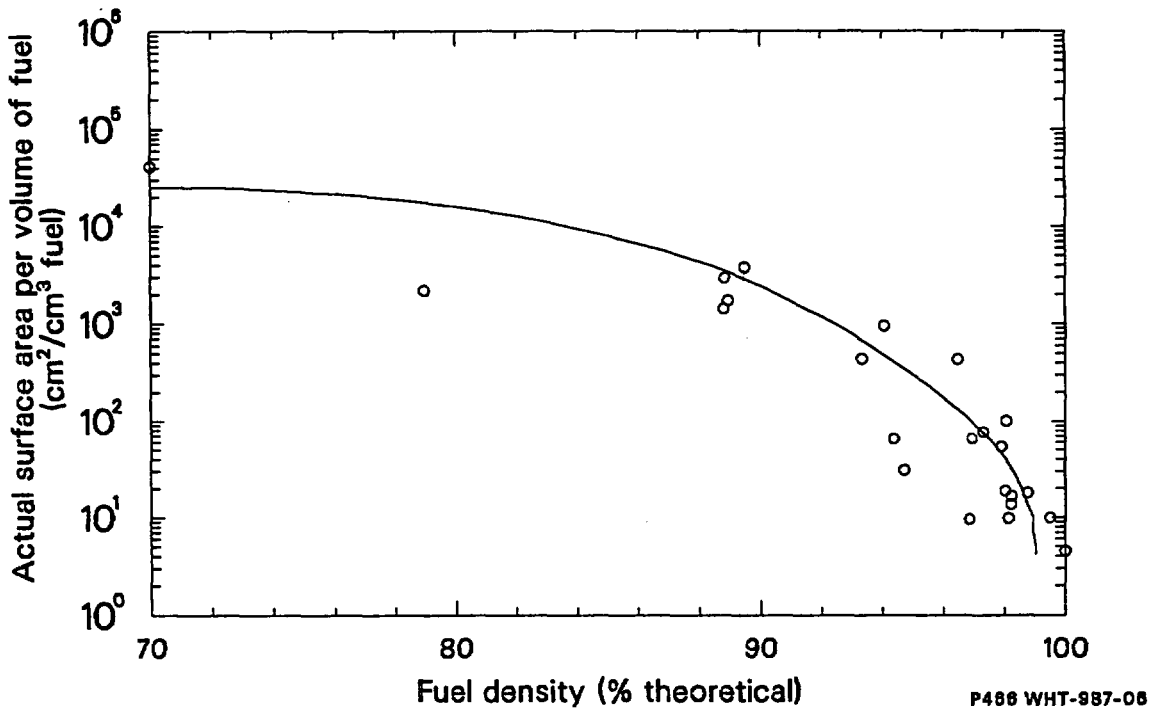

Figure 3. Effective surface-to-volume ratio as a function of theoretical density.

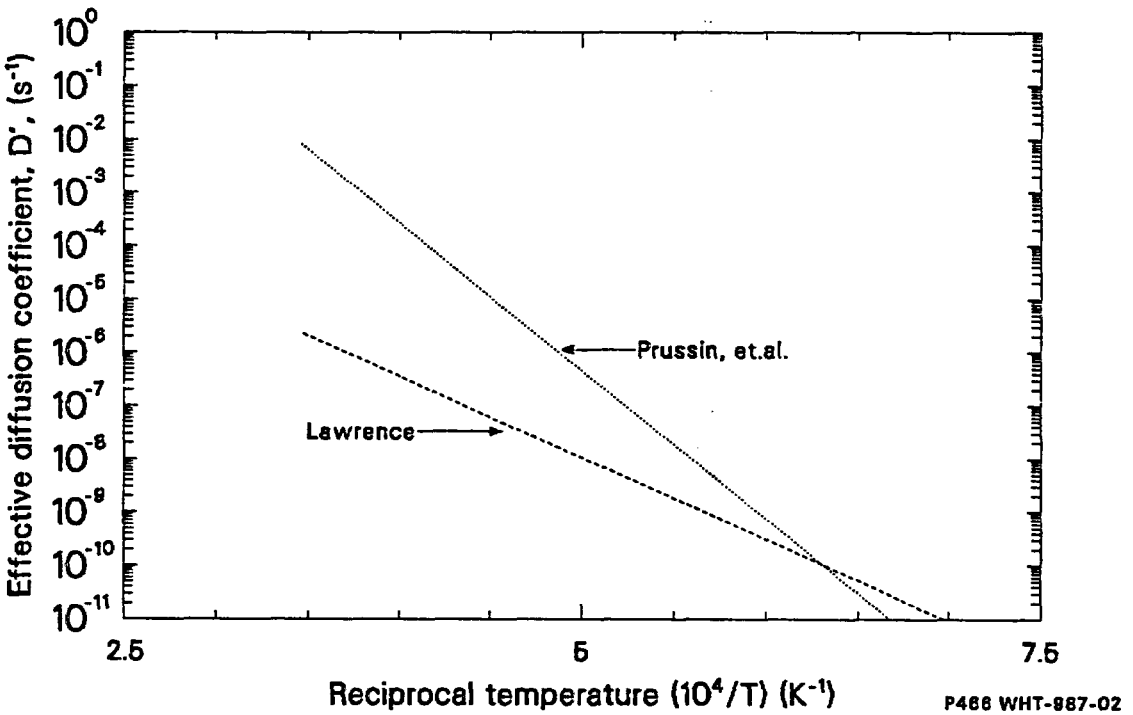

Figure 4. Diffusion coefficient correlations used in the Booth diffusional release calculation.

TABLE 3. CALCULATED DIFFUSIONAL RELEASE FROM TMI CORE DURING PHASE 2

Number	Calculation	Percent Release
1	Base case	0.02
2	$T = T_{SCDAP} + 100$	0.05
3	$T = T_{SCDAP} - 100$	0.01
4	a = 0.02 cm	0.002
5	a = 0.002 cm	0.09
6	Tmax = 2800 K	0.68
7	Tmax = 1700 K	0.002
8	Prussin results	1.77
9	All parameters at maximum values	27.0
10	All parameters at minimum values	0.000

Though the core-average release was in the range between 0 and 27%, individual nodes were calculated to have released up to 60% of their inventory, depending on their location in the core and the temperature history. The range of core nodal release fractions is indicated in Figure 5 which shows the release fraction histories for the nodes experiencing the maximum and minimum releases as calculated for the base case and maximum release calculations, respectively. Also included is a node which experienced a release near the average for each case. As shown in the figures, the minimum nodal release was approximately 0 for both calculations while the maximum nodal release was approximately 60%.

The specific calculation, described above, was for the release of fission product Xe from the TMI-2 core. It has been assumed in this analysis that other gaseous and high volatile fission products (Kr, I, Cs, and Te) diffused at approximately the same rate. While it is obvious that there are differences in the diffusion of these different fission products, these differences are expected to be smaller than the uncertainties in the other parameters governing diffusion (e.g., calculated versus actual core temperatures, fuel stoichiometry, etc.). The effect of these differences on the release fractions is included within the sensitivity calculations already discussed.

A direct comparison of the calculated release fractions with measured data from the core cannot be made, primarily because of the difficulty involved in identifying the conditions experienced by individual samples extracted from the core and the uncertainty in identifying the original enrichment and burnup (both of which affect the initial fission product inventory) in the sample. Additionally, there are no samples available that experienced only the first two phases of the accident; therefore the measured fission product release fractions are a result of fission product release during the entire accident. Within these uncertainties, however, some general comparisons between measured and calculated fission product release can be made. Volatile fission product release measured in samples extracted from the upper

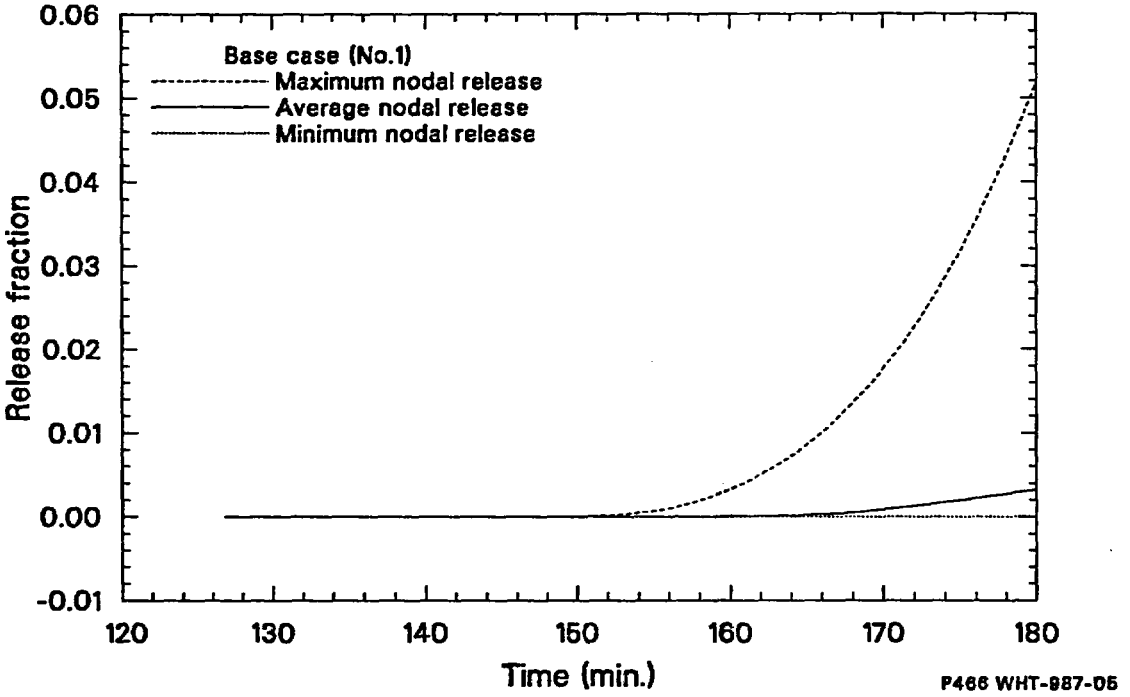

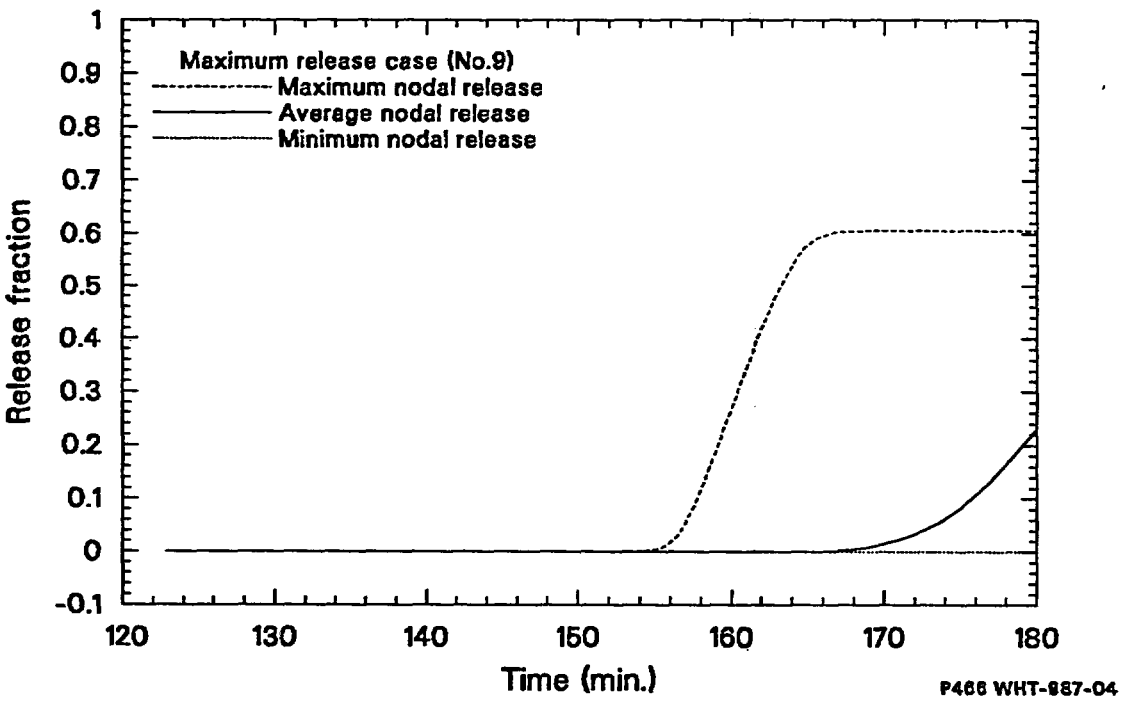

Figure 5. Nodal fractional release histories from the Booth diffusional release calcuations.

debris bed is judged to have occurred primarily during Phases 2 and 3a since during Phases 3b and 4 this debris was covered with water and was in the process of being quenched. No data on noble gas release from these samples are yet available (but will become available in the future). Release of I and Cs from these samples ranges from 69 to 87% for I and from 60 to 92% for Cs. The calculated Phase 2 nodal releases for both of these species range from 0 to 60%, depending on the temperature and diffusivity parameters used in the calculation for the particular mode. Significant additional release is expected to have occurred during Phase 3a, as discussed in Section 4. Thus, these volatile fission product release calculations are generally consistent with the data obtained from the upper debris samples.

In general, Te release from the fuel pellets is roughly similar to the Xe diffusional results. However, separate effects test data indicate that Te tends to become bound to unoxidized Zr in the cladding. When the zircaloy oxidizes, the Te is released. It is recommended in Reference 15 that when the local Zr oxidation is less than 70%, the calculated Te release should be reduced by a factor of 40. It is indicated in Reference 16 that the global Zr oxidation was of the order of 50% (based on an analysis of the hydrogen that was evolved from the core). However, since approximately 40% of the core was largely undamaged (i.e., remained predominantly in an unoxidized rod-like geometry), the hydrogen generation estimate indicates that the damaged portion of the core could have been heavily (~80%) oxidized. Therefore, it is expected that in the undamaged core regions where the local oxidation is less than the 70% threshold, any Te released from the fuel would be sequestered by the cladding. However, for the heavily damaged areas of the core, significant Zr oxidation probably occurred, suggesting that the Te release from these regions could be large.

3.2 Other Factors Affecting Fission Product Release During Heatup

There are factors other than simple diffusion that affect fission product release from UO_2 during heatup of solid fuel. Two of the more important are fuel oxidation and fuel burnup. Fission product gases migrate to fuel grain boundaries during irradiation under normal operating conditions and collect in bubbles in the boundaries. Above burnups of ~5000 MWd/MTU, depending on the fuel temperature, the density of gas bubbles in the boundaries becomes great enough that the bubbles tend to interconnect to form a continuous tunnel network of voids in the grain boundaries that reaches to the pellet surface. This tunnel network provides a path of rapid escape for fission gases and vapors that reach it from the grain interiors. Because the average burnup in the TMI-2 core was <4000 MWd/MTU, this tunnel network would not be expected to be well developed prior to the accident. The microstructures of fuel in regions of the TMI-2 core not exposed to high temperatures in the accident confirm this expectation (Figure 6).

Oxidation of the fuel by steam enhances atomic mobility in the UO_2 and thus the release rates of fission products. Enhancements in release due to fuel oxidation by factors of 2 to 4 have been reported.[17] One of the evidences of the effect of increased atomic mobility is accelerated grain growth. The process of grain boundary sweeping during grain growth can be an important

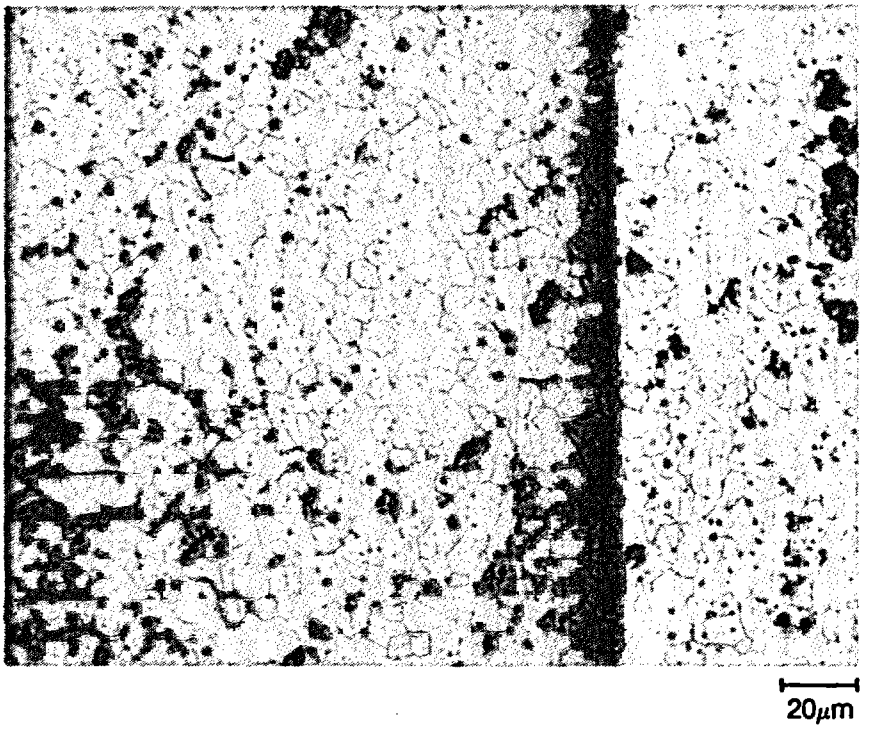

Figure 6. Optical photomicrograph of etched fuel below lower crust showing microstructure typical of low burnup fuel, i.e., little porosity redistribution. Sample from location D4, 1.05 m above bottom of core.

mechanism for accelerating the migration of fission products to grain boundaries during heatup. However, in low burnup fuel such as in TMI-2, the fission products accumulated at the grain boundaries during heatup are trapped until the boundaries are opened or otherwise changed by other phenomena. Therefore, although some evidence of at least localized fuel oxidation in TMI-2 exists,[18] the possible effects on fission product release are accommodated within the sensitivity study (discussed in Section 3.1) that varied the magnitude of the diffusion coefficient in the Booth model. Two additional phenomena that can affect the structure of the grain boundaries and the release of fission products trapped in them are fuel liquefaction and fuel cracking. Fuel liquefaction by interaction of UO_2 with molten zircaloy occurs upon heatup and is discussed in the following section, whereas fuel fracturing is of concern principally upon cooling and is discussed under Phase 3a.

3.3 Fission Product Release from Liquefied Fuel

Laboratory studies [19] of the liquefaction of UO_2 by molten zircaloy show that the process proceeds by the diffusion of oxygen from the UO_2 preferentially along grain boundaries into the zircaloy. The depletion of oxygen leads to reduction of the UO_2 to liquid uranium metal in the grain boundaries. The boundaries are weakened by this process and grains of UO_2 are separated from the surface of the fuel and are surrounded by molten zircaloy. The high surface area of the individual grains contributes to their rapid dissolution by the zircaloy. Once the UO_2 has been dissolved in the molten zircaloy, the release of fission gases and vapors is governed by the coalescence and rise of bubbles in the liquid to a free surface. This behavior is considered in the Phase 3b analysis.

It has been argued,[20] based on theories of atom and bubble mobilities, that the liquefaction of grain boundaries in low burnup fuel should cause an increase in the release rate of fission gases and volatile fission products (such as iodine and cesium), but should cause no significant change in release rates for high burnup fuel with interlinked porosity at grain boundaries. On-line measurements of fission product release rates from some in-pile bundle tests using trace-irradiated fuel have been interpreted in terms of enhanced release rates upon fuel liquefaction,[21,22] but these experiments are complex and not readily amenable to unambiguous interpretation. A reduction in fission product release rates has been calculated by Rest [23] for grain boundary liquefaction in out-of-pile release tests performed on high burnup fuel at Oak Ridge National Laboratory.[24] As will be discussed in Section 4.2, fuel fragments in the upper debris bed exhibit some degree of interlinked porosity in grain boundaries typical of higher burnup because of time at high temperature. Therefore, for the analysis of fission product release during the heatup phase in the TMI-2 accident, the effect of grain boundary liquefaction in TMI-2 fuel would not change fission product release rates significantly and that the effect is accommodated within the sensitivity study varied the magnitude of the diffusion coefficient in the Booth model. The effect of bulk dissolution of UO_2 by molten zircaloy is analyzed in Phase 3b where

bubble coalescence of fission product gases and vapors is considered and is found to have a pronounced effect on release from the liquid state.

4. FISSION PRODUCT RELEASE DURING PHASE 3A

Phase 3a is defined as the time period between 174 and 180 min when the B-loop pump was restarted and injected a large quantity of liquid into the vessel. No "first principles" models exist to characterize fission product behavior during the quenching of the fuel and formation of the debris bed which occurred in Phase 3a. Therefore, this section is limited to a discussion of in-pile experiments that were quenched from high temperature, and the results from metallurgical examination of the upper debris bed samples from the TMI-2 core.

4.1 Fission Product Release during Fuel Fracturing and Fragmentation

The Power Burst Facility Severe Fuel Damage Scoping Test (SFD-ST) [22] and the Loss-of-Fluid Test (LOFT) FP-2 experiment [25] are the only two severe fuel damage in-pile experiments in which the fuel bundle was cooled with a rapid reflood of water into the bundle. In SFD-ST greater than 90% of the fission product release occurred after initiation of reflood and preliminary information suggests that a similar release behavior occurred in the LOFT FP-2 experiment. The fuel burnup in these experiments was very low, less than 450 MWd/MTU. As was discussed above, one would expect fission products to migrate to grain boundaries in low burnup fuel during a high-temperature transient. The fuel will crack as it is subjected to thermal-mechanical stresses during cooling as a result of reflood. Transgranular and intergranular cracking have been observed in fuel cooled rapidly from high temperature. Intergranular cracking has been explained [26] based on quenching from above the equicohesive temperature (about 1900 K in UO_2) where the ultimate tensile strength sharply decreases due primarily to decreasing grain boundary strength and ductile failure along grain boundaries. (Note that in the SCDAP/RELAP5 calculation described in Section 3, nearly 90% of the upper half of the core reached temperatures in excess of 1900 K prior to the B-pump transient.) Some fracture along grain boundaries was observed in SFD-ST but this phenomenon was not widespread. Transgranular cracking can intersect accumulations of fission products trapped at grain boundaries and enhance release. This kind of cracking is prevalent in both SFD-ST and in the particles that make up the upper debris bed in TMI-2 (Figure 7).

4.2 Fuel Morphology of TMI-2 Upper Debris Bed Samples

Samples from the upper debris bed have been examined to characterize the fuel morphology that is important to fission product release before and during the pump transient. Specifically, the examination focused on characterizing grain boundary porosity and interconnection, the degree of fuel oxidation, fuel fracturing, and amount of grain growth. Figure 8 shows that the grain boundaries contain a great deal of porosity and that some interconnection to form tunnels along grain edges may have occurred.

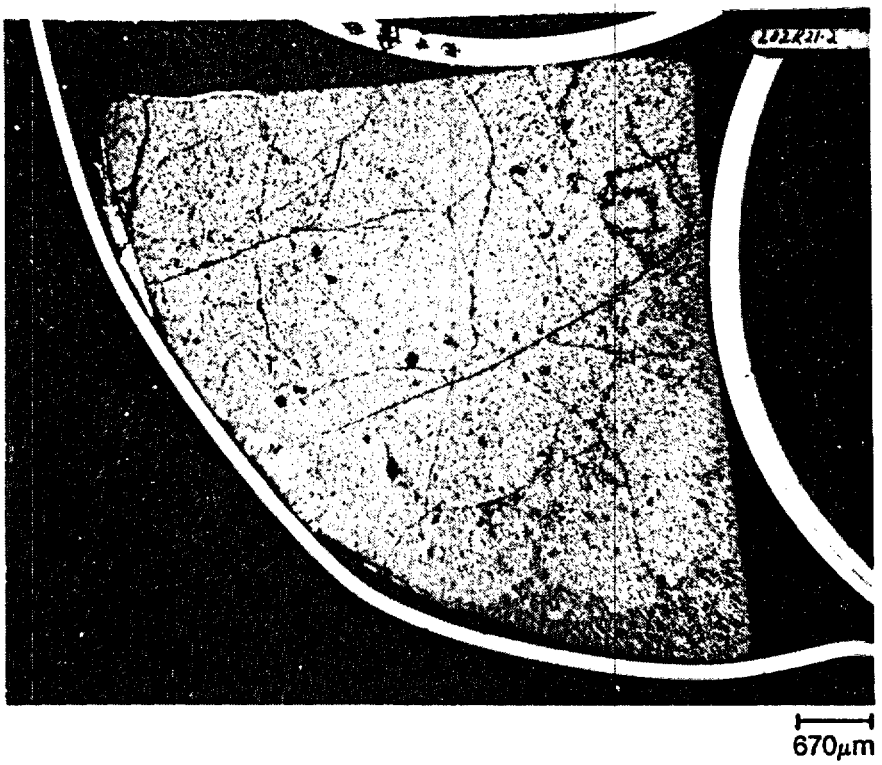

Figure 7. Macrocracking of fuel fragment in upper debris bed.

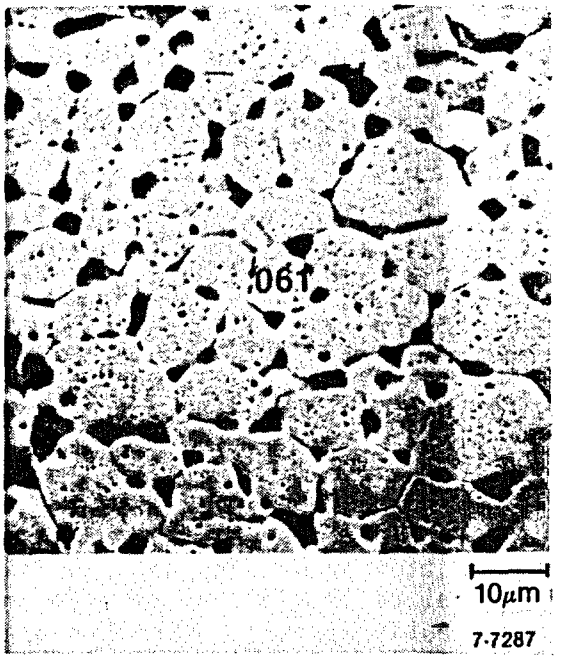

Figure 8. Scanning electron microscope image showing interlinked porosity at grain boundaries in fuel in the upper debris bed.

Based on the microstructure of fuel that was not overheated in the accident (Figure 6) and previous work,[20,24,27] it is expected that fission gas bubbles migrated to the grain boundaries primarily during the heatup in Phase 2 of the accident. To the extent that open pathways developed along grain boundary edges, fission gases and vapors could be released in this phase of the accident at a rate exceeding simple diffusion as calculated in Section 3.1. However, evidence of interaction of the fuel with molten zircaloy is widespread in the upper debris bed (Figure 9) and this interaction produces liquid uranium metal in the grain boundaries of the fuel,[19] tending to slow release along previously open pathways. Despite some Auger measurements indicating localized oxidation of the fuel, the absence of U_4O_9 in the microstructure suggests that fuel oxidation was not widespread. This observation is consistent with the observed lack of grain growth. There was a large amount of macrocracking evident in the fuel cross sections (Figure 7) and fuel pullout during preparation (Figure 10) indicating that grain boundary separation or intergranular cracking also occurred. The intersection of macrocracks with porosity trapped at grain boundaries has been used to explain fission gas release upon cooling from high temperature transients.[27] Additionally, grain boundary separation can contribute to fission product release upon reflood.

In summary, the microstructure of the fuel in the upper debris bed suggests that fission gas bubbles migrated to grain boundaries during the heatup period of the accident (Phase 2) and that some interlinkage accelerating fission product release from the fuel may have occurred. However, the reduction of UO_2 to uranium in grain boundaries by the interaction with zircaloy would be expected to occur in a similar temperature regime (2200 K) and, therefore, in a similar time frame, as the interlinkage of porosity along the boundaries. The net result is that fission product release during Phase 2 may not have been greatly affected by either grain boundary interlinkage or the initial stages of fuel liquefaction. The range of diffusivities employed in the Booth diffusion study of fission product release in Phase 2 is intended to encompass uncertainties in the phenomena discussed above. Although the release is not expected to be affected by the initial stages of fuel liquefaction, the release of fission gas bubbles from the liquid formed by bulk dissolution of UO_2 can be rapid as is discussed in the Phase 3b analysis. The macrocracks and fuel intergranular fracturing observed in the fuel in the upper debris bed suggest that considerable additional release of fission gases and volatile fission products could have taken place upon reflooding at the time of the B-loop pump transient.

5. FISSION PRODUCT RELEASE DURING PHASE 3B

Phase 3b is defined as the time period between 180 and 224 min when the consolidated mass of molten material was in an uncooled geometry surrounded by water. During this phase, this mass continued to heatup and form a large molten pool. This molten mass was surrounded by a crust which was covered with a debris bed. The core was covered with water as a result of the B-loop pump transient. Fission product release during this phase can come from three separate fuel regions: fuel still in a rod-like geometry, the debris bed, and the molten pool. Because the rods and debris bed were relatively

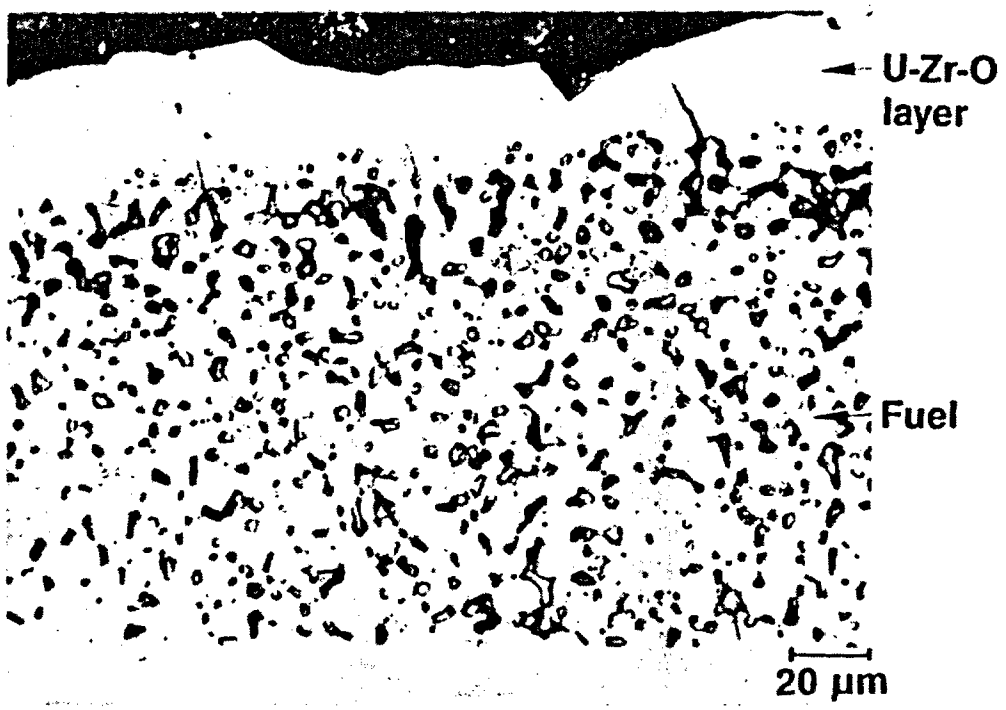

Figure 9. Optical photomicrograph showing interaction of molten zircaloy with fuel in upper debris bed.

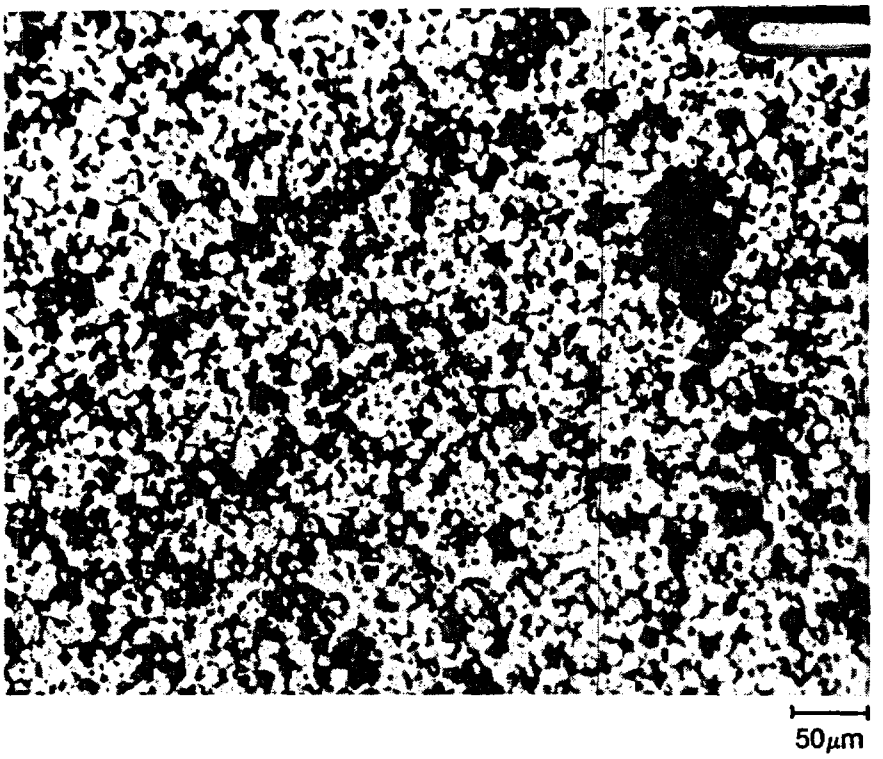

Figure 10. Optical photomicrograph showing fuel pullout due to intergranular fractures in fuel in the upper debris bed.

cool, very little fission product release is expected from these sources. As a result, only fission product release from the molten pool is considered here.

Details of the geometry of the molten pool used in all calculations in this section are given in Section 5.1. Different mechanisms are thought to govern the release of the high and low volatile fission products from the molten mass. Because the volatile fission products are gaseous at high temperature (>2800 K) their release is expected to be dominated by bubble dynamics in the molten pool. Section 5.2 examines bubble dynamics in a convective pool to determine the amount of gas that can be released from the melt. Medium and low volatile fission products (Sb, Sr, Eu, Ce) will tend to exist as condensed phases in the melt. Hence, their release is probably controlled by convective mass transfer from the melt. The oxygen content of the melt will be used to determine the dominant chemical form and volatility of these fission products. The behavior of the medium and low volatile fission products will be discussed in Section 5.3. The effect of a crust of U-Zr-O material surrounding the melt will be investigated in Section 5.4.

5.1 Geometry of the Molten Pool

For all fission product release calculations, the pool was assumed to be a hemisphere, 1.45 m in radius and 6385 L in volume. The details of pool growth during Phase 3b have been neglected. This volume represents 35% of the original core material. Based on metallurgical examination of samples that relocated from this region into the lower plenum, the material was found to be stoichiometric $(U,Zr)O_2$ with a melting point of ~2800 K. Potential fission product inventories in the pool are 35% of the total core inventories given in Table 1. Physical properties of the molten $(U,Zr)O_2$ used in these calculations are listed in Table 4.

TABLE 4. VALUES OF PHYSICAL CONSTANTS OF MOLTEN $(U,Zr)O_2$ AT 2800 K[a]

Constant	Value	Range
Density, ρ (kg/m^3)	8700	--
Viscosity, μ (kg/m-s)	5.1 E-03	±25%
Heat capacity, c_p (J/kg-K)	500	±50%
Coefficient of thermal expansion, β (K^{-1})	9.3 E-05	+100%/-50%
Thermal conductivity, k (W/m-K)	4	±25%
Thermal diffusivity, α (m^2/s)	9.1 E-07	±50%
Kinematic viscosity, ν (m^2/s)	5.9 E-07	±25%

a. From References 13 and 33.

5.2 Volatile Fission Product Release from the Melt

The release of noble gases, Kr and Xe, and the volatile fission products, I and Cs is expected to be dominated by bubble dynamics in the molten pool because these high volatile fission products are gaseous at the high temperatures (>2800 K) in the melt. Results from the heatup analysis of this molten mass suggest that a large temperature gradient existed between the center and periphery of the melt and that the pool was probably in natural convection during Phase 3b.[28] As a result, gas bubbles in the melt can only be released if the buoyant velocity of the bubble is large enough to overcome the convective velocity in the pool. Comparison of the bubble rise velocity with the convective velocity in the pool will determine the critical bubble size that can escape from the pool and be released. This approach should provide a conservative estimate of the critical bubble size because it is assumed that the convective pool forces always oppose the buoyant forces of the bubble. However, given the circular nature of convection cells, it is recognized that sometimes the convective and buoyant forces act together to bring bubbles to the surface.

The rise velocity of a spherical gas bubble is found by balancing the drag and buoyant forces on the bubble. Hence

$$V_{rise} = 2\rho g r^2/9\mu \qquad (8)$$

where

ρ = density of melt (kg/m^3)

g = acceleration due to gravity (m/s^2)

r = radius of bubble (m)

μ = viscosity of melt (kg/m-s).

The convective velocity can be obtained from an energy balance and is given by

$$V_{conv} = 2Q/\rho A c_p \Delta T \qquad (9)$$

where

Q = total decay energy in the pool (J)

A = area for convection (m^2)

c_p = heat capacity (W/m-K)

ΔT = temperature gradient from pool center to surface (pool superheat) (K).

The velocity given by Equation (9) more closely represents the velocity in the boundary layer than the velocity in the pool because most of the temperature gradient across the pool is in the boundary layer. The pool velocity is probably significantly larger than that given by Equation (9).

The criterion for bubble escape is given by

$$V_{rise} > V_{conv} \quad . \tag{10}$$

Solving for the critical diameter yields

$$d_{crit} > (18\mu V_{conv}/\rho g)^{1/2} \tag{11a}$$

$$d_{crit} > (9Q\mu/\rho^2 g A c_p \Delta T)^{1/2} \quad . \tag{11b}$$

Values for the variables used in Equations (8) through (11) are given in Tables 4 and 5. Realistic estimates of the ranges of these parameters are also listed in the table. Substituting the nominal values of the variables yields a minimum critical diameter of about 37 μm. The major uncertainty in this calculation is the pool convection velocity (V_{conv}), which in turn depends on the pool superheat (ΔT). Because most of the temperature gradient is in the boundary layer of the convecting pool, the nominal value of Δt is probably too high. A lower temperature gradient through the pool would cause V_{conv} to increase. As a result, convection velocities between 0.1 and 10 cm/s were used to bracket the range of d_{crit}. Using these upper and lower estimates on the pool convection velocity results in a range for d_{crit} between 33 and 328 μm.

Having calculated the critical diameter of bubbles that will escape the pool, the amount of gas in the melt that is in bubbles greater than d_{crit} needs to be estimated. Most of the initial volatile fission product inventory will be in bubbles much less than d_{crit}. The initial bubble size in the pool is probably governed by the initial bubble distribution in the fuel grains prior to liquefaction. For the low burnup fuel in TMI-2, the gas bubbles in solid fuel are rather small (~100 A). However, as the fuel is dissolved and temperatures increase, diffusion of volatile fission product atoms in the fuel matrix and bulk diffusion of the intragranular gas bubbles in the fuel will cause most of the gas to reside in bubbles. These bubbles will interact and grow by coalescence. Coalescence theory can be used to determine the growth characteristics of the bubble size distribution in the molten pool and hence estimate how much gas release can be expected during Phase 3b.

The rate of coalescence of a bubble of radius r is given by [29]

$$dn_k/dt = 0.5 \sum_{i+j=k} B(r_i,r_j)n_i n_j - n_k \sum_{i=1}^{\infty} B(r_k,r_i)n_i \tag{12}$$

TABLE 5. VALUES OF PARAMETERS USED IN PHASE 3b RELEASE CALCULATION

Parameter	Value	Range
Pool internal heat generation, Q (MW/m^3)	1.75	±0.25
Pool superheat, ΔT(K)	198	128-320
Pool velocity, V_{conv} (cm/s)	0.13	0.1-10
Critical diameter, d_{crit} (μm)	37	33-328
Raleigh number, Ra	4.81 E+15	5.10 E+14/3.68 E+16
Prandtl number, Pr	0.65	--
Diffusion coefficient (cm^2/s)		
Ru	1.31 E-04	
Sr	4.24 E-05	
Sb	6.58 E-05	
Eu_2O_3	3.27 E-05	
Ce_2O_3	3.24 E-05	

where

$B(r_i,r_j)$ = coalescence frequency function (cm^3/s)

n_k = number concentration of bubble of size r_k (p/cm^3).

The first term represents the rate at which bubbles of size k are formed by collisions of particles of size i and j. The second term represents the rate at which bubbles of size k disappear due to coalescence with bubbles of all other sizes. Two processes are assumed to cause bubble coalescence: turbulence in the molten pool and differential bubble rise due to buoyancy. For each mechanism, a coalescence frequency function can be determined. Although not exactly applicable to the case of turbulence in the pool, a correlation for aerosol agglomeration in turbulent pipe flow is used.[30] It is given by

$$B(i,j)_{turb} = 1.3(r_i + r_j)^3 (\epsilon_d/\nu)^{1/2} \quad (13)$$

where

$$\epsilon_d/\nu = (4/d_m)(f/2)^{1.5} V_{conv}^3 \quad (14)$$

and

ϵ_d = eddy diffusivity (m^2/s^3)

ν = kinematic viscosity (m^2/s)

d_m = pool diameter (m)

f = fanning friction factor (= 0.004)

V_{conv} = pool convection velocity (m/s).

The rate of coalescence due to turbulence is found to be more sensitive to the velocity of the convecting pool than to the size of the bubble. For differential bubble rise in the pool, the frequency function is given by [30]

$$B(i,j)_{rise} = \pi(r_i + r_j)^2 \, |V_i - V_j| \quad . \tag{15}$$

As can be seen by examination of Equation (15), two bubbles of the same size will never coalesce through bubble rise since they rise at the same rate. For the analysis here, it is assumed that the overall collision frequency function is given simply as the sum of the turbulent and bubble rise functions. Figure 11 is a three-dimensional plot of the overall collision frequency function B(i,j) as a function of the diameters of the two coalescing bubbles. As indicated in the plot, the frequency function increases dramatically as the size of either of the two coalescing bubbles increases. This result basically reflects the fact that large bubbles can sweep out more of the gas in the pool than small bubbles due both to their greater surface area and larger rise velocities. An examination of Equation (15) indicates that a factor of 10 increase in bubble radius will cause a factor of 10^4 increase in the coalescence frequency function. Separate examinations of the turbulent and bubble rise mechanisms indicate that turbulence is only important for very small bubbles. At large sizes, coalescence is due primarily to bubble rise in the pool. In Equations (12) through (15) it is assumed that each collision results in coalescence. This is a common assumption used in both UO_2 fuel swelling analysis and aerosol agglomeration theory.[29,30] Despite this fact, it is not clear that this assumption is correct for very small bubbles. The effects of bubble surface tension may result in only a fraction of all collisions producing coalescence. Nevertheless, the assumption that all collisions produce coalescence is used for this scoping type of study.

Due to the large uncertainty in many of the input parameters in this model, several calculations have been performed to bound the amount of gas that is released from the melt as a function of time. Three parameters were thought to control gas release from the pool. They are: (a) the amount of gas initially in the melt, (b) the initial size of the bubbles in the pool, and (c) the velocity in the pool (which determines the critical bubble diameter for escape and the rate of coalescence due to turbulence). Analysis of diffusional release during Phase 2 indicates that between 0 and 60% of the volatile fission products would have been released from individual fuel pellets (depending on their location in the core) prior to the formation of the molten mass. The fuel fracturing that occurred during the pump transient could have increased these values to close to 100% for some of the small fuel fragments. Because of this range in release estimates, no single initial inventory of gas in the melt can be estimated with certainty. As a result,

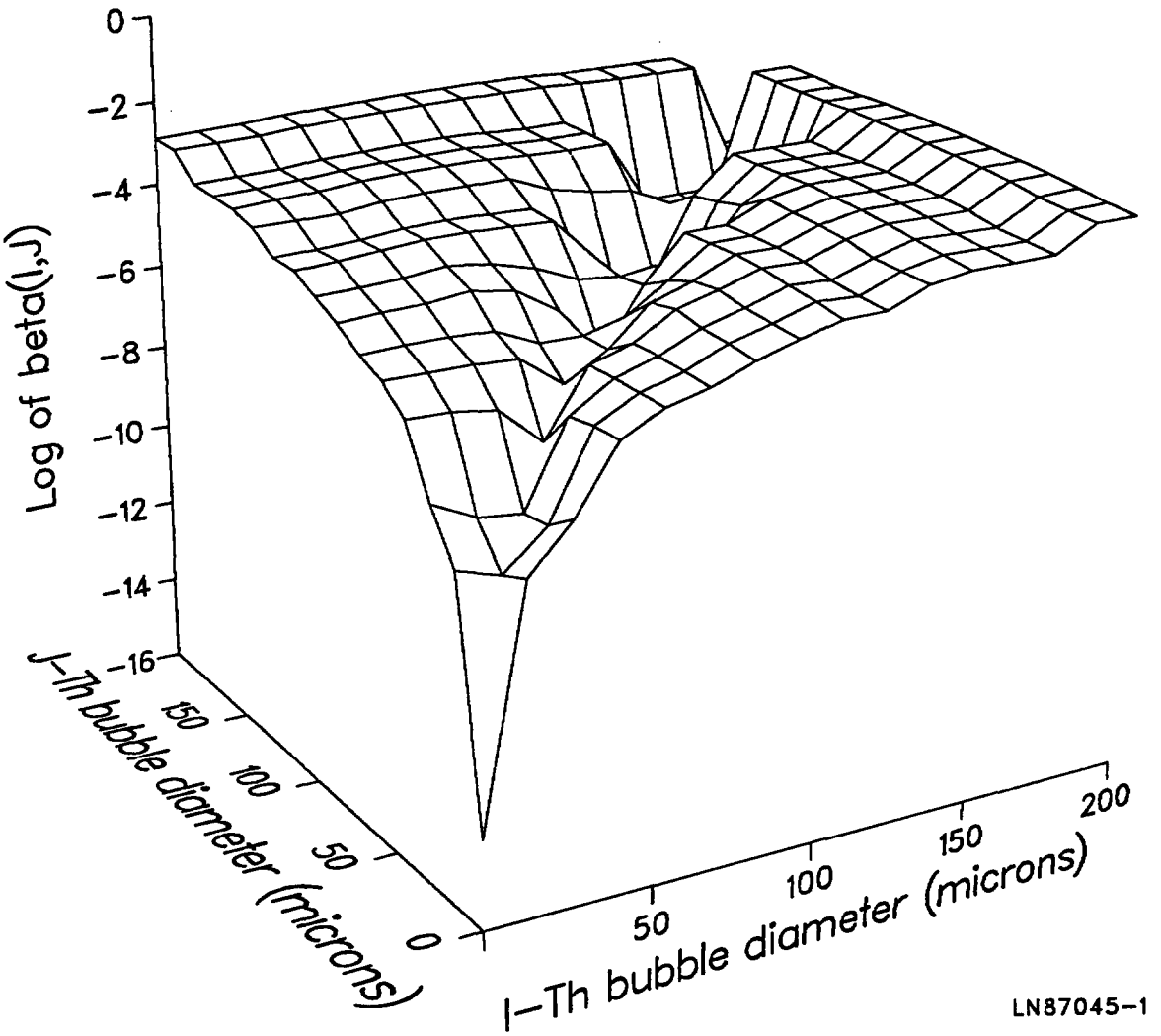

Figure 11. Coalesence frequency function, $B_{i,j}$, as a function of bubble diameter.

the sensitivity calculations were performed assuming that the pool contains 100%, 50%, and 10% of its initial inventory. Three initial bubble sizes of 0.01, 0.1, and 1 μm were chosen for the analysis. Finally, as stated earlier, due to uncertainties in pool thermal parameters, natural convection pool velocities ranging from 0.1 to 10 cm/s were chosen for this analysis.

The amount of gas release as a function of time for the best estimate case is shown in Figure 12. As indicated in the figure, release is very small early in time as the initial bubble distribution coalesces into larger bubbles. Once a sufficient quantity of large bubbles have developed, the amount of gas escaping the melt increases dramatically due to the sweeping effect of these bubbles. The results from this best estimate case indicate that most of the gas would be released from the melt during Phase 3b very quickly (<5 min). The times to release 75% of the volatile gas inventory from the melt for all the sensitivity cases are listed in Table 6. The results of all of the calculations indicate that virtually all of the gas would be released from the melt during Phase 3b. These results agree with the iodine retention estimates from the lower plenum samples, yet are in disagreement with the Cs retention data. Thus, it is postulated that the high cesium retention in the lower plenum samples is not the result of a physical process, but may be because the retained cesium is in a less volatile (as yet unknown) chemical form which reduces it volatility in the melt. Silicates, zirconates, and borates of cesium are three potential low volatile chemical forms that might be stable at 2800 K. Silicates could be formed from SiO_2 impurities in the stainless steel, borates could be formed by the interaction of B_4C burnable poison rods with the cesium, and zirconates could form by reaction of the cladding with cesium.

TABLE 6. VOLATILE FISSION PRODUCT RELEASE RESULTS FOR VARIOUS BUBBLE COALESENCE PARAMETER VALUES

d_o (μm)	V_{conv} (cm/s)	Fraction of Initial Inventory (%)	Time to Release 75% of Inventory (s)
0.1	0.1	100	109
0.1	1.0	100	67
0.1	10.	100	29
0.01	10	100	66
0.1	10	100	29
1.0	10	100	8
0.1	10	100	29
0.1	10	50	57
0.1	10	10	291
0.1	10	100	369[a]

a. Coalescence rate determined from turbulence alone. Bubble rise was not considered.

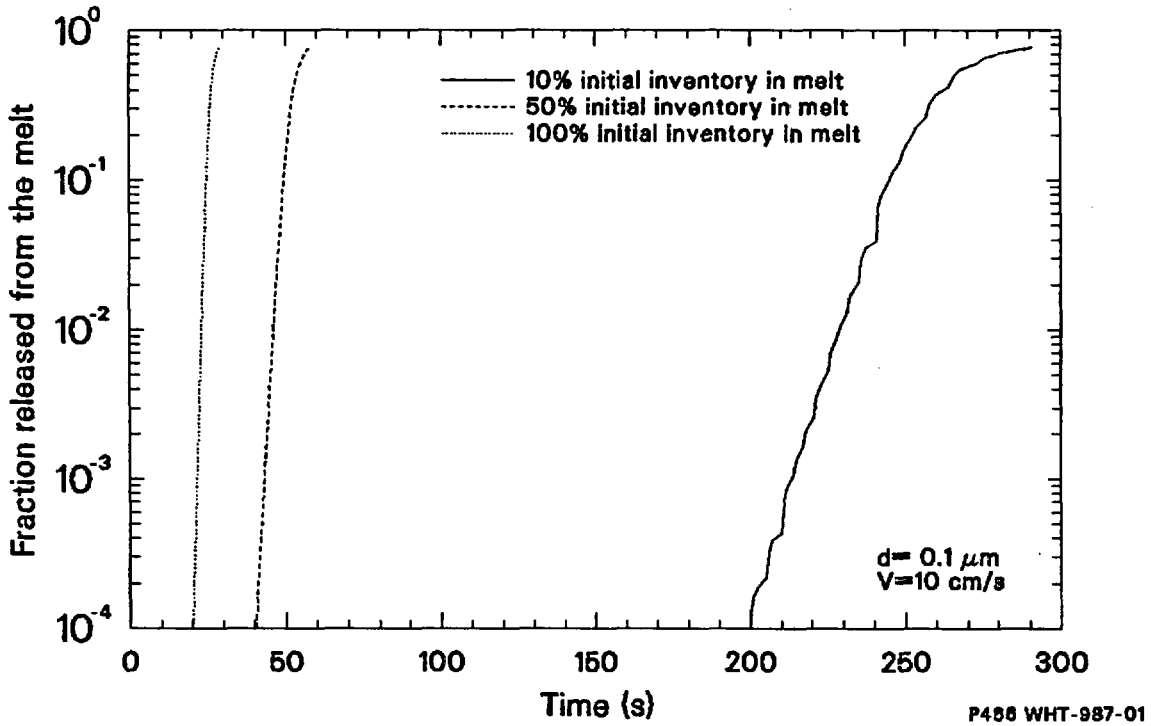

Figure 12. Volatile gas release from the melt due to bubble coalescence and rise.

5.3 Medium and Low Volatile Fission Product Release from the Melt

Unlike the volatile fission products, the medium and low volatile fission products will tend to remain as condensed phases in the melt because of their low vapor pressures. The chemical forms of the lower volatile fission products in the melt are determined by the oxygen potential in the melt. As indicated in Figure 13, the high oxygen potential of stoichiometric $(U,Zr)O_2$ at 2800 K (- 590 kJ/mole O_2) suggests that Eu and Ce will exist as oxides (i.e., Eu_2O_3, and Ce_2O_3) whereas Ru, Sr, and Sb will exist as metals because of their low oxidation potentials.

Release of these materials from the molten pool can be calculated based on mass transport through a liquid. The rate of mass transport of a species in a liquid is given by

$$M_{vap} = k_c A(C_{bulk} - C_{surface}) \tag{16}$$

where

k_c = mass transport coefficient through the condensed phase (m/s)

A = surface area for vaporization (m^2)

C_{bulk} = bulk concentration of species in the melt (kgmole/m^3)

$C_{surface}$ = concentration of species at the surface (kgmole/m^3).

Assuming that the concentration at the surface is much smaller than the bulk concentration, a mass balance on the pool yields

$$dC/dt - -M_{vap}/V = -(k_c A/V)*C \tag{17}$$

where V is the volume of the pool. The solution to Equation (17) is a simple exponential with a time constant of (V/k_cA). The time constant is a function of the geometry and mass transport coefficient. The mass transport coefficient is determined by the hydrodynamics of the pool. Three extreme cases have been examined: (a) a stagnant pool where mass transport is controlled by diffusion, (b) a well-mixed pool where mass transport is controlled by natural convection of vapor to the pool surface, and (c) mass transport of vapor to the volatile fission gas bubbles in the pool.

For the pure diffusion calculation, the pool was modeled as a parallelpiped with a volume and height equal to that of the hemispherical pool (V = 6385 L, R = 1.45 m). For this geometry, the mass transport coefficient is given by [31]

$$k = (3 + \pi)\pi D/[R(1 + 4\sqrt{2\pi/3})] \tag{18}$$

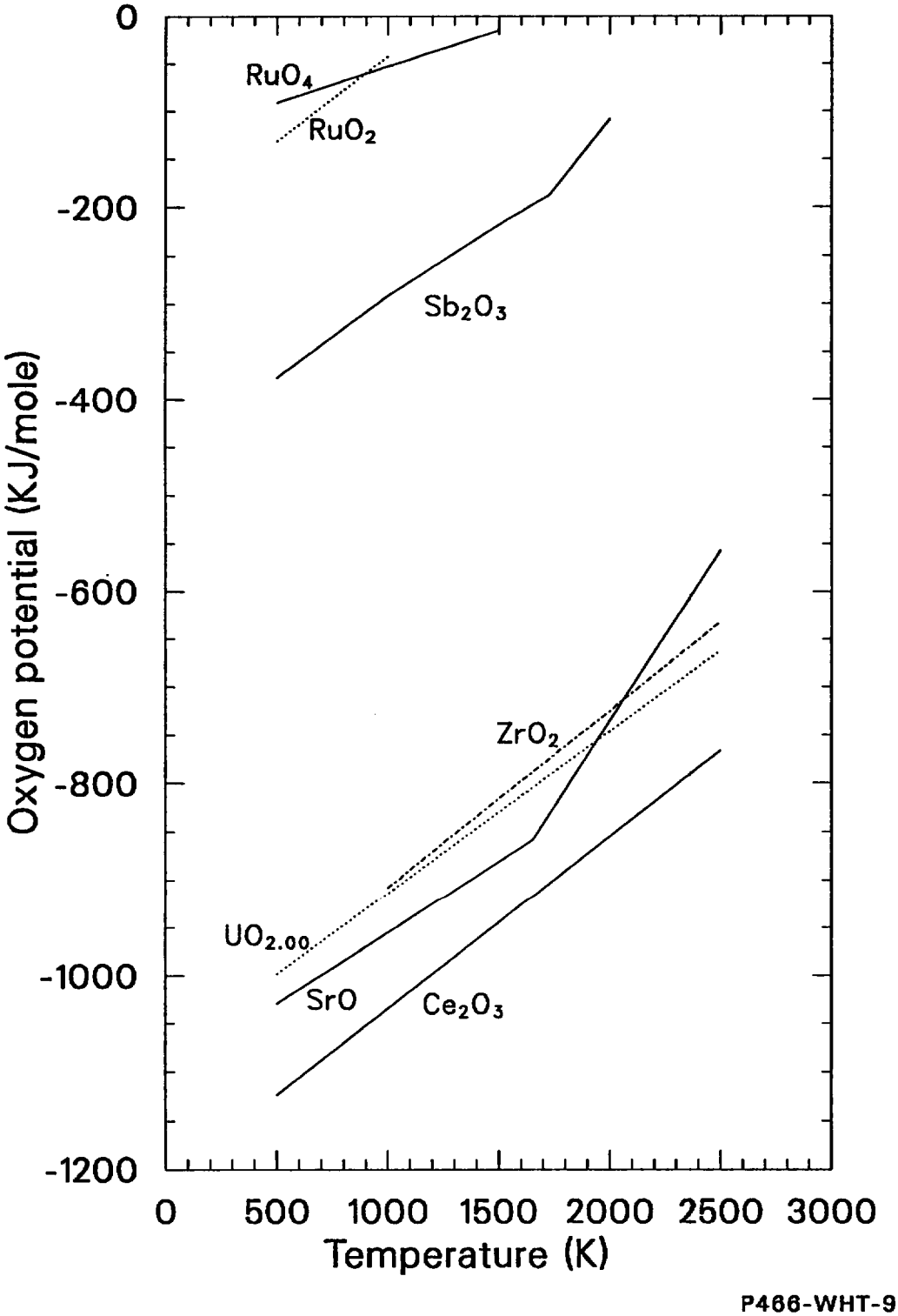

Figure 13. Free energies of formation for core material oxides.

where

D = diffusion coefficient of condensed phase in the melt (m^2/s)

R = radius of pool (m).

For the case where transport in the pool is controlled by natural convection, the mass transport coefficients for the top and bottom of the pool can be obtained from heat transfer correlations and the mass transfer analogy.[32] Thus

$$Nu_{top} = 0.36\ Ra^{0.23}\ (Sc/Pr)^{0.23} \tag{19}$$

$$Nu_{bottom} = 0.6\ Ra^{0.2}\ (Sc/Pr)^{0.2} \tag{20}$$

where

Ra = Rayleigh number of the pool

Sc = Schmidt number

Pr = Prandtl number.

The Rayleigh, Schmidt, and Prandtl numbers are given by

$$Ra = (gBQR^4/\alpha\nu k),\ Sc = \nu/D \text{ and } Pr = \nu/\alpha \tag{21}$$

where

B = thermal expansion coefficient (K^{-1})

Q = volumetric heat generation in the pool (W/m^3)

α = thermal diffusivity (m^2/s)

k = thermal conductivity (W/m-K).

The average mass transport coefficient for the pool is given by surface area averaging Nu_{top} and Nu_{bottom}

$$k_c = (D/R)(Nu_{top} + 2Nu_{bottom})/3\ . \tag{22}$$

The diffusion coefficient for a condensed phase in the melt is given by [33]

$$D = 8.2\ E\text{-}10\ [1 + (3v_b/v_a)^{2/3}]\ T/(\mu_b v_a^{1/3}) \tag{23}$$

where

D = diffusion coefficient (cm^2/s)

μ_b = viscosity of the melt (g/cm-s)

v_a = molar volume of the melt (cm^3/gmole)

v_b = molar volume of the condensed phase (cm^3/gmole)

T = temperature of melt (K).

For the case of mass transport to the volatile gas bubbles, a transport time can be estimated using the equation for diffusion to a sphere [31]

$$\tau = R^2/(\pi^2 D) \qquad (24)$$

where the characteristic size, R, is the radius of the bubble. Values of the parameters used to calculate the mass transport results are listed in Table 5.

Time constants have been calculated for the various fission product species using Equations (17) through (24). The results are presented in Table 7. The time constants associated with pure diffusion to the pool surface are extremely long for all species due to the small surface to volume ratio of the molten pool. As expected, the time constants for the well-mixed pool are smaller than those for diffusion. By contrast, the time constant associated with diffusion to a 10-μm bubble for all species is well under one second. This rapid transport time does not indicate however, that large release of the medium and low volatile fission products would be expected. The vapor concentration, C_{bulk}, of these fission product species in the melt needs to be examined. Raoult's law can be used to estimate the vapor concentration of the fission product oxides (Eu_2O_3, Ce_2O_3) because they are soluble in the ceramic melt. The low vapor pressures of Eu_2O_3 and Ce_2O_3, combined with their low mole fractions in the melt, result in a very small vapor concentration. Although the metallic fission products (Ru and Sb) have moderate vapor pressures at 2800 K, their vapor concentrations in the pool are also very small because of alloying of these species with other metallic components (Fe, Ni, Cr) [34,35] and the low mole fraction of metallic material in the molten pool. All of these thermodynamic arguments indicate that despite the potential for very quick diffusional transport times to the volatile gas bubbles, very little release of these medium and low volatile fission products would be expected because of their low upper pressures and mole fractions in the molten pool during the accident. However, if the material that did not relocate to the lower plenum remained hot for many hours, then the results in Table 7 indicate that some release might have occurred very late in the accident. All of these results agree with the lower volatile fission product retention data in Table 2. For the fission product oxides (Eu_2O_3, Ce_2O_3), very little release was noted. The low retention of the metallic fission products (Ru and Sb) in the lower plenum ceramic samples is not the result of vaporization. Rather, the low

TABLE 7. TIME CONSTANTS FOR DIFFUSIONAL FISSION PRODUCT RELEASE FROM THE MOLTEN POOL

Species	Diffusion Without Convection[a] (days)	Natural Convection (h)	Diffusion to a 10 μm bubble (s)
Ru	96	3.9	7.70 E-04
Sr	297	9.4	2.38 E-04
Sb	197	8.8	1.53 E-03
Eu_2O_3	386	11.5	3.13 E-03
Ce_2O_3	389	11.6	3.12 E-03

a. For a rectangular parallelpiped of the same volume as the pool and a height corresponding to the pool radius of 1.45 m.

retention in these ceramic samples reflects the fact that Ru and Sb are tied up with the other metallic components (Fe, Ni, and Cr) in the melt that were not sampled.

5.4 Effect of a Surrounding Crust

It is not expected that the crust would have any open cracks in it due to its self-sealing nature. Because the material at the crust/pool interface is at the melting point, any crack in the crust would tend to be plugged by the molten material and refreeze thus preventing release of volatile fission products until the large relocation of material at 224 min.

6. FISSION PRODUCT RELEASE DURING PHASE 4

Very little fission product release is expected during the core relocation in Phase 4 because it occurred so rapidly. Release during this phase is probably governed by the break-up dynamics of the molten column as it entered the water in the lower plenum. The extent of release will be a function of the amount of melt surface area and trapped fission products exposed to water during and following the relocation. Estimating fission product release under such conditions is very difficult because of the difficulty in characterizing the cracking and breakup of the molten material as it entered the lower plenum. Posttest examination of the fuel bundle in Test SFD 1-1 [21] indicated that significant cracking of the molten U-Zr-O mass contributed to the large fission gas release upon cooldown. Thus, the potential existed for significant release of volatile gas inventory during Phase 4, depending on the extent of fragmentation as the debris entered the lower plenum. However, based on the results from the Phase 3b coalescence calculations, very little gas is expected to be trapped in the molten material at the time of relocation.

7. SUMMARY AND CONCLUSIONS

Based on this preliminary analysis of fission product behavior during the TMI-2 accident, the following conclusions can be drawn concerning high, medium, and low volatile fission product release:

Volatiles (Noble gas, I, Cs, Te):
Volatile fission product release during Phase 2 was dominated by diffusion up to the point that significant liquefaction of the fuel occurred. Based on a series of sensitivity calculations, the average core-wide fission product release during this phase was within the range of 0 to 27%, though individual locations within the core may have experienced up to 60% release. The macrocracks and fuel intergranular fracturing observed in the fuel in the upper debris bed suggest that considerable additional release of fission gases and volatile fission products could have taken place upon reflood following the B-loop pump transient. These volatile fission product release results are generally consistent with the iodine and cesium retention data obtained from the upper debris samples.

Although in general Te release from the fuel pellets would be roughly similar to the Xe diffusional results, separate effects test data indicate that Te tends to become bound to unoxidized Zr in the cladding. As the Zr oxidizes, the Te is released and transported from the cladding. Therefore, it is expected that those areas of the TMI-2 core that experienced a high degree of oxidation should have high Te releases while more Te retention is expected in areas of low oxidation.

Bubble coalescence calculations indicate that following liquefaction and consolidation of the molten material into a large pool, volatile fission products should be released very quickly from the melt due to sweeping of small gas bubbles by large ones to the melt surface. However, the gas would probably be trapped inside the crust until it failed at 224 min. The molten fuel breakup and macrocracking that occurred during Phase 4 can result in release of any trapped volatile gas bubbles. The magnitude of the potential release depends on the extent of debris breakup as the molten material entered the lower plenum. These results are in agreement with the iodine retention data for the lower plenum samples. However, these results also indicate that the high cesium retention in the lower plenum samples is not the result of physical bubble trapping in the molten pool. It is postulated that the cesium is in a less volatile (as yet unknown) chemical form which reduces it volatility in the melt. Silicates, zirconates, and borates of cesium are three potential low volatile chemical forms that might be stable at 2800 K.

Medium (Ru, Sb) and Low (Eu, Ce) Volatile Fission Product Release:
The chemical forms of the medium and low volatile fission products are determined by the oxygen potential of the system. The oxygen potential of the molten $(U,Zr)O_2$ pool in TMI-2 suggests that Eu and Ce will exist as oxides (i.e., Eu_2O_3 and Ce_2O_3) while Ru, Sr, and Sb

will exist as metals. Very little medium and low volatile fission product release was calculated to have occurred during the TMI-2 accident primarily because of the low volatility of these species in both the solid and molten fuel and the low surface-to-volume ratio of the melt. These calculational results agree with the lower volatile (Eu, Ce) fission product retention data. The low retention of the metallic fission products (Ru and Sb) in the lower plenum ceramic samples is not the result of vaporization. Rather, the low retention in these ceramic samples reflects the fact that Ru and Sb are tied up with the other metallic components (Fe, Ni, and Cr) in the melt that were not sampled.

The fission product retention estimates developed in this study have been compared, to the extent possible, with retention data from lower and upper plenum samples. This analysis has been able to explain some of the measurement results, however additional work is still required to explain the high cesium retention in the lower plenum. The results from this study will be factored into the accident scenario to provide additional insight into the accident. In addition, the results of this study will be used to help resolve outstanding severe accident and source term issues relating to fission product release, transport, and chemical form.

8. REFERENCES

1. E. L. Tolman et al., TMI-2 Accident Evaluation Program, EGG-TMI-7048, February 1986.

2. E. L. Tolman et al., TMI-2 Accident Scenario Update, EGG-TMI-7489, December 1986.

3. B. G. Schnitzler and J. B. Briggs, TMI-2 Isotopic Inventory Calculations, EGG-PBS-6798, April 1985.

4. D. W. Akers et al., "Fission Product Behavior in the TMI-2 Core: Preliminary Evaluation of Transport and Chemistry," Proceedings of the Symposium on Chemical Phenomena Associated with Radioactivity Releases During Severe Nuclear Plant Accidents, Anaheim, CA, September 9-12, 1986.

5. R. H. Barnes et al., Xenon Diffusion in Single-Crystal and Sintered UO_2, BMI-1533, August 1961.

6. J. B. Melehan et al., Release of Fission Gases from UO_2 During and After Irradiation, BMI-1623, March 1963.

7. D. F. Toner and J. L. Scott, "Study of Factors Controlling the Release of Xenon-133 from Bulk UO_2," The 64th Annual Meeting of the American Society for Testing and Materials, Atlantic City, NJ, June 1961.

8. S. G. Prussin et al., "Release of Volatile Fission Products from UO_2," Proceedings of the American Nuclear Society Meeting on Fission Product Behavior and Source Term Research, Snowbird, UT, July 15-19, 1984.

9. A. H. Booth and G. T. Rymer, Determination of the Diffusion Constant of Fission Xenon in UO_2 Crystals and Sintered Compacts, CRDC-720, August 1958.

10. G. A. Berna et al., RELAP5/SCDAP/MOD0 Code Manual, Volume 1: Code Structure, System Models, and Solution Methods, Draft Preliminary Report, EGG-RTH-7051, September 1985.

11. G. T. Lawrence, "A Review of the Diffusion Coefficient of Fission-Product Rare Gases in Uranium Dioxide," Journal of Nuclear Materials, 71, pp. 195-218, 1978.

12. J. Belle, (ed.), Uranium Dioxide: Properties and Nuclear Applications, Naval Reactors, Division of Reactor Development, USAEC, 1961.

13. D. L. Hagrman and G. A. Reymann (eds.), MATPRO-Version 11, A Handbook of Materials Properties for Use in the Analysis of Light Water Reactor Fuel Rod Behavior, NUREG/CR-0497, TREE-1280, February 1979.

14. TMI-2 Accident Core Heat-up Analysis, A Supplement, NSAC-25, June 1981.

15. M. Silberberg et al., Reassessment of the Technical Bases for Estimating Source Terms, NUREG-0956, July 1986.

16. Analysis of Three Mile Island--Unit 2 Accident, NSAC-80-1, March 1980.

17. R. R. Hobbins, D. J. Osetek, and D. L. Hagrman, "In-Vessel Release of Radionuclides and Generation of Aerosols," Proceedings IAEA Symposium on Source Term Evaluation for Accident Conditions, Columbus, OH, October 28-November 1, 1985, International Atomic Energy Agency, 1986.

18. D. W. Akers et al., TMI-2 Core Debris Grab Samples--Examination and Analysis Part 1, GEND-INF-075, EG&G Idaho, Inc., September 1986.

19. W. Dienst, P. Hofmann, and D. K. Kerwin-Peck, "Chemical Interactions between UO_2 and Zircaloy-4 from 1000 to 2000°C," Nuclear Technology, 65, pp. 109-124, April 1984.

20. A. W. Cronenberg et al., "An Assessment of Liquefaction-Induced I, Cs and Te Release from Low and High Burnup Fuel," Proceedings of the International Meeting on Light Water Reactor Severe Accident Evaluation, Cambridge, MA, August 28-September 1, 1983.

21. Z. R. Martinson, D. A. Petti, and B. A. Cook, PBF Severe Fuel Damage Test 1-1 Test Results Report, NUREG/CR-4684, EGG-2463, October 1986.

22. A. D. Knipe, S. A. Ploger, and D. J. Osetek, PBF Severe Fuel Damage Scoping Test--Test Results Report, NUREG/CR-4683, EGG-2413, August 1986.

23. J. Rest and A. W. Cronenberg, "Modeling the Behavior of Xe, I, Cs, Te, Ba and Sr in Solid and Liquefied Fuel during Severe Accidents," Journal of Nuclear Materials (in press).

24. M. Osborne et al., "Experimental Studies of Fission Product Release from Commercial Light Water Reactor Fuel Under Accident Conditions," Nuclear Technology, 78, 2, August 1987, pp. 157-169.

25. G. D. McPherson, R. R. Hobbins, and P. North, "U.S. Department of Energy Severe Accident Technology and Analysis Program," International Conference on Nuclear Power Performance and Safety, Vienna, Austria, September 28-October 2, 1987, IAEA-CN-48/192.

26. A. W. Cronenberg and T. R. Yackle, "Intergranular Fracture of Unrestructured UO_2 Fuel During Film-Boiling Operation," Journal of Nuclear Materials, 84, pp. 295-318, 1979.

27. P. J. Fehrenbach et al., "High Temperature Transient Fission Gas Release from UO_2 Fuel: Microstructural Observations," Proceedings of the International ANS/ENS Topical Meeting on Thermal Reactor Safety, San Diego, California, February, 2-6, 1986.

28. M. Epstein and H. K. Fauske, The TMI-2 Core Relocation--Heat Transfer and Mechanism, FAI/87-49, July 1987.

29. D. R. Olander, Fundamental Aspects of Nuclear Reactor Fuel Elements, TID-26711, 1976.

30. S. K. Friedlander, Smoke, Dust and Haze: Fundamentals of Aerosol Behavior, New York: John Wiley & Sons, 1977.

31. H. S. Carslaw and J. C. Jeager, Conduction of Heat in Solids, Cambridge: Oxford University Press, 1959.

32. M. Jahn and H. H. Reineke, "Free Convection Heat Transfer with Internal Heat Sources, Calculations and Measurements," Proceedings of the 5th International Heat Transfer Conference, Tokyo, Japan, September 1974, Paper No. 28.

33. D. A. Powers et al., VANESA: A Mechanistic Model of Radionuclide Release and Aerosol Generation During Core Debris Interactions with Concrete, NUREG/CR-4308, SAND85-1370, July 1986.

34. R. K. McCardell et al., "TMI-2 Core Bore Examination Results," 15th Water Reactor Safety Meeting, Gaithersburg, MD, October 26-29, 1987.

35. G. W. Parker et al., "Source Term Evaluations From Recent Core Melt Experiments," Proceedings IAEA Symposium on Source Term Evaluation for Accident Conditions, Columbus, OH, October 28-November 1, 1985, International Atomic Energy Agency, 1986.

NRC FORM 335 (2-84) NRCM 1102, 3201, 3202

U.S. NUCLEAR REGULATORY COMMISSION

BIBLIOGRAPHIC DATA SHEET

SEE INSTRUCTIONS ON THE REVERSE

1 REPORT NUMBER (Assigned by TIDC add Vol No., if any)

NUREG/CP-0091
Vol. 6

2. TITLE AND SUBTITLE

Proceedings of the Fifteenth Water Reactor Safety Information Meeting

3 LEAVE BLANK

4 DATE REPORT COMPLETED

MONTH: January | YEAR: 1988

5. AUTHOR(S)

Compiled by Allen J. Weiss, BNL

6 DATE REPORT ISSUED

MONTH: February | YEAR: 1988

7. PERFORMING ORGANIZATION NAME AND MAILING ADDRESS (Include Zip Code)

Office of Nuclear Regulatory Research
U. S. Nuclear Regulatory Commission
Washington, D. C. 20555

8 PROJECT/TASK/WORK UNIT NUMBER

9 FIN OR GRANT NUMBER

A-3283

10. SPONSORING ORGANIZATION NAME AND MAILING ADDRESS (Include Zip Code)

Same as Item 7 above

11a. TYPE OF REPORT

Proceedings of conference on safety research

b. PERIOD COVERED (Inclusive dates)

October 26-29, 1987

12. SUPPLEMENTARY NOTES

Proceedings prepared by Brookhaven National Laboratory

13. ABSTRACT (200 words or less)

This six-volume report contains 140 papers out of the 164 that were presented at the Fifteenth Water Reactor Safety Information Meeting held at the National Bureau of Standards, Gaithersburg, Maryland, during the week of October 26-29, 1987. The papers are printed in the order of their presentation in each session and describe progress and results of programs in nuclear safety research conducted in this country and abroad. Foreign participation in the meeting included twenty-two different papers presented by researchers from Belgium, Czechoslovakia, Germany, Italy, Japan, Russia, Spain, Sweden, The Netherlands and the United Kingdom. The titles of the papers and the names of the authors have been updated and may differ from those that appeared in the final program of the meeting.

14. DOCUMENT ANALYSIS – a. KEYWORDS/DESCRIPTORS

reactor safety research
nuclear safety research

b. IDENTIFIERS/OPEN-ENDED TERMS

15 AVAILABILITY STATEMENT

Unlimited

16 SECURITY CLASSIFICATION

(This page) Unclassified

(This report) Unclassified

17 NUMBER OF PAGES

18 PRICE

UNITED STATES
NUCLEAR REGULATORY COMMISSION
WASHINGTON, D.C. 20555